

07

ATKINS

Technical Journal

Papers 099 – 119

Plan Design Enable





Welcome to the seventh edition of the Atkins Technical Journal which has been given a refreshed appearance, but continues to showcase the impressive breadth and depth of the excellent technical solutions we offer our clients. A gratifying aspect of this edition is that our authors come from a full staff cross section of Graduate Engineers through to Directors with a seamless blend of quality.

This edition demonstrates the extent to which we are leading research to push back the boundaries of codes of practice and drive innovation. Sometimes this research is to facilitate more reliable decision making, such as the need to better understand how ground movement associated with the construction of new tunnels impacts on existing tunnels in congested urban environments. Frequently our research is targeted at generating more sustainable solutions for our clients, such as the use of fabric formwork for concrete structures (being investigated with Bath University) which allows shaping of beams to follow the flow of force and eliminate unnecessary material. However, when adherence to codes of practice is required, we have experts who understand their background and can apply them to most efficient effect, as is illustrated by our geotechnical teams' expertise in UK and European geotechnical standards.

Asset Management represents a growing share of what we do and we have an impressive array of projects showcasing our abilities to prolong the efficient service life of infrastructure. The use of forensic engineering, advanced analysis and remote monitoring techniques on projects like Runway 9/27 Houston, Texas and the Midland Links Viaducts in the UK (co authored with the Highways Agency) are two examples amongst several within this Journal.

Of course, the environmental aspects of sustainability are not forgotten in our projects and the consideration of protection to a wide range of natural environmental features and habitats are covered in this Journal, including those for newts and badgers.

I hope you enjoy the selection of technical papers included in this edition.

Chris Hendy

Network Chair for Bridge Engineering
Chair of H&T Technical Leaders Group

Atkins



Technical Journal 7

Papers 099 – 119

Asset Management

- 99 Rehabilitation of runway 9-27 at George Bush Intercontinental Airport (Houston, TX) 5
- 100 Fatigue management of the Midland Links steel box girder decks 13

Defence

- 101 The use of "off the shelf" data with limited integrity in a safety critical avionics environment 23
- 102 The application of high pressure water mist as part of a holistic fire fighting system 29

Geotechnical

- 103 Update on new and future earthworks standards in the UK and Europe 41
- 104 Lightweight backfill materials in integral bridge construction 47

Highways

- 105 Safety governance of complex highway projects 55
- 106 Monitoring the use of badger tunnels on highways agency schemes 59

Intelligent Transport Systems

- 107 M4 J24 – J28 VSL: modelling and calibration 63
- 108 Motorway-to-motorway: a potential technological solution to motorway congestion 67

Structures

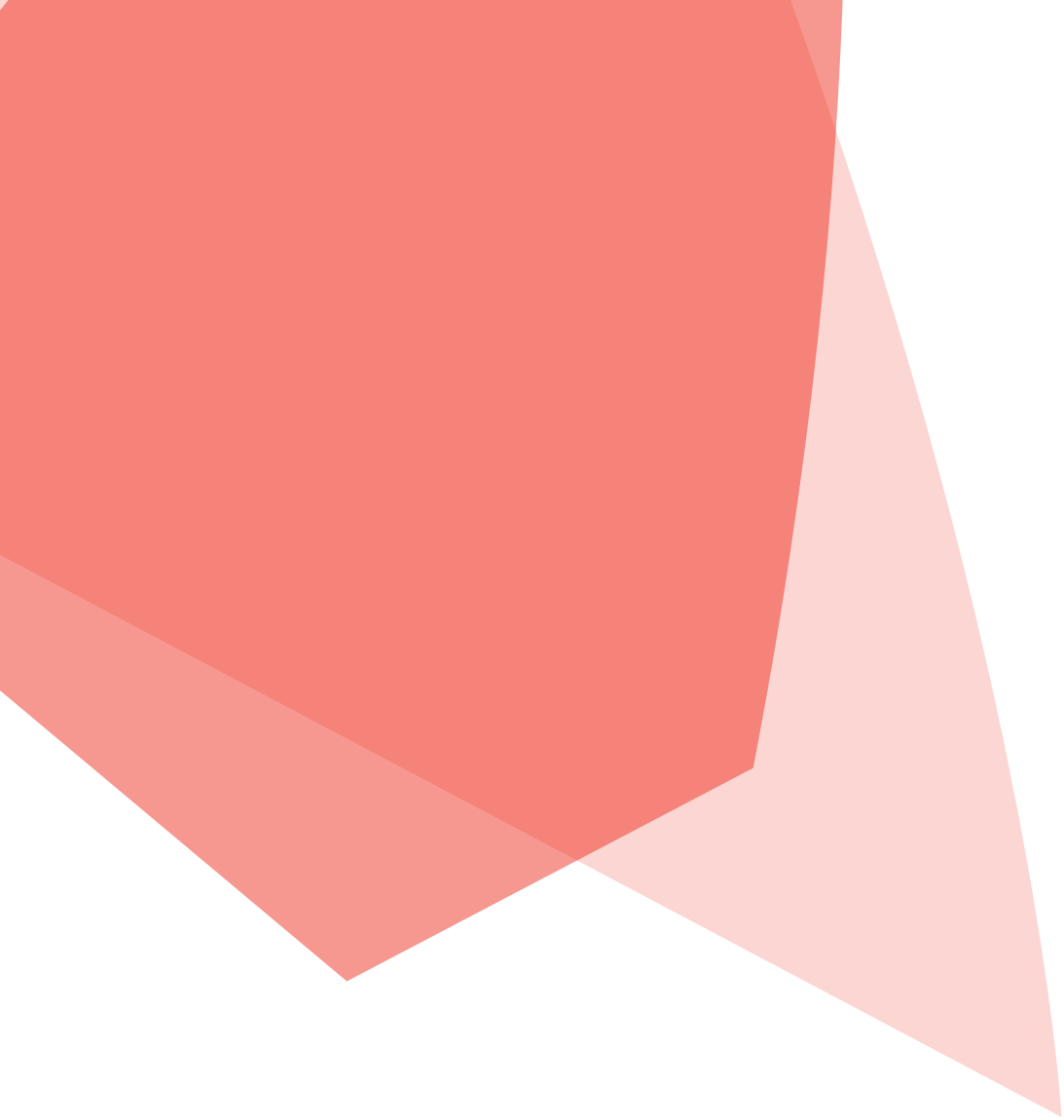
- 109 Load capacity rating of an existing curved steel box girder bridge through field test 75
- 110 Wind loads on steel box girders during construction using computational fluid dynamic analysis 83
- 111 The design and construction of Cliffsend Underpass 93
- 112 Concrete structures using fabric formwork 97

Tunnelling

- 113 Adit mining in high permeability, interbedded sandstone, Red Line, Dubai Metro 107
- 114 Assessment of ground movement impacts on existing tunnels 113

Water & Environment

- 115 Mineral extraction alongside great crested newts 121
- 116 Bank stabilisation by redirective structures on the Santa Clara River, Ventura County, CA. 125
- 117 The Olympic Park – a biodiversity action plan in action 133
- 118 Long term modelling at the East and West Flower Garden Banks 2004-2008 137
- 119 Risk and uncertainty in hydrological forecasting 143





Justin P. Jones

Vice President/Business
Sector Manager

National
Aviation Group

Atkins North America



**William G.
Stamper**

Senior Engineer

National
Aviation Group

Atkins North America



Adil Godiwalla

Assistant Director
of Aviation

Design &
Construction Division

Houston Airport
Systems



Jim Hall

Senior
Principal Engineer

Applied Research
Associates, Inc.

Vicksburg, Mississippi



Dallas Little

Snead Endowed Chair
in Transportation
Engineering

Civil Eng. Dept., Texas
A&M University

CMS Engineering
Group, LLC, Texas

Rehabilitation of Runway 9/27 at George Bush Intercontinental Airport, Houston, Texas

Abstract

A combination of finite element method (FEM) analysis, traditional pavement design methods, and forensic analysis can reveal information about a pavement's history and its future performance that cannot be determined with traditional evaluation methods alone. Engineers and researchers recently applied this three-tiered approach to the rehabilitation of Runway 9/27 at Houston Airport System's George Bush Intercontinental Airport. The results of the investigation demonstrate the utility of a new generation of tools for site-specific pavement evaluation and rehabilitation design and suggest a change in the way engineers approach these projects in the future.

For Runway 9/27, the investigative team had to discover the root causes for crazing, tearing, and shoving of the asphalt at the landing areas and high-speed exits. Using X-ray computed tomography, the relationship between air void and crack distributions was evaluated from core samples and the distresses observed in different runway areas. The results revealed high air-void content consistently at a depth of approximately 3 inches, indicating a point of separation or slippage boundary.

Based on the forensic evaluation and FEM analysis, investigators concluded that the distress in the pavement was likely due to high shear stresses resulting from the braking and cornering action of aircraft and to the geometry of the asphalt layers. The synergistic effects of a stiff, polyethylene binder, oxidative aging in the top inch of the pavement, and the high, near-surface shear stresses all resulted in shoving and crazing.

Ongoing advances in computer technology open the door for the development of increasingly sophisticated programs to analyze pavement conditions, allowing for more cost-effective, yet more thorough, investigations.

Deficiencies in the traditional pavement analysis approach can be mitigated not only by supplementing the investigation with forensic analyses to determine causes for apparent distress, but also by using three-dimensional FEMs to analyze relationships between weak interlayers (identified on the basis of visual examination), shear stresses, and permanent deformation.

Typically, airports demolish airfield pavements at the end of their 20 year design lives and build new ones. In contrast, by deploying forensic engineering practices, airports can save costs, expedite construction, and mitigate the environmental impact associated with pavement replacement.

Background

The Houston Airport System is the fourth-largest airport system in the United States and the sixth-largest in the world. To bring air service to the metro area's population of more than 5.5 million, the Houston Airport System has three facilities: George Bush Intercontinental Airport, William P. Hobby Airport, and Ellington Airport. The three-airport system served more than 49.5 million passengers in 2010, including more than 8.5 million international travelers.

Together these facilities form one of North America's largest public airport systems and position Houston as the international passenger and cargo gateway to the south central United States and a primary gateway to Latin America.¹

After a complete rehabilitation, Runway 9/27 at George Bush Intercontinental Airport was re-opened in 2009 and is now equipped with state-of-the-art approach capabilities. The runway began accepting ARC's Category III approaches in February 2009. According to FAA Advisory Circular (AC) 150/5300-13, Airport Design, the Airport Reference Code (ARC) is a coding system used to relate airport design criteria to the operational and physical characteristics of the airplanes intended to operate at an airport. The upgraded runway allows pilots the greatest precision in landing aircraft in low and reduced visibility flight conditions.

The rehabilitated runway now places Houston's hub airport in a league among a few airports in the nation that currently operate three parallel Category III runways. The Houston Airport System combined the fast-tracked rehabilitation project with the addition of the navigational aid that was completed at the same time.²

George Bush Intercontinental Airport is located approximately 20 miles north of downtown Houston, Texas. Named after George H.W. Bush, the 41st president of the United States, the airport is one of the fastest growing in the nation and the 17th busiest in the world, serving nearly 43 million passengers annually.³

One of the airport's five existing runways, the 10,000 foot long Runway 9/27 was originally constructed in 1987 with 300 foot Portland concrete cement (PCC) pavement at each end and asphalt pavement in the center with a lime cement fly ash (LCF) base. The 9,400 foot asphalt portion of the runway received an asphalt overlay in 1998, and portions of



Figure 1. Shoving of wearing course on Runway 9/27



Figure 2. Cracking/tearing of wearing course on Runway 9/27

the taxiways have been reconstructed and repaired since the original construction.

A pavement condition investigation conducted in 2005 indicated that pavement rehabilitation on Runway 9/27 was necessary. Visible defects to the runway were recorded, with shoving (**Figure 1**) and crazing/tearing (**Figure 2**) evident at the landing areas and high-speed exits.

An extensive investigation of the existing runway was performed to determine the potential cause of the distress and to develop a cost effective, site specific design to accommodate the anticipated loading for the next 20 years. The investigation included a topographic survey, geotechnical investigation, forensic study of cores, and finite element analysis of the existing pavement structure.

A new paradigm was used for the analysis and design. LEDFAA and the finite element computer program ISLAB 2000 were used to determine the corner pavement stresses and strains, edge stresses and strains, thermal stresses and strains, and deflections in the various pavement layers. LEDFAA is a computer program used to perform thickness design of airport pavements. It implements advanced design procedures based on layered elastic theory developed under the sponsorship of the Federal

Aviation Administration.⁴ A host of other analyses including non-destructive testing, X-ray computed tomography, and electronic image scanning were also performed for the forensic analysis. The finite element analysis included deteriorating load transfer efficiency for the concrete panels for the next 20 year design cycle.

Evaluation of existing conditions

A confident assessment of the existing pavement structure is the basis of an effective rehabilitation strategy and structural design; consequently, identifying and evaluating the material properties of the existing pavement was the focus of the initial design phase. This activity was performed specifically to determine the condition, capacity, and material properties of the existing pavement. The evaluation comprised four main components:

- Review of previous pavement study;
- Review of record drawings;
- Geotechnical investigation;
- Laboratory testing and forensic evaluation.

The development of existing material properties was pursued using two methodologies. The first involved evaluating the previous pavement study data against cores taken during the geotechnical investigation; the second included a forensic evaluation of the cores recovered from the geotechnical investigation.

This parallel approach provided the necessary checks and balances to ensure that the rehabilitation design was developed on an accurate assessment of existing conditions.

Review of record drawings

The review of the record drawings provided an understanding of the construction of the existing pavement. The review revealed that the center 9,400 foot runway portion consisted of a 7 inch asphalt (including a 0.5 inch stress absorbing membrane interlayer [SAMI] layer) surface course on a 28 inch LCF base course and a 30 inch stabilized sub-base course. The first 300 feet on each end of the runway consisted of 14 inch PCC and a 3 inch asphalt concrete (AC) separation layer on a 14 inch LCF base course and a 30 inch stabilized sub-base course.

These data were verified through a total of 17 cores to a depth of 10 feet and 24 cores through the existing asphalt pavement taken during the geotechnical investigation.

Geotechnical investigation

Analytical procedures were used to compute or back calculate the elastic properties of the individual pavement layers and sub-grade. The data used for the analysis were calculated during the previous pavement study and from cores obtained during the geotechnical investigation.

The deflection data from the heavy weight deflectometer (HWD), along with thicknesses from the geotechnical investigation, were used with the proprietary back calculation software Deflexus to determine the modulus of the pavement layers and the sub-grade.

Figure 3 and **Figure 4** show the back calculated moduli for the AC and LCF layers. Upper and lower limits were set in Deflexus for the AC, LCF, and sub-base layers, which served as a maximum and minimum allowable moduli for each layer. The limits are necessary to control the range of the outputs. The standard deviation, however, was still large for the AC, LCF, and sub-base layers. A likely cause for the wide range of data within each feature was due to averaging layer thicknesses for each feature and the variability of the strength of each layer. By averaging layer thicknesses for each feature, Deflexus was used to perform the analysis assuming that the averaged thicknesses were exact thicknesses within each feature. To account for the data fluctuation, the design values for each layer were conservatively determined as the mean minus one standard deviation.

Representative moduli for each feature, based on this analysis, were developed as follows:

- The average AC layer modulus minus one standard deviation was approximately 434,568 pounds per square inch (psi);
- The average LCF layer modulus minus one standard deviation was approximately 458,034psi;
- The average stabilized sub-base layer modulus minus one standard deviation was approximately 73,510 psi, which is below the lower limit;
- The average sub-grade modulus minus one standard deviation was approximately 24,770psi.

AC Moduli

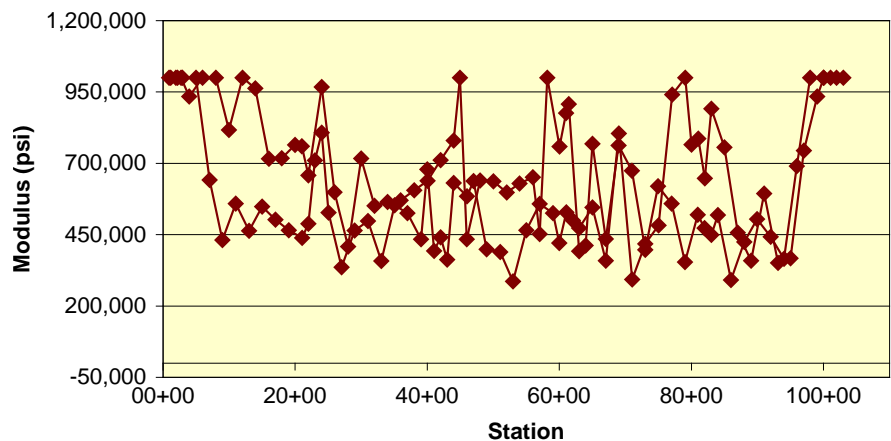


Figure 3. Modulus of asphalt concrete for Runway 9/27

LCF Moduli

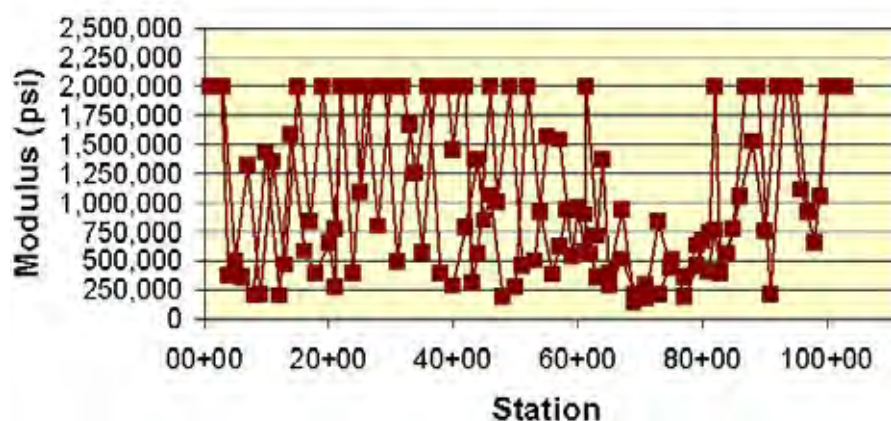


Figure 4. Modulus of lime-cement-fly ash for Runway 9/27

Laboratory testing forensic evaluation

The forensic evaluation of the existing pavement included the following main components:

- Visual inspection of field cores;
- Evaluation of air void distribution using X-ray computed tomography;
- Finite element analysis of the influence of weak interlayers in the pavement structure on shear stresses and their impact on shoving and top-down cracking within the asphalt layer.

The forensic evaluation focused on the relationship between the air void and crack distributions in the cores and the distresses observed in different runway locations. In this analysis, weak interlayers are defined as either poorly tacked interfaces between pavement

layers or those having the presence of a SAMI that is either too thick or too near the surface. Experience has shown that SAMI locations and thicknesses play an important role in the development of shear-induced shoving of the asphalt surface. The presence of a well-designed and sufficiently deep SAMI layer may reduce the potential for both reflection cracking and the propagation of cracks from the bottom up due to a favorable dissipation of energy at the SAMI interface rather than through crack growth or shoving in the asphalt surface.

Observations Regarding Core and Runway Condition

Figure 5 shows representative core samples (Cores F10A and F10B). **Table 1** summarizes the measurements and visual inspection of core samples taken as part of the geotechnical investigation.

X-ray computed tomography analysis of air void distribution

X-ray computed tomography is a nondestructive technique used to visualize the internal characteristics of opaque objects. An X-ray source sends out a beam of known intensity through the analyzed sample. The beam then reaches a detector where the attenuated beam intensity is measured. The sample rotates 360 degrees with respect to its center so that a full two-dimensional image can be created. The sample also moves at a given fixed gap in the vertical direction so that images at different



Figure 5. Representative core samples (F10A and F10B) showing air void and crack distributions in runway core samples

Label	Location	Total Thickness (Inches)	SAMI Location (Inches) and condition	Core condition	Location condition	Notes
F15	Taxiway SA	6.0	5.0	Separated at SAMI	Depression in the Taxiway	
F14	Taxiway SA	4.0	3.0 (distorted layer and non-uniform)	Separated in a lower SAMI layer	Depression in the Taxiway	Aggregate of darker color
F10C	Near the intersection of Runway and Taxiway SH	8.5	7.0 (uniform and thin layer)	No evidence of separation	Good condition	
F10A	Near the intersection of Runway and Taxiway SH	7.0	6.0 (uniform and thin layer)	Separated at 2.0 inches	Raveling (loss of asphalt concrete from the surface) Longitudinal crack (0.75 inch opening and 1.5 inch deep) Closure of grooves	
F10B	Near the intersection of Runway and Taxiway SH	7.0	5.0 (thin layer)	No top layer	Shoving north of F10A with mix moving to the west	Thin mixes below the SAMI
F8	Intersection of Runway and Taxiway SG	8.0	5.0 (thin layer)	Separated at 3.0 inches	Good condition	
F7	Between F8 and C	8.0	5.0 (thin layer)	Separated at the base	Good condition	
D2	East side of Runway just east of Taxiway SH	8.0	6.0	Separated at SAMI disintegrated	Good condition	
B3	West side of Runway just west of Taxiway SG	5.5	5.0	Separated at 3.0 inches	Good condition	
C1	Near the middle of Runway between Taxiway SH and SG	8.5	6.0 (thin layer)	Separated at 3.5 inches	Good condition	

Table 1. Summary of core measurements and visual inspection

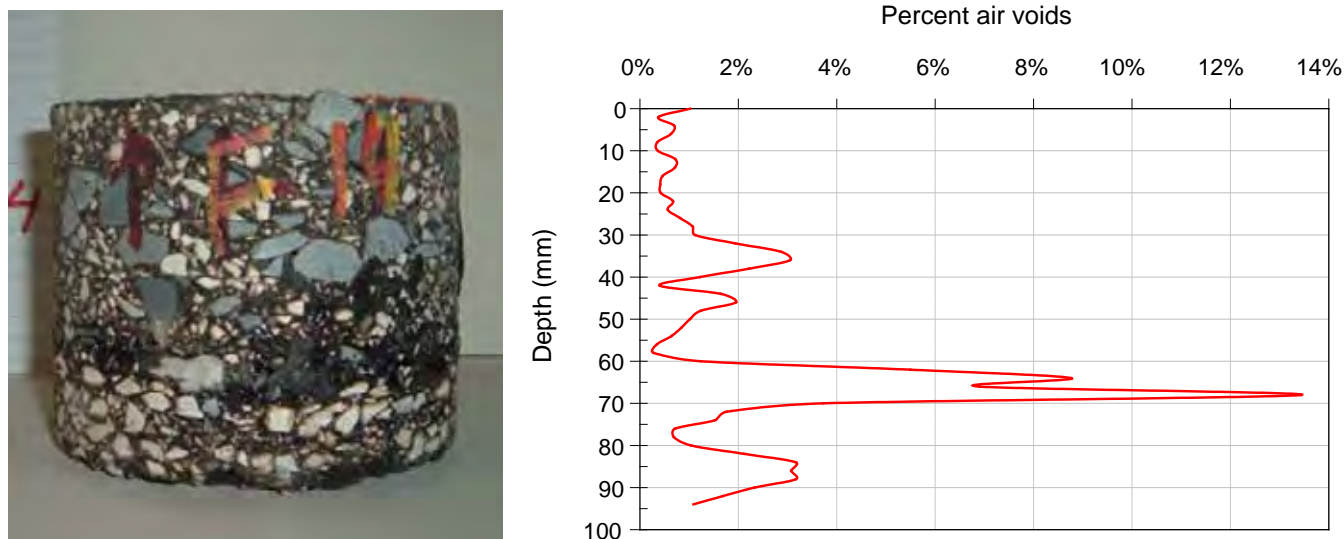


Figure 6. Air void distribution in Core F14

height locations can be obtained and thus describe the entire sample volume. X-ray computed tomography was used to evaluate the internal air void distribution in cores C1, F10A, F10B, F10C, and F14.

Results from Core F14 provide an indication of the data developed from this analysis. Core F14 exhibited low air voids except in the location of the SAMI layer (**Figure 6**). The low void content is an indication of mix instability or shoving, which was observed in this location during the site visit. This location has three characteristics that differentiate it from all other sections. First, the SAMI

layer in this core is thicker than in the others. Second, the SAMI layer is at a depth of about 3 inches from the surface, which is the smallest depth to SAMI among all cores. Third, the aggregate source, which is a darker aggregate, appears to be different from the aggregates used in the rest of Runway 9/27. **Figure 7** shows images captured at different depths within the core. **Figure 8** shows the three-dimensional distribution of air voids in Core F14. These images show that the percentage of air voids in the SAMI layer is much higher than in the rest of the core.

Finite element analysis of the influence of weak interlayers

An elasto-visco-plastic finite element model was used to analyze the permanent deformation of an airfield pavement section. The objective of this simulation was not to model the Runway 9/27 structure and material properties (because that requires extensive material testing) but rather to demonstrate the influence of the location of a SAMI layer on shear stresses and permanent deformation.

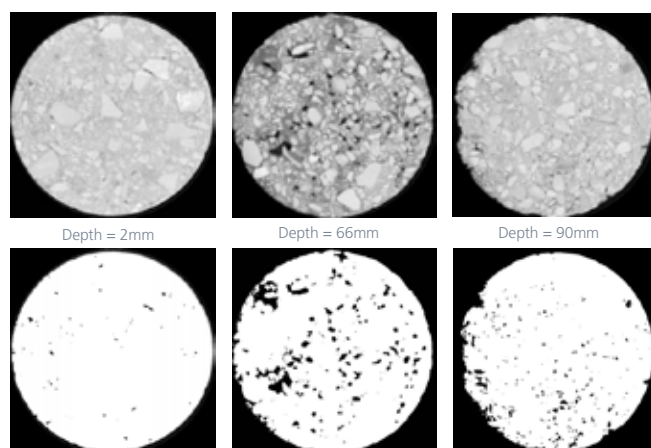


Figure 7. Images taken at different depths within core F14

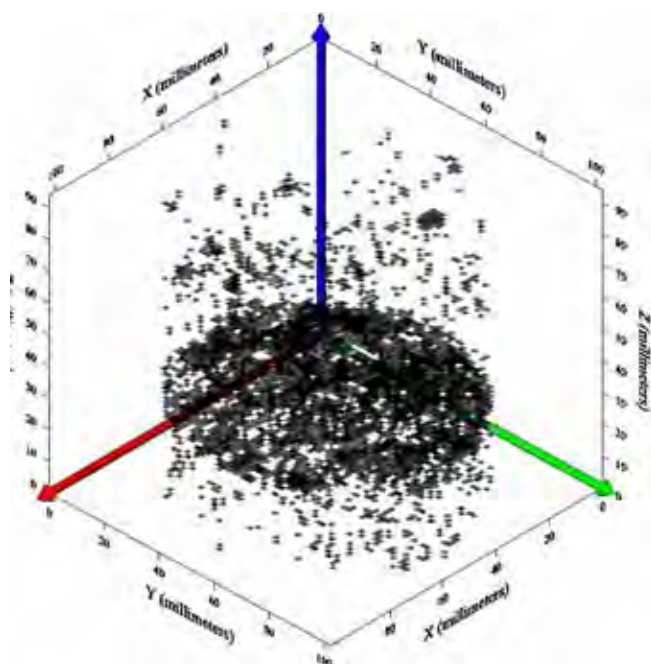


Figure 8. Three-dimensional air void distribution in core F14

The analysis was conducted using an axisymmetric finite element model. The asphalt mix material properties were selected to represent the properties of a typical asphalt mix that was evaluated at Texas A&M University at a high temperature of 58°C. The applied load was that of a B-737-300 aircraft (see **Table 2**). **Figure 9** shows the axisymmetric finite element model with the applied forces. The asphalt layer thickness is 6 inches, and the width is 120 inches. The SAMI was modeled as a 1 inch layer with an elastic modulus equal to 40 percent of that of the surrounding hot mix asphalt layers. However, the visco-plastic model parameters were maintained at the same level for both the SAMI and asphalt mixture. **Figure 10** shows the maximum permanent deformation in the three sections.

Gross Weight lbs (tons)	140,000 (63.503)
Tire Pressure psi (kPa)	201 (1386)
Percent Gross Weight on Gear	47.5%
Dual Spacing in (mm)	30.5 (774.7)
Tire Contact Width in (mm)	11.47 (291.4)
Tire Contact Length in (mm)	18.36 (466.3)

Table 2. B-737-300 loads used in the finite element model

It should be noted that a pavement section with the SAMI layer 2 inches below the surface experiences more permanent deformation than the section without the SAMI layer (about an 11 percent increase in permanent deformation). The section with the SAMI layer located 4 inches below the surface experienced only a 4 percent increase in permanent deformation compared with the section without SAMI. It is also important to note that as the SAMI layer is moved closer to the surface, the shear stresses within the hot mix asphalt surface are increased (**Figure 9**). This condition could lead to near surface distortion and could possibly contribute to groove closure or distortion of the groove pattern. The system with a SAMI layer at 4 inches below the surface induces a favorable combination of low permanent deformation and low surface shear stresses. The system with no SAMI layer gives the least permanent

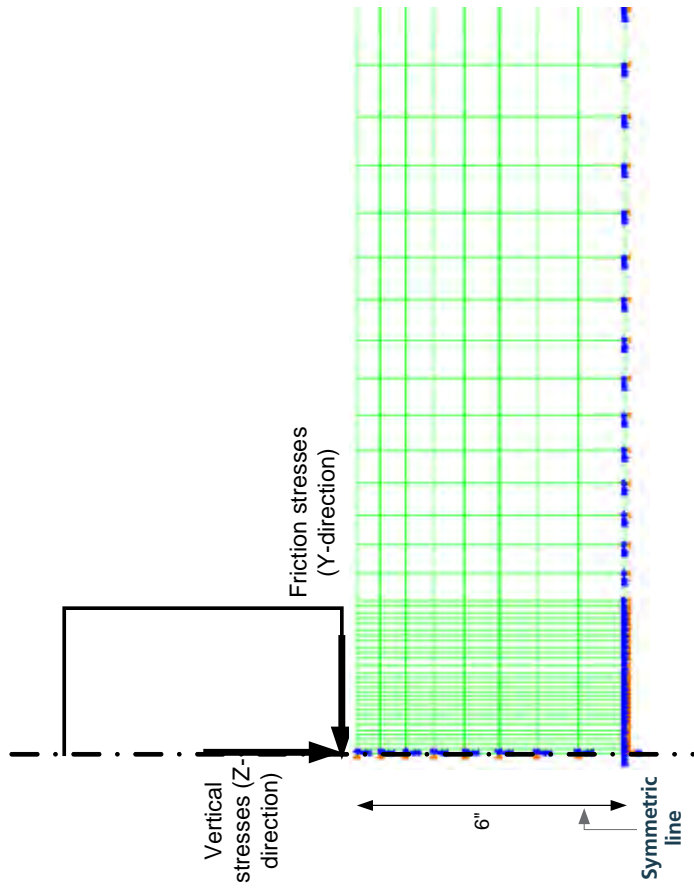


Figure 9. Applied loads in the finite element model

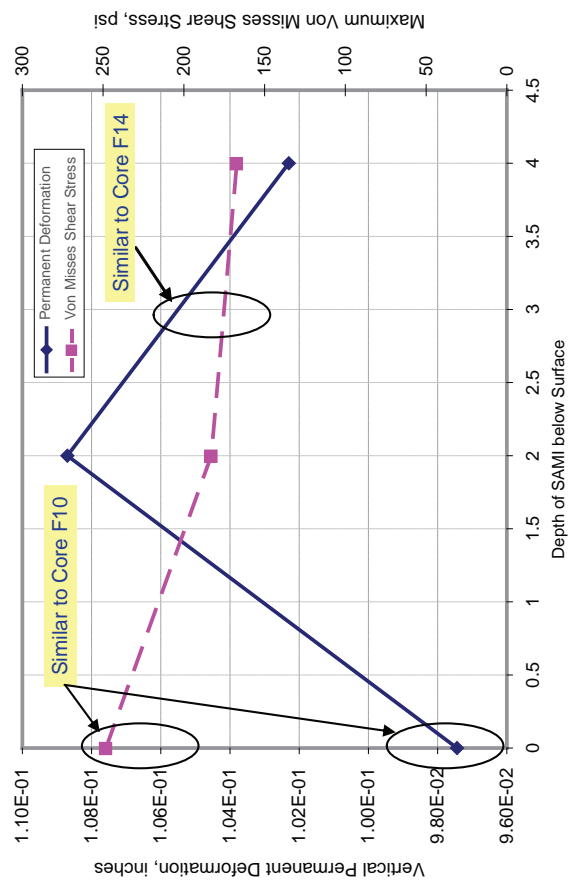


Figure 10. Permanent deformation and shear stresses in asphalt layer due to different SAMI layer depth deformation but the highest surface shear stresses.

Reconciliation

In addition to analyzing the influence of weak layers, the parallel forensic evaluation tested intact LCF cores in the laboratory; these cores yielded elastic moduli of around 4,000,000psi, significantly higher than that resulting from the back calculation analysis. While this high result may be true of an intact specimen, it is estimated that cracking in the LCF layer and poor bonding among the multiple LCF layers yielded

a composite layer with a much smaller modulus, matching that resulting from the back calculation.

A three-phase approach was undertaken to reconcile the differences between laboratory measured compressive strengths, resilient moduli, and field back calculated values. The hypothesis of the analysis was that both the laboratory-measured compressive strength and modulus values and the back calculated values from HWD testing were probably correct and could be reconciled. The

basis for this reconciliation is that while an intact section of the LCF (such as that evaluated in the laboratory) may have a high compressive strength and modulus, the “slab” effect may be considerably lower due to the cumulative effect of shrinkage cracks and smaller, load-associated cracks. These cracks are not likely to be tested in all intact laboratory samples. Further, the intact sections tested in the laboratory may not reflect field performance due to a lack of bonding between compaction planes. This is a distinct possibility because the LCF layer was constructed in approximately seven individual sub-layers. Theory dictates that the combined stiffness of several partially bonded or unbonded stiff sub-layers is substantially less than the stiffness of a monolithic layer of the same thickness and stiffness.

The conclusion from that work is that the residual hot mix asphalt surface can be reasonably modeled in the ISLAB analysis (ISLAB is a finite element analysis software) as a Totski interface with an interlayer constant of $0.75 \times 10^6 \text{psi/in}$, the LCF layer can be modeled as a 28 inch thick layer with an effective modulus of 500,000psi, and the composite sub-base-sub-grade interlayer can be modeled with a composite k-value of between 200 and 300pci, a result comparative to that established through back calculation of HWD data.

Conclusions of forensic evaluation

In addition to finalizing the material properties, the forensic evaluation also revealed that the distress was likely due to high shear stresses resulting from the braking and cornering action of aircraft and the nature of the asphalt layer placed. The asphalt binder used was very stiff. The synergistic effects of a very stiff, polyethylene binder, oxidative aging in the top inch of the pavement, and the high, near-surface shear stresses resulted in shoving and crazing (closely spaced top-down cracking). Initial assumptions that the SAMI layer was a major contributor to the distress were therefore proved unfounded.

The analysis also identified the benefits of maintaining a section of the existing AC in the final overlay design. This layer, approximately 2 or 3 inches after milling, provides at least two favorable functions: (1) it acts as a cushioning effect for the PCC overlay that will reduce corner stresses imposed by loading and temperature-induced curling; and (2) it acts as a bond-breaker between the PCC overlay and the LCF structural layer that allows the PCC overlay and the LCF to function as two separate layers, thereby

reducing the bending stresses within the LCF. The analysis also enabled the development of a model for use during the design of the overlay solution.

Forensic analysis and rehabilitation design

An LEDFAA analysis was performed to prepare paving alternatives using the material properties for specific pavement areas, with results for a PCC overlay ranging from 8.5 to 14.5 inches.

After the LEDFAA analysis was performed, the finite element based ISLAB computer model was used to further evaluate the PCC overlay thicknesses predicted by LEDFAA. A four-step analysis was performed using ISLAB:

1. Determine the critical location and critical stresses imparted by the critical aircraft listed.
2. Assess the fatigue life consumption of the rehabilitated (overlayed) pavement due to the design traffic.
3. Evaluate the impact of overlay thickness on damage of the LCF layer.
4. Compare and evaluate the impact of the actual thickness of the LCF with an effective LCF modulus (from HWD back calculation) versus effective thickness of the LCF layer based on the laboratory measured moduli.

For these studies, the following model was used, based on the findings of the forensic evaluation discussed above:

- Model the residual hot mix asphalt layer as a Totski interlayer with a “spring constant” of approximately $3.0 \times 10^6 \text{psi/in}$, which is consistent with a resilient or dynamic modulus of approximately 750,000psi;
- Model the LCF as a 28 inch thick layer with an effective modulus of 500,000 psi. This is the more critical case as compared to modeling the LCF with a higher modulus ($4 \times 10^6 \text{psi}$) with a reduced or effective thickness of 12 to 14 inches;
- Model the composite sub-base and subgrade with a k-value of 200pci.

This analysis demonstrated an unusual trend because the bending stresses actually decreased when the PCC overlay thickness is less than about 10 inches. However, an overlay thickness below 12 inches induced high bending stresses at the bottom of the LCF layer, which may be a potential for excessive damage in that layer. Curling stresses were conservatively considered in the analysis, and although the analysis demonstrates

the high bending stresses that can occur in the LCF, the acceptable performance of this layer over more than 20 years of service tempers that assessment. Further, traditional transfer functions, such as the one used in the fatigue consumption analysis, are highly sensitive to the stress ratio. Increasing the PCC rupture modulus from 650psi to 750psi increases the performance life to 20 years or more.

The results of this analysis demonstrate that a PCC thickness between approximately 10 and 15 inches has little impact on critical PCC stresses. However, the thickness of the PCC significantly impacts critical stresses in the LCF, particularly when a Totski interface is not considered.

Subsequently, the design thickness was developed with two goals in mind: (1) to limit the stress in the PCC, and (2) to minimize the stress in the LCF layer. Based on the results of this analysis (shown in **Figure 11** and **Figure 12**), it is apparent that the optimum thickness is approximately 14 inches, which would provide adequate support to protect the PCC as well as the bottom LCF layer. A thickness of 10 inches would likely provide the needed support for the PCC layer, but degradation would likely occur in the LCF layer over time.

Benefits of forensic evaluation

During the preliminary engineering phase, the runway underwent an extensive and rigorous investigation, which exceeded the normal limits of project development and included a forensic evaluation of the existing pavement.

Summary

As part of the project’s preliminary engineering phase, Atkins, assisted by Applied Research Associates (ARA) and CMS Engineering Group (CMS), undertook an extensive and rigorous investigation of the existing runway to determine the potential cause of the evident distress and to develop rehabilitation alternatives that would be evaluated in more detail as part of the Preliminary Engineering Report submission.

Given the unusual nature of the existing pavement, the design team determined that a more rigorous design approach was needed; therefore, an extensive forensic investigation was undertaken to determine the existing conditions, identify the cause of failure, and provide analytical

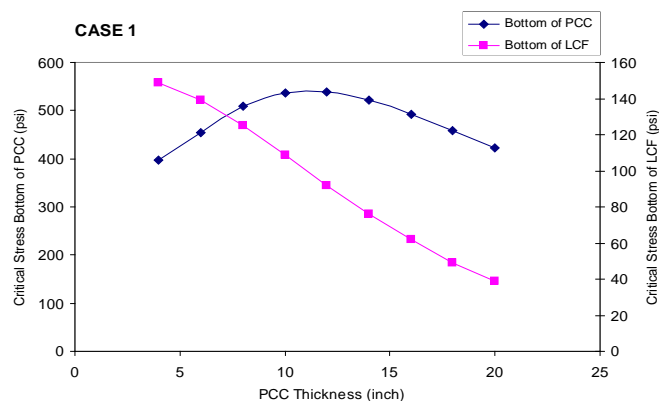


Figure 11. Case 1: Hot mix asphalt as Totski interface (with temperature gradient)

data to allow the team to develop a cost-efficient solution.

This investigation went beyond the normal limits of project development and included a forensic evaluation of the existing pavement. This rigorous approach enabled the team to develop an efficient site-specific solution, balancing initial cost, longevity, and construction schedule to best meet the challenges. The cost of this additional investigation was less than 0.3 percent of the final construction cost, yet the savings achieved as a result were far greater by factors of ten.

The project (**Figure 13**) demonstrated the correct application of engineering principles and innovative approaches and illustrated how up-to-date equipment can benefit a project. The result is a highly successful project – recipient of the Federal Aviation Administration's Program of the Year Award – that will comfortably ensure air operations into the airport's 60th anniversary in 2029.

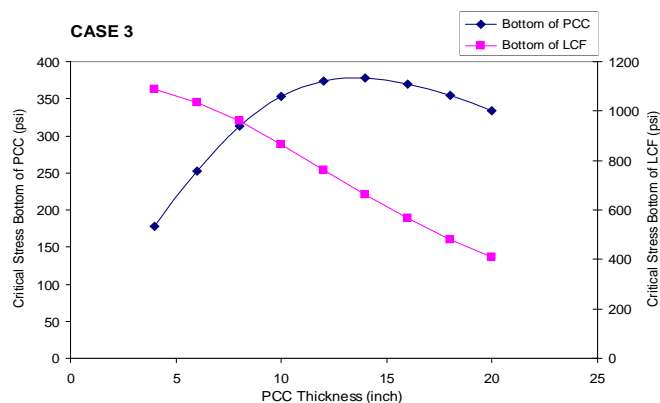


Figure 12. Case 3: Hot mix asphalt and lime-cement-fly ash as composite layer (with no temperature gradient)



Figure 13. Runway 9/27 at George Bush Intercontinental Airport, Houston, Texas

References

1. <http://www.fly2houston.com/about-has-history>. Accessed August 3, 2011.
2. <http://airportnews.aero/airline/19461/59/George-Bush-Airport-receives-state-of-the-art-upgrades>. Accessed July 28, 2011.
3. <http://www.houston-iah.airports-guides.com/>. Accessed July 28, 2011.
4. <http://www.airporttech.tc.faa.gov/Pavement/26ledfaa.asp>. Accessed July 28, 2011.

**Chris R Hendy**Head of Bridge Design
and TechnologyHighways
and Transportation

Atkins

**Sibdas
Chakrabarti OBE**Independent
consultant

Fatigue management of the Midland Links steel box girder decks

Abstract

The Midland Links Motorway Viaducts, carrying M5 and M6 around Birmingham, have been subject to a regular programme of assessment, repair and strengthening since 1989 after corrosion problems, primarily due to chloride contamination, were first detected in 1979. A number of the longer spans comprise multiple steel and concrete composite box girders and some of these superstructures are supported by steel box girder cross beams. Assessment showed areas of very high overstress in the web plate at the locations of internal bracings. These overstresses affected ultimate, serviceability and fatigue limit states and arose because of poor detailing of the cross braces and stiffeners.

The greatest concern was the fatigue stresses produced in the web at the end of the transverse stiffeners at the internal bracing locations. This was caused by the distortional stiffness of the bracing coupled with the termination of the transverse stiffener in the web. Acoustic emission sensors were installed to determine if the predicted fatigue activity was actually occurring and elastic shell finite element modelling was undertaken for an improved determination of stresses. Plastic redistribution was considered to demonstrate adequate ultimate limit state (ULS) performance and an analysis was undertaken with potential fatigue damage modelled to prove the structure would not collapse with such damage at the ultimate limit state. In-situ strain monitoring was undertaken both under known test vehicle loading and under normal traffic conditions to derive more accurate fatigue stress spectra. These results were used not only to calibrate the finite element results but also to improve the predicted fatigue life and allow preparation of a long-term strategy for managing and monitoring fatigue activity using a damage tolerant approach.

Background

The Midland Links Motorway Viaducts have been subject to a regular programme of assessment, repair and strengthening since 1989 after corrosion problems, primarily due to chloride contamination, were first detected in 1979. This has mainly involved repair to reinforced concrete cross beams and the concrete decks of steel-concrete composite spans. However, a number of the longer spans comprise multiple steel and concrete composite box girders supported on full-width rocker bearings. The assessment and management of these steel box girder superstructures were more complex and form the subject of this paper.

Typical steel-concrete composite box girder spans are shown in **Figure 1** with a general arrangement of the cross section and internal diagonal bracing shown in

Figure 2. All steel is mild steel; the web and top flange are in accordance with BS 15¹ and the bottom tension flange is in accordance with BS 2762² (Type Notch Ductile IIB). The box decks were initially analysed using grillage models. The end diaphragms were found to be overstressed under the torque produced at the rocker bearings but after the torsion constant for individual load cases was softened in the analysis, to allow for the distortional flexibility of both the box cross section and the internal bracing, this overstress was eliminated. A method for softening the torsion constant in this way is given in reference 3. The assessment, however, predicted areas of very high overstress in the web plate at the locations of internal diagonal bracings.



Figure 1. Typical steel-concrete composite box girder spans

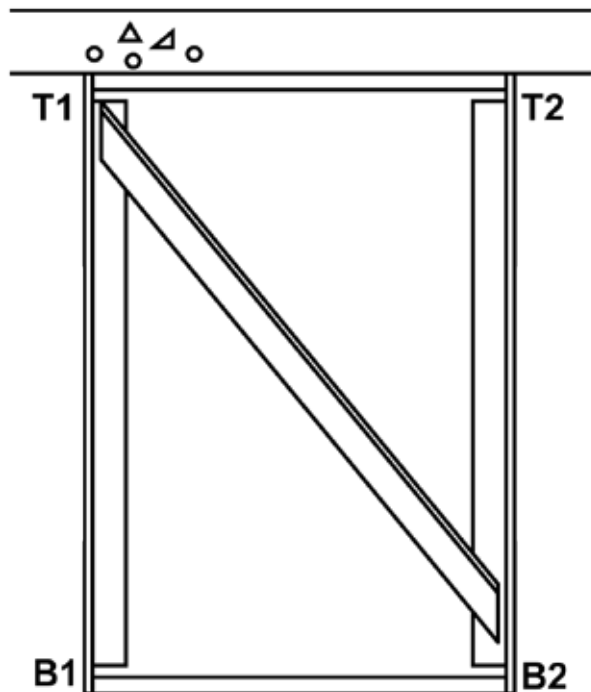


Figure 2. Typical steel-concrete composite box girder cross section

This remaining overstress at bracings affected ultimate, serviceability and fatigue limit states and arose because of poor detailing of the bracing and stiffeners. The stiffeners terminate short of the flanges and thus distortional forces acting on the box cause a high local

bending moment in the web between stiffener and flange (**Figure 3**). The problem is exacerbated by the presence of a fillet weld connection between web and flange giving rise to a Class W fatigue detail in the weld and Class F detail in the web in accordance with BS 5400 Part 10⁴.

Since neither adequate strength nor service life could be demonstrated by using conventional assessment, despite the fact that the viaducts showed no signs of distress, further investigation and assessment was required to ensure safe operation.

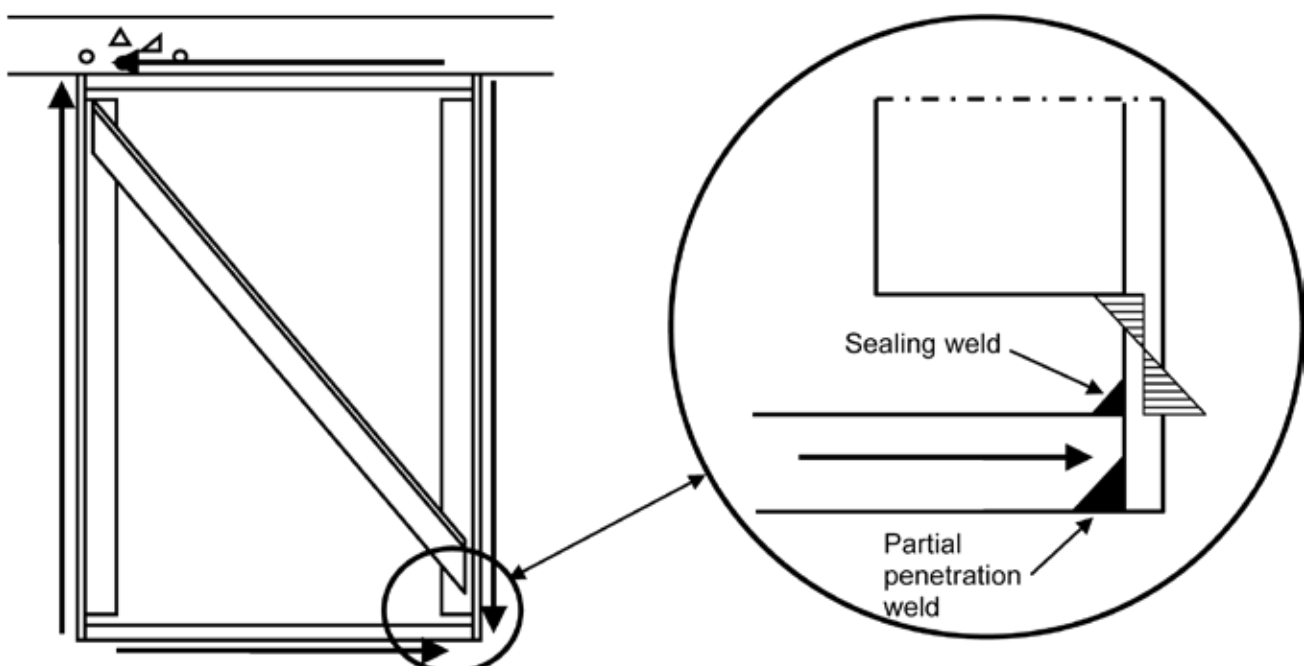


Figure 3. Bending moment induced in web at bracings due to distortional forces

Acoustic emission monitoring of the viaducts

The critical detail for fatigue just above the sealing weld (**Figure 3**) was located inside the box girders. Since there was no access provision to the box girders it was necessary to find a way of inspecting and monitoring the boxes from the outside. A programme of acoustic emission monitoring (AEM) and ultrasonic inspection was therefore undertaken. AEM trials were carried out in 1999, when potential problem areas were first identified, at two locations – Bescot Viaduct and Bromford West Viaduct. There were indications that fatigue activity might be occurring at the bracing locations. The AEM trial carried out at Bescot Viaduct was repeated in 2006 which indicated similar activity. However, ultrasonic investigations found no signs of cracks and subsequent visual inspection (by entering the box through newly formed access hatches) found lengths of missing sealing weld dating back to the original construction but no cracks. This cast doubt on the suitability of AEM to locate fatigue defects in a large steel viaduct such as the Midland Links. It clearly detected increased activity at the fatigue-prone details; the emission hot spots coincided with the areas of predicted overstress in the structural analysis. However the AEM was a poor predictor of actual fatigue damage when compared with visual inspection and ultrasonic inspection.

Verification of ultimate limit state strength

As-built analysis

It was clear that the use of grillage analysis was too crude to investigate this particular problem properly; the bracing had been included in the grillages, but only as shear flexible members. The critical boxes were therefore remodelled using shell finite elements. Complete spans (comprising ten or more box girders and concrete deck slab) were modelled. Beam elements were typically used for the stiffeners and bracing members but the most heavily loaded bracing locations in each box were modelled using shell elements for the stiffeners and bracings and a finer mesh was used in the web in the area of peak stresses at the ends of the stiffeners. An extract of one fish-bellied girder from a typical model is shown in **Figure 4**, together with a view of the detailed mesh at one of the bracing frames being investigated.

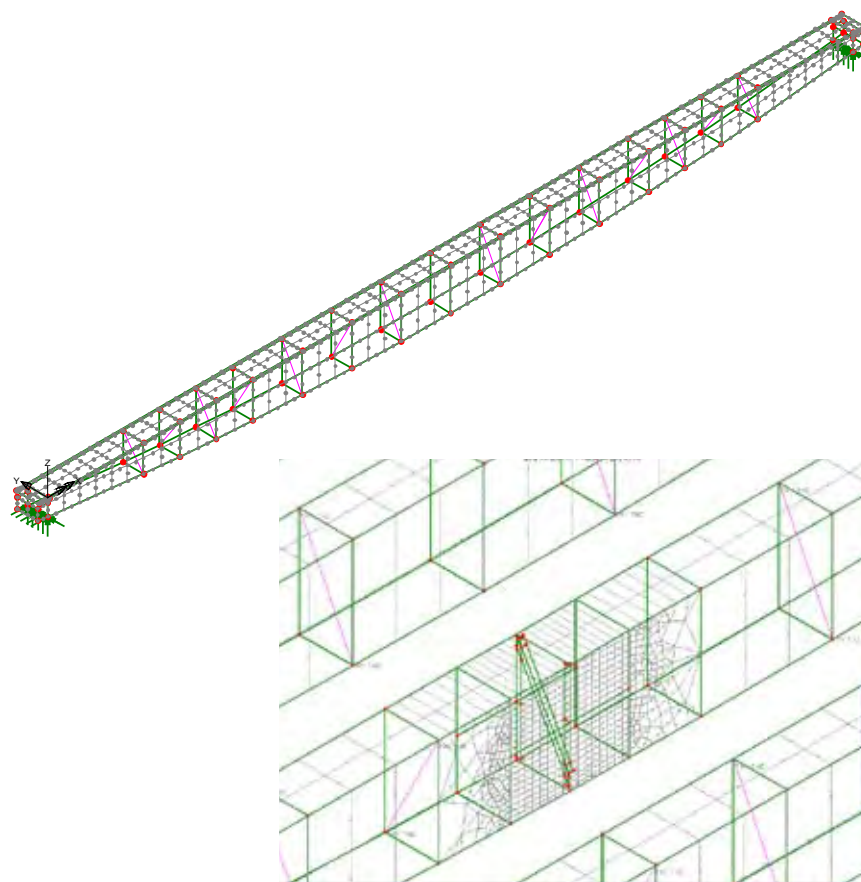


Figure 4. Layout of typical bracing bay finite element model showing detail at chosen

Ultimate limit state

Stresses at the ultimate limit state were shown by linear elastic finite element analysis to be well in excess of the yield stress of 247 MPa (up to 450 MPa) in the webs as a result of the distortional stresses attracted to the web by the diagonal bracing – see **Figure 5**. The extent of the material with stresses exceeding yield along the box was very small; only around 100mm. With plasticity in the bracings or at the web-stiffener connection, these high stresses could potentially be shed safely or redistributed to a larger zone; it was therefore suspected that ultimate limit state (ULS) would not be a governing limit state. In order to verify ULS performance, two separate checks were performed. First, the yielded material was removed and cross-section checks repeated. Second, an analysis was performed removing the cross bracings altogether and linear elastic analysis repeated. This approach was preferred to a full non-linear analysis because of the time involved in conducting such an analysis on such a large model.

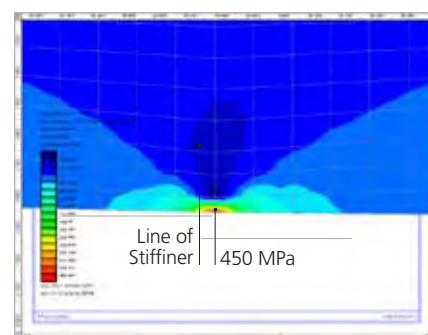


Figure 5. Typical vertical stresses in web at stiffener location

Removal of yielded material

It was calculated that the distortional moment in the part of the web plate where yield was exceeded could be carried by a length of web plate equal to just over 200mm acting at yield. This was estimated simply by calculating the moment carried by the yielded portion and redistributing the moment over the length required to attain equilibrium with the material stress limited to yield. This calculation ignored the reduction in distortional moment that would arise due to the reduction in stiffness caused by the yielding material. To verify that the cross-section as a whole was adequate for global effects, a reduced effective cross section was used in global stress checks, ignoring the yielded portion of web entirely in the cross section properties. The effects of secondary bending around these idealised holes in the cross section were also considered. This showed that the cross section overall remained adequate.

Cross bracings removed

If excessive yielding were to occur in the web between stiffener and flange, the cross bracing could be rendered ineffective because of the loss of stiffness. To investigate this, the analysis was repeated removing the cross bracings completely to check whether the box girders would still have adequate strength to resist the applied loading.

Removal of the cross bracings led to an increase in distortional flexibility which significantly reduced the distortional stresses in the web adjacent to flange and stiffener; the distortional stresses reduced from 450MPa to just over 100MPa at ULS. The reduced torsional stiffness however, also increased the box girder midspan, sagging moments by up to 5% because of the reduced transfer of loads between the boxes. It was therefore necessary to verify that the boxes remained adequate with this moderate increase in moment. The strength of the concrete slab was also checked as the reduced torsional stiffness of the boxes increased the transverse bending moments on the concrete deck. There proved to be adequate reserve of strength in both elements.

The conclusion from these two analyses was that the boxes had adequate ultimate limit state strength.

Serviceability limit state

The stresses in the web plate at serviceability limit state (SLS) also exceeded yield on Bescot and Oldbury. As

serviceability “failures” do not threaten the integrity of the boxes and as there was no sign of actual distress in the corners of the box (for example disruption of the paint), the SLS predicted failures were not considered to be of concern on their own. It was also considered likely that in-situ stresses would actually be much lower than predicted in the analysis because of additional joint flexibility in the bracings that was not modelled and because of composite action with the deck surfacing. The apparent overstress was eliminated when the scale factor from in-situ strain measurement, determined from the load testing described in a following section, was applied to the calculated SLS stresses.

These findings led to the conclusion that the serviceability performance of the boxes was adequate.

Fatigue limit state - damaged condition and damage tolerance

Fatigue was, however, of greater concern. Stress ranges determined from the initial grillage analyses were found to be extremely high and the stress ranges determined from the subsequent

shell finite element models were only moderately reduced from these values.

Figure 6 shows the influence line surface plot for the maximum force in one typical diagonal bracing member; the force is proportional to the distortional stress in the web. The plot shows that large influence surface ordinates only occur in areas in close proximity to the cross frame in question. The influence of other vehicles remote from the bracing being considered is small.

The estimated fatigue lives for the deck with and without the diagonal bracing are shown in **Table 1** at the locations shown in **Figure 2**. The case without bracing was investigated by way of a potential “strengthening” scheme as the work described in a previous section showed that the boxes had adequate ULS strength without them. These results were produced using the fatigue method of clause 8.3 of BS 5400 Part 10⁴. The lowest fatigue life predicted was just less than 1 year in the web at the toe of the web-flange sealing weld. The fatigue spectrum approach of clause 8.4 of BS 5400 Part 10⁴ was then used as a refinement; the vehicles were applied in turn and the damage summed using Miner’s rule. The predicted fatigue life based on stresses from the finite element model

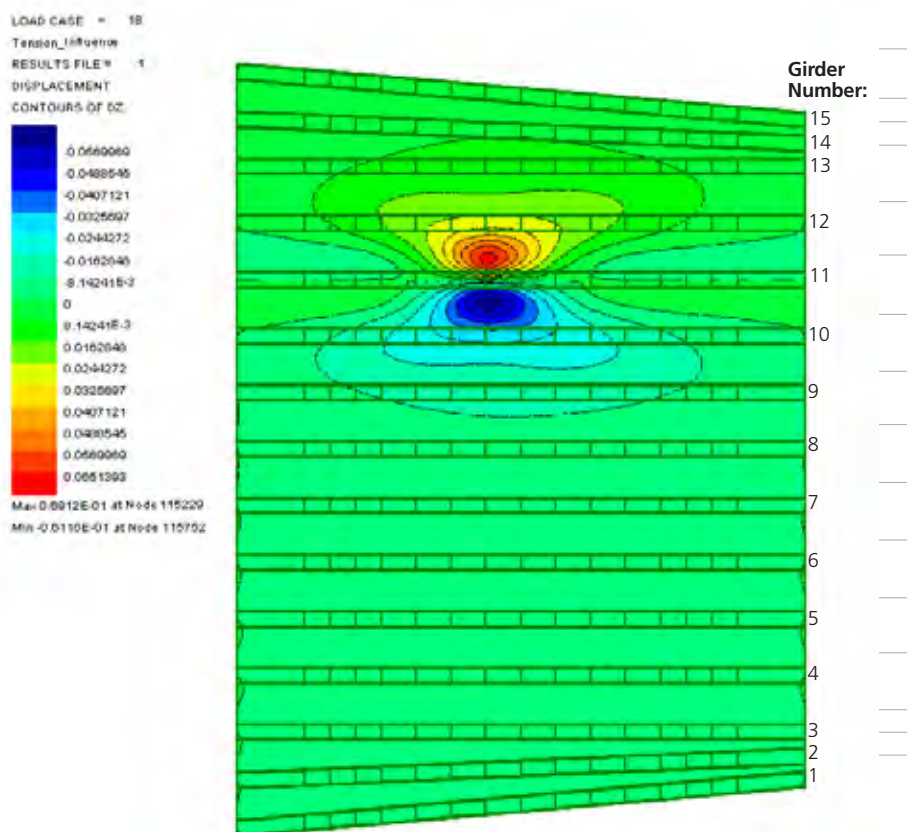


Figure 6. Influence surface for maximum axial force in typical diagonal bracing on girder 11 of a Bescot Viaduct deck

and the Part 10 spectrum was 5 years. It was considered that the spectrum was representative of the Midland Links motorways with little, if any, in-built conservatism. A proposal was, however, made to collect actual traffic spectrum data during subsequent load testing, this is described in a following section of this paper.

Damage tolerance

Although it was possible to demonstrate adequacy of the boxes at the ultimate limit state if plastic redistribution was allowed for, the boxes could not be shown to have adequate fatigue life and therefore the plastic redistribution assumed might not be able to occur if a fatigue crack was to first result in fracture. As a result, the consequences of a propagating fatigue crack were considered.

A full height crack was introduced in one web of a box. This was done to investigate if the bridge could remain standing, albeit with plastic damage, should one fatigue crack form at a bracing location and propagate in the web until finally tearing through the full height of the web by brittle fracture. The crack was represented as a gap in the mesh over the full height of the web. A vertical crack was placed in the model at the support to investigate the worst shear case. In a separate model, a crack was added at midspan to investigate the worst bending case. 45HB and HA loading was considered and the live load effects were combined with the dead and superimposed dead load effects and the sections checked to BS5400 Part 3⁵.

The situation was analysed elastically, rather than non-linearly, which is conservative because no allowance was made for plastic redistribution between boxes after the fatigue crack had formed. Web buckling and yielding checks were carried out for the worst bending and shear cases. In checking strength, all load and material factors were removed which is consistent with the accidental combination used in BS EN 1990⁶ for extreme events. It was found that the bridge could just sustain the full loading in this condition by virtue of the loss of elastic stiffness of the damaged box and the shedding of load to adjacent boxes. The webs all passed the web buckling checks and their stresses did not exceed the yield stress (247MPa). The maximum bending case caused partial plastification of the bottom tension flange adjacent to the ineffective cracked web, but the yielded zone was relatively small and equilibrium was still maintained.

		With bracing		With bracing removed	
Location and BS 5400 Part 10 fatigue detail classification		Estimated fatigue life (years)	Estimated fatigue life (years)	Estimated fatigue life (years)	Estimated fatigue life (years)
		T1	T2	T1	T2
Cracking in welds	Sealing weld (Class W)	6.4	>1000	>1000	>1000
	Part-pen weld (Class W)	136	>1000	>1000	>1000
Cracking in web plate	Web-flange weld location (Class F)	0.8	>1000	>1000	>1000
	Web stiffener location (Class F2)	112	>1000	600	600
Location		B1	B2	B1	B2
Cracking in welds	Sealing weld (Class W)	>1000	144	>1000	>1000
	Part-pen weld (Class W)	>1000	>1000	>1000	>1000
Cracking in web plate	Web-flange weld location (Class F)	>1000	1.0	>1000	>1000
	Web stiffener location (Class F2)	>1000	134	700	700

Table 1. Fatigue life predictions with and without bracing

The conclusion of this work was that propagation of an undetected crack would not lead to sudden collapse of the superstructure and therefore there would be time to intervene in such an event. It was therefore decided that the Midland Links boxes could continue in operation without traffic restrictions provided an ongoing programme of inspection of the key welds at bracings was made, which in turn would require a programme of access provision for internal inspection. This is essentially a "damage tolerant" approach to fatigue design as permitted by BS EN 1993 1-9⁷ which permits reduced factors of safety for fatigue design provided two main conditions are fulfilled:

- The boxes must be inspectable with an inspection regime in place;
- There must be redundancy in the event of fatigue crack propagation.

The first criterion was partially satisfied in that external inspection of the web was possible, as was ultrasonic testing. Provision of future access to the box voids would enhance inspectability. The second

criterion was shown to be satisfied above; a full depth web crack could be sustained without collapse of the box girders. This "damage tolerant" approach is different from the usual design "safe life" approach where the design aims to ensure adequate fatigue life without the need for inspection.

In order to assist inspection, fracture mechanics techniques were also considered to determine a critical crack length which would propagate by fast fracture. Knowledge of such a critical crack length would clearly inform the inspection regime and facilitate determination of when a crack should be repaired. However, no records of fracture toughness were available and the range of fracture toughness expected for BS15 steel was very wide. A pessimistic estimate of toughness led to predictions of very short critical crack lengths which would not easily be detected. Consequently, this study was abandoned in the secure knowledge that there was redundancy available in the event of a propagating crack forming.

Revised fatigue assessment using in situ strain measurement

Although the damage tolerant approach to fatigue proved that the structure was suitable for monitoring, it did not provide information on the time available to plan a maintenance strategy, nor predict when significant cracking might start to appear in the boxes. In fact, the codified analysis indicated that cracking should have initiated some time ago when inspection had shown no signs of cracking. There were a number of possible reasons identified to explain the difference including:

- (i) The real spectrum of traffic being less onerous for fatigue than that in the design code;
- (ii) The in-situ stresses being lower than predicted in the analysis due to incidental composite action with deck furniture and surfacing or due to additional joint flexibility;
- (iii) Better in-situ material properties for toughness than assumed in the assessment;
- (iv) The possibility that the as-built details on the drawings differed from those actually present.

The fatigue assessment was therefore repeated based on in-situ strain measurement for both a single known controlled load and also from measured in-situ strains during operation. The results are discussed below.

Load test

Following the fatigue assessment and recommendations above, a load test was carried out on Bescot and Oldbury Viaducts with strain measurement on the box diagonal bracing and web-flange junctions. Access holes were installed in the boxes to facilitate attachment of the equipment.

The testing employed a six-axle 40 tonne articulated lorry with a 40foot flat barrier trailer loaded with 11 concrete temporary vehicle restraint barriers. This lorry type represents the second most common commercial vehicle configuration, accounting for 27-33% of all HGV types on the M6 (2.3 million vehicles per year) and M5 (1.6 million vehicles per year) respectively. As the response of the structure was likely to involve both composite action with the surfacing and some tension-stiffening in the concrete deck slab and the effect of both of these are load dependent, it was



Figure 7. Load testing M5, North Bound (Oldbury Viaduct)

important to ensure that this test vehicle was representative both of common vehicle configurations and also the weight of the heavier ones. Use of a light vehicle could overestimate the benefit of these effects for real heavy vehicle loading and hence underestimate steel strains for heavier vehicles.

The testing involved driving the test vehicle in designated paths (load cases) over each span while recording the induced strains in the relevant diagonal bracing bays – see **Figure 7**. The load cases were designed to replicate both normal traffic loadings and the theoretical worst cases. As the stress at the box diagonal bracing locations were very sensitive to vehicle position, it was essential to ensure that the strain measurements were accurately matched to vehicle position. Consequently the vehicle position was accurately recorded during each load test by using a total station which automatically tracked a prism attached to the rear of the trailer. The time on the total station was synchronised with the strain-monitoring computer to enable correlation with the strain results. The vehicle was driven slowly to eliminate any dynamic impact effects.

The strain monitoring equipment to be used was given careful thought. Measurement of the highly localised strains in the web with a high strain gradient over its height required gauges of very short length to avoid excessive averaging out of the stresses, thus underestimating the peak values. Uniaxial electrical resistance strain gauges were chosen as being most appropriate for this purpose. Numerous gauges were provided in order to determine the stress gradient. The strain was measured three ways in order to give some degree of cross-checking:

- (i) By installation of a grid of strain gauges directly on the web in the area of interest between bottom of stiffener and top of bottom flange. A typical layout is shown in **Figure 8**. This allowed direct comparison with the predictions for the strain in the web in the shell finite element model.
- (ii) By installation of strain gauges on the diagonal braces. A typical layout is shown in **Figure 8**. This allowed comparison with the predictions for the strain in the cross bracing in the shell finite element model. The stress in the web is proportional to the axial force in these diagonal bracings. A large number of gauges were placed on the bracings to allow determination of flexural effects and average axial stress.
- (iii) By use of laser shearing interferometry to measure strains directly in the web in the area of interest between bottom of stiffener and top of bottom flange. This was intended to overcome the averaging limitation of conventional strain gauges. Laser shearing interferometry (LSI) uses a green 532nm laser beam which is expanded and collimated before illuminating the target surface (the web stiffener interface). Saving an image of the unstressed target and then subtracting all subsequent images obtained during loading of the structure produces a strain field, which is visible as fringes in the subtracted video and allows the strain changes under loading to be calculated. The image has a resolution of 1024 x 768 which is equivalent of approximately 786,000 strain gauges over a circular area of 150mm diameter.

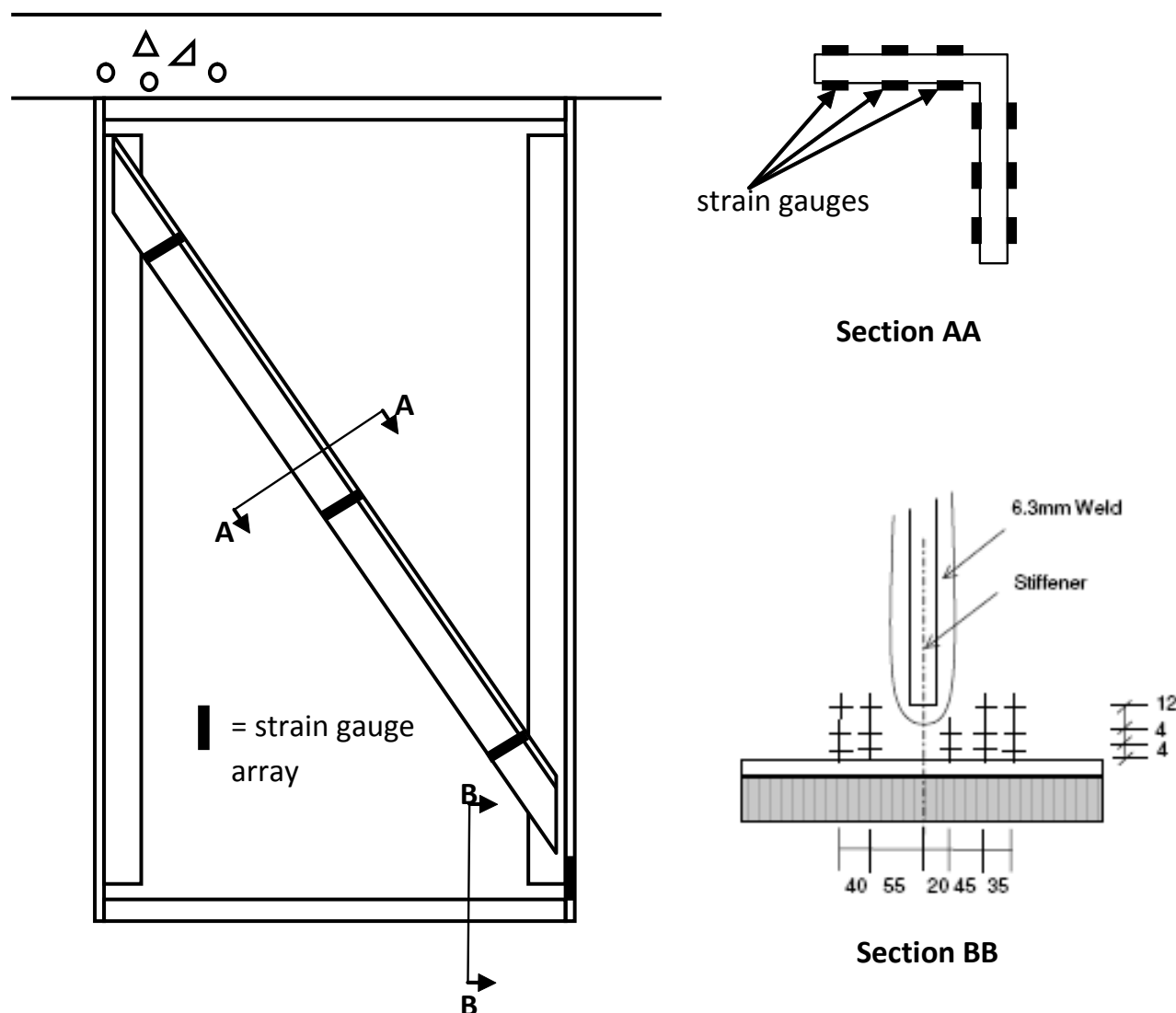


Figure 8. Location of strain gauges on bracing and web

Typical strain readings at the base of the web are shown in **Figure 9**. The in-situ strain measurements for the known vehicle were used to calibrate the finite element model. A series of load cases modelling both transverse and longitudinal test vehicle position were analysed and the results from the finite element model compared to the in situ strain measurements. A scale factor for fatigue stress range derived from the finite element model was obtained and the fatigue life revised. Depending on vehicle position and bracing location, and whether the strain in the web or the cross bracing was used to derive the stress in and adjacent to the weld, the ratio of in-situ strain measurement to strain predicted by the finite element model was between 40% and 60%. This ratio was then used to scale down the effects of the fatigue vehicle as determined in the finite element model. Two approaches

were then taken to calculating the revised fatigue life based on the methods of clause 8.3 (fatigue vehicle method) and clause 8.4 (design spectrum) of BS5400 Part 10⁴.

Clause 8.3 (fatigue vehicle method)

For this check, the scale factor of 0.4 between site and finite element results was deemed appropriate because, although this ratio varied from 0.4 to 0.6 depending on vehicle position, the load cases causing peak stresses in the web and weld occurred when this ratio was closest to 0.4. Based on the simple method of assessment and this scale factor, the 1 year fatigue life, as discussed previously, was extended to 40 years.

Clause 8.4 (design spectrum method)

For this check, the scale factor of 0.6 between site and finite element results

was deemed appropriate because the model could not be calibrated realistically against the whole range of traffic expected (since vehicle axle configurations, lengths, widths vary significantly from the test vehicle) and since the scale factor was sensitive to vehicle position as well, a more conservative ratio of 0.6 was considered appropriate. Based on the simple method of assessment and this scale factor, the 5 year fatigue life discussed previously was again extended to 40 years.

In situ strain continuous monitoring

In addition to the load test above, continuous monitoring of strain was also carried out on a number of girders over a period of three weeks. The intention was to use the strain readings to derive a

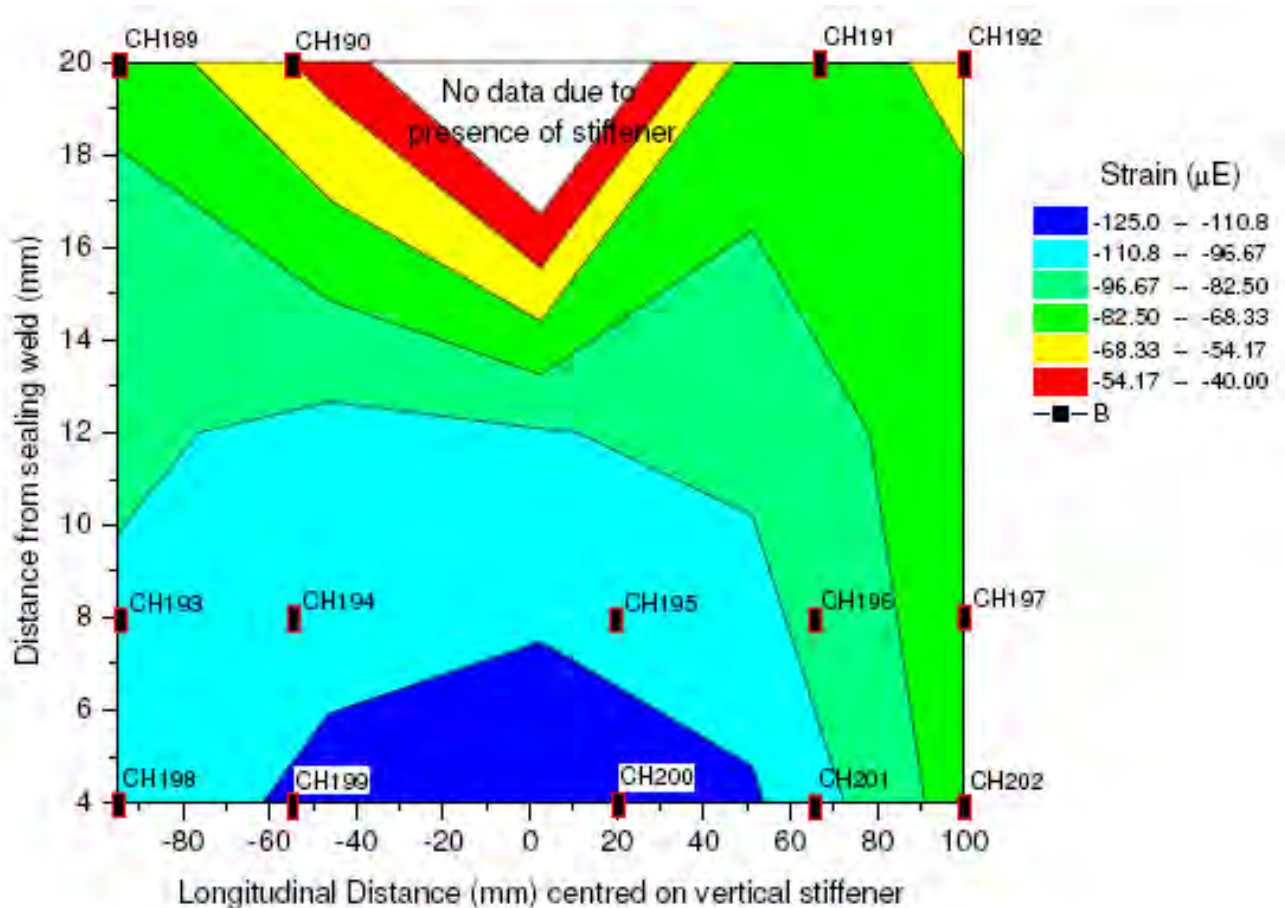


Figure 9. Typical strain gauge readings

stress spectrum under traffic directly and hence a prediction of fatigue life based on actual traffic conditions. Three weeks was considered to be a satisfactory period to allow average annual conditions to be determined. The period was chosen to avoid public holidays.

An upper bound life was first derived from this traffic data by considering only the damage from the largest stress range in three days and assuming this occurred every three days. This led to an upper bound design life of 83 years based on design material properties. Attempts to include smaller vehicles indicated that any benefit over the methods discussed previously would be very small. Since this upper bound value was still less than 120 years, this method was not pursued further. The full data from three weeks of monitoring could have been used to produce a better estimate of fatigue life. However, the amount of data was enormous and difficult to process and a pragmatic interpretation would have been needed to produce a simplified spectrum from it, rather than trying to consider the fatigue damage from every measured cycle using rainflow counts.

Realistic fatigue life and asset management proposals

Realistic fatigue life prediction

The revised fatigue assessment based on the use of in situ strain measurements to modify the results of the previous shell finite element model led to a reduction in stress and therefore an increase in predicted fatigue life, measured from the opening of the viaducts, to 40 years. However, it was considered that this codified prediction of fatigue life was still very much on the conservative side for a number of reasons:

- The calculation assumed that the current codified spectrum of vehicles has been in operation since the opening of the bridge. It is difficult to quantify this effect due to the lack of suitable historic data. Draft BD77⁸ contained a means of approximating this effect via a formula for equivalent fatigue age of the bridge, Y_e , from the actual age, Y_a , and the age at which the traffic reached saturation point, Y_s , taken as the bridge's age in the year 2000:

$$Y_e = 40(1 - e^{-Y_s/40}) + (Y_a - Y_s)$$

- For the Midland links boxes, $Y_a = 38$ years, $Y_s = 30$ years so the equivalent fatigue age of the bridge, $Y_e = 29$ years. This is 9 years younger than the bridge's actual age which would therefore add 9 years to the predicted fatigue life measured from the opening of the viaducts. This implies the fatigue life is 49 years.
- The choice of scale factor used previously was the most pessimistic for the data collected. If the mid-range value was taken, i.e. 0.5, the calculated fatigue life would have increased to 80 years.
- The worst 2.3% fractile material properties (two standard deviations from the mean) were also used i.e. there is a 2.3% probability of failure in the reported fatigue design life. If mean properties are considered, the life rises to 91 years without any of the above other considerations included in addition, but there is a 50% chance of a fatigue failure in that time which is an unacceptable probability. However, if access is to be provided for inspection, an increased probability of fatigue cracking

could be considered. If properties corresponding to one standard deviation from the mean were used, this would give a 15.9% probability of failure in 60 years. This increased probability of failure when inspection is possible and planned is consistent with the Eurocode's damage tolerant approach.

In view of these further considerations, it was considered that a realistic fatigue life from the day of opening could be taken as 50 years. It was emphasised in the report to the Highways Agency that this still did not mean that cracks would form after this. It only implied that the likelihood of this event occurring will increase beyond this time.

These results of the various analyses and the absence of any detected cracks suggested that the Midland Links boxes could be allowed to continue to operate without traffic restrictions provided that:

- An ongoing programme of inspection of the key welds at cross frames was maintained;
- Any weld cracking discovered was repaired;
- A programme of providing access for internal inspection was instigated for future maintenance operations unless other monitoring capable of detecting cracks inside the box is installed.

Intervention required if cracks occur

It was also necessary to have a strategy in place in the event of cracks being found by the inspection regime. Cracks in welds could be repaired by grinding out the damaged areas and re-welding. Short lengths of cracks in the web plate could be arrested by drilling through the crack tips. Larger defects could potentially, however, lead to the need for strengthening (together with crack repairs or arresting measures), for which there were several alternatives including:

- Connecting the stiffeners to the bottom flange which eliminates the high web distortional stresses.
- Installing external ring frames around the box bracing locations to carry the distortional forces. This would minimise the amount of working inside the boxes.
- Removing the diagonal braces to reduce the distortional forces attracted.

The impact of future Active Traffic Management (ATM)

The introduction of Active Traffic Management (ATM) on the hard shoulders of the motorway was initially viewed with concern given the low predicted fatigue life of the boxes and the lack of proven service performance of the boxes below the hard shoulder; the boxes beneath lane 1 had at least proven themselves in service. However, the extended life predictions from the load testing reduced this concern and it was consequently not considered that the introduction of ATM would have an adverse effect on fatigue life. In fact, the introduction was considered to dilute the traffic density for a time and shift some of the highest stress range fatigue cycles on to the previously unloaded boxes with consequently greater residual fatigue life. It was therefore considered that the effects of ATM would be beneficial, but further consideration would need to be given to quantify the benefits.

Conclusions and key lessons learnt

For the first time in 25 years, the Midland Links Viaduct steel boxes have been assessed to have adequate capacity to carry abnormal traffic loads without restriction. This has been possible as a result of the cooperation and combined efforts of all parties including Client (Highways Agency), Assessing Engineer (Atkins), Checking Engineer (Faber Maunsell) and Maintaining Agent (Amey Mouchel). However, like other structures, routine inspections and monitoring will continue to ensure continued safe operation of the viaducts.

A number of lessons were learnt in the course of the Midland Links box girder project, many of which were utilised in the assessment of the viaducts. These are summarised below:

Stress analysis

- High peak stresses in the vicinity of details with local stress concentrations may pose no threat at the ultimate limit state where there is scope for plastic redistribution to the surrounding area;
- The actual stresses in the structures can be significantly less than those determined from global analysis for a number of reasons as discussed in the main text (e.g. conservative design loadings, incidental composite action with deck furniture and presence of additional material not shown on

as-builts). In-situ strain monitoring can confirm this, without necessarily identifying the specific reasons for the difference.

In-situ testing and strain monitoring

- In-situ testing can be beneficial for determining yield strength for use in SLS and ULS verifications, but is less readily applicable to the fatigue limit state because fracture toughness is a more variable property than yield strengths;
- In-situ strain monitoring is a good tool for determining SLS and fatigue stresses while the structure remains in an elastic condition. It would not, however, be a suitable means of predicting ULS performance because many of the aspects of behaviour leading to reduced stresses (such as concrete tension stiffening and composite action with surfacing) could be lost at ULS. Load testing vehicles should be of a comparable weight to actual heavy vehicles using the road so as not to overestimate these beneficial effects;
- Strain monitoring equipment needs to be appropriate to the situation being investigated. LSI can be considered in conjunction with electrical resistance strain gauges where there is very localised high strain in order to give greater certainty in the accuracy of results;
- Care is needed when choosing strain monitoring equipment and fixing monitoring locations because of the averaging effect of strain gauges over their own length. It is appropriate to have several strategies for obtaining the same information so cross-checking can be employed.

Acoustic monitoring

- Acoustic emission monitoring is an effective tool for identifying potentially fatigue prone areas. It may not however be a reliable predictor of actual damage. It was not therefore particularly suited to monitoring the boxes for indication of when to intervene.

Fatigue assessment

- Inspection of key details is very important where fatigue damage is predicted by calculation. Where inspection of the key details is not possible, assessment should be based on safe life principles;
- A more relaxed approach to managing fatigue can be applied where damage tolerant conditions

apply, that is where the structure has a monitoring regime in place, is inspectable for cracks and has structural redundancy in the event that a propagating crack is undetected;

- Residual fatigue life predictions, particularly for older structures, can be quite pessimistic because of the lower traffic volumes experienced earlier in their lives as compared to the current design traffic spectra. Since fatigue damage is a cumulative occurrence the effects on the early stages were usually minimal. Consideration of this reduced damage during the early years can

provide additional fatigue life. (It is ideal if the client authority keeps records of the traffic volumes and weights experienced by the structure throughout its life);

- S-N curves in design codes are typically based on a lower bound estimate of test results assuming a 2.3% probability of failure i.e. two standard deviations from the mean values. Consideration could be given to using less conservative values, such as one standard deviation below the mean, in consultation with the client, particularly for structures where damage tolerant conditions apply.

Consideration of the above led to the fatigue life of the viaducts being increased from 1 year after the initial finite element assessment to 50 years. This was sufficient to allow the motorway to be kept open without traffic restrictions while a maintenance strategy was put in place. The current management strategy uses the damage tolerant approach in conjunction with the creation of inspection openings in the critical longitudinal box girders to permit early identification of fatigue problems.

Acknowledgements

The authors wish to acknowledge the contributions of Wasfe Ali and Richard Harris from the Highways Agency's Network Services for their technical advice, support and coordination of the project, George Lawlor of AECOM for his support and helpful suggestions throughout his independent check and Peter Gilbert, Amey (AmeyMouchel) Structures Asset Manager for planning and executing the in-situ testing and monitoring and allowing results to be reproduced here. **Figures 1, 7 and 9** are reproduced courtesy of Amey.

References

1. BS 15 (1961) Mild steel for general construction purposes, British Standards Institution, London
2. BS 2762 (1956) Notch ductile steel for general structural purposes, British Standards Institution, London
3. BS 5400 Part 10 (1980): Steel, concrete and composite bridges – Part 10. Code of practice for fatigue. British Standards Institution, London
4. BS 5400 : Part 3 (2000): Design of steel bridges. British Standards Institution, London
5. BS EN 1990 (2002): Eurocode - Basis of structural design. British Standards Institution, London
6. BS EN 1993-1-9 (2005): Design of Steel Structures. Part 1.9: Fatigue. British Standards Institution, London
7. Design Guide for Composite Box Girder Bridges (1994), SCI Publication P140, Ascot, UK
8. Draft BD77/98 Assessment, inspection and monitoring of existing steel bridges for fatigue life, Highways Agency, UK



Ian Glazebrook

Senior
Principal Consultant

Defence, Aerospace
and Communications

Atkins

The use of “off the shelf” data with limited integrity in a Safety Critical avionics environment

Abstract

“Integrity” and “assurance” are key attributes of any system and each needs to be addressed as part of the Safety Case for any system. This paper outlines some of the issues associated with the use of data and databases which have integrity and assurance issues. The paper focuses on possible techniques which could be deployed, whilst addressing recent developments from the civil sector and suggesting potential mitigation strategies, which may be used or considered when developing systems which access and/or utilise “off the shelf” databases and data sets.

Introduction

This paper deals with the use of databases and data sets, often used by systems, detailing ways of addressing integrity and assurance issues which need to be considered when accessing such “off the shelf” data. A distinction has been drawn between what constitutes “data” and “software”. For the purposes of this paper databases and data sets are considered to be sets of values which are called or executed in order for a computer programme to execute or function correctly. This paper therefore focuses on discussing ways of ensuring data correctness and quality. RTCA DO 200A is the civil aerospace standard covering aeronautical databases³ and it defines a database as being:

“One or more files of data structured to enable data to be extracted from the files and for them to be updated. This primarily refers to data stored electronically and accessed by computer, rather than in files of physical records.”

there is still a requirement to protect the integrity of the implementing system at all stages of the system execution and operational lifecycle. This is particularly true of navigation computer systems and applications which, are highly complex and integrated.

As noted, obtaining sufficient assurance evidence is often difficult and there may be a limited number of suppliers. The primary source is commonly a national body/institution which does not always accept responsibility for the quality attributes of the data being provided. Integrity assured databases and data sets with proven levels of integrity are not therefore always readily available for commercial and military applications resulting in issues associated such as “data granularity” and “validity”. Lower resolution databases are used such as terrain databases from the National Oceanic and Atmospheric Administration (NOAA) and the U.S. Geological Survey (USGS, GTOPO30).

Operational context

Access to accurate and robust data is a requirement for most modern systems. This coupled with the drive towards greater standardisation as systems become increasingly “inter-operative” means access to complex databases either bespoke or off the shelf is, becoming more prevalent. As part of a system architecture, there is often a requirement to access and use data, which may have limited assurance evidence. However,

Legal context

The Database Directive⁷, provides for protection under copyright law where the “selection” or “arrangement” of the content, the data and the structure, is considered sufficiently novel as to constitute an intellectual creation and Intellectual Property (IP) rights can be attributed to it. The Database Directive does not however provide accuracy or quality provisions, dealing primarily with access rights and

Detailed in Box 1 are two examples of databases, which are commonly available for avionics applications. The integrity and assurance attributes for each are addressed on a system-by system basis.

Shuttle Radar Topography Mission (SRTM)

NASA's National Geospatial Intelligence Agency (NGA) made available Shuttle Radar Topography Mission (SRTM) data following completion of the SRTM in February 2000. SRTM data is widely used, providing access to the results of a C-Band radar measurement of the earth undertaken by Endeavour over an eleven-day period. This captured elevation data for approximately 80% of the earth. This is now considered as being one of the most comprehensive digital topographic databases of the earth with absolute vertical accuracies of 3m to 15m¹.

Digital Aeronautical Flight Information File (DAFIF)

The Digital Aeronautical Flight Information File (DAFIF) is a data set, which details aeronautical information such as the location of airports, nav aids and waypoints. The data set was initially provided by NASA's NGA, who developed the data set for the US military. DAFIF was publicly available through the internet until October 2006, however, it was subsequently removed from public access. Its removal from public access was as a result of increasing numbers of organisations claiming intellectual property rights over the data coupled with a specific move by the Australian Government to apply copyright to the source. The Australian Government Corporation Air Services Australia in September 2003 also started charging for access to Australian data and rather than exclude the Australian data, the NGA opted to stop making the data available to the public. In the UK the MoD source for DAFIF data is "No 1 AIDU" who provide distribute and access to DAFIF data.

Box 1. Commonly available avionics database applications

responsibilities, namely IP. Annex 15 of the Convention on International Civil Aviation (ICAO)⁶, supplemented by EUROCAE ED-76 and ED-77 does however provide data quality characteristics for avionics systems which are dependent upon aeronautical and topographical data. ICAO Annex 15 states that:

"The Contracting States shall ensure that the integrity of aeronautical data is maintained throughout the data process from survey/origination to the next intended user".

Navigation systems often have operational requirements which require access to and use of data which may require a higher level of aeronautical data quality evidence than that which is currently available. ICAO provides quality requirements via ICAO Annex 15 for accuracy, resolution, traceability and timeliness. Reliance upon data requiring a high level of integrity means obtaining assurance with a minimum of one error in 100,000,000 for failures which could result in a catastrophic Failure Condition (see ARP 4754 and 4761). Aeronautical data integrity requirements are based upon the potential risk (accounting for probability and severity) resulting from the corruption of the data and the following classification and data integrity levels are generally applied:

- Critical data, integrity level 1×10^{-9}
- Essential data, integrity level 1×10^{-5}
- Routine data, integrity level 1×10^{-3}

This is often very difficult to demonstrate and satisfying the aeronautical data quality requirements required by ICAO is a known problem. Therefore there has often been a low compliance rate in achieving specific aeronautical data compliance. As part of the Single European Sky (SES) initiative, the European Commission (EC) has been working for a number of years to improve the availability, accuracy and therefore indirectly "integrity" and "assurance" attributes of aeronautical databases for critical applications such as Precision Area Navigation in terminal airspace. The Aeronautical Data Quality (ADQ) Regulation⁸ was developed by Eurocontrol on behalf of the EC and is a specific regulation providing a requirement to ensure the quality of aeronautical data, via an Implementing Rule which was adopted by the EC on 26th January 2010, as EC regulation 73/2010⁸. This entered into force in February 2010 with the first provisions within the regulation expected to come into force in July 2013.

The data chain

All data has an "integrity" attribute attached to it irrespective of criticality, and needs to be managed to limit/control errors from the database/data set being introduced by any of the stakeholders. A key tool in achieving this is through managing the data chain. An aeronautical data chain is a "conceptual representation of the path that a set, or element, of aeronautical data takes from its creation to its end use" (Section 1.5.4.1³). Use of and access to "off the shelf" data and databases has implications for all stakeholders within the data chain. Data chains are programme specific and an example data chain is detailed in Figure 1.

In order to ensure the integrity at all stages of the operational lifecycle, and at all stages in the data chain, it is essential that the data process is fully identified, mapped and understood by all stakeholders. Historically, not all

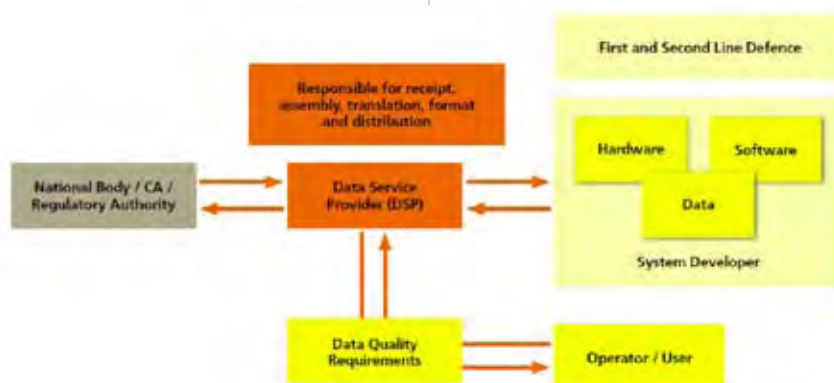


Figure 1. Example of an aeronautical Data Chain

parties have had the awareness of their obligations within the data chain, which can result in errors not being identified or mitigated or updates not being passed on to the operator. Responsibility for maintaining the accuracy and quality characteristics for data rests ultimately with the operator. RTCA DO 200A Section 1.4 notes that “The ultimate responsibility of ensuring that data meets the quality for its intended application rests with the end-user of that data”. Maintaining and ensuring integrity has an impact on the protection defence mechanisms, including both first line and second line implemented by system engineers.

The implementation of the EC73/2010 regulation discussed previously has implications for all involved in the aeronautical data chain. Service Level Agreements (SLAs) are of particular use in this area enabling agreement on:

- Timeliness – when information is required;
- Content – what information is to be provided;
- Format – how information is to be presented;
- Means – how information is to be provided;
- Approval – how the resultant publication is approved for release⁵.

Guidance for each of the stakeholders is detailed in US DOT FAA Advisory Circular 20–DB.

An example of the guidance as it equates to data suppliers is shown in **Table 1**.

Integrity management

The design and assessment of a system will determine what is permissible with regard to accessing data and how to best use and access said data. Safety assessment as a key part of the system engineering activity determines the criticality of the system/functions being implemented and the integrity and assurance requirements for the data providing:

- The baseline requirement for a specific data set;
- An indication of what integrity is appropriate based on the safety assessment indicating whether it is acceptable to use the dataset;
- What additional controls and limitations may be required to support the use of the data set, and these

3-1	Foreign Suppliers must be identified	AC 7
3-2	Type 2 LOA must be associated with specific equipment	AC 8a(2)
Compliance Plan		
4-1	Compliance Plan must be developed per 200A, sect 2.2.	AC 11b(1)
4-2	Compliance Plan shall be prepared to address all aspects of data process It shall identify the 5 items in 200A, sect 2.2	200A 2.2
Data Quality Requirements (DQR s)		
5-1	Documentation of DQR's per 200A, sect 2.3	AC 11b(2)
5-2	Mutual agreement of DQR's between Type 2 LOA holder and its data suppliers	AC 11b(2)
5-3	Changes to DQR's must be coordinated between Type 2 LOA holder and its data suppliers	AF 11b(4)
5-4	Changes to DQR's that result in major changes to TSOA article must obtain new TSOA	AC 8d(3Xii)
5-5	DQR;s must be under configuration control	AC 11b(2)
5-6	The data shall have the agreed data accuracy	200A 2.3.2
5-7	The data shall have the agreed data resolution	200A 2.3.2.
5-8	The data shall have the agreed data assurance level	200A 2.3.2.
5-9	Level 4 data must be distinguishable from any 200A compliant data	AC 11b(5)
5-10	Documentation must show traceability between identification of installed data with version of DQR's	AC 8c(4)
5-11	The data shall have the agreed data traceability	200A 2.3.2.
5-12	The data shall have the agreed data timelines	200A 2.3.2.
5-13	The data shall have the agreed data completeness	200A 2.3.2.
5-14	The data shall have the agreed data format	200A 2.3.2.

Table 1. Application of 200A to Data Suppliers⁹

may be flowed to the operator in the data chain.

However, system designers and operators are often faced with the requirement to use a specific data source as there is no other option or solution available GOTOPO 30 and DAFIF (as previously discussed). When considering the implications of using or relying on data from these sources, the safety related functions associated with the use of the data might require a higher level of integrity than currently available and therefore additional safeguards will be required. As part of any system, which uses “off the shelf” data sets and databases, mitigation techniques will be required either “procedural” or “strategic” depending upon the implementation

requirements and operational context. Strategic mitigation (primary) is systematic mitigation within the system boundary preventing or limiting failure such that failure is extremely remote. “Procedural mechanisms and mitigation” including implementing procedures placing operational restrictions/deviations which mitigates the effects from system failure as a result of a data error should be used as secondary lines of defence. Data Quality considerations are dealt with through application of RTCA DO 200A³, which defines data quality for databases as being:

“A degree or level of confidence that the data provided meet the requirements of the user. These requirements include levels of accuracy, resolution,

assurance level, traceability, timeliness, completeness, and format”.

Data quality characteristics need to be a set of criteria agreed by all stakeholders in the aeronautical data chain by ensuring data:

- Accuracy
- Resolution
- Assurance level
- Traceability
- Timeliness
- Completeness
- Format

Responsibility in accordance with RTCA DO 200A³ is the responsibility of the end-user, as per Appendix B, which details: “the final responsibility for meeting the data quality requirements remains with the end-user”.

Determining the level of integrity attached to a database is achieved through application of RTCA DO 200A³.

Table 2 defines the assurance level approach to support the definition of integrity requirements for the data process, which is commensurate with the design assurance level approach from the civil aircraft standards.

Assurance Levels	Related requirement assurance level on state provided data (ICAO)
1	Critical
2	Essential
3	Routine

Table 2. Assurance level

RTCA DO 200A, **Table 3** provides the link between failure condition categories and data process assurance level.

The provenance of any database or dataset is a key factor in influencing how and what data may be used and what associated reliance may be placed upon it within the operational context for the system. Where commercial databases and assurance evidence are available this is often costly and is implementation specific, ie there is no guarantee that assurance achieved from one implementation is transferable to another. Updates are available for some databases

maintained by national bodies resulting in slightly higher levels of resolution with updates provided covering their own specific territory, which in some instances provide quality factor heuristics.

Different techniques are available where additional assurance is required, these are considered as being either “first line” or “second line” mitigation strategies/mechanisms which are used when additional checks and/or protection mechanisms can be implemented or are required.

Protection is the first line of defence and provides the greatest level of assurance. It is extensively used in safety critical applications. Protection mechanisms are provided as the first line of defence when architecturally mitigating the effects from integrity violations, which could be caused by:

- Software or hardware errors;
- Deliberate/malicious intrusions;
- Operational errors/deviations.

Architectural protection and avoidance provide the optimum solution and are generally considered as the “first line” of defence when ensuring and assuring data integrity. Some common techniques include:

Protection

- Isolation – isolating data from other processes eg wrappers or binary blobs, while the dataset is being accessed or excised;
- Cyclic redundancy checks (CRCs) – protecting the data by setting constraints and defensive mechanisms such as CRCs to ensure data integrity.

Avoidance

- Segregation: segregate the data as the first line of defence. This should be used in conjunction with a protection mechanisms such as CRC;
- Partition: temporal and spatial partitioning of the data from core
- Other “first line” techniques which are termed “low first line” due to the fact that they need to be considered in addition to a “first line” mechanism outlined above include:

Detection

- Parity checks;
- Check summing: enabling identification of any integrity violations;
- System mirroring: mirroring through replication or mirroring using techniques such as execution mirroring and CRC’s help ensure data reliability;
- Dynamic validation: constant validation through the allocation and setting of cross variable data validation testing.

“Second line” strategies include:

Recovery

- Recovery – recovery strategies can be used to provide for data recovery following a violation, ie the safe and steady state. Recovery should be seen as a secondary line of defence and is often used in conjunction with a mixture of protection and detection acting as the primary lines of defence. Strategies for recovery can include majority vote and parity, and redundancy strategies such as RAID.

Closing remarks

Access to worldwide databases with validated quality attributes is obviously the best solution. This does however require a common requirement and level of agreement and consensus which is often difficult to reach, increasingly so from a military perspective. The requirement for standardisation when dealing with data integrity including the agreement on appropriate attributes and assurance requirements is a key requirement. Standards offer the best solution to this as emerging legislation may drive this as systems become more integrated. This coupled with the increase in “systems of systems” means that the availability and requirement for validated databases and datasets for navigation will increase. In computer science “integrity” is a well understood subject and a clear definition can be sought from the Biba Integrity Model², which notes that a system possesses the property of “integrity” if it can be trusted to adhere to a well-defined code of behaviour. Therefore we can say that “data integrity” attributes ensure that the data are complete and consistent both at creation and at all times during execution and/or use. Integrity is demonstrated through formal verification and validation, which ensures that the

Failure condition category	Effect	Design assurance level	Data process assurance level
Catastrophic	Failure conditions that would prevent continued safe flight and landing	A	1
Hazardous / severe – major	Failure conditions that would reduce the capability of the aircraft or the ability of the crew to cope with adverse operating conditions to the extent that there would be: (1) a large reduction in safety margins or functional capabilities; (2) physical distress or higher workload such that the flight crew or (3) adverse effects on occupants including serious or potentially fatal injuries to a small number of those occupants.	B	
Major	Failure conditions that would reduce the capability of the aircraft or the ability of the crew to cope with adverse operating conditions to the extent that there would be, for example, a significant reduction in safety margins or the functional capabilities, a significant increase in crew workload or in conditions impairing crew efficiency, or discomfort to occupants, possibly including injuries.	C	2
Minor	Failure conditions that would not significantly reduce aircraft safety, and that would involve crew actions that are well within their capabilities. Minor failure conditions may include, for example, a slight reduction in safety margins or functional capabilities, a slight increase in crew workload, such as routine flight plan changes, or some inconvenience to occupants.	D	
No safety effect	Failure conditions that do not affect the operational capability of the aircraft or increase crew workload.	E	3

Table 3. Assurance level/failure condition mapping

system executes correctly under normal and abnormal operating conditions. The level and complexity of this formal verification and validation is dependent upon the criticality of the system, which is executing the data being assessed. The use of data integrity modelling is an important technique which assists as systems become more increasingly open and interoperational. Integrity Modelling provides ancillary first line protection through:

- Integrity validation through logical and rule based testing;

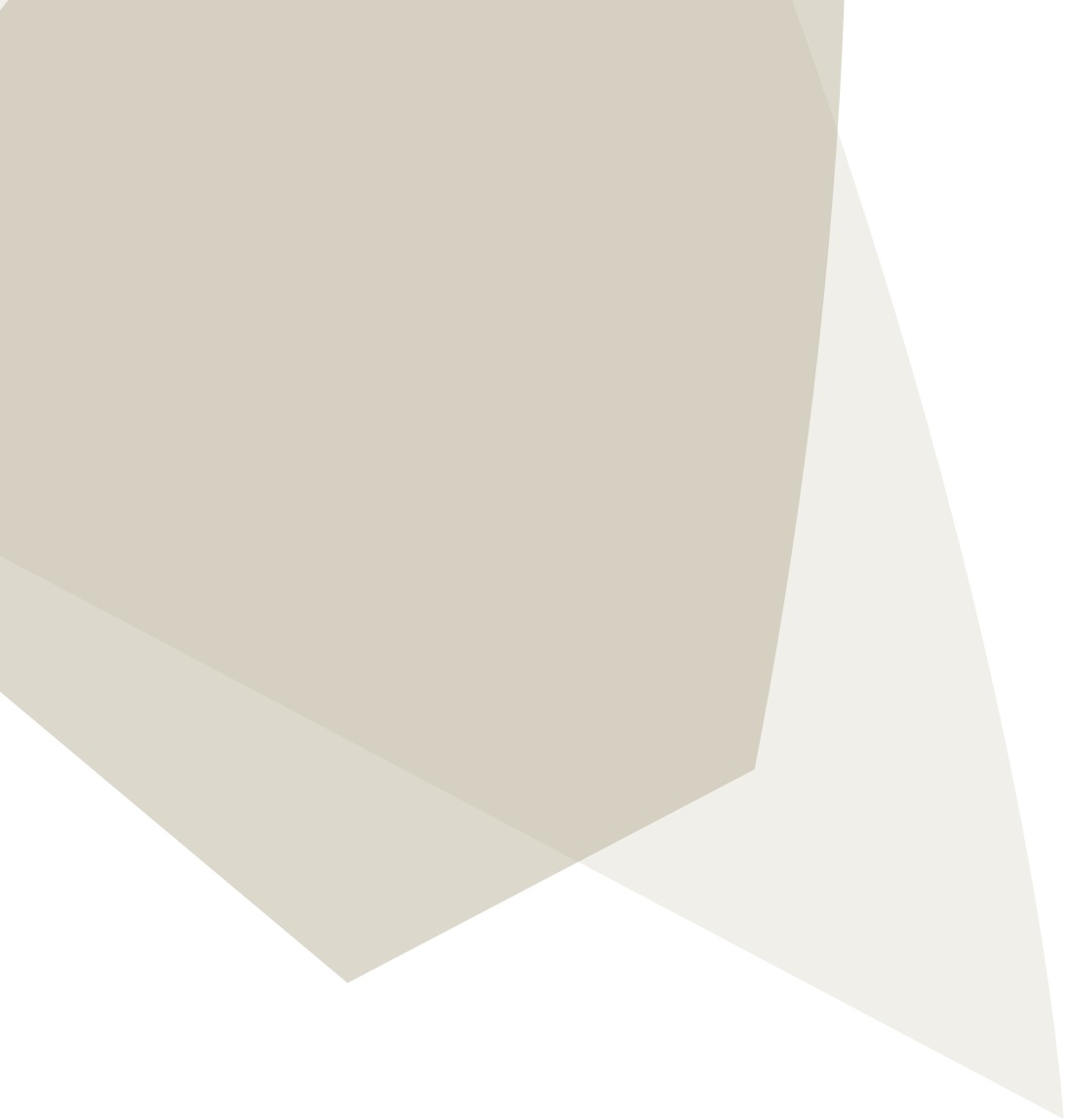
- Continuous integrity monitoring and checking and validation including the setting and activation of protection triggers.

As previously noted the use of data, irrespective of its “integrity” or the “assurance” requirements associated with the data sets, needs to be considered within the context for how the data and/or the system is to be used, to what are the data going to be for accounting for both normal and abnormal operating conditions. For safety critical applications, accessing flight critical and essential critical

and navigational aeronautical data (eg runway height) additional checks will be required. As a general rule of thumb safety critical applications may not use or rely on the data, which have an unknown pedigree. The strategies discussed are never considered in isolation. Ensuring data integrity will require a combination of first and second line protection to ensure that sufficient assurance is available to maintain and demonstrate the integrity of the system.

References

1. A worldwide SRTM terrain database suitable for aviation use; Jeppesen, Denver, CO, USA
2. Biba Integrity Model, K.J. Biba, 1977
3. RTCA DO 200A; Standards for Processing Aeronautical Data
4. RTCA DO 201A, “Standards for Aeronautical Information”.
5. Data Integrity: A Practical Guide; CHAIN 0072; Section 2.10
6. International Convention on International Civil Aviation (ICAO), ANNEX 15
7. European Database Directive 96/9/EC and the Proposed World Intellectual Property Organisation (WIPO) Database Treaty 1996
8. EC regulation 73/2010; Aeronautical and Information Quality Implementing Rule
9. US DOT FAA Advisory Circular 20–DB





**Simon
E Ratcliffe**

Graduate Engineer

Defence

Atkins

The application of high pressure water mist as part of a holistic fire fighting system

Abstract

Current accommodation standards consume significant space on board ships. The development of a holistic approach to fire fighting would enable a reduction in the requirement for trained ships crew and in turn in accommodation. This will drive savings in a reduced hull size, propulsion requirements, and reduce the number of people exposed to risk in the event of a fire.

This study aims to explore the use of High Pressure Water Mist (HPWM) to provide ship wide reactive fire fighting by considering its application to a generic area of the Type 26 Frigate in peacetime and battle scenarios. This study also offers a brief discussion of the surrounding issues associated with implementing such a system, including estimated technology readiness levels.

Acronyms

BD	Battle Damage
BGCV	Branch Group Control Valve
CMS	Combat Management System
DNV	Det Norske Veritas
FAR	Firefighters' Assistance Robot
FN	Frame Number
FPA	Fire Protection Association
FSC	Future Surface Combatant
GB	Glass Bulb
HPWM	High Pressure Water Mist
IMO	International Maritime Organisation
IR	Infrared
NDP	Naval Design Partnering Team
O	Open
PD	Positive Displacement
PT	Peace Time
RN	Royal Navy
TRL	Technology Readiness Level
US	United States (of America)

Introduction

The cost of a ship relates directly to its size, both in the concept phase and in service. Being able to reduce the size of a ship enables savings to be made over an otherwise larger vessel. However, one of the most significant drivers for the size of a ship is the manpower needed to crew it. Current crew living standards consume significant space due to accommodation, stores, black and grey water requirements etc.

Where advancements in technology, particularly navigation and combat management systems, have enabled the number of crew needed to sail the ship to be reduced, these savings are often not realised. The sticking point is the manpower required to fight fires on board, especially in damage and threat situations. Current fire fighting techniques and systems require a certain amount of manpower in order to function. This underlying factor prevents ships crews from being reduced below a minimum level.

The development of a fully automated and holistic approach to fire fighting onboard Royal Navy (RN) ships would enable a reduction in the requirement for trained ships crew. With fewer crew to support this would allow ships to be designed with a smaller hull size whilst still delivering the same capability. This will see savings in;

- The cost of building the ship;
- Reduced propulsion requirements;
- Reduced ships services requirements;
- Lower ships emissions;
- The number of personnel exposed to risk in the event of a fire;
- Ultimately, investment in a modern fire fighting solution will bring savings in the through life cost of a platform.

Ships fire fighting principles

The following section outlines the basic principles for optimised fire prevention, fighting and protection. The FPA report¹ discusses a progressive and scaled approach to fire protection, beginning with prevention in the first instance and leading through to fire fighting as a last resort. This approach is summarised in **Figure 1**.

Prevention and protection

In any fire management policy, the avoidance of fire should play as great a role as fire protection. The first step of fire prevention encompasses removing and reducing fire hazards and risks to avoid any incident. Techniques for doing so might include changing 'process' to reduce failure paths that may lead to fire, or changing the design of equipment to remove fire hazards altogether.

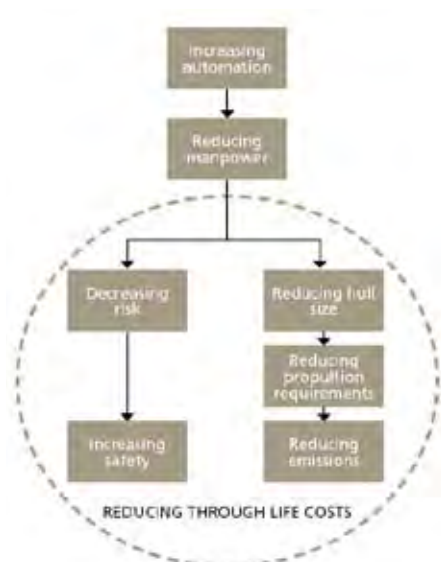


Figure 1. Reducing through life costs by an increase in automation

Fire prevention also includes the detection and prediction of fire scenarios long before the outbreak of fire. Fires and explosions are generally preceded by a series of events that lead step by step to the fire situation. Depending on the nature of these events, there may be opportunities to intervene and detect a fire scenario early. Detecting these events leading up to a fire is often outside the boundary of traditional fire detection systems. For example, monitoring an engine's vibration, fuel consumption and pressure may provide clues as to whether or not mechanical failure which could lead to fire is imminent.

Damage limitation and response

The damage and consequence resulting from a fire can be characterised into two areas; the primary damage resulting directly from the fire and its by-products, and the secondary damage and consequences of the implemented fire suppression strategy. The extent of the damage resulting from a fire and its suppression is a function of the scale of the fire and hence the scale of the response. The earlier that fires are detected, prevented and suppressed, the greater the benefits are for reducing both primary and secondary damage. Early detection also allows a better balance between a rapid but high impact response against a measured and proportionate (directed) response causing less overall damage.

Traditionally, ships fire fighting methods are not predictive by nature and, following the failure of first aid fire fighting, accept large amounts of damage as alternative means are readied. The modernising of fire fighting response requires the replacement of the 'man with an extinguisher' with automated on the spot alternatives such as equipment control, local suppression and aimed systems designed to reduce the impact of secondary damage.

Redundancy and integrity of systems

Fire safety systems and the supporting infrastructure generally embody safety factors to ensure availability and effectiveness when required. These factors may include;

- System duplication;
- System over-specification;
- System protection (resource guarantee);
- Manual backup;

- Assigning 'worst case' threshold and designing infrastructure to cope with it.

High pressure water mist systems

General description

In suppressing a fire, traditional low-pressure sprinkler and deluge systems often cause significant water damage that can be greater than the damage caused by the fire itself.

HPWM offers equivalent or better fire suppression than traditional systems with minimal water discharge, minimising damage to property and reducing the time and cost of clean-up.

High pressure water is dispersed by fixed nozzles which create an ultra fine mist over the protected area. The mist fights fires in three main ways;

- **Cooling** – Millions of tiny water droplets produce a very large heat collecting surface and rapidly reduces the temperature of the air in the space;
- **Smothering** – The vapour displaces the oxygen volume in the fire itself, rather than in the entire space. This means that it does not present an asphyxiation hazard to personnel;
- **Attenuation** – The mist absorbs radiant heat.

Ultra fine mist has the advantage that it requires very little water and consequently does minimal damage to equipment. If de-ionised water is used HPWM systems can also be applied to live electrical fires. In machinery spaces the major benefit of water mist is that since it is harmless to people, the system can be activated the second a fire is detected, without any need to first evacuate. Nor is there any need to shut off vents or close openings before evacuation, as the water mist will not escape the space, as gases would. This possibility for immediate activation means that the fire damage is kept at a minimum.

Once the fire has been extinguished, the water mist will quickly cool down the space and thus prevent re-ignition.

Flash suppression

A fire protection system designed to provide 'flashover suppression' aims to keep air/gas temperatures in compartments too low for materials and fuel sources to ignite. One of the advantages of flashover suppression is that it can be achieved with less water

with a high pressure mist system than a traditional sprinkler extinguishing system. Live fire tests conducted by the US Navy on the ex-USS Shadwell have demonstrated that flashover suppression can be achieved using fewer water mist nozzles in each compartment than would be needed using a conventional marine sprinkler system².

Pre-emptive action

A networked system of HPWM sprinklers could be used to pre-emptively cool certain spaces. This might be a reaction to developing fire conditions, ie equipment telemetry reporting increased risk, or as a precautionary measure during a fire scenario. For example, water mist could be used to cool an established escape route reducing the chance of it being blocked by fire.

Blast mitigation

The use of water mist has been shown to have benefits for mitigating the effects of blasts on Navy ships. Navier-Stokes simulations performed by Ananth et al³ and the experimental results found by Thomas et al⁴ suggest that latent heat absorption is the primary mechanism behind water mist explosion suppression in a confined space. The shock front that propagates ahead of the thermal front immediately following a detonation causes the water mist droplets to break up; this increases the heat absorbing surface area and results in an increase in the droplet vaporisation rate. This cools the gasses in the region between the shock and thermal fronts.

The second mechanism by which water mist mitigates blast energy is through momentum absorption. Simulations by Schwer and Kailasanath⁵ concluded that quasi-static pressures produced by small explosions were suppressed by water mist. The droplets interact with the front as it is reflected multiple times absorbing energy and changes of momentum.

In 2009 the US Naval Research Laboratory conducted a series of detonation experiments designed to establish a link between the mist density conditions of a sprinkler system and its ability to reduce blast impulse in a confined space⁶. The results of these experiments show that the higher mist density conditions outperformed lower mist concentrations in suppressing blast effects. This shows a significant opportunity for building water mist into a ship's defensive suite.

System configuration

Water mist systems can be configured in various ways;



Figure 2. Type 26 Frigate concept. Source: <http://www.defenseindustrydaily.com/Britains-Future-Frigates-06268/>

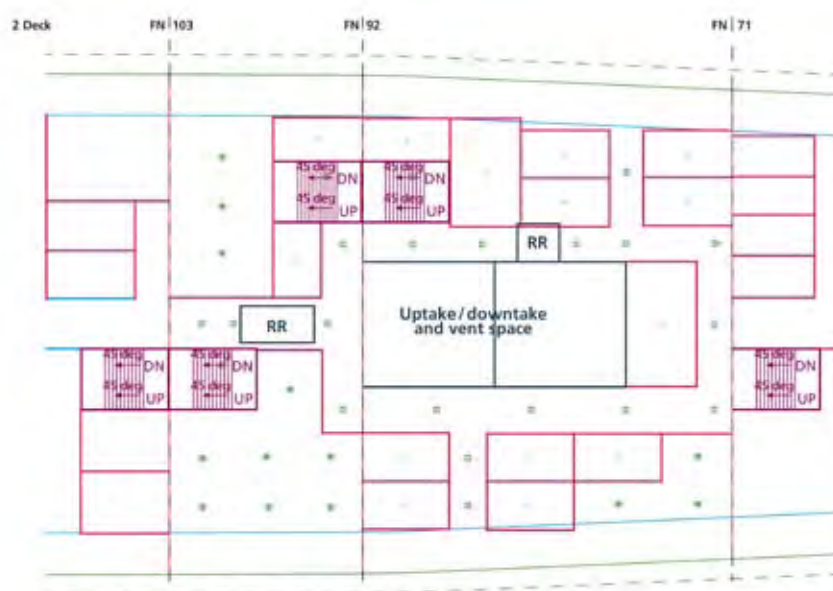


Figure 3. Fire zone 2, 2 deck arrangement and sprinkler layout

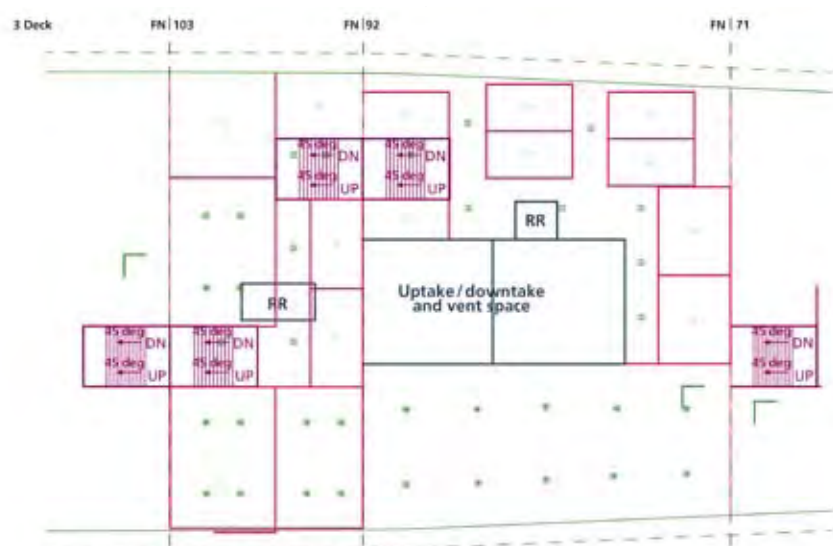


Figure 4. Fire zone 2, 3 deck arrangement and sprinkler layout

Thermally activated (Wet pipe) -

Wet pipe systems are typically used in accommodation and similar areas where solid materials are the combustible media. When ambient temperature exceeds a given limit, the activation bulb of the sprinkler bursts and water mist is discharged from that particular sprinkler.

Deluge - A deluge system normally has open spray heads with water flow controlled by closed valves. When a valve is opened, water mist is discharged by all spray heads in the section controlled by that valve. Deluge systems are typically used in spaces where fuel fires could occur.

Class A fires

Class A, or 'ordinary combustible' fires are those started from solid organic material, such as wood, paper, cloth etc. Typically, spaces containing Class A fire hazards are protected by thermally activated sprinklers, ie localised heat sources cause the sprinkler in the immediate vicinity to activate. Class A fires typically spread outwards from a single point, so initially only the closest sprinklers will open, tackling the fire directly. As the fire spreads, more nozzles will open and the water demand from the system will increase.

Class B fires

Class B, or flammable liquid fires, are those started from liquid fuels, oils, chemicals etc. Machinery spaces present numerous Class B hazards. Since highly flammable liquids like petroleum can spread quickly and set alight almost instantaneously, it is necessary to cover the entire area with water mist from the offset. In such spaces open nozzle deluge systems are used.




System design and application

Subject area – T26 baseline 2v0

For the purpose of this study, an area of T26 Frigate concept design was selected to provide a framework on which to demonstrate the use of HPWM, see **Figure 2**. The deck area was split into four 'Fire Zones' separated by water tight bulkheads.

One fire zone across two decks was isolated for use as a representative area for the application of HPWM.

Frame 71 to Frame 103 on 2 Deck T26 Baseline 2v0 was chosen to act as a single 'Fire Zone'. This zone represents a typical area on a Surface Combatant. It houses common functions and utility spaces that represent a range of potential fire conditions.

IMO Compartment	Cabins, <16m ²	Public spaces, >16m ²	Public spaces, 2 deck height	Corridors and stairways	Storage areas	Machinery spaces
Naval equivalent	Cabins/Small compartments	Large compartments	Large compartments, 2 deck height	Passage and stairways	Storage areas	Machinery space
Max deck height	2.5m	2.5m	5.0m	2.5m	2.5m	Vertical distance from object 1.5m – 5.5m
Nozzle type ^a	1B 1MB 6MB	1B 1MB 6MB	1B 1MC 6MC	1B 1MB 6MB	1B 1MC 6MC	4S 1MC 8MB
Symbol						
Glass Bulb ^{b)} (GB) or Open (O)	GB	GB	GB	GB	GB	O
K factor [lpm/ bar ^{1/2}]	1.45	1.45	2.5	1.45	2.5	1.9
Flow rate at 120 bar [lpm] ^{c)}	15.9	15.9	27.4	15.9	27.4	20.8
Max spacing	One per room	3.5m ^{d)}	3.5m	3.75 m, centred	2.65m	4.0m ^{e)}
Max distance to bulkhead	2.850m	1.750m	1.750m	1.875m	1.325m	-
Max coverage area	16m ²	12.3m ²	12.3m ²	14.1m ²	7m ²	16 m ²
Nominal water density [lpm/ m ²]	1.0	1.3	2.2	1.1	3.9	1.3

Notes on Table

- a) Nozzle designation code: 1B 1MB 6MB or 4S 1MC 8MB
- 6MB or 8MB 6 or 8 mist orifices surrounding the centre jet,
 - 1MB or 1MC 1 mist orifice on centre axis, B = 0.7mm diameter, C = 1.0mm diameter
 - 1B or 4S 1 = 120 degree cone angle, thermally activated; 4 = 90 degree cone angle, open nozzle; B = Brass; S = Stainless Steel
- b) 2mm, Job 57oC (orange code) bulbs
- c) Maximum system working pressure is 140 bar, while minimum initial working pressure at the sprinkler heads is 120 bar. A minimum of 100 m² is to be covered at 120 bar pressure, whereas 280 m² should be covered at minimum 60 bar (measured at the nozzle).
- d) This sprinkler head may also be used at ceiling height of 3.0m and 3.5m. The sprinkler head spacing should then be reduced to 3.30m and 3.05m respectively.
- e) Spray heads should be installed outside of the protected area a distance of at least 1/4 of the maximum nozzle spacing, in this case 1.0 m outside at the periphery of the protected object (see IMO MSC/Circ.913, annex 3.4.2.1).

Table 1. Sprinkler spacing and layout requirements

Commercial water mist system selection

In order to design for and demonstrate the application of a HPWM system in this study, it was necessary for a commercially available HPWM system to be selected for inclusion in the design. In this case the HI-FOG Marine System by Marioff, Finland was chosen on the basis of its pedigree as a marine fire fighting system.

Nozzle layout

Nozzle layouts have been mapped for 2 and 3 Decks between Frame Numbers 103 and 71. See **Figure 3** and **Figure 4**.

The spacing rules are shown in **Table 1**. These were derived from the Type Approval Certificates for the HI-FOG System issued by Det Norske Veritas (DNV)^{7,8}.

The HI-FOG system meets the fire test protocols for 'Accommodation areas, public spaces and service areas' on civilian ships. The International Maritime Organisation (IMO) terminology of 'Accommodation Areas', 'Corridors', 'Public Spaces' and 'Service Areas' correspond in RN terminology to 'Small spaces', 'Passageways', 'Large spaces' and 'Storage areas' respectively.

For the purposes of this paper, both open deluge and closed thermally activated nozzle types are used. It has been assumed that Branch Group Control Valves (BGCV) will control the flow to each branch pipe. This will allow nozzles to be activated remotely without the need for the local temperature being high enough to thermally trigger the bulb. Thus, the system will still maintain the reactive nature of thermally activated bulbs but also allow a central control system to pre-emptively open branch groups to protect spaces in advance of fire or blast situation.

Distribution architecture options

In this section, different possible High Pressure Water Main distribution architectures will be discussed. In particular, the way in which they might contribute to enabling a holistic and survivable water mist system capable of intelligent self diagnosis and damage control will be considered. Key factors are the degree of redundancy in pump sources, the number of routes available for water to reach any portion of the piping network, the degree of separation between redundant components and the arrangement of control valves and sprinklers. Other factors that effect survivability are the integrity of the power supply to pumps and valves, communications and logic systems, location, mounting and armouring of risers and valves etc all of which are excluded from this discussion

Three distribution architectures will be considered;

- Centre main distribution;
- Dual main distribution;
- Sectional loop architecture.

Centre main

Centre main architectures consist of a single main running down the centre line on each deck of the ship. Sectional control valves are located at the zone boundaries and at riser connections, which are spaced so to bring water from the pumps on the lower decks to each level. Sprinkler heads are connected in branch groups which in turn are connected to the centre main via a BGCV. If a pipe was to be ruptured between risers on one deck, valves on the mains would close to isolate that length of pipe. Water would still be able to flow to the intact portions of the main on that deck through the adjacent risers. The centre main in this case must be large enough to accommodate the combined flow of all the branch groups.

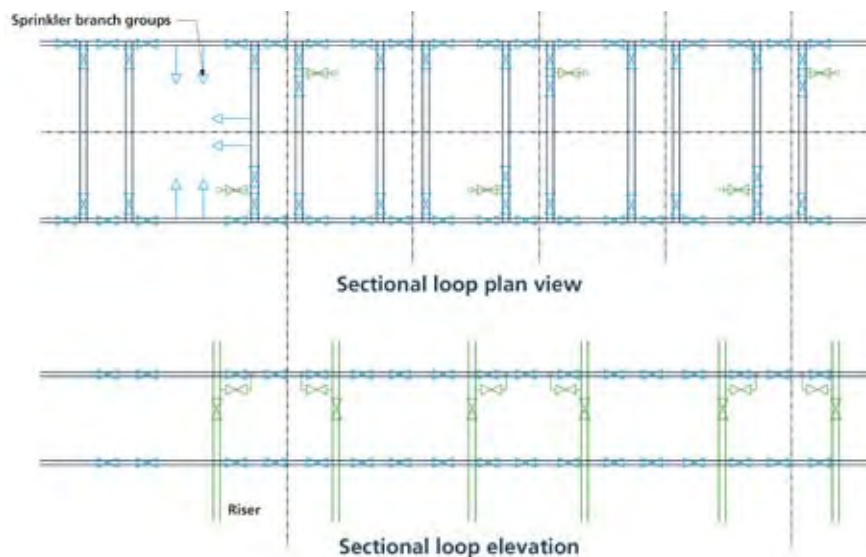


Figure 5. Sectional loop architecture

The level of redundancy in the centre main design is low; the options for re-routing the water around isolated sections is limited and as a result the number of branch groups that can be kept active in the event of damage is low.

Dual main

A step further from the centre main concept is the use of a dual main. This features mains running down both the port and starboard side of each deck with vertical risers spaced at intervals along the length of the ship supplying the mains on each side. Branch group lines are connected to either the port or starboard main via BGCVs. Zonal valves are placed at intervals along the two mains so that damaged sections can be isolated. Any undamaged branch lines within a compartment that are fed from the undamaged side of the ship will still be functional. This architecture can be modified to include crossover mains and valves to create 'offset loops'.

Sectional loop

Sectional loop architectures are similar to dual main arrangements in that a high pressure main runs along the port and starboard side of each deck of the ship, with vertical risers placed at regular intervals along the length of the ship, see Figure 5. The network of pipes is separated into 'loops' by valves and crossover mains. Each loop is served by its own riser, which can supply that loop with water or any of the loops adjacent to it. Risers alternate between port and starboard sides along the length of the ship in order to minimise vulnerability. Unlike the dual main architecture,

however, crossover mains connect port and starboard mains on the same level, one on either side of each water tight bulkhead.

The advantage of sectional loop architecture is the ability it has to recover from damage with minimal loss of functionality. Valves are placed so that each loop can be supplied in two independent ways;

- With all the supply coming up the riser serving that particular loop;
- The riser can be closed off so that the supply must come from an adjacent loop.

Sectional loop architectures allow for the subdivision of the main network into small cells that can be individually isolated. The greater the number of cells the better the ability to recover from damage while leaving as much of the network operational as possible.

Sectional loop architectures also offer hydraulic advantages in that the number of pathways for water to flow to any one demand point is maximised. A large demand at a particular point will distribute across multiple mains and risers, thus allowing for lower flow rates through the mains, requiring smaller diameter piping⁹.

It is for these reasons that using a sectional loop architecture offers the greatest potential for providing a flexible and survivable HPWM system. Sectional loop architecture will be considered from here on.

Branch group layout

Figure 6 and **Figure 7** show the nozzles and branch lines connected to the main on each deck. Typically a branch group connects four nozzles to the main and is controlled by a branch group control valve.

Where possible, branch lines are arranged so that nozzles can provide a curtain of water across the beam of the ship. Each nozzle would be connected to the branch line by a branch vein (not shown), sized to only need to carry the flow for one individual sprinkler, regardless of where it is in the system ie regardless of how many sprinklers are 'in front' of it.

Water flow demands

A system configured to provide flashover suppression cover across an entire platform has the advantage that its flow demand grows progressively to match the spread and intensity of the fire. As the fire spreads through the ship, more branch groups can be brought online as needed. For the purpose of this study, the water flow demands will be calculated for two damage scenarios; peace time and battle damage scenarios.

Table 3 compiles the nozzle count and estimated water flow demands for the HPWM system based on the layouts shown in Figure 4 and Figure 5. For simplicity, it has been assumed that each branch group holds four sprinkler heads with a K-factor of $1.45 \text{ lpm} / \text{bar}^{1/2}$, except for the machinery space where a K-factor of $1.9 \text{ lpm} / \text{bar}^{1/2}$ is used.

Pumping strategy

There are several possible approaches for providing the pumping capacity for the HPWM system. Some high level options are discussed in **Table 2**.

Option B

Option B affords 100% redundancy while also separating the two pumping assets. The sizing of both pumps to provide the total design flow rate guards against the loss of a single pump through routine mechanical breakdown and the separation of the units ensures that the risk of losing both through battle damage is greatly reduced.

However, option B may not offer the scalability or design flexibility required when considering much larger or much smaller ships. As the number and size of fire zones increases the demand flow rate will also increase. Sizing a single pump unit to provide 100% of the design flow rate in all circumstances may not be sensible.

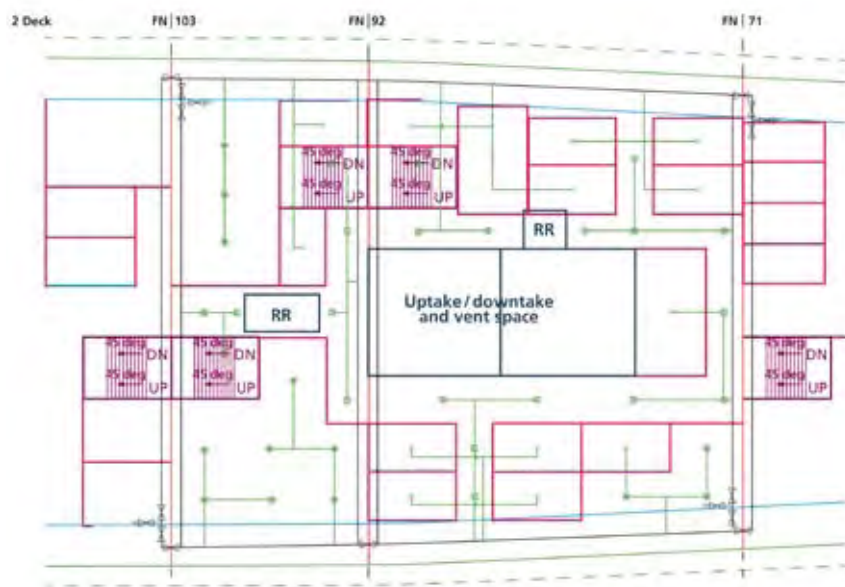


Figure 6. General arrangement of 2 deck showing sprinklers, branch groups and water main

Option	High level pumping strategy	Comments
A	One large pump unit sized to meet the full design flow rate, connected to a distribution main supplying multiple risers	Option A has no redundancy and is not discussed further
B	Two pump units in parallel, one aft of midships, and one forward serving a common distribution main and multiple risers; each pump unit sized to meet full design flow, so that one unit is redundant.	Provides for 100% redundancy and can assume at a reasonable cost for connections, power and filtration. Pump units are adequately separated so that at least one should be functional at all times
C	Four pump units in parallel, one for each fire zone; each pump unit sized for 1/3 of the full design flow, so that three units will meet full design flow with the largest out of service	Provides for redundancy in a way that permits each pump unit to be smaller than arrangement C, such that redundancy can be achieved with three of the four pumps. Can assume that smaller pump units will be cheaper to run

Table 2. High level pumping strategy

Option C

Option C maintains a reasonable level of redundancy in four pumps each providing a third of the design flow rate. The use of one pump per fire zone ensures that pump units are adequately separated and distributed throughout the ship. Options C offers advantages over Option B in the size and the scalability of the pumps required. Running several smaller pump units rather than relying on large pumps sized to meet the entire demand should

enable savings to be made in running costs and enable a more flexible design. The remainder of this study assumes Option C.

Pump type

Selecting a pump to supply a high pressure water mist system presents a challenging problem. Such a system demands a very high pressure, but also requires the flexibility to vary the flow rate as the demand changes. Potentially, the

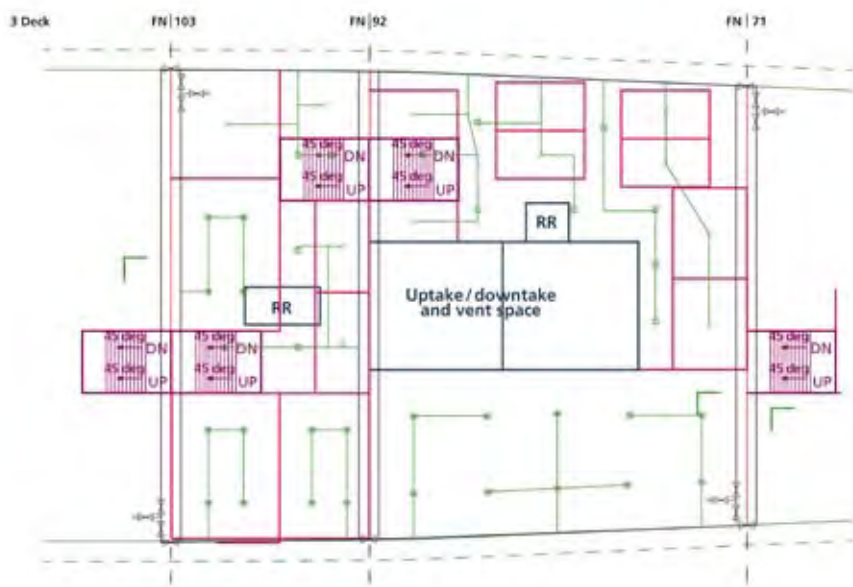


Figure 7. General arrangement of 3 deck showing sprinklers, branch groups and water main

Scenario	Branch groups	Nozzles	Flow rate (120bar, K 1.45)
Average branch group	1	4	63.6 Lpm
PT1 3 branch groups active in immediate fire area.	3	12	190.8 Lpm
PT2 3 branch groups active plus 1 branch group in corridor	4	16	254.4 Lpm
BD1 Branch groups in adjacent spaces including 4 branch groups immediately above the damage area.	7	28	445.2 Lpm
BD2 As BD1 but increasing to a further 2 branch groups on the same deck and 4 branch groups above damage area.	13	48	763.2 Lpm
BD3 As BD2 but including further 2 on deck and 3 above	18	72	1144.8 Lpm
MS1 machinery space drench system activated (Nozzle type 4S 1MC 8MB, K factor 1.9)	2	8	166.4 Lpm
BP1 nozzles in the outer most compartments of the ship open in the vicinity of an expected weapons strike. This may be on one or more decks depending on the accuracy of the prediction.	6	24	381.6

Table 3. Water flow demands

pumping system could need to go from providing high pressure fluid at a low flow rate in a single compartment to very high pressure high flow rate fluid across several fire zones.

The high pressures required of the water mist system (up to 150bar) mean that the pumps selected need to be of high quality and high capability. Traditionally, centrifugal pumps are used with sprinkler systems because they allow a constantly varying flow rate to be delivered at with relatively simple equipment. However, at high pressures, multi-stage centrifugal pumps are required. These have the potential to be more complex and require significant maintenance.

More reliable high pressure pumps come in the form of piston type positive displacement (PD) pumps. PD pumps, by nature of their design, deliver a fixed volume of fluid and as such are not best suited to variable demand sprinkler systems. However, PD pumps can be coupled with special design features to match the fixed volume output of the PD pump to a system of variable demand.

PD pumps applied to water mist systems

To design for the BD3 scenario (Table 3) each pumping unit would need to be sized to provide a flow rate of 381.6 litres/minute.

The use of PD pumps to drive HPWM systems has been demonstrated on the ex-USS Shadwell by the US Naval Research Laboratory⁹. Their approach is summarised here.

We can assume that in basic terms, each pump unit consists of two smaller pumps, a primary and a secondary pump, driven by a single motor. The two pumps might be connected by a check valve, held closed by the high pressure from the primary pump and preventing flow from the secondary pump entering the system. This excess flow from the secondary pump flow might be bypassed by a suction line via a flow bypass valve and re-circulated to the reservoirs. As long as the system demand is less than or equal to the capacity of the primary pump, the system pressure remains 'high'. Thus the first nozzles to operate at the early stage of a fire deliver water mist with maximum velocity and flow rate.

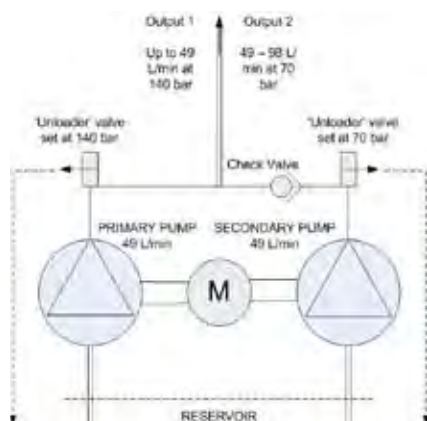


Figure 8. Diagram of a PD pump pair consisting of two PD pumps driven by a single motor

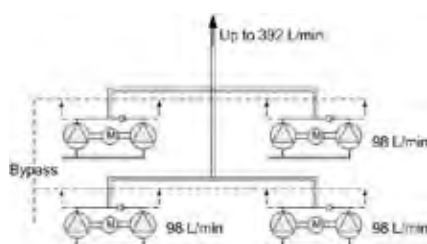


Figure 9. Diagram of an assembly of pump pairs connected in parallel to provide a range of flows

As more nozzles open and the volumetric demand of the sprinkler system exceeds the capacity of the first pump, the system pressure will drop. Once it drops to the setting of the secondary pump flow bypass valve, this will allow flow from the secondary pump to enter the system, albeit at a lower pressure. A schematic of this arrangement is shown in **Figure 8**.

For a large HPWM system, several pump pairs could be assembled in a skid to form one 'pump unit'. The minimum demand for the system, for example one or two nozzles operating in peacetime conditions could be met with one pump operating. As more nozzles open, the system pressure will drop until it falls below the setting of the next flow bypass valve. That valve then closes and the flow from that pump then enters the system to make up the demand. In this way the pump unit self adjusts to match the demand from the sprinkler system. **Figure 9** shows an assembly of pump pairs to form one of four 'pump units' sized to meet one third of the maximum expected demand.

Sensors and control

Being able to detect fires quickly and accurately is key to ensuring a ship's survivability and protecting life at sea. Early detection allows the ships systems

Human faculty	System
Optical detection Eyes	<ul style="list-style-type: none"> IR cameras Machinery monitoring Casualty location Real-time situational feedback
Electronic Nose	<ul style="list-style-type: none"> Ionising and photoelectric smoke detectors CO and CO₂ detectors Heat sensors
Acoustic monitoring Ears	<ul style="list-style-type: none"> Machinery monitoring Shock/blast detection
Brain power	<ul style="list-style-type: none"> Micro processors Intelligent control Pattern recognition Neural networks
Voice!	<ul style="list-style-type: none"> Alarms Situational feedback Personal address

Table 4. Fire fighting systems approximated to human sensory faculties.

and crew to deal with the fire and limit its damage. Generally, on most surface ships there is poor integration between sensors and suppression systems, limited use of multiple sensor types and a strong reliance on human input, leading to slow detection and numerous false alarms¹⁰. The principle fire detection system on ships is still routine human watch keeping; arguably simple, but slow and potentially dangerous for the personnel involved.

The aim of a fire detection system should be to provide comprehensive, fully integrated, multi criteria fire detection cover across the entire ship, intelligently interfacing with fire suppression systems, fluid control systems and ships crew. Without this advanced functionality, pre-emptively reacting to fire conditions using HPWM systems will be limited. A novel way of thinking about this is to emulate the sensory functions that humans use to detect fire (**Table 4**).

The basis of an intelligent sensor network would be the employment of multiple sensor types and analysis to 'diagnose' whether there is a fire rather than merely detect one of the 'symptoms'. Multiple sensors working together can provide more accurate clues as to whether a fire has started or not and more importantly if a fire is likely to start. Like the human

crew, the system should be able to make a reasoned judgement as to the fire situation based on all its data. The advantage over the human crew is that the ship can be monitored in all places, 24 hours a day.

In order for the system to correctly match sensor readings to fire scenarios, a database of fire signatures and sensor patterns would need to be established for different types of fire and typical false alarms. The more sensor patterns and fire signatures the system has access to, increased accuracy of diagnosis is achieved. However, given that no two fires are identical, the system would need to include the capacity to 'learn'.

Network integration

A holistic system will rely on multiple systems 'talking' to each other in order to co ordinate the response to a fire or damage situation. The key elements that might be involved are shown in **Figure 10**. It shows the breakdown of the Fire Control system into two main components; the Sensors and the HPWM system, ie sensing and reacting. Crossovers exist where GB sprinklers both sense and react to fire events. It also shows how the combat management system might feed into the fire and damage control system. Threat

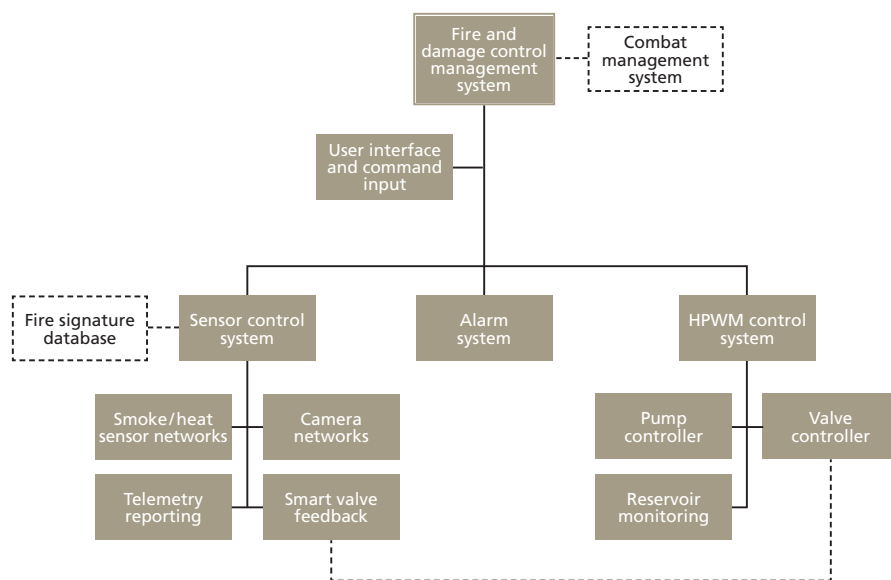


Figure 10. Fire and damage control system hierarchy

information can be used to coordinate blast suppression response using water mist. A key challenge is the design of a coordinating management suite that can effectively interface with other ships systems and coordinate action. The position of the human operator in the management system will also present interesting questions regarding accountability and autonomy.

The control system will need to digest information regarding the fire itself, the suppression response, the location and movement of personnel, any damage control efforts and the health of the fire fighting infrastructure. An ideal system will be able to react instantly to a fire situation by activating relevant branch groups and then continuing to monitor the progress of that fire and 'watch' for new events. New fire situations might come in the form of further sensor readings from multiple sources, a manual activation at an alarm call point or the bursting of a glass bulb sprinkler.

Supporting technologies

The following section discusses some of the novel technologies that would be necessary to enable a fully integrated HPWM system that provides a pre-emptive fire fighting capability

Smart valves

Valves that can autonomously open or close depending on the flow conditions that they 'see' are essential to providing a fire fighting system that removes the need for human input and decision making. Positioned at critical points in the distribution main, these motorised

valves incorporate pressure sensors and flow meters to monitor the conditions in the main.

A balance must be achieved between the benefits and the cost of installing smart valves in the distribution mains. The spacing between the valves determines the size of the area that will be non-functional if valves must be closed to isolate a rupture. When considering the sectional loop architecture, the maximum level of control for isolating damaged piping and rerouting flows could be achieved by installing a valve on each end of every pipe connecting two separated grid points. So for a T-intersection this would mean having a valve on all three branches. This strategy would result in a high valve count and, depending on the type of valve used, be prohibitively expensive. An alternative might be to use 'valve nodes' at each T-intersection; ie consolidating actuators and logic circuits into one housing capable of operating each valve individually. This would take advantage of the proximity of the valves at each intersecting node in the pipe network and achieve some economies of design.

Heat sensors

Heat sensors will form a key part of an advanced fire detection system. Rising temperature conditions indicate the increased likelihood of a fire. When coupled with other sensor types such as smoke or visual recognition, heat sensors can provide an accurate picture of a developing fire and how it is spreading. This information can be used to coordinate and prioritise the response to the fire. Heat sensing also has the

potential to provide feedback to the control system on the effectiveness of the fire suppression being applied.

Use of infra-red cameras

Infra-red (IR) cameras can also be used to spot and identify fires. In particular, they are able to spot fires in hot environments, where heat sensors may give false alarms. IR cameras measure the intensity of the IR radiation emitted from objects and surfaces. Using image recognition software the difference between a flame flare can be distinguished say from the hot casing of an engine. This sort of image processing and software recognition is not completely foolproof, flares and reflexions might give rise for false alarms. IR cameras can, however, provide clear unambiguous information on the situation as it develops by feeding live pictures back to an operator. This allows them to question whether the cause of alarm is false or a real fire and direct actions accordingly.

Technology readiness levels

This section offers a brief discussion on the maturity of the technology required to implement a holistic fire fighting system. It does not seek to provide a definitive answer with respect to technology readiness levels, but more so a 'food for thought' and provides estimates of the technology readiness levels of each solution on a scale of 1 to 10.

HPWM system

HPWM technology is well established. It forms a natural progression from 'traditional' low pressure sprinkler systems. HPWM systems are made by a variety of specialist manufacturers and can be found currently in use across a wide range of civilian vessels and increasingly land installations. Military Naval use is known, the US navy investigating its application as early as the year 2000⁹. HPWM systems can be found in small fixed system set ups eg machinery spaces, and also protecting larger spaces providing the primary means of fire fighting. Class Society Certification for passenger and cruise ship applications exists for most systems, including the Marioff products. Estimate at a technology readiness level of 8-9.

Sensors and control

The sensor technology required to drive a holistic system should be widely available and in use. Smoke detectors, heat detectors, IR cameras etc are all relatively mature technologies. The oil and gas industry are often at the forefront of innovation in this area, using

fuel mist detection to spot fire situations early and IR cameras to identify fires and false alarms. The processing of the data they gather is where the key technology questions lie. Creating a management system that can 'learn' the difference between characteristics of a real fire and a false alarm is not beyond the realms of modern computing power but may require investment in specific examples and programmes to drive forward. Technology readiness level 4 – 7.

Smart valves

Smart valves in various forms are common across the energy and process industries. The drive for greater efficiencies from deep sea drilling operations has demanded large investment from the subsea sector. Schemes have been designed and implemented for use off-shore, for example Unocal, now part of Chevron, installed intelligent pump and valve systems to boost the efficiency of its Monopod platform in the Cook Inlet Basin, Alaska¹¹. The controller technology that powers such valves is where the key development lies – the logic behind the actuated valves. Since their use in high pressure mains to provide automated damage repair and optimisation response is less well documented, valve solutions will be custom built to meet the specific needs of their applications. Technology readiness level 7.

Whole system

The key to creating a holistic system is linking the different technologies together. Sensor suites combining with suppression systems to fight fires; potential blasts being detected and mitigated against; intelligent controllers spotting false alarms and rerouting around damage will require the system to be greater than the sum of its parts. This will present the greatest challenge. For manpower savings to be realised it will require a change of doctrine, process and attitude, away from current techniques and further towards pre-emptive and instant response. Technology readiness level 4.

Conclusions

This report raises the issue that current ships fire fighting techniques are old fashioned and slow to act failing initial first aid fire fighting efforts. If ships' crews are to be reduced on future vessels, attention will need to be paid to developing a holistic and intelligent fire fighting system that can remove the 'man with an extinguisher' as far as possible.

This report sees that HPWM is an excellent solution for providing comprehensive cover across a surface ship. It allows for an instant response to a fire situation, in that it is non-toxic, does not require spaces to be sealed and can be deployed in HV and machinery spaces. The mist acts in several ways to fight fire but can also be used to prevent flashovers and pre-emptively cool compartments. Water mist has also been found to offer blast mitigation. Mist systems in outlying compartments could be activated ahead of a weapon strikes to reduce the potential damage of internal explosions.

In order to provide comprehensive cover however, the entire ship needs to be covered by high pressure sprinkler nozzles that can either be triggered locally by rising temperatures or on command from a control system. It is this 'total coverage' element that means personnel are not required in the large numbers that currently operate in fire fighting onboard surface ships. Installing and supplying such a large system presents its own complexities. Possible savings could be made if certain areas of a platform were prioritised for HPWM cover. This could be limited to high risk areas or priority escape routes and passageways for personnel.

A sectional loop architecture was found to provide the most scope for enabling an effective HPWM system, both in terms of hydraulic efficiency and protection against ruptures. The three dimensional grid with multiple flow paths provides hydraulic advantage in that it enables a reduced pumping energy requirement or a reduction in the distribution pipe size.

The use of sectional valves at crossover points either side of each bulkhead offers protection and flexibility in the event of blast damage to any particular section. The subdivision of the network into small 'cells' that can be individually isolated, or supplied from alternate routes, offers the advantage for developing a fast recovery from blast damage.

The disadvantage of such a system lies in the expected extra cost in labour, design space and material needed to install the necessary crossover mains, and the number of nozzle heads needed. The requirement of smart valves at each pipe node may also present a significant cost.

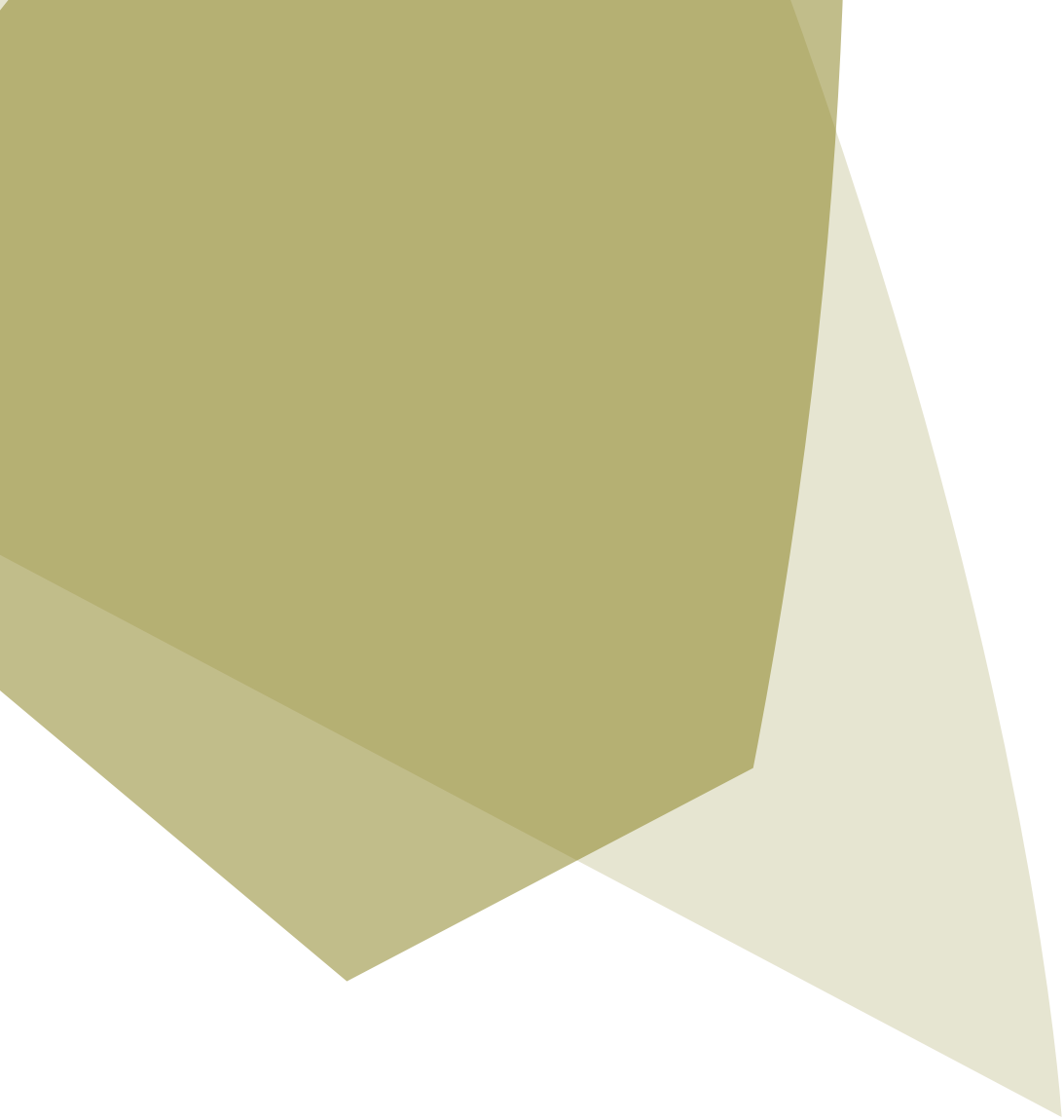
PD pumping technology was highlighted as an appropriate means to supply the network. PD pump pairs could be arranged in parallel in a skid to achieve a range of flow demands. Each fire zone should contain its own pump unit and each should be sized to meet a third of the demand. Water would need to be provided from a fresh, de-ionised source and could not be supplemented from the Sea Water Main.

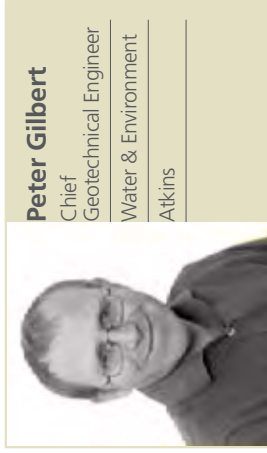
A truly holistic system will require advanced control and management. The integration of smart sensors, a control system and human operators will be vital to ensuring the full implementation of an intelligent fire fighting system. A range of telemetry and joined up sensing processes need to be combined with a sophisticated control system that can 'diagnose' fire as well as detect its symptoms. The more automated this detection and diagnosis process is, the greater the potential for saving time taken to respond to a fire and the scale of the response required to control it. Integration with Combat Management System (CMS) offers potential for building in reactive protection.

Aside from the technical challenges this presents, it will also require comprehensive rethinking of how fires and damage control are managed presently and how they are pictured in the future. A full analysis of the costs of such a system would need to be assessed against the savings made in manpower and ships size, also taking into account the reduction in risk to personnel as a result of the system being implemented. Provisionally however, the use of HPWM is recommended for meeting the reduced manning objectives set out by this report. Coupled with smart sensor and control technology it enables a swift and intelligent response to fire across the entire ship with little or no need for 'the man with an extinguisher'.

References

1. FIRE PROTECTION AGENCY, 'NA-FS Firefighting Improvement Initiatives as part of the Future Surface Combatant (FSC) Fire Policy', Final Report (Revision 2), Ref. FPA/001020, 17 March 2009.
2. Mawhinney, J.R., DiNenno, P.J., and Williams, F.W., "Water Mist Flashover Suppression and Boundary Cooling System for Integration with DC-ARM: Summary of Testing," NRL Memorandum Report 8400, September 30 1999.
3. R.Ananth, H.D.Ladouceur, H.D.Willauer, J.P.Farley, F.W.Williams, "Effect of Water Mist on a Confined Blast", Presented before the Suppression and Detection Research and Applications – A Technical Working Conference (SUPDET 2008), March 2008 Orlando Florida.
4. G.O.Thomas, A.Jones, M.J.Edwards, "Influence of Water Sprays on Explosion Development in Fuel-Air Mixtures", Combustion Science and Technology, 1991, 80, Pages 47-61
5. D. SCHWER, K. KAILASANATH, 'Blast Mitigation by Water Mist (3) Mitigation of Confined and Unconfined Blasts, Center for Reactive Flow and Dynamical Systems, Laboratory for Computational Physics and Fluid Dynamics, NRL/MR/6410--06-8976, July 14, 2006
6. Heather D. Willauer, Ramagopal Ananth, John P. Farley, Gerald G. Back, Victor M. Gameiro, Matthew C. Kennedy, John O'Connor Frederick W. Williams, 'Blast Mitigation Using Water Mist: Test Series II', Navy Technology Center for Safety and Survivability, Chemistry Division, NRL/MR/6180--09-9182, 12 March 2009.
7. Det Norske Veritas Type Approval Certificate, Certificate number F-18732, 7 August 2008.
8. Det Norske Veritas Type Approval Certificate, Certificate number F-18536, 16 November 2007.
9. JR Mawhinney PJ DiNenno, 'New Concepts for Design of an Automated Hydraulic Piping Network for a Water mist Fire Suppression System on Navy Ships', Naval Research Laboratory, Ref NRL/MR/6180-01-8580, September 2001
10. Michelle Peatross and Dr Fred Williams 'An Overview of Advances in Shipboard Fire Protection', Hughs Associates Inc
11. Jim Banks 'Take Control: Smart valves Step Forward', offshore-technology.com, dated 18 June 2008, viewed





Peter Gilbert
Chief
Geotechnical Engineer
Water & Environment
Atkins

An update on new and future Earthworks Standards in the UK and Europe

Abstract

This paper was prepared to accompany the presentation delivered at the Ground Engineering conference "Slope Stability 2010" entitled "Understanding the implications of the updated BS 6031 for earthworks designs." Over the past four years the author has been actively involved in developing earthworks standards for the UK and Europe. This paper presents personal views on certain topics that are believed to be fundamental to understanding the direction that these earthworks standards have taken.

In the paper, aspects of BS 6031:2009¹ are referred to in a selective manner to illustrate the topics presented, no attempt has been made to cover all of its content because it is available for people to read and use. An insight into the current moves towards European standardisation in the field of earthworks is also provided. The author has endeavoured to deal with the UK and European activities in a joined up manner to show where there are similarities and differences; with the aim that this paper will provide a helpful briefing note for earthworks practitioners and encourage you all to read the new British Standard.

Background

In 2006 BSI called together a Steering Group tasked with undertaking an update of BS 6031, the Code of Practice for Earthworks (see Acknowledgements). The version available was published in 1981, but included a lot of content from the original version published in 1959; consequently it was out of date with industry practice. BS 6031:1981 was no longer widely referenced, being used most often to justify common practice of requiring a Factor of Safety of 1.3 for slope stability design; this was in fact an oversimplification of the Standard.

The challenge was to ensure that the revised BS 6031 document would be in line with both current good practice in the UK, and the framework that is created by the Eurocodes (as explained in the BS 6031 Foreword). The size of the document was to be reduced by including references to other existing documents. The revised BS 6031 was published in December 2009 as an all-encompassing code of practice covering all forms of earthworks (with the exception of the special requirements of dams).

Progress towards European Earthworks Standards

In recent years the European geotechnical community has started to link up to endeavour to share good practice and research in the field of earthworks. This process was initiated by the French who hosted an International Seminar on Earthworks in Europe in 2006. The second seminar took place in London in June 2009 with participation by delegates from many European countries (see **Figure 1**).

In 2008 the European Committee for Standardisation (CEN) requested that interested European countries provide delegates to a Working Group to explore whether it was appropriate to develop European earthworks standards. BSI requested that the author attend as the UK delegate to champion our earthworks form a major part of civil engineering projects but the topic is very poorly covered by CEN activities, and understanding of each other's National practices is poor (which is a barrier to trade). In addition many countries in



Figure 1. Publicity information from the 2nd International Seminar on Earthworks in Europe, June 2009. Photo of earthworks for reinforced soil slope at Midland Quarry in Nuneaton (Huesker Geosynthetics).

Europe have limited standards in the field of earthworks. Also there is an underlying concern that the changing nature of the earthworks industry is resulting in a significant reduction in the number of highly experienced earthworks practitioners. These factors would restrict the ability to utilise poor quality fills and thus inhibit environmental sustainability.

Following the Working Group Report, CEN established a new Technical Committee CEN/TC396:Earthworks in September 2009 with the task of delivering an appropriate level of standardisation. One of the stated aims is to harmonise national guidelines and recommendations throughout Europe to ensure mutual understanding and cooperation. A UK team of experts was together to cover the various work items.

Layout of BS 6031:2009

The initial meetings of the Steering Group identified that a full re-write of BS 6031:1981 was required, and agreed the overall nature of the content. It was considered important to ensure that all topics would continue to be covered.

The 1981 standard had covered temporary excavations with vertical or near vertical sides that require support in order to ensure stability (e.g. traditional trench shoring systems). Most engineers today would not immediately think of

these as an earthworks activity, therefore the specific content of the standard that is only relevant to such works is separated into Section 3 of the new standard (No further comments on this section of the revised BS is provided in this paper).

Section 1 and Section 2 of BS 6031:2009 respectively cover general matters and design/management of earthworks. These sections form the majority of the new standard and address the topics most engineers today would consider for earthworks. Section 2 includes temporary excavations which are designed to be self supporting. If the excavation requires soil reinforcement (e.g. soil nails) then general matters (including construction of fill and global stability) are covered by BS 6031, and reference is made to BS 8006-1 which was revised and published in October 2010 for all other aspects relating to reinforced soil (including internal stability).

The structure of the new standard was set out to reflect the sequence of processes that might be followed on a typical project to deliver the earthworks, as it moves from planning to design, then construction and on to use. It attempts to set out the contents to aid the various parties who may have some

involvement in determining the final nature of earthworks (client, consultant and contractor).

The approach followed is to consider earthworks activities within clauses that follow the "lifecycle of an earthworks project" (see **Figure 2**). This approach avoids the need for repetition of processes that are common to both construction of new earthworks and repair of existing earthworks; where there are significant differences these are highlighted.

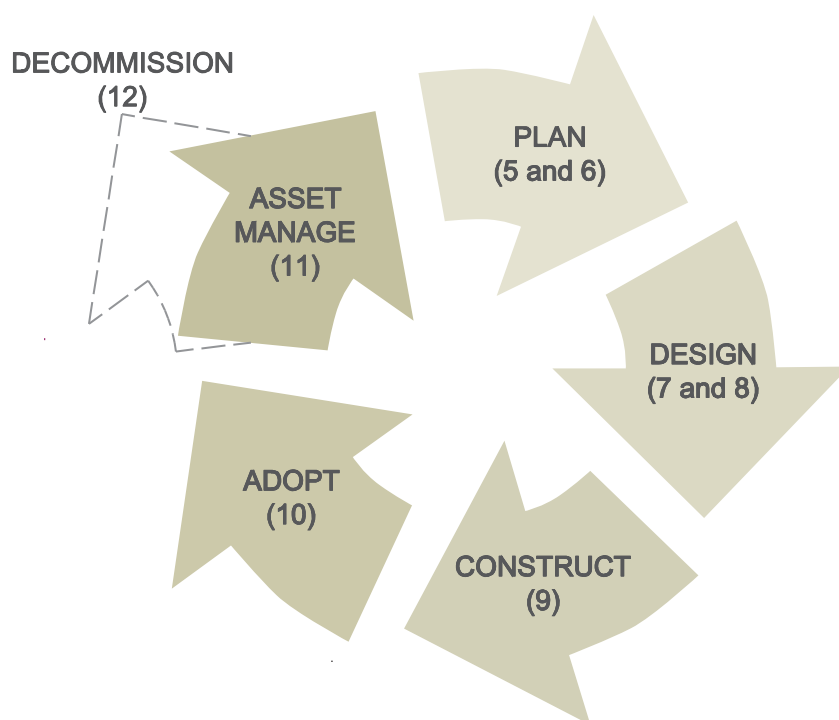
There are a number of underlying principles that run through BS 6031, which reflect the fact that decisions will be taken by a number of different individuals and companies on an earthworks project. These principles are:

- Management of risk through the life of the project;
- Requires earthworks design, construction and maintenance to be undertaken by personnel who are competent for the task;
- Plans schemes with a view to construction and to enable environmentally sustainable earthworks;
- Undertakes ground investigation that will meet the needs of all parties;
- Addresses the needs of new build, modification and asset management of earthworks.

BS 6031 relationship to other documents

The standard is set up to link with other fundamental documents, the most notable being:

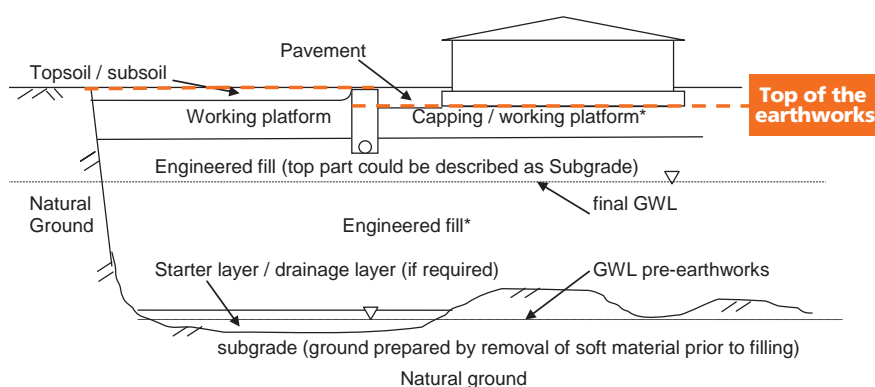
1. Specification for Highway Works (SHW) 600 series² – this is set as the default approach for earthworks specification unless stated otherwise by the Designer (see below).
2. Eurocode 7 (EC7) Parts 1 and 2^{3,4} – BS 6031 summarises the aspects of EC7 that form the overall framework for undertaking earthwork projects, provides interpretation of certain key points and adds some commentary to explain how to apply the "dry rules" of EC7; in so doing it forms non-conflicting complementary information (NCCI).
3. CDM Regulations 2007⁵ – all projects involving earthworks come under the requirements of CDM, BS 6031 advises on how this is best applied at the various life cycle phases of an earthwork project.



Note 1: Recommendations for each stage in the clauses numbered in the figure.

Note 2: During the asset management phase, if problems are identified that require construction work, the cycle has to begin again.

Figure 2. Flow diagram of lifecycle of an earthworks project (reproduced from BS 6031:2009)



*** Engineered fill specification considers:**

- Required level of compaction to deliver low air voids
- Acceptable moisture content range assessed based on both standard and modified proctor compaction tests
- Performance requirements for building (bearing capacity / settlement)
- Settlement of fill due to inundation of water to final groundwater level

Figure 3. Illustration prepared for TC396 to illustrate the special earthworks issues associated with infilling former quarries and common terminology used in the UK

Earthworks specifications

A fundamental topic for earthworks is the Specification that details how the fill is to be placed and compacted in order to form a body of fill. Different approaches can be followed depending on the particular situation being considered.

The use of the SHW 600 series for the construction of earthworks is widespread. The SHW is one of only two major documents in Europe that include a detailed Method Compaction system, the other being part of the French earthwork standards⁶, both of which were developed by extensive laboratory testing and site trials. The UK testing was between 1946 and 1990⁷, and in France mostly in the 1960s and 1970s, it is a process that is unlikely ever to be repeated. This has been recognised in BS 6031 by making the SHW the default approach for earthworks specification, other options are recognised and can be followed if an alternative specification is provided by the Designer. In this way it was possible to ensure that BS 6031 could meet the aims described above, and retain the advantages of the SHW which can be updated on a regular basis by the Highways Agency (HA) as new information becomes available.

Various sections of BS 6031 draw upon the work of the Building Research Establishment with regard to the special requirements for earthworks undertaken to form large bodies of engineered fill (e.g. infilling quarries) or to provide a platform for buildings. In these situations the designer's task of managing the self weight settlement of the fill and determining the required degree of compaction become particularly onerous. It is recognised that these are situations that extend beyond the intended scope of the SHW. **Figure 3** is an attempt to summarise the particular issues associated with this form of earthwork.

BS 6031 has been written as a framework that enables a project to use either a method, end product or performance specification, and to enable flexibility to suit the type and scale of the earthworks project. This is an approach that European earthworks standards hope to embrace (with the addition of continuous compaction control where appropriate). It is important to realise that even when end product or performance specifications are utilised there will be one member of the earthworks team who has to consider the method that will be required to compact the fill in order to achieve the required result (this is a design activity regardless of who undertakes it).

Design of earthworks

Clause 7 is the largest section of the revised BS, it deals with the topic of earthworks “design” and describes issues to be considered by the designer. The topics covered fall into two general groups:

1. Geotechnical design -this being principally assessing slope stability and settlement below an embankment. These activities have a significant numerical calculation aspect that needs to follow the approach set out within EC7 part 1.
2. Earthwork fill design -the management of the earthworks (including Specification) and the process of fill selection for a particular earth structure. This includes fill classification and identifying the requirements to achieve an adequate degree of compaction (which leads on to assessment of appropriate site control methods, estimation of self weight settlement, etc). It is fair to say that EC7 never intended to focus on these activities.

The concept of an earthworks design covering both of these elements is well established in the UK (partly because SHW Table 6/1 requires information to be added by the Designer). However, the action of “designing” earthworks does not translate well in Europe. For example, in French the closest applicable description for this task would be “conception”, but that is used only to describe the role of the architect for buildings. It has become evident from our involvement with European standards that in most countries earthworks are undertaken by following well established procedures (with the onus on the earthworks contractor to judge which procedure to follow) and using common fill materials, such that the role of the designer is limited to the geotechnical design. However, attempts to bring earthworks practices together across Europe, and the environmental requirement to use all available materials as fill, have resulted in recognition across TC396 that there is a process of decision making that extends beyond numerical calculation and is simplest to describe as “design”.

The current intention for the drafting of future European earthworks standards is to cover the earthworks fill design topics, and leave geotechnical design entirely within EC7 part 1. The agreed logic for TC396 to follow is to make the following separation:

- “Earth structures” are products. Earth structure design is covered by EC7;

- “Earthworks” is a process. Earthworks design is the process of determining what material is appropriate for construction of the earth structure, and will be covered by TC396.

It will be interesting to see how clearly the division can be made, e.g. will the standards extend to guidance on assessing self weight settlement or earthworks drainage requirements. The topic of earthwork fill design will draw heavily from certain sections of BS 6031, but we had the advantage of being able to provide a comprehensive “code of practice” covering all aspects related to design of earthworks (CEN standards are not traditionally of that format).

Fill classification

In drafting BS 6031 we realised that there is a need to clarify the differences in how a soil may be classified depending on whether the designer is undertaking geotechnical analysis or considering fill material suitability. This is a topic that tends to be taken for granted by geotechnical engineers in the UK, and a fairly consistent approach is followed. We endeavoured to capture this at BS 6031 clause 3.1 to set a fundamental underlying assumption. The clause clarifies how this approach does in fact follow the logic of EC7 and related documents. The key criterion for earthworks fills is whether a composite soil has sufficient fine fraction (passing the 63 micron sieve) to determine the engineering properties of the soil:

- >15% fines classifies a soil as a “cohesive fill” (in accordance with SHW);
- >~35% fines would generally be assessed as a fine soil for geotechnical design (the actual amount varies depending on grading curve and hence when the matrix dominates behaviour).

Study of other practices in Europe shows that there is general agreement on the matter of when a composite soil is classified as a fine grained fill; although there are national differences on the actual percentage of fines and the sieve size for this criterion. Another significant difference is that the UK is relatively unusual in placing little emphasis on plasticity to sub divide cohesive fills.

BS 6031 clarification of EC7

A significant part of the content of BS 6031 deals with the application of EC7 parts 1 and 2 on an earthwork project. The aim is to provide an explanation of how the dry rules of EC7 should be applied for earthworks, and clarify some aspects that are less easy to follow, which should help to ensure a common approach across the industry.

Clause 6 (Site Conditions and Investigations) describes the approach for undertaking and reporting on the site investigation for an earthworks project, it links this with commentary on earthworks testing and soil and rock classification (and hence onto the SHW).

Clause 7 (Design of Earthworks) covers a wide range of subjects including the following (the main BS

6031 clause numbers for these topics are given in brackets):

- Factors governing the stability of slopes and modes of failure (7.2.1 & 2);
- Actions, including surcharge loads (7.2.3);
- Selection of design parameters, including the influence of strain on soil strength (7.2.4);
- Options for modelling pore water pressures within an earthwork (7.2.5);
- Methods of design of soil and rock slopes (7.3.1 & 2);
- Application of partial factors in Design Approach 1 for slopes (7.3.3);
- Variation of partial factors where appropriate (7.4.1);
- Concepts of design life and serviceability for slopes (7.4.2);
- Earthworks drainage systems (7.5);
- Assessing overall stability and deformation (settlement) of bodies of fill (7.6.1–3);
- Selection of required fill material properties to ensure the engineering design assumptions are satisfied, including determination of acceptability limits, see **Figure 4** below (7.6.4);
- Selection of appropriate form of compliance testing for the works (7.6.5);
- Use of marginal fill materials (7.6.6–8, refers to relevant sources of information).

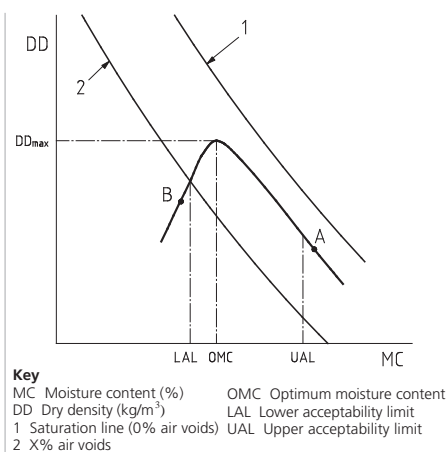


Figure 4 – Determination of acceptability limits for fine soils using relationship testing data (copy of BS 6031 Figure 10 reproduced purely for illustrative purposes)

Fill design, specification and construction

One theme throughout BS 6031 is to encourage good design practice to determine the required fill properties. This process requires the engineer to consider soil classification and fill design, and to carry the identified requirements through to the specification. Conventional compaction theory is used to show that there is a common logic that underlies this aspect of earthworks design (it is not simply a case of requiring >95% of maximum dry density) and this can provide a framework for the various different earthworks specification approaches used across Europe.

Having undertaken the tasks of design and construction the ultimate success of an earthworks project will always rely on the expertise of the Contractor's site team. It is for this reason that planning for construction is set as a focus right through the document. Clause 9 of the revised BS attempts to set out the broad range of topics that need to be considered and managed, the aim being to ensure that expertise developed over generations is not forgotten (a real risk under the current UK market conditions).

Future European Earthworks Standards

The second plenary meeting of CEN/TC396 in September 2010 was called to draw together the initial work of the five working groups of TC396. The tasks were to agree a set of documents for the working groups to develop, and to decide how these would interact to cover the subject areas. **Table 1** aims to summarise

	Title (UK delegates)	Comment on content
1	Principles and general matters* (Peter Gilbert, Atkins)	An "umbrella standard" giving general instructions, recommendations and guidance in order to express the philosophy of Earthworks (in a similar way to BS 6031). It will also introduce the other parts of the standard.
2	Classification of materials* (Richard Hocking, Cornwall Council & David Norbury, David Norbury Limited)	Description and classification systems applicable on all kinds of earthworks (it may encompass a variety of practices to suit different climatic and geological conditions). Test methods appropriate for earthworks will be identified, and test standards prepared or modified where appropriate.
3	Construction procedures* (Niall Fraser, Blackwells & Lee Parry, Mott MacDonald)	Specifications and guidelines for earthwork construction procedures for optimal use, excavation, transport, trafficability, laying, compaction, and additional operations to ensure adequate performance of the fill, in relation to classifications and national practices.
4	Soil treatment (with binders)* (Niall Fraser, Blackwells & Lee Parry, Mott MacDonald)	The treatment of natural, artificial and recycled materials with binders (lime, cement, hydraulic road binders, fly ash and slag), for earthworks construction and maintenance. Covering both fill improvement and stabilisation.
5	Quality control* (Alex Kidd, HA & Alan Phear, Arup)	Guidance on the techniques to be used to demonstrate that earthworks have been constructed appropriately. In situ and on site testing will be covered, and cross references made for appropriate texts on soil instrumentation.
6	Dredging and land reclamation, Mechanical excavation and filling underwater	A standard covering all aspects of underwater excavation and (hydraulic) placement of fill material by dredging or mechanical excavation and filling for the purpose of land reclamation and structural support. It will cross reference CIRIA's Hydraulic Fill and Rock Fill manuals.
7	Hydraulic placement of soils and mineral waste (Mike Cambridge, Cantab Consulting)	Placement of engineered soils and mineral wastes for the purposes of structural support and for mining waste disposal and reclamation.

Table 1. Expected core parts of a new family of European Earthworks Standards

Note - Parts 1 to 5 will cover earthworks undertaken on the land (rather than under water). It is intended that existing National method specifications (such as SHW) will become acceptable options under the European system. Any requirements of the standard will need to be written such that they do not prevent that approach, this will require flexibility in the agreement of classification systems.

the seven agreed parts that are expected to form the new family of documents (note: Part 1 is expected to be similar to BS 6031).

It should be noted that the total number of documents produced will exceed seven for the following reasons. Any laboratory or in situ tests will be covered under individual test standards in the normal

CEN way. Some items may prove to be best covered in separate standards, e.g. working with another TC to adapt an existing standard so that it extends to cover earthworks (e.g. for stabilised fills or laboratory tests). Working groups may opt to produce a European Standard and/or another form of document, such as a Technical Specification or Technical Report.

At this stage the agreed resolutions identify the parts as potential future new work items in the work programme of CEN/TC 396, as summarised in **Table 1**. These are described as 'potential' in line with CEN programme procedures; this gives flexibility for the final nature of the likely document(s) to be clarified as work progresses.

Table 1 provides an introduction to the work that is now in progress. Working groups from across Europe are now developing European standards on earthworks in which the UK is actively involved.

Conclusions

The updated version of BS 6031 provides the UK civil engineering industry with a Code of Practice that covers most common forms of earthworks undertaken in the UK. The SHW is set as the default specification for earthworks in the UK. This enables the application of a well established Method Specification that is underpinned by a wide body of knowledge. It also provides a framework for utilising end product or performance specifications. Standardisation of earthworks practices across Europe

are now in hand, our experience from developing BS 6031 is being fully utilised because it is seen as the sort of inclusive approach that is needed to harmonise European practices. In this way TC396 aims to enable good practice to be shared and various approaches accommodated to the benefit of all earthworks projects across Europe.

Acknowledgements

BSi policy is that British Standards no longer include the names of the authors so I'd like to take this opportunity to acknowledge the hard work of those who had the largest involvement with the preparation of BS 6031 (2009), who were as follows: Steering group members and authors: Donald Lamont (Chair, HSE), Phil Dumelow (Balfour Beatty), Peter Gilbert (Atkins), Tony Gould (Groundforce Shorco), Richard Hocking (representing the County Surveyors Society), Alex Kidd (HA), Brian McGinnity (LUL), Eifion Evans (NR). BSi content developer: John Devaney (BSi). Those who provided content for certain chapters: Bob Stork (Atkins), Andrew Charles (BRE), Lee Parry (Mott MacDonald). Reviewers/advisors regarding EC7 compatibility: Andrew Bond (Geocentrix), Brian Simpson (Arup), John Powell (BRE/GeoLabs). The team would also like to thank the Highways Agency and Network Rail who provided some funding for the task, and all those who reviewed the Draft for Public Comment, in particular Chris Danilewicz (Halcrow) who undertook a very thorough and helpful review.

References

1. BS 6031:2009 Code of practice for earthworks. British Standards Institute.
2. Manual of Contract Documents for Highway Works, Volume 1 -Specification for Highway Works, Series 600 – Earthworks. Highways Agency.
3. BS EN 1997-1:2004, Eurocode 7: Geotechnical Design -Part 1: General rules
4. BS EN 1997-2:2007, Eurocode 7: Geotechnical Design -Part 2: Ground investigation and testing
5. GREAT BRITAIN. Construction (Design and Management) Regulations 2007 (CDM)
6. Laboratoire Central des Ponts et Chaussées (LCPC). Practical manual for the use of soils and rocky materials in embankment construction (2003).
7. Parsons A W (1993). Compaction of Soils and Granular Materials – a review of research performed at the TRL.



Luke Davies
Graduate Engineer
Atkins



Tomasz Kucki
Senior Engineer
Atkins



Chris Fry
Head of Technology
Atkins



Jamie Bull
Senior Sustainability
Consultant
oCo Carbon

Lightweight backfill materials in integral bridge construction

Abstract

Analysis of integral bridge structures shows that lateral earth pressures on the end abutments have a dominant influence on the sizing of bridge components. Thermal cyclic movements induced by deck expansion cause densification of backfill material, leading to the build up of high pressures behind the abutments.

Measures to reduce these pressures by the use of alternative backfill materials can be highly beneficial to the structure as a whole, with extra expenditure on the backfill material being offset, and in some cases exceeded, by savings in material quantities in the rest of the structure and build time.

This paper examines three contrasting backfill options that were considered during the design of Cottington Road Overbridge in Kent: 6N granular backfill; lightweight expanded clay; and expanded polystyrene (EPS) blocks. Although more expensive than the other options investigated, the EPS block option was selected as the most economical solution for this particular structure due to material savings elsewhere in the structure.

Although it did not form part of the decision making process, this paper also shows a significant saving in transport-related carbon dioxide emissions through preferring EPS blocks to expanded clay.

Introduction

Maintenance issues with articulated bridge structures typically generate whole life costs due to the need to replace bearings and expansion joints, and provide for safe/adequate inspection access. Severe durability problems can also arise from the ingress of de-icing salts into the bridge deck and substructure.

In accordance with Highways Agency design procedure BA 42/96⁶, bridge decks up to 60m span with skew angles not exceeding 30 degrees are generally required to be continuous over intermediate supports and integral with abutments to address such issues.

Case study: Cottington Road Overbridge

Kent County Council is currently constructing Phase 2 of the major arterial highway corridor – East Kent Access (EKA).

Phase 2 involves upgrading two lengths of highway (the A299 and the A256), together with the provision of a new link between these two strategic highways.

See **Figure 1**: Cottington Road Overbridge location plan.

The existing single carriageway of the A299 fronting Kent International Airport between Minster Roundabout and Cliffsend Roundabout will be replaced with a new dual carriageway, and the existing A256 between Richborough Roundabout and Ebbsfleet Roundabout will be improved to two-lane dual carriageway standard. The new link will be provided between Cliffsend Roundabout and Ebbsfleet Roundabout, with a new roundabout at Sevenscore with an exit towards Lord of the Manor.

Nomenclature

d	Thermal displacement at top of wall
H	Retained height
K*	Earth pressure coefficient in accordance with BA 42/96
K ₀	'At rest' earth pressure coefficient
K _p	'Passive' earth pressure coefficient
L	Length of EPS layer
Q	EPS grade
q	Pressure
ε	Strain
Φ'	Effective internal friction angle

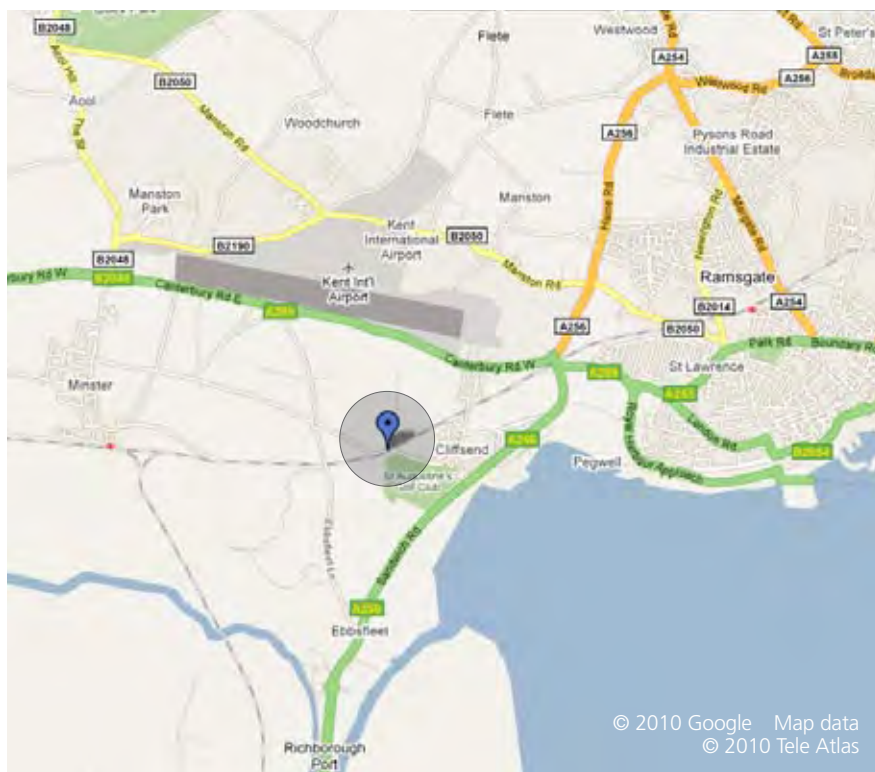


Figure 1. Cottington Road Overbridge location plan

This work involves two highway crossings of the Ramsgate to Minster railway line, requiring an underpass at Cliffsend and an overbridge at Cottington.

The structure

The structure proposed at Cottington is a two-span integral, steel and concrete composite deck, with a 30 degree end skew and a 32 degree intermediate pier skew. Each span is 30.7m long skew (26.6m square) measured along the EKA principal road centreline.

See **Figure 2:** Cottington Road Overbridge elevation.

The end abutments will comprise 1.5m thick, 10m high, reinforced concrete (RC) walls on 900mm diameter RC bored piles with independent RC wing walls. The intermediate pier will comprise 6 no. 750mm diameter RC columns at 7.5m spacing, with each column founded on a 900mm diameter RC mono-pile.

Ground conditions at this site are fairly uniform and comprise Made Ground

overlying Head, Thanet Sand and Chalk. This ground strata dictates the use of deep piled (rather than spread foot) foundations.

Backfill options

Three abutment backfill options were considered at design stage and a solution was chosen predominantly in terms of structure capital expenditure.

6N granular backfill

Usually, a granular backfill material is provided behind abutments. This limits selection to 6N or 6P material as described in Table 6/1 of the 'Manual of Contract Documents for Highway Works - Volume 1 - Specification - Series 600'⁵. As one of the most widely used and well understood backfill materials, this was first considered as it is a standard design solution.

Unfortunately, the high density of the backfill material coupled with the substantial height of retained material resulted in large moments being applied to the abutment wall piles, and equally

large hogging moments experienced at the deck/abutment interface. Resisting moments of this magnitude would require 28 no. 1200mm diameter RC piles with a two-layer cage of T40 reinforcement per abutment wall. Additionally, there would be a need to provide two rows of 900mm diameter piles spaced at 2m centres to support the wing walls, the design being dictated by the need to control lateral deflection at the top of the wall. This option was evidently a costly solution and alternative lightweight-backfill options were then considered.

Expanded clay

Expanded clay was first used in the 1950s to provide insulation to roads, railways and ditches. It is formed by heating and firing natural marine clay in a rotary kiln at temperatures up to 1150 degrees centigrade. The process transforms the clay into various-sized lightweight ceramic granules, which have a hard ceramic shell and a porous core. In this form, the material has excellent insulating properties and is also extremely lightweight with a unit weight of approximately 4 kN/m³ (compared to 19kN/m³ for 6N), greatly reducing lateral pressures on bridge abutments and retaining walls¹.

Expanded clay is much less dense than regular backfill material. However, the internal angle of friction (ϕ) is greater and leads to increased passive earth pressure. This coupled with the requirement to provide a 6N granular backfill capping layer, means that the initially realised savings are diminished.

There are a number of design considerations to take into account if specifying expanded clay backfill:

- The porous particles will absorb moisture after placement, increasing unit weight;
- Expanded clay should not be placed below the water table or in areas prone to flooding as the particles may become buoyant;
- The particles have a lower crushing strength compared to natural soils, and so ordinary test methods such as the California Bearing Ratio test are not suitable;



Figure 2. Cottington Road Overbridge elevation

Material	6N Granular backfill	Expanded Clay	EPS blocks
Advantages	<ul style="list-style-type: none"> Well understood material Cheap and readily available Ability to use normal compaction plant and testing methods 	<ul style="list-style-type: none"> Eliminates settlement period Free draining 1m compaction layers Chemically inert Resistant to fire and frost Re-usable, no special requirements for disposal Placed using same methods as normal backfill 	<ul style="list-style-type: none"> Placed by hand No compaction required Inhibited water absorption Immune to attack from bacteria and mould Minimises settlement issues Can be recycled
Disadvantages	<ul style="list-style-type: none"> High unit weight 0.25m compaction layers Susceptible to settlement issues Susceptible to frost heave issues 	<ul style="list-style-type: none"> Heavy winds can blow the finer material increasing dust levels Aggregate dust containing quartz can constitute a long term health risk No accepted test for measuring density in-situ 	<ul style="list-style-type: none"> Susceptible to attack from hydrocarbons Expensive
Unit weight, γ_d (kN/m ³)	19	4	0.5
Angle of friction, ϕ (degrees)	35	37	N/A
Cost (£/m ³)	35	40 - 50	60 - 80

Table 1. Backfill materials comparison

- A capping layer is required (see previous) to spread traffic loads sufficiently to ensure that the particle (in its mass) crushing limit is not exceeded.

In the case of Cottingham Road Overbridge, assessment showed that the use of expanded clay backfill allowed the foundations to be reduced from 28 no. 1200mm diameter piles (in the case of 6N granular backfill) to 21 no. 900 mm diameter piles (per abutment), although heavy reinforcement would still be required and the wing walls would still require two rows of piles to control deflection.

EPS blocks

Focus then turned to the use of EPS blocks. EPS can almost eradicate lateral pressures on civil engineering structures as surcharge loads are taken vertically to the ground beneath.

EPS has a proven track record as a fill material and has been used in the construction of embankments since the 1970s offering the benefits of removing specialised foundations, eliminating long surcharge periods and reducing settlement problems after construction².

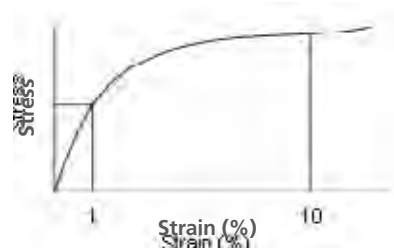
Lateral pressure is applied to the abutment walls by the EPS blocks in response to longitudinal temperature

movements and braking forces introducing stresses with accompanying strains in the EPS blocks.

See **Figure 3**: Typical EPS stress strain curve³.

There are a number of design considerations to take into account when specifying EPS blocks:

- Chemical attack: EPS is vulnerable to attack from hydrocarbons. So, if it is to be used in highway or railway embankments, it must be protected by concrete encasement, or by use of high density polyethylene (HDPE) sheets;
- UV resistance;
- Fire protection;

**Figure 3.** Typical EPS stress strain curve

- Density: where higher load bearing capacities are required, higher grade EPS blocks are specified but these have a higher density;
- Localised damage: the use of HDPE will also require a capping layer of granular backfill to spread applied loads sufficiently to prevent localised damage to the EPS blocks or HDPE membrane.

The use of EPS as an alternative backfill material had significant economic benefits for the Cottingham Road Overbridge structure. The abutment foundations were able to be reduced from the 28 no. 1200 mm diameter piles of the '6N' backfill option to 21 no. 900mm diameter piles using a single layer cage of T40 reinforcement, and the wing wall foundations could be reduced to a single (rather than double) row of piles eradicating the need for a pile cap.

See **Table 1**: Backfill material comparison.

Alternative backfill study

In order to provide a numeric comparison of loads applied to an integral bridge structure by the three backfill materials discussed, and the varying effects that this has on the structure, a simple integral bridge structure will be analysed and the results discussed below.

The integral bridge structure analysed for the purpose of this study is an overall 60m, (equal) two span bridge, 25m wide with no skew. Main girders are spaced at 2.75m. Abutments are 1500mm thick RC walls and founded on 18 no. 900mm diameter RC piles each. The central pier consists of 9 no. 750mm diameter RC columns, each column being founded on a single 900mm diameter RC pile.

SuperStress is used to model the structure as a frame with fixed connections between deck and supports, the piles are modelled using spring supports.

See **Figure 4**: Simplified study General Arrangements.

For transparency, results are given for lateral pressures on the abutments only, all other dead and live loads being ignored.

It should be noted that pressures exerted on the abutment walls by EPS blocks will only be experienced in Combination 3⁶ of BD37/01 Loads for Highway Bridges as this is the only case where restraint to movement temperature effects are taken into account.

6N granular backfill

Earth pressures exerted on the abutment walls are related to compression stresses in the retained soil. However at the top of the wall, higher earth pressures will be experienced because of wall friction.

'BA42/96 - The Design of Integral Bridges'⁷ suggests earth pressure distributions for different structural forms. For the purposes of this study a full height frame abutment form is assumed. Clause 3.5.3 of BA 42/96 suggests a distribution comprising:

- A uniform value of K^* over the top half of the retained height of the wall, with;
- Lateral earth pressure then remaining constant with depth as K^* drops towards K_0 ;
- If the lateral earth pressure falls to K_0 then below that depth pressures are applied in accordance with the in situ value of K_0 .

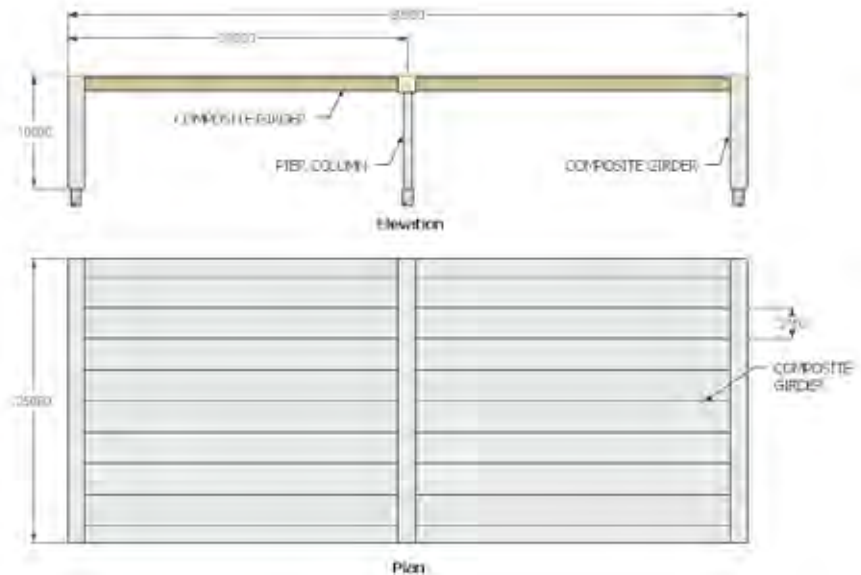


Figure 4. Simplified study General Arrangements

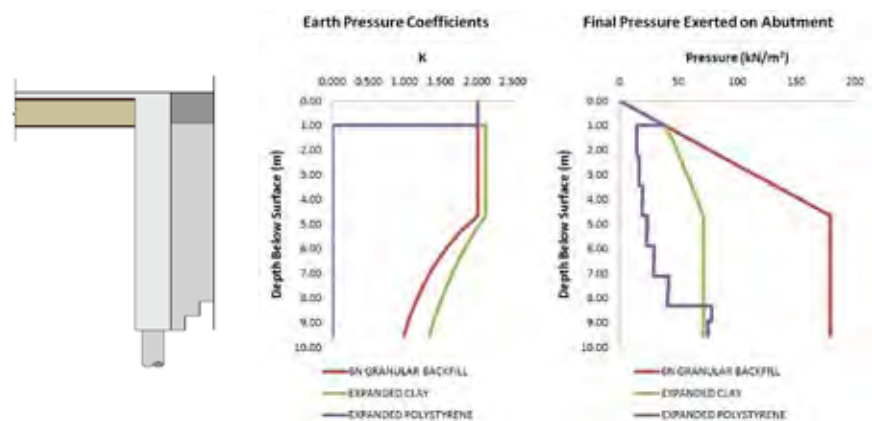


Figure 5. Earth pressure distributions

BA 42/96 gives an equation to calculate the relationship between K^* , the height (H) and thermal displacement at the top of the abutment (d):

$$K^* = K_0 + (d/0.05 H)^{0.4} K_p$$

This equation uses K_p obtained using the Eurocode 7 approach, for 6N granular backfill with $\phi' = 35^\circ$, $K_0 = 0.426$ and $K_p = 6.5$.

BA 42/96 clause 2.10 states the characteristic thermal strain for composite deck construction in the UK can be taken as ± 0.0005 , therefore:

$$d = 0.0005 \times 30000 = 15 \text{ mm}$$

$$K^* = 0.426 + (15/0.05 \times 10000)^{0.4} \times 6.5 = 2.02$$

Lateral earth pressure at the top of the wall = 0 kN/m^2

Lateral earth pressure half way down the wall = $K^* \gamma_{\text{soil}} z = 2.02 \times 19 \times 5 = 191.9 \text{ kN/m}^2$

This earth pressure then remains constant to the base of the wall since it does not fall below the earth pressure value calculated using its K_0 coefficient up to this point.

See **Figure 5 (a)**: Earth pressure distribution - 6N granular backfill.

Expanded clay

The calculation of build-up of lateral earth pressures behind the abutment when using expanded clay is identical to that for normal granular fill, in accordance with BA42/96.

The expanded clay backfill 'wedge' abuts the vertical rear face of the abutment wall and is set to a '1 in 1' incline in relation to the 'normal' embankment fill behind. A 1000mm capping layer of 6N granular backfill is assumed to prevent crushing of the expanded clay by applied dead and live loading.

Lateral earth pressure at the top of the wall = 0 kN/m²

Lateral earth pressure at capping layer interface = $K^* \gamma_{\text{soil}} z = 2.02 \times 19 \times 1 = 38 \text{ kN/m}^2$

K^* then increases to reflect the expanded clay material properties with $\phi' = 37^\circ$, $K_0 = 0.398$ and $K_p = 7.0$:

$K^* = 0.398 + (15 / 0.05 \times 10000)^{0.4} \times 7.0 = 2.12$

Lateral earth pressure half way down the wall =

$K^* (\gamma_{\text{exp_clay}} z_{\text{exp_clay}} + \gamma_{\text{soil}} z_{\text{soil}}) = 2.12 (4 \times 4 + 19 \times 1) = 74 \text{ kN/m}^2$

This earth pressure then remains constant to the base of the wall (as per '6N granular backfill').

See **Figure 5 (b)**: Earth pressure distribution – Expanded clay.

EPS blocks

14 layers of EPS blocks abut the end supports, each layer increasing in length at '1 in 1' benching steps to the interface with embankment backfill. Using this slope gradient limits lateral earth pressures exerted on the back of the EPS blocks.

A 1000mm capping layer of 6N granular backfill is assumed to prevent localised damage of the EPS blocks and HDPE membrane by applied dead and live loads. Lateral earth pressures exerted by this layer will be identical to those in 3.1 and 3.2.

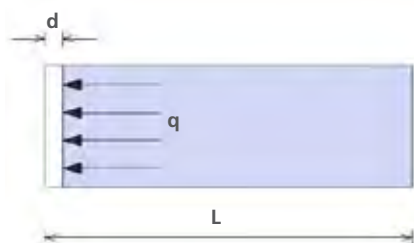


Figure 6. Development of EPS pressure

Node	Depth (m)	Deflection (mm)	Layer length (mm)	Strain (%)	Pressure (kN/m ²)
1	0.00	-	-	-	0
2	1.00	-	-	-	38
3	1.64	13.9	8540	0.16	20
4	2.29	13.7	8540	0.16	19
5	2.93	13.6	7320	0.19	22
6	3.57	13.4	7320	0.18	22
7	4.21	13.2	6100	0.22	26
8	4.86	12.9	6100	0.21	25
9	5.50	12.7	4880	0.26	31
10	6.14	12.4	4880	0.25	30
11	6.79	12	3660	0.33	39
12	7.43	11.7	3660	0.32	38
13	8.07	11.3	2440	0.46	56
14	8.71	11	2440	0.45	54
15	9.36	10.6	1220	0.87	104
16	10.00	10.2	1220	0.84	100

Table 2: EPS lateral earth pressures exerted on abutment wall

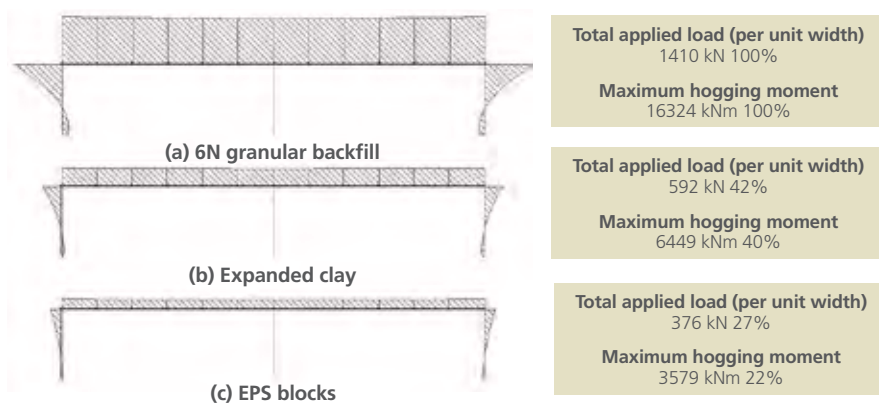


Figure 7. Bending moment diagrams

Lateral earth pressure at the top of the wall = 0 kN/m²

Lateral earth pressure at capping layer interface = $K^* \gamma_{\text{soil}} z = 2.02 \times 19 \times 1 = 38 \text{ kN/m}^2$

Pressure exerted on the abutment wall by the EPS blocks occurs as described previously. Abutment wall deflections due to thermal expansion of the deck (d) are used to calculate the strain (ϵ) in each EPS layer, this then relates to a pressure (q)

depending on the grade of EPS selected.

See **Figure 5 (c)**: Earth pressure distribution – EPS blocks.

Figure 6 shows a polystyrene block length (L) being deformed by a distance (d).

For example, assuming EPS grade (Q) of 90 kN/m², deflection (d) of 10mm and layer length (L) of 6000mm:

$$\epsilon = d / L = 10 / 6000 = 0.167\%$$

$$q = \epsilon Q = 0.167 \times 90 = 15 \text{ kN/m}^2$$

See **Table 2**: EPS lateral earth pressures exerted on abutment wall.

Results

Analysis of the effects of the three different backfill materials on the structure is carried out using structure analysis software.

Figure 7 shows the bending moment diagrams produced when the various backfill loads are applied to the structure.

Applying 6N granular backfill to 10m high integral abutments produces huge moments in the deck and at the top of the wall. In this case there is a maximum hogging moment at the top of the wall of over 16.3 MNm per metre width. In order to withstand moments of this magnitude, very large heavily reinforced sections are required.

Using expanded clay backfill to abut the end supports reduces the applied load to 42% of that seen using 6N backfill, reducing the maximum hogging moment by 60% to 6.4 MNm per metre width.

When EPS block loads are applied to the structure the bending moments produced in the structure are significantly lower than those produced by either 6N granular or expanded clay backfill. In this case the maximum hogging moment is 22% of the 6N value at 3.6 MNm per metre width.

Environmental impacts

As well as final structure cost, there are other factors that need to be considered when selecting an appropriate backfill material. Over the past decade, initiatives to curb global warming, and make new construction more sustainable, have led to an increased interest in the environmental impacts of new structures. This section looks primarily at the carbon emissions associated with the two lightweight fill options.

Carbon footprint

The carbon footprint of a construction project includes all sources of emissions including those associated with:

- Production, processing and transport of materials;
- The process of construction itself;
- Any maintenance required;
- Disposal of materials at the end of their service life.

Scope and functional unit

This study looks at the carbon footprint of the two lightweight backfill options – expanded clay and EPS. The scope is limited to the carbon footprint of the materials used and transport of

Embodied carbon of EPS and expanded clay backfill

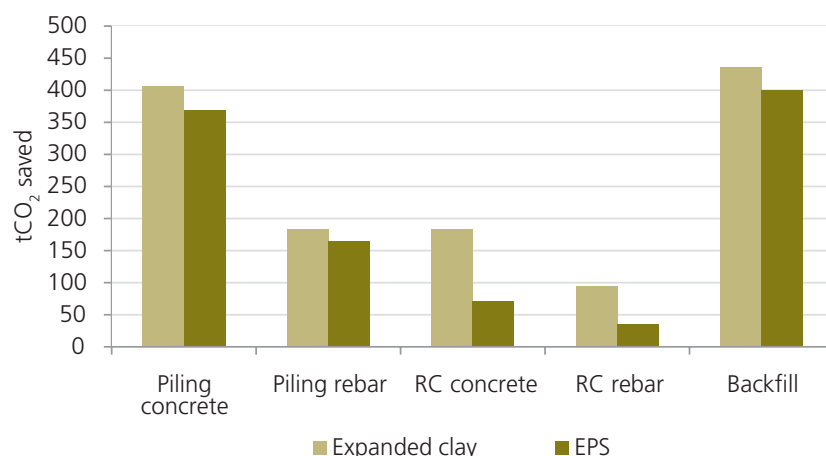


Figure 8. Embodied carbon footprint comparison

Transport carbon of EPS and expanded clay backfill

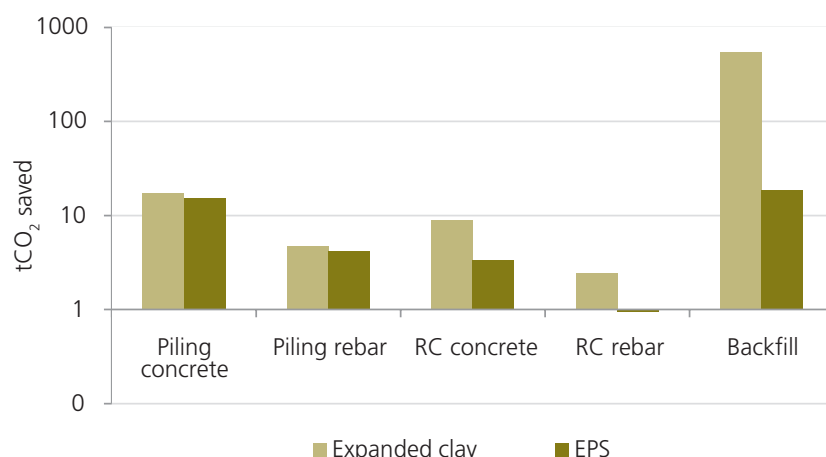


Figure 9. Transport carbon footprint comparison (note the logarithmic scale)

those materials. Emissions during the construction process are expected to be similar for the two options, and there are methodological issues with end of life costs such as the impossibility of predicting how materials such as EPS will be recycled in the future, especially given the long service life of a road bridge.

In a carbon footprint assessment it is important to define the functional unit to be assessed. As there are several factors affecting the amount of materials used in the Cottingham Road Overbridge, the only suitable functional unit is the bridge structure taken as a whole. Both options are assumed to have the same service life (the risk of failure due to hydrocarbon ingress has been assumed to be designed out).

The main change between the two cases is that less material is required in the

EPS case due to the reduced structural requirements and also the lower density of the backfill material.

Embodied carbon emissions

Many of the materials used in construction are highly processed and so contribute to carbon emissions by the energy required to process them. The figures used are sourced from the Inventory of Carbon and Energy⁴. Average values are used for the embodied carbon of materials rather than assessing the individual raw materials extraction and manufacturing processes of the products specified. This means that the results and recommendations can be more easily generalised to other situations.

The raw material used in the protection of expanded clay is quarried but further energy-intensive processing is needed for expanded clay to achieve its final

state. Due to lack of specific data, the embodied CO₂ of expanded clay has been taken as that of "General simple baked clay products" at 0.22kgCO₂/kg.

Conversely, the production of plastics is an energy intensive process. The embodied CO₂ per kg is over 10 times that of the expanded clay at 2.5kgCO₂/kg. This might be expected to make EPS blocks the least sustainable option in terms of backfill material, however it neglects the difference in weight.

As with cost the footprint should be measured per m³ which makes the two options much closer. On this metric the expanded clay gives 88kgCO₂/m³ and the EPS gives 75 – 100kgCO₂/m³ depending on the density of EPS specified.

See **Figure 8**: Embodied carbon footprint comparison.

Transport carbon emissions

Construction materials can also be heavy which leads to a lot of transport related carbon emissions. In the case of bridge structures, the two materials which make up the majority of transport emissions are reinforced concrete and backfill as they are the major components by weight.

Unprocessed aggregates, despite their low embodied carbon per tonne, are heavy materials and so the carbon footprint of transporting them can be quite high. This also means that the total emissions are very sensitive to the distance they are transported. For the most part they are not transported far from the place they are produced.

6N granular fill is a quarried material, with a number of source locations scattered over the UK meaning that transport distances are kept to a minimum.

Of the processed materials, there are a number of concrete plants in the East Kent area and so this does not require much transport. EPS and expanded clay have to be transported greater distances to site.

See **Figure 9**: Transport carbon footprint comparison.

Resource use

The use of non-renewable materials has impacts beyond embodied carbon and emissions associated with transport. All materials must be disposed of at the end of their service life. None of the materials used are renewable, although they can all be re-used or recycled to some extent.

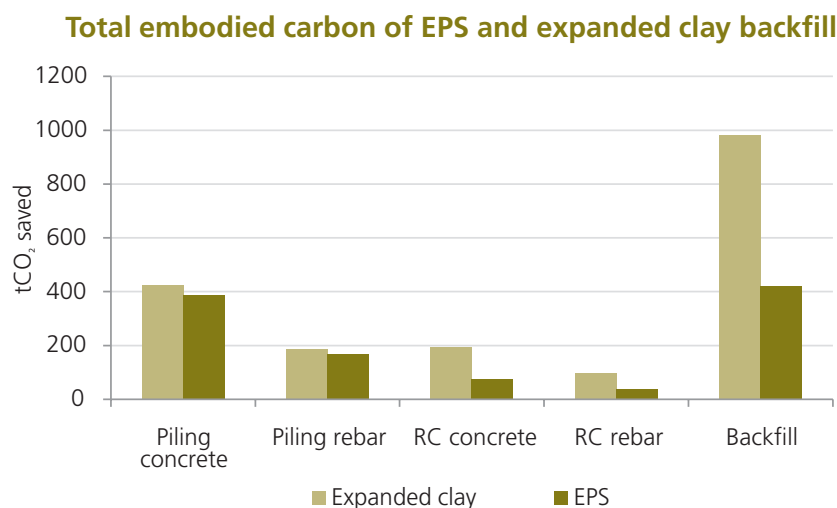


Figure 10. Carbon footprint comparison

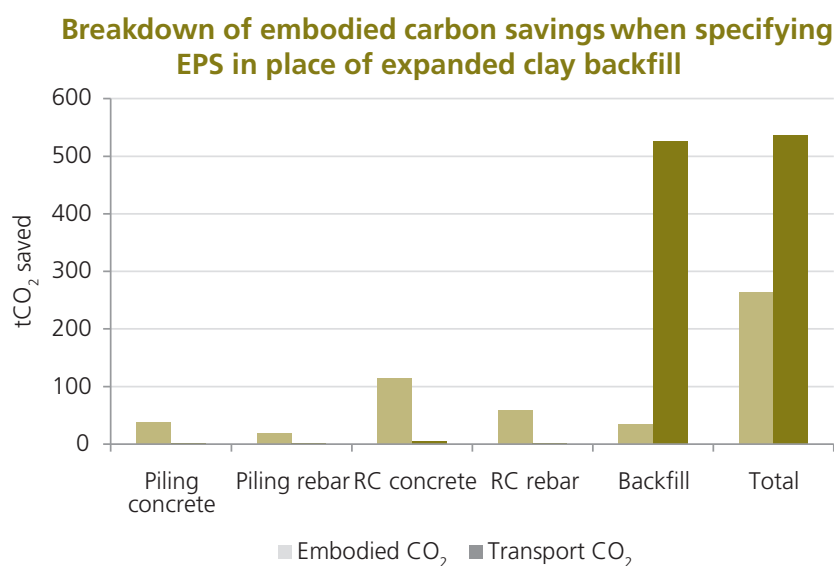


Figure 11. Breakdown of carbon footprint savings

6N granular fill and expanded clay are easy to reuse or dispose of while EPS blocks are not easy to reuse, and would need to be disposed of correctly or recycled. This could include incineration with energy capture which would offset its carbon footprint to some extent.

Other environmental impacts

There are a number of other impacts which are beyond the scope of this paper. These include toxicity of materials used, emissions to air other than carbon dioxide (such as sulphur dioxide, nitrous oxides, etc). Without carrying out a more in depth life cycle analysis it is impossible to say which of the options will have the lowest impact in these other categories.

Results

The expanded clay option has a carbon footprint of 1,880 tonnes while the EPS option has a carbon footprint of 1,083 tonnes. Relative to the expanded clay, the EPS design saves approximately 800 tonnes of carbon dioxide emissions.

See **Figure 10**: Carbon footprint comparison.

The vast majority of the savings comes from avoided transport of heavy materials. In fact the savings on transportation of fill material to site has the greatest impacts on the carbon footprint of the finished structure. Fill and expanded clay are both heavy materials, relative to EPS. Embodied carbon is proportional to the weight of material used and so the embodied carbon of

the EPS option is significantly lower than the expanded clay option due to its lower density.

See **Figure 11**: Breakdown of carbon footprint savings.

Conclusions

Although the results show the use of EPS blocks abutting the end supports of an integral bridge structure greatly reduces pressures exerted on the walls and design loads experienced by the bridge components as a result, it is often less economical to use this as a solution than expanded clay backfill material. Regarding the integral bridge at Cottington

Road, the EPS block and expanded clay solutions had very similar cost implications on the project; however, EPS blocks were selected because of problems experienced in controlling deflection of the independent wing walls.

EPS blocks provide a good solution to design problems such as retaining wall deflection or restraints of bearing pressure; however, in the absence of these issues the use of EPS blocks is unlikely to be financially worthwhile.

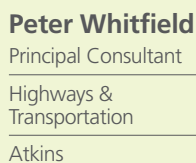
The recent increased emphasis on making structures more sustainable is likely to encourage the use of EPS blocks due to the major reduction in transport-related emissions. This may tip the balance in

favour of EPS in cases where the cost argument is marginal, or policy measures may be introduced which give the embodied and transport carbon saved a greater financial value.

Acting as a counter to this, the issues that arise with the need to protect the material from hydrocarbons and the huge effort required to rectify problems should the protection fail will make Technical Approval Authorities very reluctant to authorise this as a design solution. A robust technical solution to this problem would allow large reductions in the transport carbon footprint of backfill.

References

1. Maxit. (2004). Maxit LWA – Lightweight fill for civil engineering [Brochure].
2. S+B. (2010). Product Handbook – Civil Engineering [Brochure].
3. Jablite. (2010). Technical Information – Civil Engineering using Fillmaster EPS [Brochure].
4. Hammond, G.P. and Jones, C.I. (2008), Inventory of Carbon and Energy V1.6a [University of Bath]
5. Department of Transport, Manual of Contract Documents for Highway Works, Vol 1, Specification of Highway Works, Series 600, 2009.
6. BD 37(0) Loads for Highway Bridges, Highways Agency, UK
7. BD 42/96 The Design of Internal Bridges, Highways Agency, UK



Abstract

Introduction

Figure 1 shows the main components of the system.



Component parts

The purpose of each stage is outlined as follows:

Safety plan

This important document sets out for a client how the safety management process will be organised covering the following issues:

- Agreement of key staff and their competencies;
- Arrangements for project safety committees, stakeholder liaison and any workshops;
- Identification of data, documentation and published standards for design, safety and operations;
- Identification of key safety challenges ahead based on known existing safety problems or perceived risks associated with innovative proposals;
- Definition of safety baseline (typically existing accident frequencies) against which the project safety targets will be measured post-opening;
- Definition of safety objectives, both numerical and non-numerical, for the opened project and any overarching programme or client safety initiatives;
- Agreement of suitable methods for risk assessment (Hazard log);
- Links to other processes such as Road Safety Audit, Maintenance Strategy etc.;
- Links to any "micro" safety cases for the design of telematics.

Any scheme that is associated with complex operational regimes is likely to require significant consideration of future risks to road workers, emergency services and civilian traffic officers. Therefore the Safety Plan should set out appropriate safety objectives for these users as well as public users.

Hazard log

Depending on the type of project and its level of similarity to other completed infrastructure projects already in operation it is necessary to:

- Develop a bespoke hazard log; or
- Amend an existing generic hazard log (one published by the Highways Agency).

The total risk to road users within the completed project can be considered as " $R_{TOTAL(AFTER)}$ " and this is made up of individual risk components from hazards H1, H2, H3 etc.. Using this approach, as shown in **Figure 2**, it becomes easy to

understand where the main problems may arise and where the design effort should be focussed.

The relative widths of the bars in **Figure 2** represent the relative importance of each hazard. The risk score for each individual hazard takes account of:

- Frequency of incidents that may lead to harm;
- Probability of such incidents subsequently giving rise to harm;
- Severity of any injuries that may result.

The assessment considers $R_{TOTAL(AFTER)}$ and $R_{TOTAL(BEFORE)}$ and it is therefore possible to predict ahead of scheme opening if the safety objective can be met. For example in broad terms if a scheme has a safety objective of reducing accidents by 15% then the hazard log would need to predict at least a 15% risk reduction as measured by the difference between $R_{TOTAL(AFTER)}$ and $R_{TOTAL(BEFORE)}$.

The prevalence of a large number of small bands to the right of **Figure 2** is also useful in demonstrating that many issues are in fact low safety risks. This is very useful in responding to potential issues that are perceived by stakeholders to be initially significant.

As with any risk assessment the process is useful in developing a thorough understanding of accident modes and in turn this leads to the generation of mitigation measures to control the risk by attempting to break the causal chain associated with the accident mode. For example in the case of a hard shoulder running scheme, the risk of a stationary vehicle on the hard shoulder is reduced by providing emergency refuge areas and also by carrying out a systematic CCTV

camera by camera review before opening the hard shoulder to traffic at a reduced mandatory speed limit.

This process leads to the development of a list of essential inclusions and prohibitions for both the infrastructure design and operating protocols. These are termed "Safety Requirements".

Safety report (safety case)

This document is normally produced at more than one stage dependant on the scale of the project. For large projects it would be normal to produce it at the end of the design stage, pre-opening and post-opening. It describes:

- The forecast (or actual) safety performance of the scheme against safety targets;
- The Safety Requirements related to the infrastructure design or operating protocols that are intrinsically linked to the good safety performance of the project;
- How verification (audit) of Safety Requirements will (or has) taken place to ensure compliance;
- Any residual actions and safety monitoring;
- Information storage requirements.

Process versus culture

The use of a Project Safety Risk Management System should not be considered as merely a mechanical process. The use of this technique gives rise to a number of other benefits:

- It embeds safety in decision making, without dictating that safety should be the only concern;

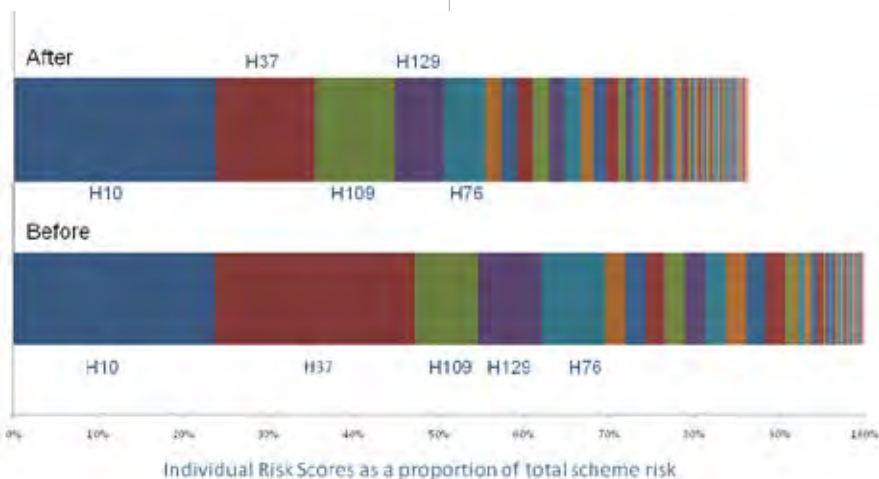


Figure 2. Example of before and after risk scores associated with individual hazards

- It allows prudent judgement to be applied to a number of design options;
- It allows stakeholders to understand issues that may affect them;
- It allows participants to challenge the “common wisdom” and standards;
- It drives cross discipline working and is therefore “lean” in its approach.

Decision making

The project Safety Plan (see above) should set out how a project makes decisions. It is normal to set up a Project Safety Risk Control Group with representation from maintainers, stakeholders and client representatives from different backgrounds. Such a group can add value to decision making whilst ensuring that safety related issues are balanced against other scheme objectives.

Experience to date

Atkins has worked on a number of projects using this methodology. These include:

- M62 J25 to J30 Managed Motorway, Highways Agency (design stage);
- M4/M5 Managed Motorway Scheme, Highways Agency (design stage);
- M6 Junctions 10a to 13 Managed Motorway Scheme, Highways Agency (feasibility stage);
- M4 Variable Mandatory Speed Limits Newport, Traffic Wales/Welsh Assembly Government (controlled motorway now open to traffic);

- Research into feasible options to improve motorway to motorway traffic flows using traffic signals.

In the case of the M4 Variable Mandatory Speed Limits (Controlled Motorway) project between J24 and J28, **Figures 3 and 4** show the novel use of verge signals that can rotate through ninety degrees and can be wound down to ground level. This allows maintenance to be carried out with minimal effect on traffic lanes and also reduced risks to operatives.

Although the implementation of a Controlled Motorway by use of lane dedicated message signs (as shown on the portal gantry in **Figure 5**) follows the practice of earlier Controlled Motorway schemes, **Figure 5** also shows that the project utilised existing variable message signs in the verge and on both new and existing portal gantries. The operational use of combinations of signals, both day to day and during incidents, was a particular challenge to ensure that the algorithms did not lead to confusing message sequences.

Does this replace road safety audit?

This technique complements road safety audit but does not replace it. Whilst it is possible to adopt a level of independence from design teams when using Project Safety Risk Management Systems, this is not necessarily desirable as understanding and influencing safety risk is linked to influencing the design and operating protocols from project inception. This also means that using an independent road safety audit team is still beneficial and in any case is still required by standards



Figure 3. Verge signal rotated to operational position (M4 Newport)


(HD19/03)¹. As with all road safety audits, the quality of the audit is dependent on the knowledge and skills of the personnel and the brief set down. Atkins has found it useful to ensure that the audit team is aware of the hazard log and also ensured that the audit team is familiar with the operational aspect of the scheme genre. It is also noted that the hazard log results have been helpful in qualifying a designer's response after a road safety auditor has identified risks without quantification. Road safety auditors are likely to possess the skills to assist with the generation of scheme hazard



Figure 4. Verge signal rotated away from carriageway to facilitate maintenance (M4 Newport)



Figure 5. Combination of existing variable message signs in verge and on gantries (M4 Newport)



logs and consideration should be given to their use in this way, although any individual involved in production of risk assessment would normally not go on to play a part in the subsequent road safety audit due to the issue of independence.

Future use of these techniques

This technique is highly adaptable to a range of project sizes and types. As with all risk assessment techniques it should be used appropriately for the circumstances. It is envisaged that the process could be

usefully adopted for large scale urban event management and for schemes with a high level of operating interfaces, such as public transport interchanges and on-street mass transit.

As well as informing funded infrastructure projects the technique is very useful in developing strategic policy interventions so that safety impacts can be estimated whilst developing strategies. Examples may include tolled lanes, pedestrian guardrail provision or setting levels of maintenance intervention.

Conclusion

Safety should be at the core of all projects and suitable systems to understand where risks might lie are likely to be of substantial benefit. Unwarranted and unquantified safety concerns have in the past been a potential barrier to innovation. Good governance of safety management from the earliest days of project inception can be a useful aid to informed decision making and promotion of suitable project options.

Acknowledgment

This paper was published in an abridged article form in Local Transport Today Issue 570 - 6 May 2011: Road Safety Supplement

References

1. Design Manual for Roads and Bridges Volume 5 Section 2 Part 2 HD 19/03 Road Safety Audit



Bonnie Eldridge

Senior Ecologist

Water and Environment

Atkins



Jules Wynn

Associate

Water and Environment

Atkins

Monitoring the use of badger tunnels on Highways Agency schemes

Abstract

It has become standard practice over the last 20 years to incorporate badger tunnels into major road schemes to mitigate the effects of habitat severance on badger populations. In order to investigate the effectiveness in terms of use by mammals (primarily badger), as well as review the tunnel design advice provided by the Highways Agency, a monitoring scheme was undertaken in 2010 on nine Highways Agency road schemes.

Background

In the UK, the Highways Agency routinely evaluates the efficacy of conservation initiatives to assess the extent to which objectives have been met. In 2010, the Post Opening Project Evaluation identified badger tunnels (culverts installed under roads to allow safe passage) as an intervention that merited further investigation to establish a) the effectiveness in terms of use by mammals (primarily European badger *Meles meles*), as well as b) the efficacy of tunnel design advice provided within the Highway Agency's Design Manual for Roads and Bridges (DMRB)³.

The primary reason for incorporating tunnels beneath highways during construction is to reduce the effects of habitat fragmentation on mammals and to minimise the risk of road traffic accidents caused by animals attempting to cross a road. When installing badger tunnels, the DMRB recommends a number of design features to guide mammals through culverts or overpasses to prevent them from directly crossing a road³. Badger tunnels should be made using 600mm diameter concrete pipes. Appropriate landscape planting should be carried out to soften the approach to the tunnel, while fencing should be installed to direct mammals to the tunnel entrance and prevent them from accessing the road. The location of badger crossings is crucial to success; it is preferable if a crossing can be located on, or as near as possible to, the site of an active badger path. The DMRB does not provide guidance on the optimal or maximum length of a badger tunnel³.

As badgers are one of the species most commonly killed on roads in the UK, this study focuses primarily upon the use of tunnels by badgers, although other mammal species are also considered.

The monitoring methodology used in this study is based upon that developed previously for mammal underpasses by Baker, Knowles & Latham¹. This involved monitoring the use of a mammal underpass using clay mats to record the imprint of mammal tracks; a simple and low-cost technique. The present study had two aims, firstly to establish whether badgers use crossings, and secondly, to identify any specific problems or factors associated with tunnel design that reduce or increase the likelihood of use by mammals.

Site selection

Nine major road schemes (dual carriageway or motorway) throughout England were chosen for study. These roads incorporated 38 mammal tunnels installed between 2003 and 2007 (**Table 1**). The tunnels varied in design in terms of materials, width and length but were straight on plan. The 38 tunnels included both concrete and corrugated iron tunnels and were an average length of 44m (max 120m to min 20m). Tunnel diameters were either 300mm, 450mm, 600mm, 700mm or 1000mm, with the most common diameter being 600mm.

Scheme name and location	Scheme type and length	Mammal tunnels	Known design issues
A590 High and Low Newton Bypass (northwest England)	3.8km 2-lane dual carriageway	4 badger tunnels; 1 tunnel proposed for use by both badger and otter	1 tunnel less than the 600mm advised by DMRB (450mm)
A66 Temple Sowerby (northwest England)	5km 2-lane dual carriageway	1 badger tunnel	Tunnel 60m long
A1(M) Wetherby to Walshford, North Yorkshire (northeast England)	5.3km 3-lane motorway	1 badger tunnel	Tunnel 60m long and with a plank bridge crossing needed to access the tunnel
A63 Selby Bypass, North Yorkshire (northeast England)	10km single carriageway	3 badger tunnels	1 tunnel less than the 600mm advised by DMRB (300mm)
A5 Nesscliffe Bypass, West Midlands (central England)	4.5km 2-lane dual carriageway	4 badger tunnels	2 tunnels larger than the 600mm advised by DMRB (i.e. 700mm and 1000mm); 1 tunnel 70m long
A6 Rothwell Bypass East Midlands (central England)	6km single carriageway	13 badger tunnels	Some tunnels deep beneath carriageway, therefore possibility of restricted air flow Close to public footpaths
A428 Caxton to Hardwick (eastern England)	7.7km 2-lane dual carriageway	4 badger tunnels	1 tunnel known to suffer from poor drainage
A120 Stansted to Braintree (Essex, southeast England)	14km 2-lane dual carriageway	6 badger tunnels	3 tunnels 70m long
A34/M34 Chieveley Junction South (Berkshire, southern England)	Junction	1 badger tunnel	Tunnel 120m long

Table 1. Road scheme and tunnel design summary

Monitoring methodology

Monitoring was undertaken from 24 August to 26 October 2010. The autumn was chosen as a suitable time for undertaking monitoring (as in the 2007 study) since the substrate used in the clay mats would remain moist and soft enough to record mammal footprints over about a week's duration. It is also the time when mammal activity levels tend to be high (post-breeding dispersal of young animals). At each study tunnel, a clay mat (45 x 45cm x 0.5cm thick) was placed just inside the tunnel entrance in late August (**Figure 1**). Notes were made on aspects of tunnel design (diameter, construction material), drainage conditions around the tunnel entrance and the condition of the associated fencing. The amount of vegetation cover around the tunnel entrance and habitat connectivity was recorded, by describing how the tunnel entrance tied into adjacent habitat features such as hedges and highway planting.

The mats were checked weekly during the trial period. Any evidence of animal tracks was recorded and species identified². The clay mat was then thoroughly wetted and smoothed over, leaving a clean surface to record future tracks.



Figure 1. A clay mat installed at the entrance of a badger tunnel to monitor use by mammals

In addition to clay mats, passive infra-red motion activated cameras were set up at two tunnel entrances (A5 Nesscliffe Bypass and A590 High and Low Newton Bypass) for one week to further assess suitability of monitoring using clay mats and to highlight any unexpected limitations associated with this technique.

Results

Mammal use

Overall, 35 of the 38 tunnels (92%) were used by mammals, with 89% used by badgers during the autumn 2010 monitoring period. Species recorded were badger, Eurasian otter *Lutra lutra*, red fox *Vulpes vulpes*, European hedgehog *Erinaceus europaeus*, brown rat *Rattus*

rattus, domestic cat *Felis catus* and domestic dog *Canis lupus familiaris*. Use of the tunnels by badgers was greater than by any other species.

In terms of the regularity of use, 37% of the tunnels were used frequently by badgers (i.e. footprints recorded on 7 or 8 of the 8 monitoring visits), 29% showed moderate levels of use (i.e. prints recorded on 4 - 6 monitoring visits) and 23% were used infrequently (i.e. prints recorded on only 1 - 3 monitoring visits).

Figure 2 shows prints on one of the clay mats. These results indicate that the tunnels installed under both dual carriageways and motorways are being used on a regular basis.



Figure 2. Badger prints on a clay mat within a badger tunnel

Design

The results of this study emphasise the importance of some elements of tunnel design, which may encourage use by badgers. The key design features that appear to be associated with more frequent use were:

- Good habitat connectivity with existing landscape features such as hedges and ditches. **Figure 3** shows that good and moderate connectivity is more likely to result in a tunnel being used than poor connectivity;
- Good vegetation cover around the tunnel entrance. **Figure 4** shows that tunnels with good cover are most frequently used by badgers;
- Good drainage; tunnels with poor drainage were never used or infrequently used;
- A tunnel width of at least 600mm – the two tunnels narrower than the standard 600mm (300 and 450mm) were never used or infrequently used by badgers, although the small sample size precludes a definitive conclusion. Tunnels wider than 600mm were regularly used, but there was no evidence that tunnels more than 600mm were used more or less often than the 600mm tunnels.

The results also indicate that use of the tunnels by badgers is not significantly influenced by tunnel construction material (concrete or corrugated steel), whether the whole of the tunnel had some degree of illumination by daylight, or tunnel length. The lack of a clear relationship between use by badgers and tunnel length was surprising (there is anecdotal evidence that badgers tend not to use very long tunnels). This is illustrated in **Figure 5**.

Effectiveness of clay mats as a monitoring method

The use of clay mats proved effective both in terms of cost and as a means of monitoring mammal tracks. The technique does have its limitations, which include drying out and cracking in hot weather, or water logging. Where water-logging occurred there was evidence that badgers tried to avoid walking on the mats (partial prints on mat edges suggested that badgers had tried to walk around them). A few simple measures could be taken to reduce these limitations, such as the use of larger clay mats (thus animals cannot pass without treading on them, placing mats further in the tunnel entrance (out of direct sunlight or rain), making drainage holes and more

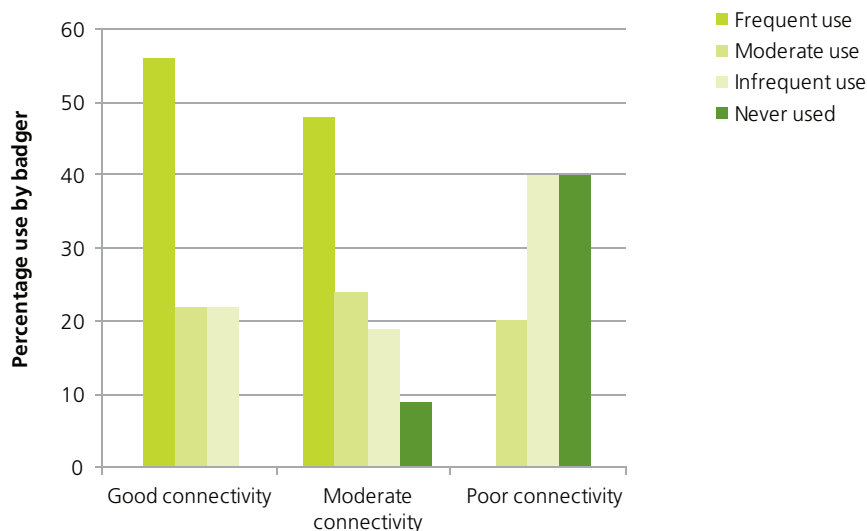


Figure 3. Tunnel use by badger in relation to habitat connectivity

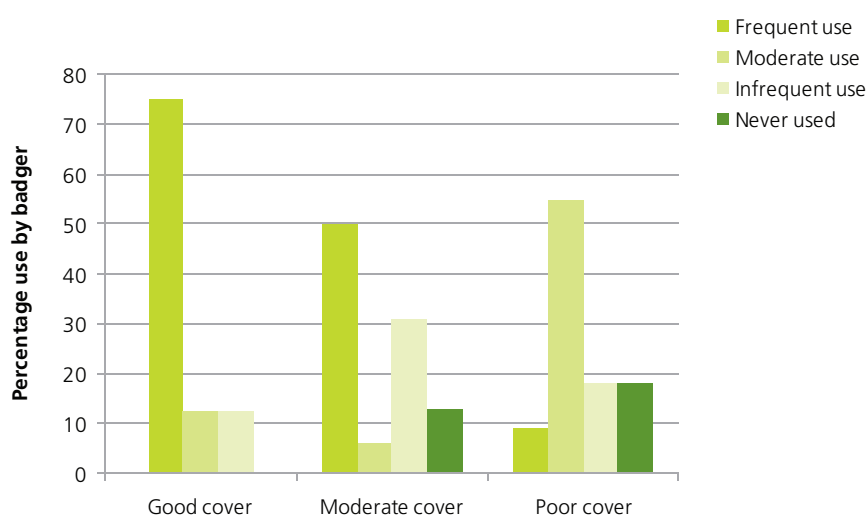


Figure 4. Tunnel use by badger in relation to vegetation cover at tunnel entrance

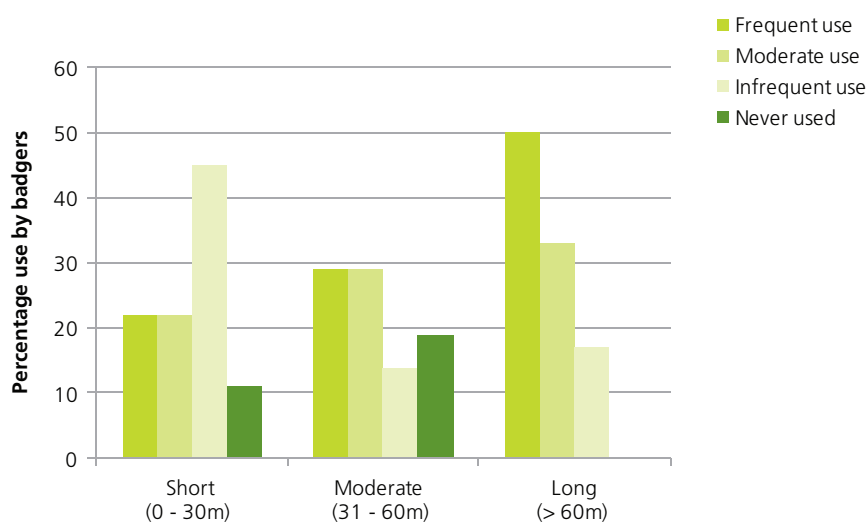


Figure 5. Tunnel use by badger in relation to tunnel length; no correlation between tunnel length and badger use was apparent



Figure 6. Motion-activated infra-red camera pictures of badger using a tunnel on the A5 Nesscliffe Bypass from motion-activated cameras

regular monitoring (every 3 to 5 days instead of every 7 days).

The use of motion-activated cameras at two sites did not identify any additional species than those identified by the clay mats. There were occasions when a camera did not pick up mammal activity, through malfunction. However, the camera did provide some excellent images of badger and otter using the tunnels (**Figures 6, 7 and 8**).

Other observations

A number of other interesting observations were made. In some tunnels, prints were sometimes recorded in one direction only. This suggests that badgers use tunnels to access feeding grounds, subsidiary or outlier setts; consequently, they may not return the same night (or for several nights). Alternatively, badgers may be using other means of returning, such as other tunnels or bridges, or directly over the road.

At three of the tunnels (on the A5 and A6), badgers had pulled bedding into the tunnels. This suggests they use tunnels as resting sites as well as underpasses. In one case, the tunnel was blocked at one end by a large boulder making it impassable to badgers, but prints were recorded regularly at the open end of the



Figure 7. Motion-activated infra-red camera pictures of badger using a tunnel on the A5 Nesscliffe Bypass from motion-activated cameras

tunnel and badgers appeared to be using the tunnel as a sett.

Conclusions

The results indicate that badgers used tunnels installed under the study roads. Therefore, tunnels help mitigate the effects of habitat fragmentation resulting from new road developments. Tunnels provide safe passage across roads for several mammal species, particularly badgers: 89% of tunnels monitored were used by badgers and 92% were used by a wider range of mammals.

Clay mats are an efficient and cost-effective means of monitoring mammal use of tunnels. This monitoring method has some limitations. For example, it cannot be used to assess the actual number of individuals using a tunnel over a given time period nor take account of changes in tunnel usage due to seasonal differences in the use of different foraging areas.

In terms of the efficacy of tunnel design advice (Highways Agency, 2001), the results suggest that to maximise the likelihood of use by badgers, the tunnel should incorporate adequate drainage and the tunnel diameter should be



Figure 8. Motion activated infra-red camera pictures of otters (bitch with 2 cubs) using a tunnel on the A590 High and Low Newton Bypass

at least 600mm; a tunnel of smaller diameter is less likely to be used and poor drainage greatly reduces tunnel usage. Tunnel material does not appear to affect use – there were no differences in the regularity of use between concrete and corrugated iron. Tunnels should ideally be located where existing habitat connectivity is good, with vegetation providing some cover around tunnel entrances, in order to increase their suitability for use by badgers and other mammals as underpass structures. Although not investigated here, it is likely that a tunnel located on or close to an existing well-used badger pathway is more likely to be used by badgers.

The results do not indicate that the current guidance for badger tunnels within the DMRB (Highways Agency, 2001) should be amended. However, the results emphasise the importance of some elements of the design of these structures. Good mammal tunnel design should optimise the factors that have been shown to be important in this study in order to maximise the suitability of tunnels under roads for use by badgers and other mammals and to increase the likelihood of their success as a mitigation measure for habitat severance by road schemes.

Acknowledgements

This study was undertaken by Atkins Ltd. as part of the Highways Agency contract number 514917. We thank Sheena Crombie of the Highways Agency, Atkins colleagues for undertaking the field monitoring and John Box CEnv FIEEM for providing a critical review of the script. A version of this paper was originally published in Conservation Evidence (www.ConservationEvidence.com) 2011, 8, 53-57 and their permission for publication here is gratefully acknowledged.

References

1. Baker A., Knowles M. & Latham D. (2007) Using clay drain seals to assess the use of dry culverts installed to allow mammals to pass under the A1 trunk road, Northumberland, England. Conservation Evidence, 4, 77-80.
2. Bullion S., Strachan R. & Troughton G. (2001) A guide to British mammal tracks and signs. Field Studies Council/The Mammal Society, UK.
3. Highways Agency (2001) Design manual for roads and bridges, Vol. 10, Section 4, Part 2, HA 59/92 as revised. Department for Transport, UK. (<http://www.dft.gov.uk/ha/standards/dmr/vol10/section4.htm>)



Joe Castle
Senior Design Engineer
Intelligent
Transport Systems
Atkins



Jill Hayden
Principal Consultant
Intelligent
Transport Systems
Atkins

M4 J24 – J28 VSL: modelling and calibration

Abstract

On behalf of the Welsh Government Atkins has managed the installation of the M4 Variable Speed Limit (VSL) scheme, between Junctions 24-28, which is intended to reduce congestion, improve safety and reduce environmental effects. This innovative scheme uses the Controlled Motorway (CM) concept but has unequally spaced gantries, with some separated by fairly large distances. Where there is a long gap between overhead gantries, post-mounted MS4 signs are used to provide repeater speed limit information to drivers. This allows significant cost savings from reduced infrastructure, while retaining the benefits of using speed control to reduce congestion. This paper presents the results of modelling performed by Atkins using PARAMICS, to investigate the impact of the scheme and verify the CM parameters used before they are used in the live system.

Introduction

On behalf of the Welsh Government Atkins has managed the installation of the M4 Variable Speed Limit (VSL) scheme, between Junctions 24-28, which is intended to reduce congestion, improve safety and reduce environmental effects. This innovative scheme uses the Controlled Motorway (CM) concept but has unequally spaced gantries, with some separated by fairly large distances. Where there is a long gap between overhead gantries, post-mounted MS4 signs are used to provide repeater speed limit information to drivers. This

allows significant cost savings from reduced infrastructure, while retaining the benefits of using speed control to reduce congestion.

Modelling has been performed by Atkins using PARAMICS, to investigate the impact of the scheme and verify the CM parameters used before they are used in the live system.

The model used a base scenario, which models and validates the existing road conditions before applying the VSL scenario.



Figure 1. M4 VSL Scheme & PARAMICS Model Area

The results showed that in severe flow breakdown conditions (i.e. Friday afternoon peak and Monday morning peak on the westbound carriageway), the journey times will be reduced by the VSL scheme. Journey time reliability should improve for all day types, in line with post operational evaluation of other CM schemes.

Study area

The M4 VSL scheme covers the M4 motorway between Junction 24 and Junction 28, a distance of approximately 12km. The scheme is intended to address congestion caused by the non-standard nature of the road including the proximity of adjacent junctions, horizontal and vertical alignments and lane drops.

Congestion problem

The main bottlenecks in the scheme are on the approaches to the Brynglas Tunnel, where the number of lanes drops from three to two. Flow breakdown occurs on the approaches to Brynglas Tunnel in both directions. On the westbound carriageway, typically congestion builds up to a point upstream of J24. This congestion can last for a period of three hours or more in the evening peak.

Fridays are usually the most congested of all week days, with Mondays and Thursdays suffering frequently but less severely.

Base model development & operation

The PARAMICS model covers the VSL scheme and the motorway beyond, a distance of 24km between a point west of Junction 29 and a point east of Junction 23. The extent of the model is shown in **Figure 1**.

Base model development

The traffic data used for the model included:

- MIDAS data, for speed and flow;
- Manual Classified Count (MCC) data, for vehicle categorisation;
- Automatic Number Plate Recognition (ANPR) camera data, for journey times.

Motorway Traffic Viewer (MTV) plots were used, plotting Traffic Count Data (TCD) from Motorway Incident Detection and Automated Signalling (MIDAS), to provide information about the location and time of flow breakdown and congestion.

Validation

Because the inputs to the CM algorithm are speed and flow, it is essential that the model accurately replicates the speed and flow conditions on the road. Therefore the following three variables were validated:

- Flow
- Speed
- Journey time

For flow, the modelled flow data was compared to the MIDAS flow data. For speed validation, observed speed data for each minute was extracted from selected MIDAS loops and compared to the modelled speed data from the corresponding loops within the model.

Observed journey time data was provided by the ANPR cameras for the M4 between Junction 24 and Junction 28 and compared to the modelled journey times.

The link flow, journey time and speed validation for the M4 model were satisfactory and the locations of modelled delay and congestion are generally on the same stretch of the M4 carriageway as observed on the MTV plots. The M4 base models were considered to be a good representation of the traffic conditions and acceptable for testing the proposed M4 VSL Scheme.

Model scenarios

Modelling the operation of the VSL required the use of the 'ATM (Active Traffic Management) Controller' module in PARAMICS and configuration of the CM algorithm and parameters before testing the scenarios.

Two scenarios were compared:

- The base model with no traffic control, i.e. no Controlled Motorway system and no MIDAS HIOCC;
- The VSL model with mandatory variable speed limits set as a result of the CM and HIOCC algorithms. HIOCC sets mandatory 40mph limits (using default MIDAS settings) and CM sets mandatory 50 and 60mph limits.

PARAMICS ATM module

The ATM PARAMICS receives the traffic data (i.e. speed and flow) from virtual loops in the PARAMICS model, then processes it and sends instructions on the VSL response (based on the Highways Agency's MIDAS signal and sign setting strategy) back to the PARAMICS model. The dynamic

interaction between the PARAMICS model and the ATM Controller enables the system to continuously respond to traffic flow and speed changes adjusting the output controlled speed limit accordingly.

Configuration and calibration of CM parameters

Due to the non-standard nature of the M4 VSL scheme, the configuration of the optimum CM parameters is key to its successful operation. Therefore the configuration exercise required some departures from standard practice.

The CM parameters were configured off-line before being calibrated using the model. The parameters were modelled iteratively using the results from the previous model run until no more significant improvements were made.

Speed and flow thresholds

Speed and flow thresholds determine the congestion levels which trigger the different variable speed limits. Speed-flow curves using smoothed data were created for all typical days.

These graphs were used to identify the rising and falling speed and flow thresholds which will trigger the variable speed limits.

Gantry pointers

Gantry pointers are required to identify which gantry signals will display variable speed limits in response to the data coming from each set of loops.

Where gantries are placed in close proximity, the same speed limit will need to be displayed on more than four upstream gantries in order to avoid speed changes in close proximity, which could cause shockwaves and driver uncertainty.

Where the distances between gantries are much longer, as few as two upstream gantries will be used. This reduces the length of road on which a low VSL will be displayed, minimising the negative impact the system will have on journey time.

Results

Journey time

Figure 2 shows a comparison of modelled journey time data between the base and the M4 VSL scenario.

It can be seen that journey times are reduced when there is severe flow breakdown and congestion, e.g. Friday afternoon peak and Monday morning peak on the westbound carriageway.

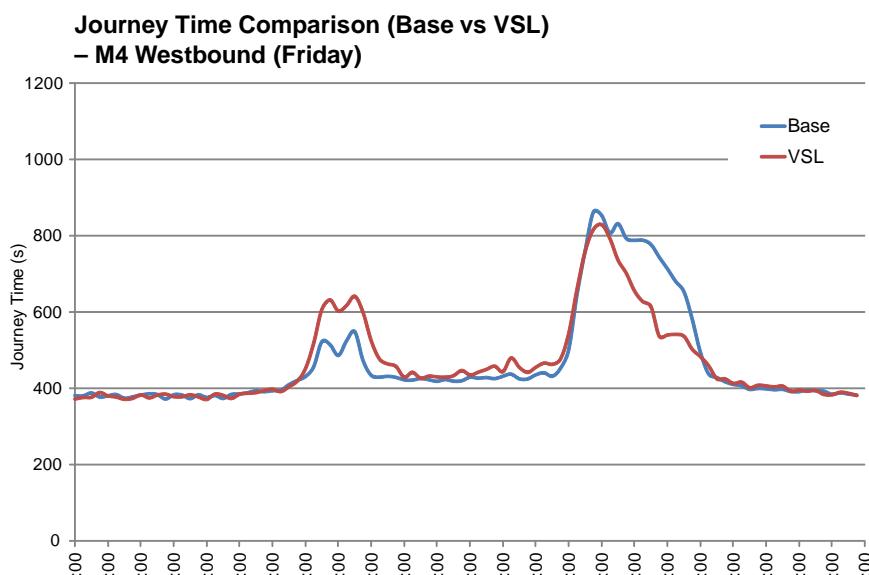


Figure 2. Journey Time Comparison (Friday)

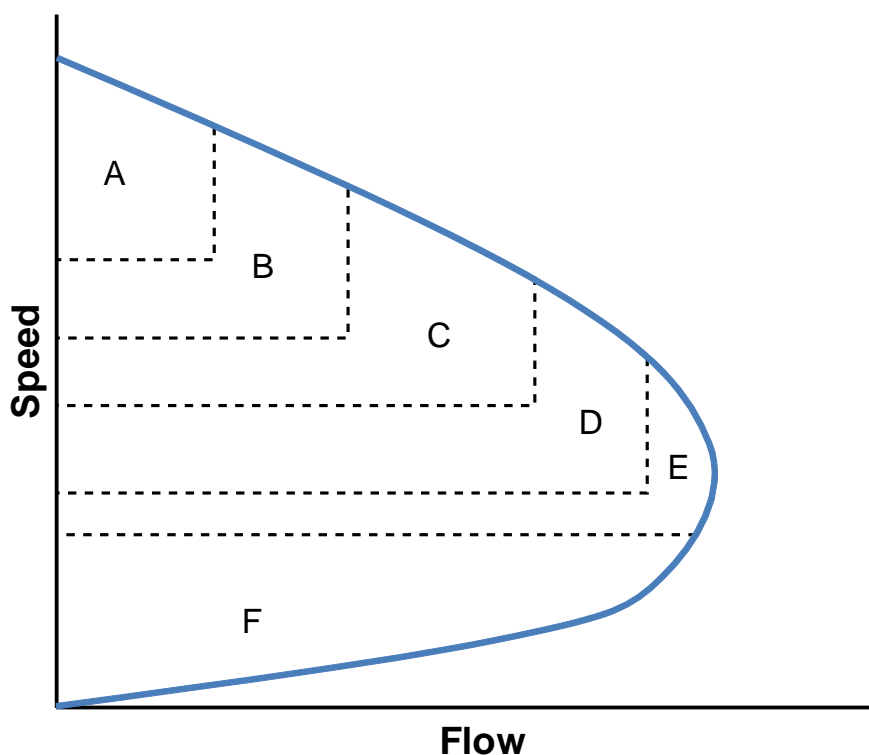


Figure 3. Relationship between Level of Service and Speed-Flow Data

In more marginal traffic conditions, the modelling showed the VSL system increasing journey time. This is because in these conditions traffic is likely to be able to travel at higher average speeds when the system is off than when obeying the mandatory VSLs.

Level of service

Speed-flow data can be used to identify 'Levels of Service' (LOS). The Highway Capacity Manual¹ gives six levels of service for highways:

- LOS A: Free-flow;
- LOS B: Stable flow;
- LOS C: Stable flow but manoeuvrability is more restricted due to higher flow volumes;
- LOS D: Approaching unstable flow. Reasonable operating speed but there is little freedom to manoeuvre. Fluctuations in flow volume can cause considerable speed drops;
- LOS E: Unstable flow as demand is at or near the capacity of the highway. Stop-start flow can occur at the level;
- LOS F: Forced or breakdown flow. At this level of service, speeds are low and volumes are above capacity. This level is found in queues which are backing up.

Figure 3 shows a typical speed-flow curve and its relationship with the levels of service².

During the Friday PM peak, the M4 westbound carriageway between Junction 24 and Junction 25 is severely congested and the benefit of the proposed VSL scheme is most apparent.

Figure 4 shows the speed-flow curves for the two scenarios at Junction 24, which is upstream of the origin of the flow breakdown. In the base, flow breakdown occurs with speed dropping to 40kph; however in the VSL scenario the speed stays above 60kph. The flow throughput in the VSL scenario is also higher than the base, suggesting that the length of the queue is likely to be shorter. Throughout the scheme, LOS for the base can drop to LOS F, whilst for the VSL scenario the LOS is generally at level D or better.

This suggests that journey time reliability is likely to be improved as a result of the VSL scheme, because more uniform speeds are associated with more reliable journey times. It is not possible to quantify these results using modelling, but journey time reliability improvements will be measured as part of the on-road evaluation of the scheme.

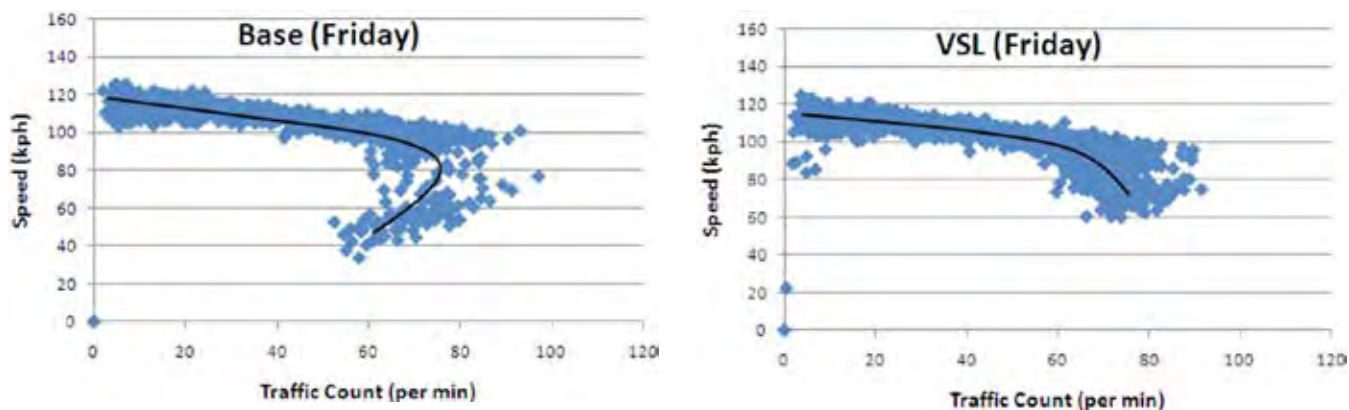


Figure 4. Modelled Speed Flow Curves for Junction 24 Westbound Friday

Discussion

The modelling exercise provided some interesting results.

The Friday afternoon peak on the westbound carriageway was identified as being the most congested of all time periods and sections of the M4 within the modelled area. During this period, the modelling showed that the application of variable speed limits should lead to improved flow throughput, reduced queuing, higher average speeds and reduced journey times.

During periods of more marginal congestion, the modelling showed that the VSL scheme tends to increase journey times. There are two main factors leading to this result:

- When the VSL scheme is operating, the 40mph speed limits set by the HIOCC algorithm for queue protection are mandatory, meaning that traffic slows down significantly as a result. Previously, these speed

limits would have been advisory, so traffic would have tended to exceed them until they meet the tail of the congestion;

- The long distance between gantries in some parts of the scheme limits the number of points where speed limits can change. This means that low speed limits are set for longer sections than required.

The Level of Service indicator suggests that journey time reliability would be improved for all modelled day types as a result of the VSL scheme reducing flow breakdown, leading to more uniform speeds.

In summary, the results show that journey times will be reduced in the most congested periods but increased overall and journey time reliability will be improved. These results are in line with the post-operational evaluation of other Controlled Motorway schemes (e.g. M25 and M42 ATM).

Other benefits that can be expected from the M4 VSL include safety benefits and reduction in emissions.

Conclusions

The modelling and off-line calibration exercise was a success in terms of understanding the requirements for the initial parameter values of the CM algorithm on this innovative non-standard CM scheme being implemented by the Welsh Government. The next step is to test the initial settings using the 'MIDAS Replay' application before inputting them to the M4 VSL site data.

Switch on of the scheme using the CM algorithm is planned for Autumn 2011; during on-site calibration these initial parameters will be fine tuned. This is important as driver behaviour on the road may differ from that assumed by the model, particularly in terms of compliance with the mandatory variable speed limits over the long distances between gantries.

References

1. Highway Capacity Manual, Transportation Research Board, Washington DC, 2000
2. Chapter 11, Highway Traffic Analysis and Design, R J Salter, Macmillan Education



Roger Higginson
Principal Engineer
Intelligent
Transport Systems
Atkins



Jill Hayden
Principal Engineer
Intelligent
Transport Systems
Atkins



Sukhvinder Ubhi
Project Sponsor
Highways Agency



Joe Castle
Senior Design Engineer
Intelligent
Transport Systems
Atkins

Motorway-to-motorway: a potential technological solution to motorway congestion

Abstract

Motorway-to-Motorway metering (M2M) is the potential application of dynamic traffic control to manage congestion at motorway-to-motorway intersections. The techniques developed as part of the M2M Feasibility Study aim to manage the road space in different ways for varying conditions to maximise capacity within a safe environment for the travelling public.

This paper details the findings of a feasibility study of deploying M2M on the Highways Agency's motorway network in several key areas, including: technical proposals, operational modelling, economic assessment, safety analysis, environmental impact and stakeholder and legal issues. These findings are based on the extensive modelling and research undertaken as part of the study. The conclusions are that M2M could reduce journey times and increase average speeds without adversely impacting on safety.

Introduction

Motorway to motorway intersections form some of the most critical parts of the Highways Agency's network. Congestion at these intersections can have significant impacts on the travelling public and the economy. Therefore any potential solution that could reduce congestion at motorway to motorway intersections should be considered further to determine its suitability for addition to the Highways Agency's toolkit for reducing congestion.

Motorway to Motorway metering (M2M) is the proposed application of dynamic traffic control to manage congestion and improve traffic flow at motorway-to-motorway intersections. A feasibility study was undertaken to determine if M2M could be both feasible and beneficial in maximising the flows through and reducing congestion at motorway to motorway intersections.

The techniques developed as part of the feasibility study aim to manage the road space in different ways for varying conditions to maximise capacity whilst providing a safe environment for the travelling public.

The feasibility study used extensive modelling and research to assess six key areas, namely technical proposals, operational modelling, economic assessment, safety analysis, environmental

impact, and stakeholder & legal issues. This paper details the key findings of that study.

Technical proposals

The objective of the M2M system is to maximise the flow through motorway intersections through specific and appropriate management of the traffic merging process using a feedback control system architecture, as shown in **Figure 1**:

A new M2M system was considered

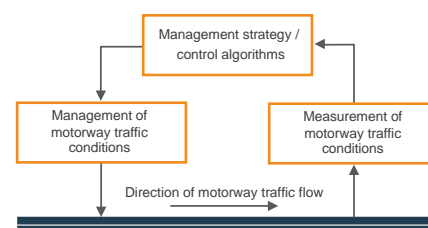


Figure 1. M2M system architecture

as the current Ramp Metering (RM) system¹ is not suitable for most motorway intersections, due to the:

- Higher flows and speeds involved;
- Operational priorities of traffic joining from each approach road;

- Need to manage merging and queuing traffic on the main line and link road;
- Safety concerns of using traffic signals and stop lines on motorways.

However RM theory and experience was used as a starting point for the proposed M2M system as operational assessment of the first 30 RM sites deployed on the Highways Agency's network showed that RM reduced journey times through congested junctions by an average of 13% and could increase capacity through the junction by 5-7%².

Measurement of motorway traffic conditions

The Highways Agency's MIDAS (Motorway Incident Detection and Automatic Signalling) system monitors traffic conditions using inductive loops at regular (nominally 500m) intervals. The data from the existing MIDAS system was used in the feasibility study to determine congestion levels and validate the model. The MIDAS system provides live data on the motorway traffic conditions such as speeds, flow and occupancy and is therefore ideal for use in the proposed M2M system, particularly as the cost and disruption of installing additional monitoring systems would be prohibitive.

Management strategy / control algorithms

An iterative process of technical proposals and experimental modelling was used to refine the proposed M2M system algorithms. Key considerations made during the development of the M2M algorithms were to:

- Maximise the flow capacity downstream of the merge;
- Maximise the flow capacity of the merge;
- Balance queues on all approaches to the merge area;
- Manage flows on all motorway approaches to the merge area;
- Suppress shockwaves upstream of the merge.

The iterative development of the M2M algorithms resulted in a combined M2M system algorithm to address the key considerations detailed above, as shown in **Figure 2**:

The combined algorithms are based on empirical evidence³ which suggests that the flow capacity can be increased by applying reduced Variable Mandatory Speed Limits (VMSLs) and the ALINEA⁴ algorithm used in RM. The modelling

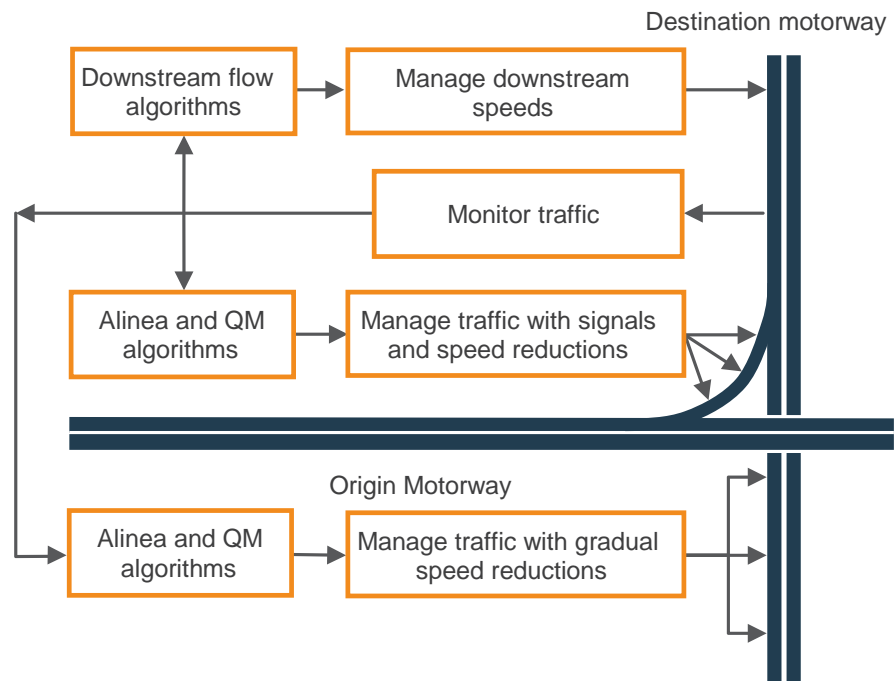


Figure 2. Combined M2M algorithms

work also highlighted the critical nature of correct set up and calibration of the algorithms. Therefore any practical implementation should include advanced automatic calibration algorithms such as Ad-ALINEA⁵ to ensure that the system maintains optimum performance under changing flow rates and prevailing conditions.

Management of motorway traffic conditions

The operation of the algorithms relies on the ability to control the flow from the mainline and merging motorways into the merge area. However, unlike the existing RM technique, M2M cannot rely exclusively on traffic signals and stop lines because of the higher flows and speeds involved, therefore other methods of managing traffic had to be developed and tested on the model(s). Three different control measures were considered for M2M as follows:

- Stop Line Control (SLC);
- Dynamic Speed Control (DSC);
- Dynamic Lane Control (DLC).

Stop Line Control (SLC)

The operation of SLC, as shown in **Figure 3**, for flow control and its limitations are well understood from RM. The advantages are that the control is relatively constant with good compliance by motorists as long as the signals are applied appropriately and various safety mitigation factors are in place.

The main limitation of SLC is the limited flow range that can be achieved, particularly the maximum practical flow per lane which is too low for most M2M applications. Therefore SLC needs to be combined with DSC to manage higher flows and to ensure safe operation. It is also not appropriate to consider using SLC on the main carriageway of the destination motorway as other techniques such as DSC or DLC are more effective.

Dynamic speed control (DSC)

Experimental modelling of a straight line section of motorway section confirmed that DSC, should give effective flow management on the approaches to the merge. An advantage of DSC is that it can be applied to main carriageway traffic as well as joining traffic, as shown in **Figure 4**.

As DSC is less restrictive than either SLC or DLC it is a useful measure for controlling flows during the onset and recovery of congestion where the M2M system must reduce flows only slightly to maintain the optimum flow capacity of the merge whilst minimising the build up of queues upstream of the junction.

Potential safety issues concerning non-compliance with low VMSLs would be prevented as very low speed limits of 30mph and 20mph would only be used when the traffic conditions are sufficiently heavy to prevent non-compliance or large speed differentials between vehicles.

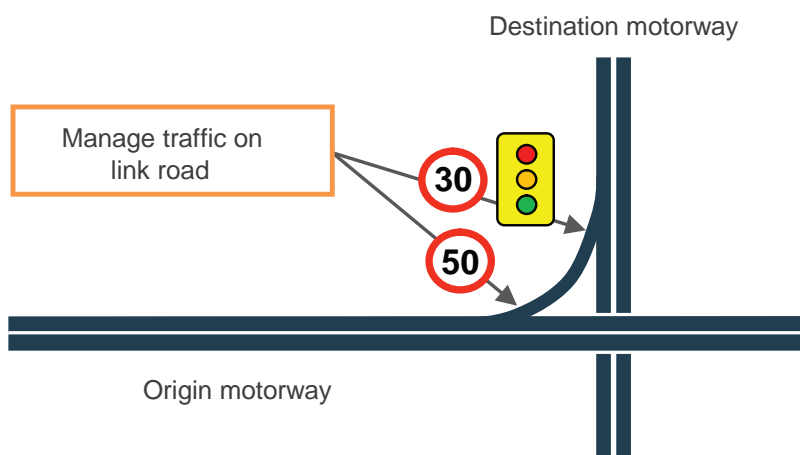


Figure 3. Stop line control

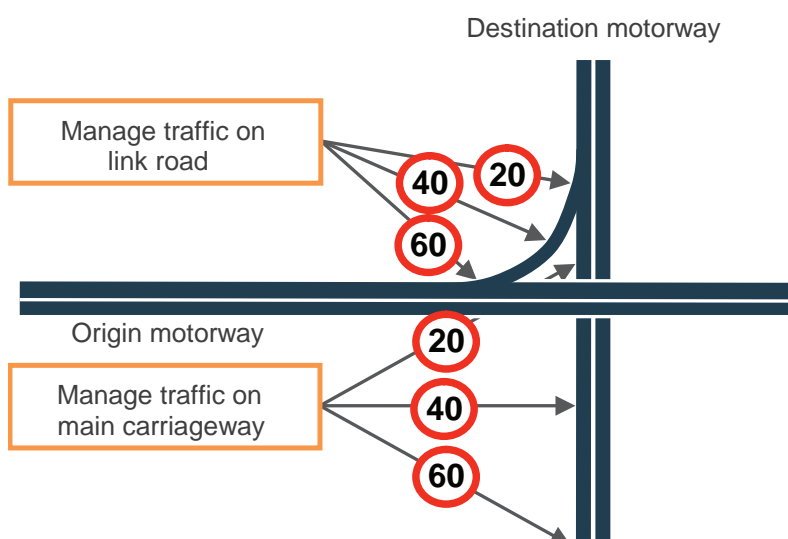


Figure 4. Dynamic speed control

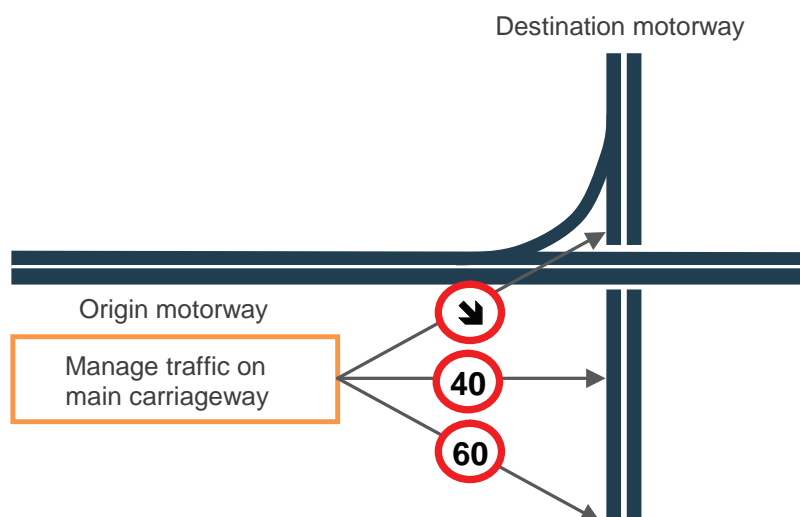


Figure 5. Dynamic lane control with dynamic speed control

Dynamic Lane Control (DLC)

The most direct way of changing capacity is by changing the number of lanes open to traffic using DLC. This type of control could be deployed on the main carriageway, on-slip/link road or both, depending on the flows and number of lanes. Merge behaviour could also be affected by changing lane configuration, as shown in **Figure 5**.

Key points of technical proposals

Several different algorithms and combinations of algorithms were designed, modelled and investigated for use in M2M systems and proved to be successful in the model. The study also identified three techniques required for implementation of the M2M algorithms.

The optimum combination of algorithms and implementation techniques would be specific to each site, therefore detailed modelling of each site would be required before considering an implementation of M2M.

Operational modelling

As the M2M proposals are new and innovative, detailed modelling was essential to check that the proposals were feasible and to gain an understanding of the possible benefits and impact. While detailed modelling results do not guarantee success of a real implementation, they give greater confidence to take the ideas forward for a potential on-road pilot.

VISSIM™ software from PTV⁶ was used due to its strength in junction modelling, both signalled and un-signalled (VISSIM is a German acronym for “Verkehr In Städten - SIMulationsmodell” (German for “Traffic in cities - simulation model”). VISSIM is a microsimulation model based on car following and lane change logic. Furthermore, it includes the Vehicle Actuated Programming (VAP) integrated package that enables complex algorithms to be modelled.

Accurate VISSIM models were developed to represent the congestion currently experienced at two sites. Each model was built based upon CAD drawings of actual junction layout and infrastructure locations. Analysis of MIDAS data and site visits were used to determine the required extents of the model based on the congestion. The models were calibrated against MIDAS and journey time data to ensure they provided accurate representations of the traffic situation during the modelled periods. The algorithms (ALINEA, Queue

Management, Release, SLC, DSC and DLC) were implemented in the VAP code and then various scenarios were tested. This involved an iterative process of viewing results, identifying areas for improvement, modifying the algorithms and then running further scenario tests, and so on.

M6 J8 Northbound, (M6 J7-9 and M5 J1 to M6 J9)

Key aspects of the M6 J8 Northbound M2M model are shown in **Figure 6**.

Table 1 shows the modelled journey times from locations upstream of the merge area on both the M5 and M6 to downstream of the merge, before the diverge to J9, with and without M2M.

The results reported in **Table 1** are for dual ALINEA with QM controllers, using a combination of SLC and DSC for merging traffic and SLC for main line traffic.

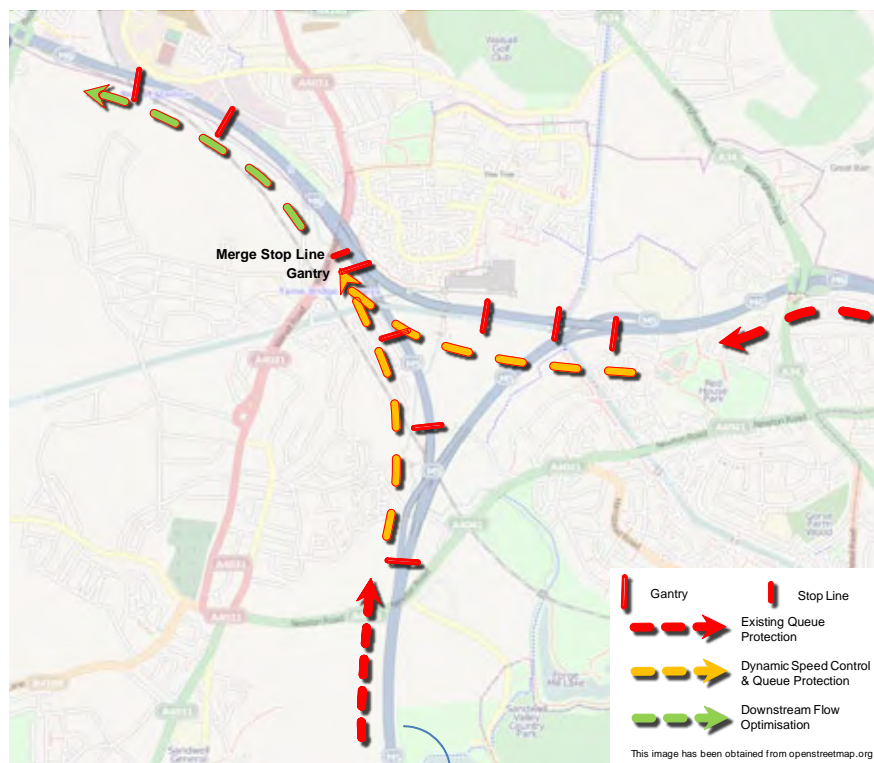


Figure 6. Location of modelled stop line and gantries for M6 J8 NB

Measure		M5 Upstream to M6 J9 Diverge	M6 Upstream to M6 J9 Diverge	Overall
1. Total number of vehicles	Base	18,602	23,420	42,022
	With M2M	18,591	23,490	42,081
	Difference	11	+70	+59
2. Average journey time (s) per vehicle	Base	457	525	N/A
	With M2M	415	388	
	Difference	-42	-137	
3. Total vehicle travel time (hrs)	Base	2,362	3,418	5,779
	With M2M	2,144	2,529	4,673
	% Difference	-9.2%	-26.0%	-19.1%
4. Average delay time (s) per vehicle	Base	212	239	N/A
	With M2M	171	101	
	Difference	-41	-138	
5. Total vehicle delay (hrs)	Base	1,098	1,556	2,654
	With M2M	882	661	1,543
	% Difference	-19.7%	-57.5%	-41.9%

Table 1. Results of modelled travel times for M6 J8 NB with and without M2M

M60 J12 clockwise, (M60 J8-13, M62 J11 to M60 J13 and M602 J1 to M60 J13)

Key aspects of the M60 J12 Clockwise M2M model are shown in **Figure 7**.

The results reported in **Table 2** are for triple ALINEA with QM controllers, using a combination of SLC and DSC for each merge.

The speed frequency chart shown in **Figure 8** is of vehicle speeds upstream of the junction on the M60. Note that without applying the M2M control algorithms there are significantly more vehicles travelling at speeds in the range 15-30mph, whereas with M2M vehicle speeds are increased towards 35-50mph.

The modelling demonstrated significant benefits could be obtained using DSC on the M60 with DSC and SLC on both the M602 and M62. The slight increase in journey times on the M602 is outweighed by reduced journey times for more vehicles on the M60 and M62.

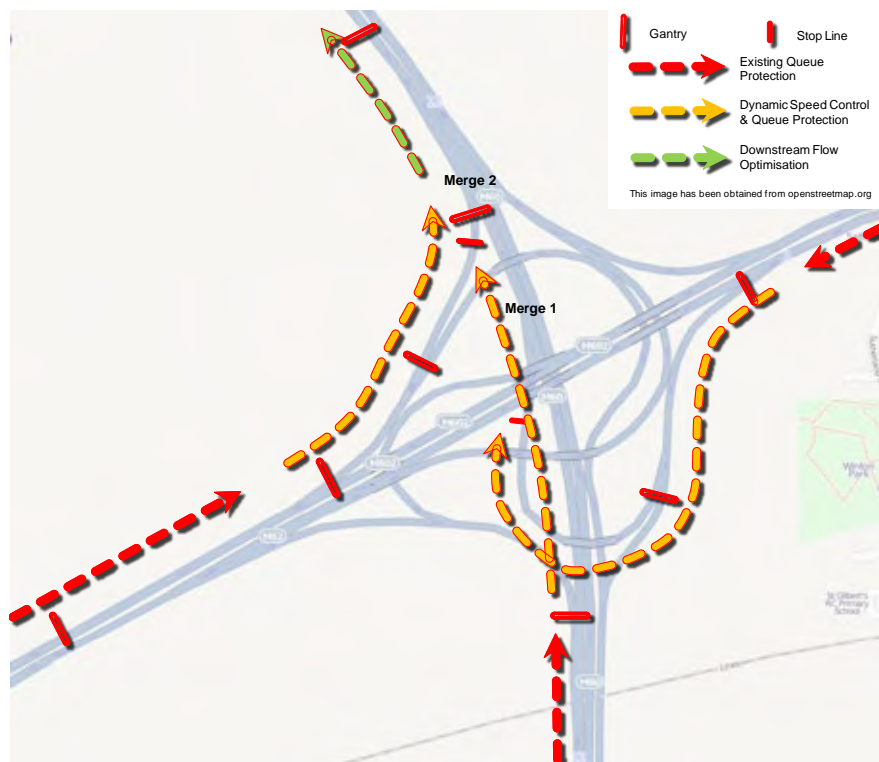


Figure 7. Location of modelled stop line and gantries for M60 J12 clockwise

Measure		M60	M602	M62	Overall
1. Total number of vehicles	Base	29,873	8,677	18,787	57,337
	With M2M	30,031	8,675	18,788	57,494
	Difference	158	2	1	157
2. Average journey time (s) per vehicle	Base	428	326	166	N/A
	With M2M	279	351	148	
	Difference	-149	25	-18	
3. Total vehicle travel time (hrs)	Base	3,554	785	866	5,206
	With M2M	2,328	846	770	3,945
	% Difference	-34.5%	7.8%	-11.1%	-24.2%
4. Average delay time (s) per vehicle	Base	229	102	60	N/A
	With M2M	80	128	42	
	Difference	-149	26	-18	
5. Total vehicle delay (hrs)	Base	1,899	246.8	314	2,460
	With M2M	668	308.5	218	1,194
	% Difference	-64.8%	25.0%	-30.7%	-51.5%

Table 2. Results of modelled travel times for M60 J12B with and without M2M

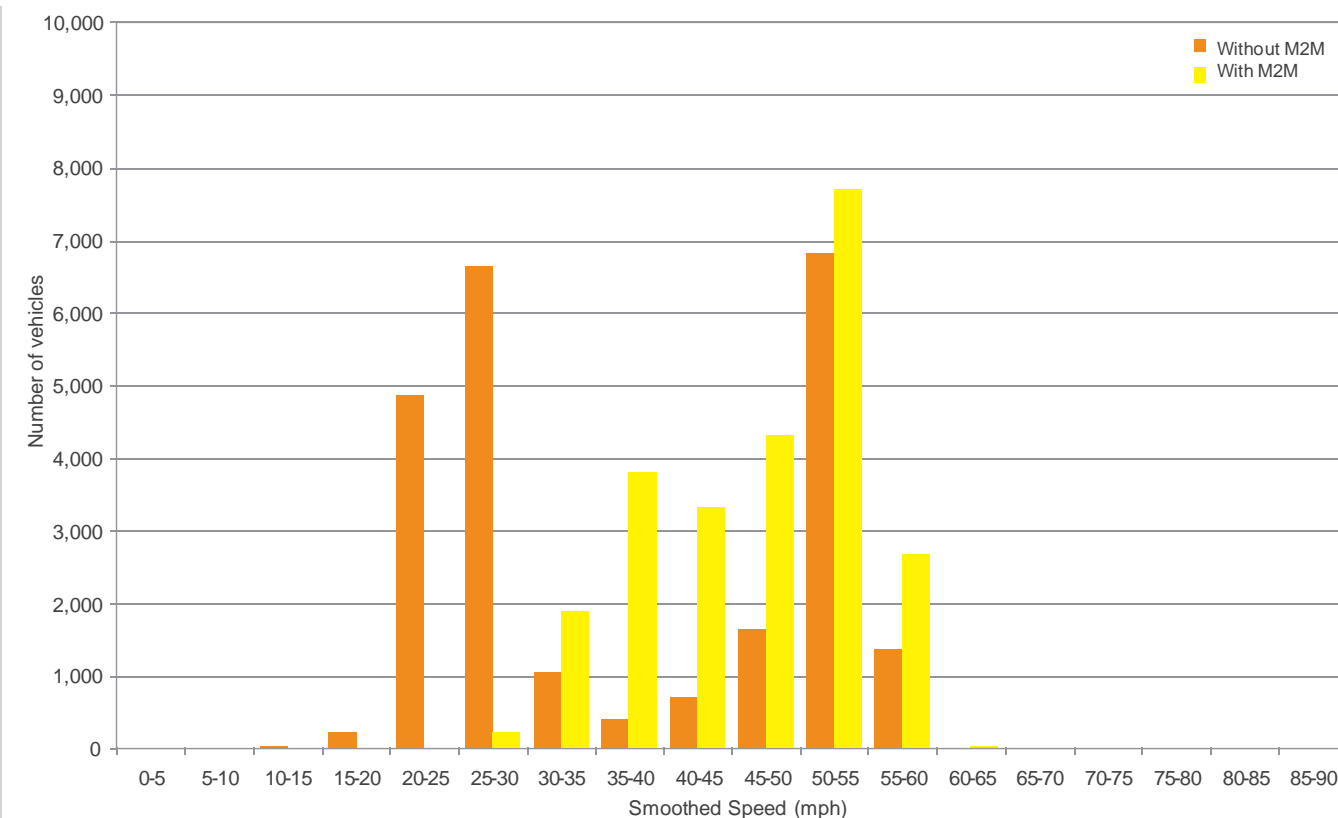


Figure 8. Speed frequency comparison for M60 J12 upstream

Key points of operational modelling

The key findings of the modelling of two M2M junctions were:

- Significant benefits for both junctions;
 - Journey times reduced by 19.1% and 24.2%; and
 - Delay times reduced by 41.9% and 51.5% at M6 J8 NB and M60 J12 CW respectively.
- Overall journey time reductions for joining traffic; (increased journey times on M60 J12 CW merge 1 are outweighed by reduced journey times on merge 2);
- Significant improvement in speed distributions, with a significant number of vehicles travelling at higher speeds with M2M.

The models demonstrated that significant benefits could be realised for both joining and main line traffic, although fine tuning of the M2M settings was critical to optimise the benefits.

Each site would need to be modelled in order to understand the potential benefits and optimum combination of SLC, DSC and DLC, as part of any outline design of any pilot site.

Increases in traffic flows due to trip re-assignment have not been modelled.

Economic assessment

Economic appraisal of a potential pilot site at M60 J12 clockwise was performed in accordance with the Department for Transport's WebTAG guidance⁷. The estimated costs for the installation and operation of a pilot scheme at this site over a 30 year period were compared with the benefits of reduced journey times, suggesting that M2M could provide an overall benefit-cost ratio of 5.6. Other potential benefits (more reliable journey times, safety and air quality benefits) were not included at this stage as they are more difficult to infer from the modelling work.

All motorway-to-motorway junctions in England were assessed to determine which sites would be suitable for installing M2M, based on congestion levels and other factors, and 18 sites were identified where the installation of M2M could provide a high or medium value for money solution to the current congestion problems.

Safety analysis

The introduction of traffic signals and stop lines on motorway intersections is a key concern for the implementation of M2M. Outline and detailed safety impact analysis as defined in the Highways Agency's Project Safety Risk Management System⁸ were performed on the potential impacts that the installation of traffic signals could have at M2M sites.

The results of the detailed safety assessment work demonstrated that the installation of SLC is not likely to result in a detriment to safety, assuming that key mitigating measures, such as queue management, high friction surfacing, improved signing and lining and variable mandatory speed limits are included. As DSC and DLC techniques are both adaptations of existing measures, it was not considered necessary to undertake detailed safety assessments at this stage. An outline assessment was performed for DSC and DLC to identify hazards that would need to be addressed through undertaking a more detailed safety analysis at an outline design stage.

The findings of the safety analysis means that key concerns associated with the use of SLC and very low VMSLs should not cause the M2M proposals to be

discounted on safety grounds. The high economic benefits, coupled with the lack of a significant impact on safety (i.e. no significant benefits or disadvantages found from the analysis performed) mean that M2M could be both feasible and beneficial.

Although the inclusion of safety benefits is not critical to the selection of an economically robust site, those sites with significantly higher than average numbers of mainline collisions may benefit most from M2M. In turn, the reduction in incident related congestion may further support the economic case.

Environmental impact

Environmental analysis of the modelling results shows that the changes in speed as a result of implementing M2M could improve air quality overall, as long as the improved traffic conditions do not lead to trip attraction. However, the implementation of SLC may result in increased emissions adjacent to the stop line; therefore care would need to be taken with the placement of the stop line in an Air Quality Management Area (AQMA) to ensure it minimises the impact within the AQMA and has an overall beneficial impact.

An air quality assessment will need to be undertaken as part of the outline design of any site, leading to an Environmental Assessment Report (EAR). As a minimum this would use detailed VISSIM modelling results to simulate vehicle emissions with and without M2M. Where feasible or relevant, dispersion modelling would also be performed.

In priority AQMAs, modelling of the wider area may also be required to assess potential traffic reassignment impacts. An assessment of air quality impacts will be required prior to the implementation of any M2M site. This could either be done using the existing models, or at pilot stage using results from VISSIM models of the pilot sites.

Legal and stakeholder issues

Given the innovative nature of the M2M proposals the following key issues:

- Use of a stop line and traffic signals on a motorway;
- Use of VMSs down to 20mph to control flows;
- Use of automatic lane closures;

would have to be addressed and may require changes in standards or regulations.

Most of the feasible M2M sites identified in the economic assessment are part of the current National Roads Programme. The deployment of M2M could therefore be seen as part of the wider congestion relief programme outlined in the National Roads Programme.

Conclusions

M2M builds on the principles of RM to address the issues at some of the most congested pinch points on the Highways Agency network, namely motorway to motorway intersections. The study identified three types of control that could be used for M2M:

- Stop Line Control (SLC) – use of a traditional RM stop line and traffic signals;
- Dynamic Speed Control (DSC) – use of dynamically variable mandatory speed limits;
- Dynamic Lane Control (DLC) – use of lane closures to control flow and to dynamically change merge profiles as required.

M2M techniques were evaluated at two modelled test sites; M6 J8 NB and M60 J12 CW. The modelling showed substantial benefits with 19% reduction in journey times at M6 J8 and 24% reduction in journey times at M60 J12 (41.9% and 51.5% reduction in delays respectively).

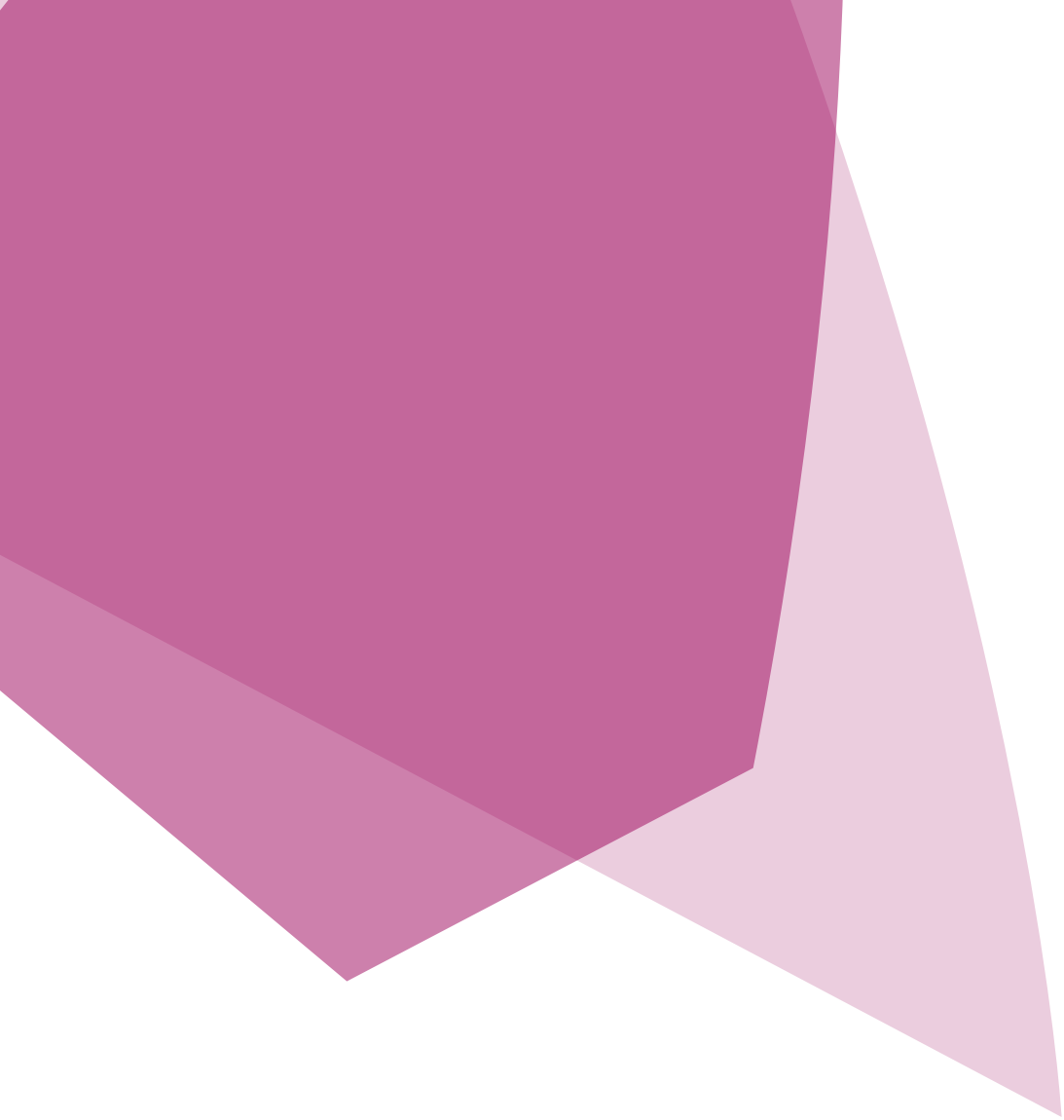
The conclusion therefore is that M2M could reduce journey times and increase speeds at congested motorway interchanges, without having a negative impact on safety or the environment. The main recommendation from the feasibility study is that an on road M2M pilot scheme is needed to confirm that the modelled benefits can be realised in practice and to prove the feasibility of M2M.

Acknowledgements

This paper draws on the work undertaken for Highways Agency Network Services Directorate © Crown and is published with the permission of the Highways Agency. The views contained in this paper are those of the authors and not necessarily those of the Highways Agency.

References

1. "Ramp Metering Summary Report", Highways Agency Report, November 2007, http://www.highways.gov.uk/knowledge/documents/SW07195_ramp_metering.pdf
2. "Ramp Metering Operational Assessment", Highways Agency Report, April 2008, http://www.highways.gov.uk/knowledge/documents/Ramp_Metering_Operational_Assessment.pdf
3. M Papageorgiou, E Kosmatopoulos, and I Papamichail "Traffic Theory for using VMSL to manage flows Effects of Variable Speed Limits on Motorway Traffic Flow, Transportation Research Record: Journal of the Transportation Research Board, No. 2047.
4. M. Papageorgiou, H. Hadi Salem, and J-M. Blosseville (1991) "ALINEA: A Local Feedback Control Law for On-Ramp Metering," Transportation Research Record, vol. 1320.
5. E Kosmatopoulos, M Papageorgiou, D Manolis, J Hayden, R Higginson, K McCabe, N Rayman "Real Time Estimation of Critical Occupancy for Maximum Motorway Throughput", Transport Research Board Journal, Volume 1959, 2006.
6. VISSIM (Verkehr In Städten – SIMulationsmodell) microsimulation model, <http://www.ptvag.com/software/transportation-planning-traffic-engineering/software-system-solutions/vissim/>
7. "Transport Analysis WebTAG guidance" Department for Transport, <http://www.dft.gov.uk/webtag/>
8. "Interim Advice Note 139/11, Managed Motorways Project Safety Risk Work Instructions" Highway's Agency Interim Advice Note, March 2011, <http://www.dft.gov.uk/ha/standards/ians/pdfs/ian139.pdf>





Dongzhou Huang

Senior Engineer IV

TS Transportation
Design South Florida

Atkins North America

Load capacity rating of an existing curved steel box girder bridge through field test

Abstract

This paper presents a load rating procedure through field test and analysis for Veteran's Memorial Bridge. The bridge is a curved steel box girder bridge, located in Tallahassee, Florida. The tests include a bending test, a shear test, and a structure system test. Test and analytical results indicate: (1) nearly all concrete areas of the bridge deck and barriers are composite with the steel box girders and effectively resist both bending and shear forces; (2) the shear capacity at the end abutment is much higher than that predicted by current Guide Specifications; (3) the bridge behaves predictably. Based on test and theoretical results, a reliable analytic model was developed. Load ratings for a total of 13 types of trucks permitted in Florida were performed according to the identified analytical model. Rating results show that the operating rating loads evaluated based on the identified model are greater by about 43% than those obtained based on current AASHTO Guide Specifications. The operating rating factor for the HS20-44 vehicle based on the identified model is 38% greater than that obtained in 1997. The rating procedure presented in this paper is instructive and can be used in bridge load-rating activities.



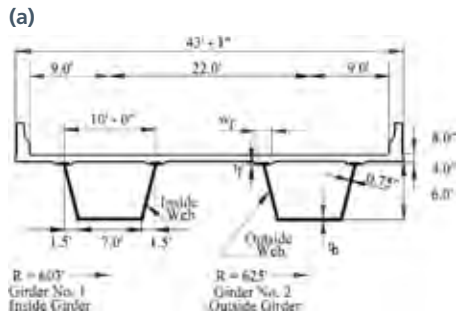
Figure 1. Veteran's Memorial Bridge

Introduction

Veteran's Memorial Bridge (see **Figure 1**) is a steel box girder bridge carrying US 319 in Tallahassee, Florida. It consists of two sections of three-span continuous girders; one section is straight and the other is curved. The bridge was built in 1997 and its capacity was determined based on the as-built plans dated that same year. The original load rating factor for an HS20-44 design load is controlled by the bending capacity of the curved unit and very conservatively estimates the capacity of the bridge. A more recent load rating of this bridge performed in 2003 indicates that the shear capacity of the curved unit at the abutments is also comparatively low, based on the current AASHTO Guide Specifications for Horizontally Curved Steel Girder Highway Bridges¹.

Many non-destructive load tests of bridges¹ show that there is a potential for demonstrating higher load capacities for bridges than those determined based on conventional analysis alone, due to the following effects: (a) actual section dimensions; (b) actual material properties; (c) unaccounted system stiffness and section, such as curb, barrier, and additional composite action; and (d) conservative design codes and other conservative assumptions. Subsequently, field-testing was conducted on this bridge to identify its actual behavior and to more accurately determine its safe load capacity.

The purpose of this paper is to present a structural system identification procedure through a combined test and analysis method, a load rating procedure, and to demonstrate potentially higher and safe capacity ratings based on actual bridge performance.



Description of bridge

Since the load capacity of this bridge is controlled by the curved section, only the curved section will be discussed; the term “bridge” used in this paper refers to the curved section only, unless otherwise indicated.

The three-span continuous curved box girder bridge with an average radius of 187.15m has a span length of 50.53-75.79-50.53m, measured along bridge centerline. The cross-section of the bridge is made of two built-up steel box girders with a center-to-center spacing of 6.71m. The steel sections are composite with the deck. All structural steel is Grade 345 (50), except that the steel of transverse stiffeners is Grade 248 (36). The deck consists of normal weight concrete with design strength of 31.03Mpa. The deck is 203mm thick and 13.13m wide from outside to outside. The design concrete strength for barriers is 23.44Mpa. The typical section is shown in **Figure 2a**. There are a total of six different box cross-sections along the bridge length. The various plate dimensions of each section of the outside girder are shown in **Figure 2b**. The spacing of cross frames is 3.09m, except that the end spacing of the cross frames is 2.71m. There is no lateral bracing between box girders, except at sections over the supports. The spacing of web stiffeners at end supports is 1.49m. Principal as-built dimensions of the bridge were verified. It was found that the haunch heights of the steel girders are different from those shown in the bridge plans. The measured haunch heights at several locations are shown in **Figure 3**. A routine biennial bridge inspection was performed in 2003. The inspection results show that both super- and sub-structures are in excellent condition. There is no evidence of significant structural damage or dimensional differences from the as-built plans.

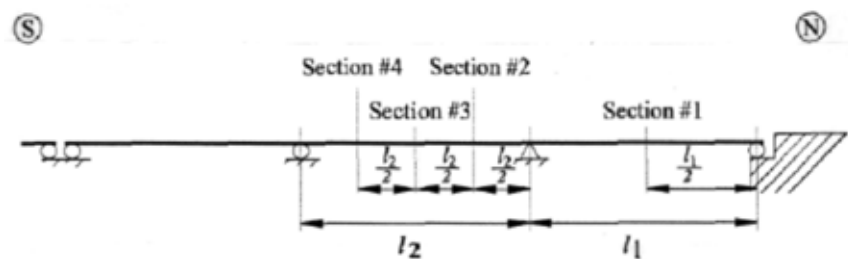
Instrumentation and

(b)

Section No.	#1.	#2	#3	#4	#5	#6	
	51' - 8"	60' - 4"	21' - 8"	44' - 0"	41' - 9"	57' - 9"	Symmetric

Cross section #	Top flange		Bottom flange	
	w _t (width) (in)	tf (thickness) (in)	w _b (width) (in)	tb (thickness) (in)
1	16.0	0.875	86.0	0.5
2	16.0	0.875	86.0	0.875
3	21.0	1.375	86.0	1.25
4	26.0	2.75	86.0	1.25
5	26.0	1.375	86.0	1.00
6	16.0	1.375	86.0	0.875

Figure 2. Bridge principal dimensions (a) Typical cross-section, (b) Longitudinal section 1ft = 0.3048 m, 1 in =25.4 mm)



Section No.	Outside girder		Inside girder	
	Outside haunch h _h (inch)	Inside haunch h _h (inch)	Outside haunch h _h (inch)	Inside haunch h _h (inch)
1	4.00	3.50	3.50	3.00
2	7.40	3.50	4.50	4.00
3	10.25	6.25	5.75	5.75
4	4.25	4.50	5.00	5.75

Figure 3. Measured haunch height (1ft = 0.3048 m, 1 in =25.4 mm)

test loading

The structure identification includes three parts of bending, shear, and system behaviors under truck loading. Both strain and deflection sensors were used to monitor the behavior of the bridge.

Strain gages and location

Four critical cross-sections were chosen for monitoring (see **Figure 4a**). The strain gages at Section #1 (**Figure 4b**) were used to monitor the shear and principal stresses. There were a total of 27 strain gages at Section #1. Sections #2 through

#4 were each instrumented with 8 strain gages oriented in the longitudinal direction of the bridge. The strain gages at Sections #2 to #4 were used to monitor the sectional bending behaviors. Their detailed locations can be found in **Figure 4c**. A total of 51 strain gages were placed on the bridge.

Deflection gages and location

A total of six linear variable differential transformer (LVDT) deflection gages were used to monitor the buckling behavior at Section #1 of the outside girder (see **Figure 5a**). Section #1 is midway

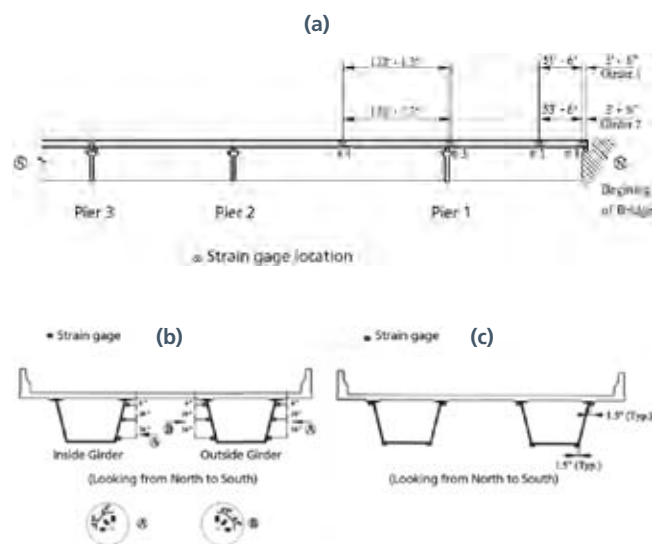


Figure 4. Strain gage locations, (a) In longitudinal direction, (b) At section no. 1, (c) At section #2 to 4 (1 ft = 0.3048 m, 1 in = 25.4 mm)

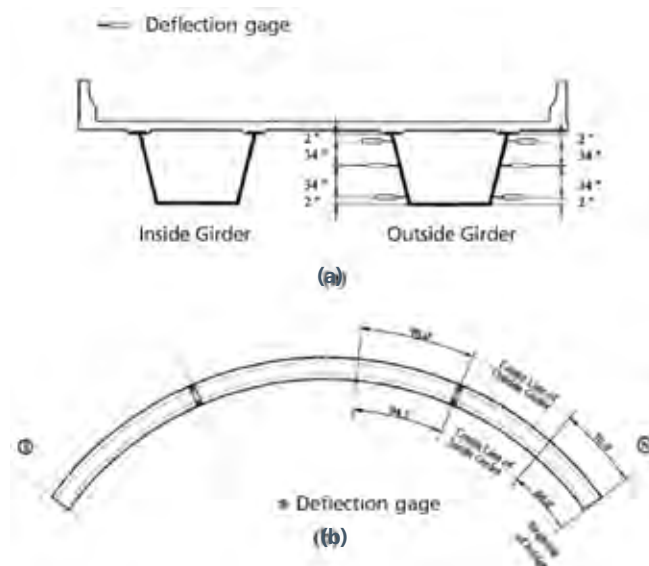


Figure 5. Deflection gage locations, (a) Horizontal deflection gages at end, (b) Vertical deflection gages (1 ft = 0.3048 m, 1 in = 25.4 mm)



Figure 6. FDOT Test truck loaded with steel blocks

between the end diaphragm and the first transverse stiffener. The top and bottom gages were used to monitor the torsion deformations of the girder, while the middle deflection gages were used to monitor the local deformation of the webs. Six DT deflection gages were mounted to the bottom flange of the box girders on the side and center spans to measure the bridge vertical displacements (see **Figure 5b**). The main purpose of this measurement was to monitor the structural integrity and to detect possible significant hidden deteriorations.

Test loading

Two Florida Department of Transportation (FDOT) Research Center test trucks (see **Figure 6**) were used to test the bridge under live load conditions. Each truck can carry a maximum of 72 concrete-filled steel blocks, a weight totaling 839.83kN. Detailed descriptions of the trucks are found in Huang, et al².

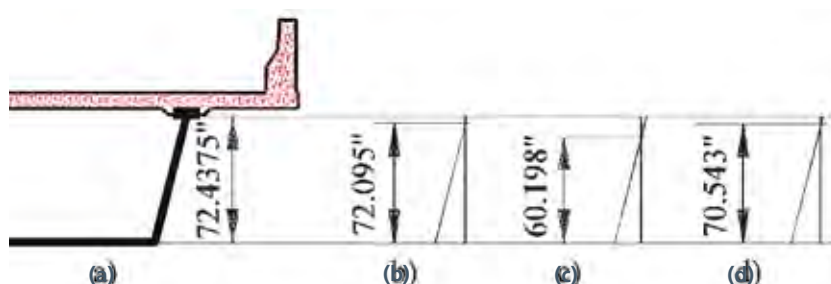


Figure 7. Comparison of neutral axis locations for section #4, (a) Half section of box, (b) Test results, (c) With original design assumptions, (d) Considering actual modulus of elasticity and entire slab and barriers concrete areas (1 ft = 0.3048 m, 1 in = 25.4 mm)

Structural identification

Deck concrete modulus and strength

Normally, after several years of service, concrete actual strength will be higher than the strength assumed for design. In order to verify the actual deck concrete strength, three concrete cores were taken from the bridge deck and tested according to American Society of Testing Materials (ASTM) Specifications. Each of the concrete cores had a length of 152.4mm with a diameter of 76.2mm. The modulus elasticity and strength of each concrete core is given in **Table 1**. In this table, the moduli of elasticity were determined according to the equation provided in ASTM Specifications Article C469-94. The average values of the test results are taken as the strength and the modulus of elasticity of the deck concrete.

Identification of bending section

To identify how much concrete areas of barriers and bridge deck are composite

Concrete core no.	Modulus of elasticity, $E_c \times 10^4$ Mpa	Concrete strength, f_c (Mpa)
1	3.608	55.78
2	4.027	54.13
3	3.983	64.54
Average	3.872	58.15

Table 1. Modulus of elasticity and strength

with the steel box girders, **Figure 7** shows the comparison between test and analytical neutral axis locations at Section #4. **Figure 7b** illustrates the test neutral axis locations determined by the average stresses of inside and outside webs. The test results were measured based on the loading condition of two trucks side by side placed over Section #4, each with a weight of 525.0 kN. The neutral axis locations shown in **Figure 7c** were determined according to the original

Web	Gage location	Micro Strain			Shear stress (Mpa)	Principal stress (Mpa)	Principal angle (Degree)
		ϵ_V	ϵ_L	ϵ_H			
Outside	Top	-103.67	29.36	-0.6	-18.15	-14.2	61.15
	Middle	-58.81	-167.35	-27.48	-19.11	-31.58	41.41
	Bottom	-24.74	-127.90	-19.18	-16.27	-22.57	44.25

Table 2. Test web shear stress distribution

Location	Maximum stress (Mpa)				Absolute difference (%)		
	Plane grid		Shell plate Case 3	Test	Plane grid		Shell plate Case 3
	Case 1 (AASHTO)	Case 2			Case 1 (AASHTO)	Case 2	
Middle	24.94	19.97	20.48	18.15	37.41	10.03	12.84
Top	24.94	21.82	21.42	19.11	30.51	14.18	12.09
Bottom	24.94	13.79	18.47	16.29	53.10	15.35	13.38

Table 3. Comparison of maximum web shear stresses at Section #1

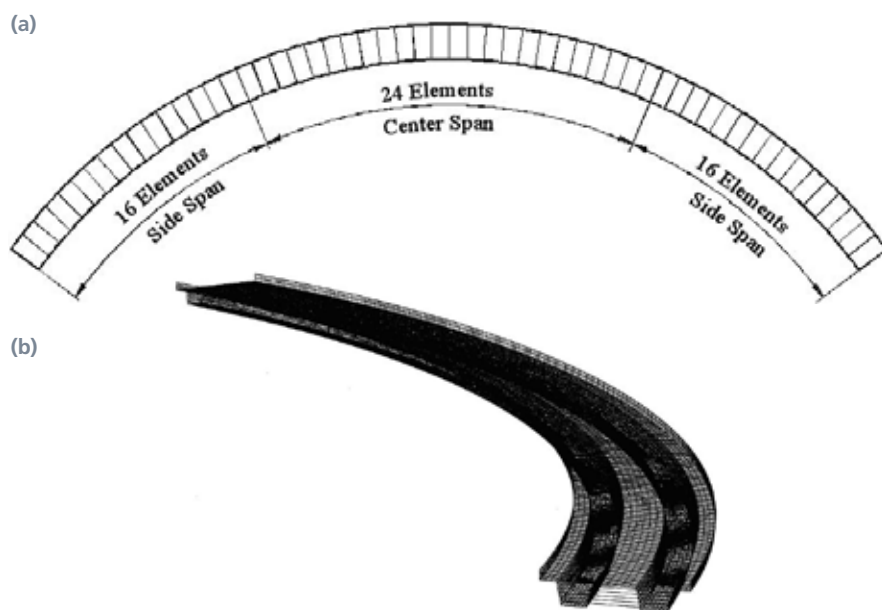


Figure 8. Analytical model, (a) Plane grid, (b) Shell-plate

design assumptions and the current Guide Specifications¹. The neutral axis locations illustrated in **Figure 7d** were evaluated based on tested deck concrete modulus of elasticity and by assuming all concrete areas are effective, including the entire deck and barriers. From **Figure 7**, we can conclude that all deck and barrier concrete sections are composite with the steel girders.

Identification of shear section

Because the first transverse stiffener at the simple end support of the bridge does not meet the requirement of AASHTO

Guide Specifications for Horizontally Curved Bridges¹, the calculated shear capacity at Section #1 is comparatively low. A diagnostic test was performed at this section. Two FDOT test trucks were positioned side by side and incrementally loaded from 473.5kN to 787.3kN. Strain and deflection readings were carefully observed and recorded for each loading case. Detailed test results can be found in Huang, et al². The distribution of shear stress and principal stress and direction for outside girder, outside web are shown in **Table 2**.

The test and analytical maximum shear stresses in the outside web of the outside girder are given in Table 3. Two different models were employed to analyze this bridge: Plane grid model and shell-plate model (see **Figure 8**).

In the plane grid model, the bridge is divided into two types of finite elements: plane grid elements and curved grillage elements³. The transverse action of the bridge deck is simulated by plane grid elements and the curved box girder is modeled with curved grillage beam elements. The side and mid spans are divided into 16 and 24 elements in bridge longitudinal direction respectively. Torsional shear stresses were determined by thin-wall theory⁴ and by assuming the steel box girder section to be rigid. In the shell-plate finite element system, the bridge deck, barriers and steel box girders are divided into a series of quadrilateral shell-plate elements, while the bracings and stiffeners are treated as three-dimensional frame elements. There are a total of 21,555 shell-plate elements and 5,417 three-dimensional frame elements. In Case 1, the vertical shear obtained by the plane grid model is assumed to be taken by the steel web according to AASHTO Guide Specifications¹. In Case 2, the vertical shear determined by the plane grid model is assumed to be taken by the whole section, effectively including the concrete deck and barriers. The shell-plate model is defined as Case 3.

In **Table 3**, the difference ratio is calculated as:

$$\text{Difference} = \frac{\text{Analytical} - \text{Test}}{\text{Test}}$$

From this table, it can be seen that the test shear stresses are much smaller than those obtained from the AASHTO codes. However, if the effect of the concrete section (Case 2) is considered, the maximum differences of the maximum shear stresses between test and analytical results obtained by plane grid model are about 15%. The actual concrete strength and area reduce shear stress by about 16% to 28%.

Table 4 shows the tested lateral deflections for the outside web of the outside girder. The web shears, including torsional shear, were determined using the plane grid model. The relative deflection at the web mid-height is defined as the deflection referenced to the straight web. From this table, we can see that the lateral deflections of the web are very small. The relative deflections are close to zero and may be due to the limited accuracy of the gages. The ratio of the relative deflection to the web depth (H) is less than 1/10000. The tested web shear can be expected to be far less than the web buckling shear strength.

Since available test loading is insufficient to field-test the web shear capacity, a full non-linear analysis of the curved box girder bridge was performed to determine the web shear capacity. The web, deck, and stiffeners were modeled as a number of quadrilateral shell-plate elements. An initial imperfection in the sinusoidal shape function was introduced and normalized to a magnitude of one hundred-twentieth of the web depth, which is the maximum allowed out-of-flatness in Bridge Welding Codes⁵. The nonlinear analytical results are shown in **Figure 9** where the abscissa represents the web maximum deflections not including the assumed initial deflection and the ordinate represents web shear force. Two different shear capacities predicted according to AASHTO Guide Specifications¹, and based on two different assumptions of non-stiffened and stiffened webs are also shown in **Figure 9**. The assumption of a non-stiffened web is based on the fact that the ratio of the stiffener spacing to web depth at the first transverse stiffener at the end supports of Veteran's Memorial Bridge does not meet the requirement specified in the AASHTO Guide Specifications¹. For this reason, engineers have to treat this web as non-stiffened,

Web shear (kN)	Deflections (mm)				
	Top	Middle			Bottom
		Measured	Relative (Δ)	$\Delta/H/100000$	
397.34	0.29	-0.32	-0.05	2.90	-0.42
443.11	0.34	-0.31	-0.03	1.45	-0.47
487.19	0.25	0.43	-0.13	7.21	-0.64
534.87	0.32	-0.39	-0.08	4.50	-0.64
581.44	0.36	-0.43	-0.09	4.78	-0.65
626.59	0.38	-0.40	-0.06	3.34	-0.76
672.40	0.38	-0.50	-0.12	6.63	-0.81

Table 4. Measured web lateral deflections

resulting in a very low web shear capacity of 1364kN. The assumption of a stiffened web is based on the fact that the first transverse stiffener spacing at the ends of the bridge meets the criteria for stiffened straight webs. If the web is treated as stiffened, the web capacity determined by the AASHTO Guide Specifications is 4146kN, which is close to the result obtained from the nonlinear analytical results. From **Figure 9**, it can be seen that the current AASHTO Guide Specifications regarding the first stiffener spacing is conservative and that the web shear capacity can be safely determined by assuming the curved web as a stiffened web.

Structural system identification

Deflection under loading is one of the most important characteristics which represent the behavior of an entire structural system. One FDOT test truck with a total weight of about 467kN crawled along both the inside and outside girder alternatively maintaining a distance of 1.219m from the curb line; the influence lines at Sections 1 to 4 were recorded. **Figure 10** shows the comparison of test-based and calculated influence lines at center span of the outside girder when the truck moved over the inside girder. The solid line represents the test data; the dash line represents theoretical results. In the theoretical analysis, the concrete modulus of elasticity was taken as 3.872×10^4 Mpa and all of the concrete areas were considered as effective based on the results of the identification procedure. The bridge was modeled as a plane grid model. From this Figure, we can see that the tested influence lines agree well with the analytical results.

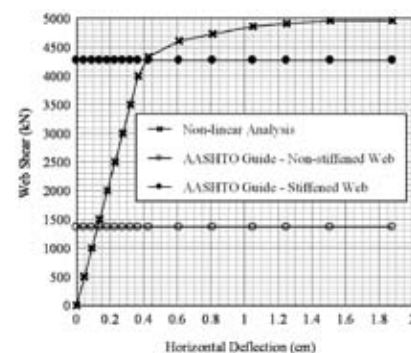


Figure 9. Variation of web lateral deflection with shear

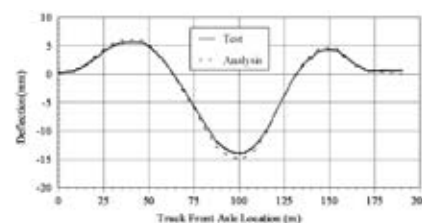


Figure 10. Deflection influence line at section #4 under inside web of outside girder

To further verify the actual structural system, typical normal stress distribution tests at critical sections with heavier loading were performed. In the testing, two trucks side by side, each with a total weight of 525.0kN, were placed at the predefined critical load positions on the bridge. The comparison between maximum test and analytical results at Sections 2 and 4 are given in **Table 5**. Case 1 cross-sectional properties were determined according to the original design assumptions, neglecting the barrier effect; while Case 2 cross-sectional properties were evaluated based on the test results with a deck concrete

Section	Girder	Maximum stress (Mpa)				Difference		
		Plane grid		Shell plate Case 3	Test	Plane grid		Shell plate Case 3
		Case 1	Case 2			Case 1	Case 2	
2	Outside	62.27	57.84	53.46	54.24	14.8%	6.6%	-1.4%
	Inside	53.37	49.13	48.16	46.41	15.0%	5.9%	3.8%
4	Outside	55.09	51.35	50.11	45.80	20.3%	12.1%	9.4%
	Inside	47.42	43.62	41.72	39.00	21.6%	11.9%	7.0%

Table 5. Comparison of maximum normal stresses at bottom flange

modulus of elasticity of 3.653×10^4 Mpa, considering the barrier section to be effective. From Table 5, it can be observed:

1. The difference ratios between the test and analytical results predicted by the plane grid model for Case 1 range from 15% to 22%, while for Case 2 they vary from 6% to 12%;
2. The maximum difference ratio between the test and analytical results predicted by the shell-plate finite element model for Case 2 are less than 10%;
3. Plane grid models are good for bridge design and analysis;
4. The actual deck concrete strength and barrier effect reduce the maximum normal stresses by about 8% to 10%.

From the deflection and normal stress comparisons between test and analysis, we can conclude that entire bridge structure is in good condition and its response to live loads can be well predicted by a plane grid model.

Bridge capacity rating

Rating model

The final rating mechanical model was determined by following the flowchart shown in **Figure 11**³. The identified bridge structure, based on the measured response, includes many effects as mentioned. Some effects may not be reliably used for determining a safe load-carrying capacity. For example, the barrier wall has expansion joints that may be removed during bridge widening. For conservative purposes, the final rating mechanical model only includes the effect of actual concrete strength and the whole deck width concrete area in bending capacity and the effect of steel webs in shear capacity. The bridge is modeled as a plane grid finite element model with 56 elements in bridge longitudinal direction.

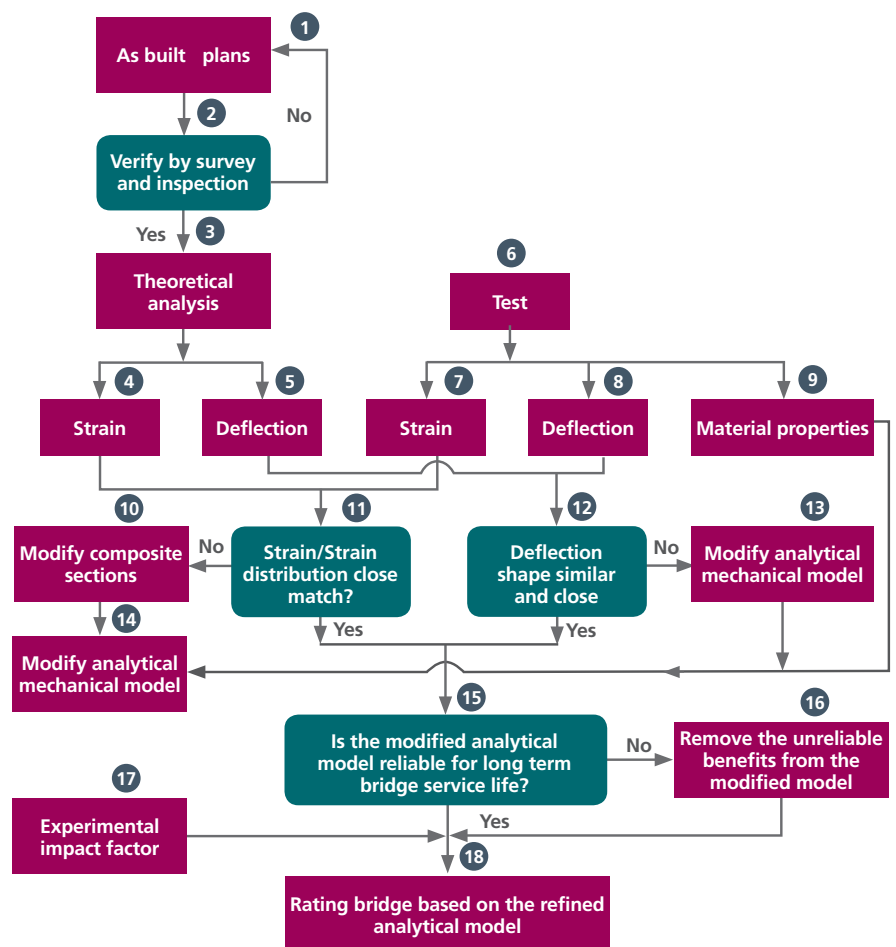


Figure 11. General flowchart for bridge rating through field test

Rating vehicles

There are a total of 13 types of trucks currently permitted in Florida. The configurations of the trucks are shown in **Figure 12**. The spacing between tires in the transverse direction is equal to or greater than 1.829 m.

Rating results

The bridge load rating factors are determined by using the following rating equation contained in the AASHTO Manual for Condition Evaluation of Bridges⁶.

$$RF = \frac{C - A_1 D}{A_2 L(1 + I)} \quad (2)$$

Where RF = the rating factor for live load carrying capacity, C = the capacity of the member, A_1 = factor for dead load = 1.3, D = service dead load, A_2 = factor for live load, for inventory level = 2.17, for operation level = 1.3, L = live load effect, and I = impact factor.

The critical section for shear is located at the end supports. The critical section for bending moment in the side-span is located 17.98m from the north side abutment, measured along the outside girder axis. The critical section for bending moment in the middle span is located 38.58m from the interior support, measured along the outside girder axis.

Shear capacity at end, according to current Guide Specifications³: $V_{cr} = C_{by} * 0.58F_y * H * t_w = 1369 \text{ kN/web}$, where C_{by} = The ratio of the elastic-shear-buckling strength to the shear-yield strength = 0.253, H = web depth, t_w = web thickness. Shear capacity at end, according to identified shear section and behavior: $V_{cr} = C_{by} * 0.58F_y * H * t_w = 3661 \text{ kN/web}$, where $C_{by} = 0.68$.

Moment capacity: $M_{cr} = F_{cr} * S_b = 31,828 \text{ kN-m}$ (side span), 45639 kN-m (middle span), 70313 kN-m (interior support), where S_b = bottom section modulus, F_{cr} = maximum allowable normal tension stress.

The inventory rating factors based on current AASHTO Guide Specifications and the identified structure are 0.923 and

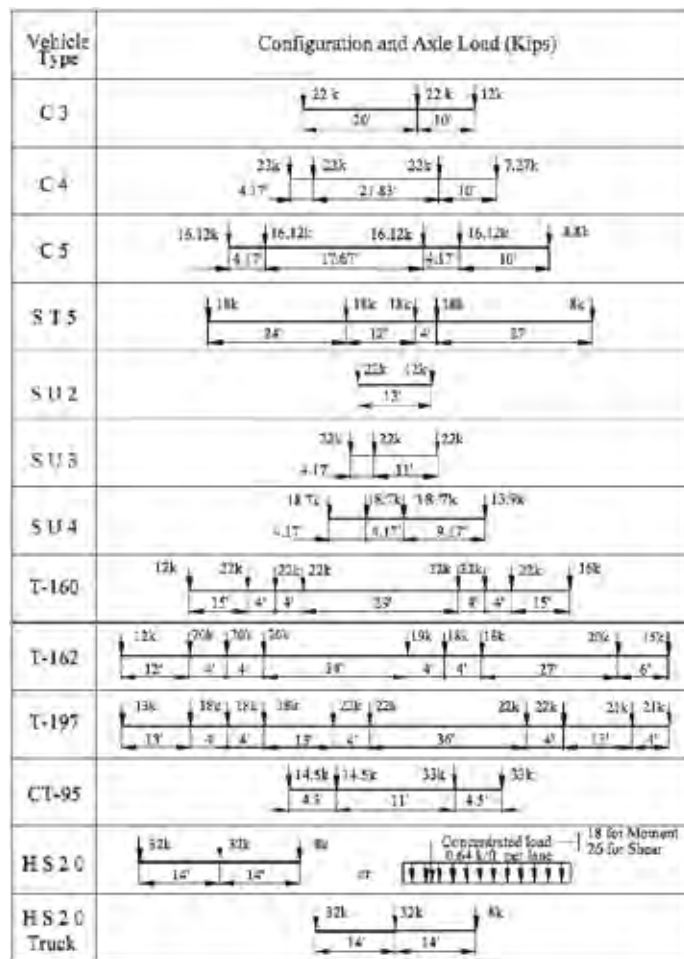


Figure 12. Rating truck designation and configuration (1 kip = 4.448 kN)

Rating vehicle	Vehicle weight (kN)	Rating based on identified (bending control) (1)	Rating based on current specs (shear control) (2)	Original rating (bending control, 1997)(3)	Difference	
					((1) (2))/(2)	((1) 3)/(3)
C3	124.5	3.730	2.379	3.307	57%	13%
C4	162.8	2.892	1.787	2.555	62%	13%
C5	162.8	2.940	1.789	-	64%	-
ST5	177.9	2.856	1.668	2.458	71%	16%
SU2	75.6	5.660	3.147	5.071	79%	11%
SU3	146.8	2.938	1.844	2.630	59%	12%
SU4	155.7	2.778	1.657	2.474	68%	12%
T 160	355.8	1.561	0.886	-	76%	-
T 162	360.3	1.754	0.985	-	78%	-
T 197	438.1	1.472	0.820	-	79%	-
TC 95	211.3	2.059	1.223	-	68%	-
HS20 TRUCK	160.1	2.804	1.763	-	59%	-
HS20 44	160.1	2.196	1.540	1.588	43%	38%

Table 6. Comparison of operation rating factors for bridge curved section

1.316 respectively. The operation load rating factors are summarized in **Table 6**.

It can be observed from this table that the operating rating loads evaluated based on the identified reliable structure have increased by more than 43% from those obtained based on the current Guide Specifications¹. The load rating capacities evaluated based on the Guide Specifications for all rating trucks are controlled by the shear capacity at the end section, while the load ratings determined based on the identified structure are controlled by bending capacities. The operating rating factor for the HS20-44 design load evaluated based on the identified system has increased by about 38% from that obtained in 1997. Note that the load rating factors obtained in 1997 did not include the shear capacity rating.

Conclusions

The following conclusions are drawn:

1. The existing bridge has a potential to demonstrate a higher load capacity than that determined based on the design assumptions and the specifications. The operating rating factors determined based on the identified structural system for Veteran's Memorial Bridge are about 43% greater than those determined based on the current AASHTO Guide Specifications¹. The operating rating factor for the HS20-44 design load determined based on the actual structure is about 38% larger than that determined in 1997. The proposed structure identification procedure can be applied to other types of bridges.
2. If the actual geometry and material properties are known, the bridge bending and shear behaviors due to live loads and its load capacity can be accurately predicted by a finite element model. For Veteran's Memorial Bridge, the difference between the maximum experimental and analytical results obtained by using a plane grid finite element model at critical sections is about 12% and 15% for bending and shear stresses respectively.
3. Current AASHTO Guide Specifications regarding the first transverse stiffener spacing at the simple end support of a girder seem to be too conservative for bridge load capacity ratings. The shear capacity for Veteran's Memorial Bridge at the simple end support can be safely evaluated as a stiffened web.
4. The test results show that nearly all concrete areas of the bridge deck and barriers are composite with steel box girders. For the Veteran's Memorial Bridge, the actual concrete strength and barriers contribute an increase of about 9% and 25% respectively to the bending and shear capacity.
5. Test and analytical results show that a plane grid finite element model with about 20 elements per span in the longitudinal direction can be used to analyze the curved multi-box girder bridges with external bracings located only over supports.
6. Experimental and analytical results show that under the bridge design loading (such as two trucks side by side) the entire bridge cross section, including the full width of deck and barriers, can be safely treated as effective concrete area for bridge internal force analysis.

Acknowledgments

The writer would like to express his sincere appreciation to Mr. Marc Ansley, P.E., Mr. Garry Roufa, P.E., and Mr. John Previte, P.E., for their valuable comments and support received during the research. Gratitude is also extended to the FDOT Structures Research Center staff for their hard work in the instrumentation, testing, data collection, and preparing some Figures contained in this paper. The opinions and conclusions expressed in this paper are those of the writer and are not necessarily those of the Florida Department of Transportation.

This paper is a revision of the paper entitled "Structure Identification and Load Capacity Rating of Veteran's Memorial Curved Steel Box Girder Bridge" by Dongzhou Huang, Journal of Transportation Research Board (TRB), TRB of National Academies, No.2200, 2010, Washington, D.C., USA.

References

1. AASHTO, (2003), "Guide Specifications for Horizontally Curved Highway Bridges", Washington, D.C.
2. Huang, D. Z., Ansley, M.(Reviewer), and Roufa, G. (Reviewer) (2004), "Bridge Test Report - Veteran's Memorial Bridge", Florida Department of Transportation, Structures Research Center, Report No. SRC-H001-04, Tallahassee, Florida.
3. Huang, D.Z., (2004). "Field Test and Rating of Arlington Curved Steel Box Girder Bridge", Journal of Transportation Research Record, No. 1892, Transportation Research Board, Washington, D.C.
4. Heins, C. P., and Firmage, D. A. (1979). Design of Modern Steel Highway Bridges, Wiley, New York.
5. AASHTO and the American Welding Society (AASHTO/AWS). (1990). Bridge Welding Code, AASHTO, Washington, D.C.
6. AASHTO, (2001). "Manual for Condition Evaluation of Bridges", Washington, D.C.

**Glenn F. Myers**Principal
Technical ProfessionalTZ Transportation
Management

Atkins North America

**Ali M Ghalib**

Senior Engineer III

Transportation Design
& Planning Southern
States

Atkins North America

Wind loads on steel box girders during construction using computational fluid dynamic analysis

Abstract

Constructibility requirements for structural steel bridges are defined in the AASHTO Guide Specifications for Horizontally Curved Steel Girder Highway Bridges and the AASHTO LRFD (load resistance factor design) Bridge Design Specifications. These requirements are intended to define conditions encountered during construction that may cause instability or inelastic deformation of the steel structure and to provide guidance on acceptable methods to alleviate these conditions. Analysis for constructibility must consider component and construction dead loads, construction live loads and wind loads. The component and construction loads are easily determined for the constructibility analysis and assumptions are typically noted in the contract plans. Wind loads need to be carefully considered for the different climatologic, topographic, and exposure conditions that occur during construction.

The critical wind exposure condition in the constructibility analysis is on the exposed partially erected girders during the various construction stages and also on the completed skeletal frame prior to the addition of forms and concrete deck. Drag coefficients to be utilized in the development of wind pressures under these conditions are not readily available. Computational Fluid Dynamic (CFD) modeling was performed to develop horizontal drag and vertical lift coefficients for the constructibility analysis, which are significantly larger than those stipulated for the completed bridge in the design specifications. The purpose of this paper is to present the analysis of the wind loading on the steel box girder skeletal frame and to report the criteria utilized in the development of the constructibility plans for the Interstate 4 (I-4)/Lee Roy Selmon Expressway Interchange (LRSEI).

Introduction

The AASHTO Guide Specifications for Horizontally Curved Steel Girder Highway Bridges¹, under which the Interstate 4 (I-4)/Lee Roy Selmon Expressway Interchange (LRSEI) project was designed. The AASHTO LRFD (load resistance factor design) Bridge Design Specifications² define constructibility requirements for structural steel bridges to establish conditions encountered during construction that may cause instability or inelastic deformation of the steel structure. These specifications also provide guidance on acceptable methods to alleviate these conditions, including provisions for temporary supports consisting of towers or cables that are added to provide the needed stability and

to control stresses. The requirements for the design of these temporary supports are defined in the AASHTO Guide Design Specifications for Bridge Temporary Works³. Analysis for constructibility must consider component dead loads, construction dead loads, construction live loads, and wind loads. The component and construction loads are fairly easy to predict for the constructibility analysis and assumptions are typically noted in the contract plans. These loads can be easily assessed and modified by the contractor based on preferred means and methods. Wind loads, however, are environmentally based, and need to be carefully considered for the different exposure conditions that occur during construction.



Figure 1. Interstate 4/Lee Roy Selmon Expressway Interchange

The I-4/LRSEI, shown in **Figure 1**, is located in Tampa, Florida, a hurricane wind zone area. This multi-level interchange is characterized by ramp structures varying from 30 feet to 100 feet above existing ground. The wind load design criterion for the finished structure is well defined in the AASHTO LRFD Bridge Design Specifications. Recent failures of partially completed structures under construction during high wind events raised concerns regarding the stability of the exposed steel box girder skeletal frame prior to casting of the deck. The critical wind exposure conditions in the constructibility analysis is on the exposed steel skeletal frame during the various construction stages and also on a completed skeletal frame prior to the addition of forms and the concrete deck.

Research into wind criteria for the partially constructed bridge found little information to provide guidance relating to appropriate wind drag coefficients. It was found that most of the research since the failure of the Tacoma Narrows bridge has been on aeroelastic instability of bridges, and that the topic of drag coefficients for stable bridges has received little attention. In order to establish appropriate drag coefficients, two-dimensional Computational Fluid Dynamic (CFD) modeling was investigated as a tool to develop these drag coefficients. The purpose of this paper is to report on the findings of the CFD analysis and the effects of constructibility wind loading on the skeletal frame. This information established criteria and implementation procedures to be utilized in the development of the design plans for the I-4/LRSEI.

Development of wind loads for constructability

The development of wind loads for constructability must consider the aerodynamic characteristics of the structural steel skeleton of these bridges. AASHTO LRFD Bridge Design Specifications defines structures exhibiting span-to-depth and span-to-width limits greater than 30 as wind sensitive, where structural aeroelastic instability needs to be examined. Steel box girders on this project are governed by the deflection criteria of the AASHTO Guide Specifications for Horizontally Curved Steel Girder Highway Bridges, which prescribes a span-to-depth ratio of less than 25 for deflection control. A check of the span-to-width ratio of the individual boxes indicates a range of 20 to 22. Both of these criteria are well below the critical aeroelastic instability limits. Therefore, the steel skeleton structure will be analyzed utilizing traditional fluid dynamic methods.

Using steady flow fluid dynamics model, velocity pressures are determined from Bernoulli's equation as a function of the mass density of air and the square of the wind flow velocity. This velocity pressure is then modified by various adjustment factors to develop the design surface pressures to be applied to the structure in question. These adjustment factors are functions of the geometric shape of the structure, its location within the project environment and probabilities of occurrence. These factors have been developed from wind tunnel and water tunnel tests and historical

performance data.

Wind flow surface pressures are typically calculated by applying adjustments to the Bernoulli equation in the following form:

$$p = 0.00256 * K_z * K_t * K_d * V^2 * I * G * C_p \quad (1)$$

where: p = Wind flow surface pressure (psf)

K_z = Velocity pressure exposure coefficient (nondimensional)

K_{zt} = Topographic factor (nondimensional)

K_d = Wind directionality factor (nondimensional)

V = Basic wind velocity (mph)

I = Importance factor (nondimensional)

G = Gust effect factor (nondimensional)

C_p = Drag coefficient (nondimensional)

The above formula is the current format shown in ASCE 7-05⁴. The various AASHTO documents reference the older ASCE 7-88 document⁵. The formula in these two ASCE publications is basically the same, except that ASCE 7-88 included the gust effect factor within the velocity pressure exposure coefficient, and applied the importance factor with the basic wind velocity and squaring the product of these two values. The wind directionality factor is a new component of equation 1, and will be discussed.

To develop the criteria for the partially constructed shape of the steel structure, the various components of this formula are addressed in the following discussion.

Basic wind velocity and wind directionality

Florida Department of Transportation (FDOT) Structures Design Guidelines (SDG)⁶ Section 6.8 requires the evaluation of the superstructure stability during construction using load criteria from the AASHTO LRFD Bridge Design Specifications and the AASHTO Guide Design Specifications for Bridge Temporary Works, which defines the wind velocity using a 50-year mean return interval (MRI) wind velocity chart. This chart corresponds to the 50-year MRI (fastest mile) wind velocity chart included in ASCE 07-88. The basic wind velocity for the project area is defined as 100mph, and is consistent with FDOT SDG Section 2.4.1.

Factors of safety are applied to the wind flow surface pressure developed from equation 1 to simulate higher storm

intensities. The methodology presented in the AASHTO Guide Design Specifications for Bridge Temporary Works is more consistent with allowable stress design (ASD) philosophy where the Factor of Safety is provided by utilizing a lower allowable stress (approximate Factor of Safety of 1.5). The AASHTO Guide Specifications for Horizontally Curved Steel Girder Highway Bridges uses a Load Factor approach by specifying a Load Factor of 1.4 on wind for constructibility. It should be noted that the current AASHTO LRFD Bridge Design Specifications has reduced this criteria, using a Load and Resistance Factor approach with a Load Factor of 1.25 on wind for constructibility and a Resistance Factor of 1.0.

Wind directionality represents the lower probability of having the wind blowing on the entire bridge at some critical angle (horizontal yaw and vertical). The current ASCE 7-05 utilizes a Load Factor of 1.6, which corresponds to a 500 year MRI for hurricane prone regions using the ASCE 7-05 wind charts. The pressure associated with this Load Factor is then modified by a Wind Directionality Factor of 0.85. The AASHTO design provisions do not include adjustments for wind directionality, but instead utilizes a Load Factor of 1.4, which already includes the Wind Directionality Factor. The application of the implied 1.6 Load Factor to the 100mph basic wind velocity represents a strength based wind velocity of 126mph, corresponding to an upper level Category 3 storm in accordance with the Saffir-Simpson Scale (111mph – 130mph).

In straight girder bridges, the probability of having the wind acting at a particular critical wind direction (in this case a wind normal to the bridge longitudinal axis) can potentially be smaller compared to curved bridges having varying orientations and therefore have higher probability to be subjected over a given section to that critical wind direction. Since the wind travels primarily in a single direction at a particular moment in time during a hurricane, the probability of having the entire curved unit loaded with full wind load may be as remote as that for a straight bridge. As such, an increase above the proposed Load Factor of 1.4 for wind for constructibility is deemed unnecessary.

Velocity pressure exposure coefficient

Velocity pressure exposure coefficients are based on the height above ground and will use the previously accepted philosophy utilized for the development of wind pressures for the fully constructed

bridge. This philosophy adopted an Exposure C classification, and for the heights of the structures within this project resulted in a K_z of 1.5.

Topographic factor

The Topographic Factor accounts for wind speed-up at embankments (escarpments). This factor was analyzed as inconsequential to the development of wind pressures for the constructed bridge and will not be considered in the constructibility analysis.

Importance factor

AASHTO does not currently apply an importance factor to wind, although they do establish essential and critical structures for probability based seismic design and vessel impact design. This factor will not be considered in the constructibility analysis.

Gust effect factor

For typical bridge structures that are not sensitive to wind-induced dynamics the gust effect coefficient, G , applied to the fastest mile wind velocity may vary between 1.25 and 1.50. For typical bridges, a G of 1.3 is usually assumed. The current philosophy of most other codes is to utilize the three second gust wind velocity with a reduced gust factor of approximately 0.85 for stiff structures that is adjusted to higher values depending of the structure's flexibility.

Drag coefficient

The drag coefficient, C_D , is a function of many variables, the most important of which are the yaw angle of attack (horizontal angle of wind), and aspect ratio (ratio of height to width of structure). For box or I-girder superstructures and solid piers with wind acting at zero yaw angle, C_D may vary between 1.2 and 2.0. A factor of 1.50 for C_D is usually assumed for design purposes for a fully constructed bridge. For unusual exposure shapes, the drag coefficient should be determined from

wind tunnel tests or by other analytical means. Assuming the importance factor and exposure coefficients are 1.0, a gust factor of 1.3, a drag coefficient of 1.5 and a wind velocity of 100mph design (fastest mile) wind velocity, the formula above yields the 50psf transverse wind load currently prescribed in the various AASHTO documents. Use of the velocity pressure exposure coefficient of 1.5, previously adopted for the taller structures within this project, resulted in the recommendation to use 75psf for the design of the completed bridge structures.

Much research has been performed over the last 60 years in the field of aeroelastic instability of long spans and their supporting towers and cables, while the performance of traditional shorter span bridges has received little attention. The configuration of steel box girders prior to the casting of the deck does not fall within the assumed parameters for typical bridges and must therefore be analyzed for temporary conditions where the drag coefficient can be significantly different from the typical final bridge structure. The development of a drag coefficient for the skeleton structure has to be considered carefully.

The principle research found for the development of drag coefficients for typical bridges was compiled by the ASCE Task Committee on Wind Forces⁷. The ASCE Task Force found that for a structure consisting of a combination of parallel plates, as is the case of a partially or fully erected pair of steel plate or box girder superstructure elements before the installation of deck, the effect of the shielding of one member by another is appreciable. For zero yaw angle of attack (horizontal) winds, the windward girder shields its leeward counterpart through the formation of a vortex wake behind the windward girder. This wake results in a suction pressure in the space between the girders. Typically, the drag on the

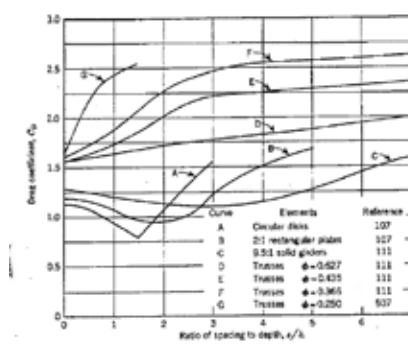


Figure 2. Effects of spacing on drag of pairs of elements

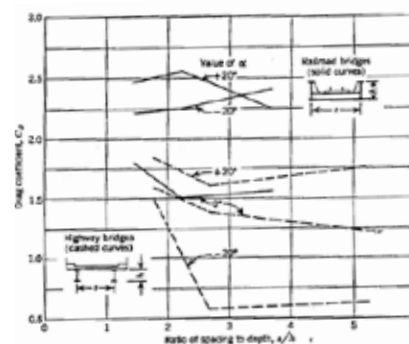


Figure 3. Drag coefficients for bridges⁶

windward girder of a bridge is larger than that on the leeward girder due to the suction pressure created behind the windward girder. At the same time the drag on the leeward girder may be positive or negative depending on the relative magnitude of the suction pressures on both sides of that girder. The total drag (sum of all pressures on all faces of the bridge girders) depends on the spacing of the girders. If the spacing is very small, the drag is the same as on a single girder. As the spacing is increased further, the wake effect is reduced resulting in an increase in the total drag on the bridge system, and would eventually equal twice that at zero spacing. Curve C in **Figure 2** shows the effect of girder spacing ratio (spacing/girder height) on the total drag coefficients of a pair of plate girders having a 9.5:1 aspect ratio due to a horizontal wind with zero yaw angle.

The wind coming from McKay Bay and across the Crosstown embankment is expected to have an upward component as it approaches the bridge ramps, which is further compounded by the superelevation of the proposed structure. Based on results from wind tunnel tests of plate girder bridges, the effect of shielding is greatly reduced with small yaw angles. As the vertical angle of attack increases, the suction pressure between the two girders decreases because ultimately this zone will become a path of flow. In addition, as the angle of attack increases, the downwind girders become more exposed and the projected area of the bridge system subject to wind pressure also increases leading to higher total "system" C_p . The solid lines in **Figure 3** show the total drag coefficient on a twin girder bridge system with no deck for varying spacing depth ratios and three values of wind angles of attack, namely -20 degrees, 0 degrees, and +20 degrees. The angle of attack is positive when the wind has an upward component. The through railway bridge system with open floor configuration resembles the twin box girder bridge system before placement of the Stay-In-place (SIP) forms and casting of the concrete deck. It is indicated that typically higher C_p coefficients are measured for both positive and negative angles of attack as compared to horizontal winds. Typically the superelevated I-4/LRSEI skeleton structure simulates the through girder bridge structure with slope of approximately 5 degrees.

The dashed curves in the same figure indicate the measured drag coefficients for a typical highway bridge after casting the concrete deck. Due to the aerofoil



Figure 4. Typical steel skeletal frame cross section

characteristics of the deck-girder bridge system, and for reasonable yaw angles of attack (± 20 degrees), the drag pressure on all but the windward girder is very small. In addition, there is little drag on the relatively smooth upper surface of the deck for winds with negative angle of attack. It is indicated that the presence of the deck (metal SIP or concrete deck) reduces the total drag coefficient on the bridge system for these angles of attack. This condition was considered non-critical and was not considered further in this study.

For the I-4/LRSEI constructability analysis, a design yaw angle of approximately 10 degrees plus the maximum superelevation will be selected for the analysis of all bridge units, or approximately 15 degrees. Based on the research, a conservative C_p value of 2.5 would be assumed for these bridges; however, advanced modeling techniques are available for determining appropriate drag coefficients using CFD modeling. No information on lift coefficients was available from the research. The lift coefficient was assumed to be proportional to the ratio of the AASHTO provided default uplift (20psf) to the default horizontal pressure (50psf), or 0.4 times C_p . This yields a lift coefficient of -1.0 (upwards).

Computational fluid dynamic modeling

The use of CFD modeling software was investigated to develop more reliable information related to the drag, lift and torsional coefficients to be utilized in the design. Of the many CFD software packages available, Bentley's RM software was chosen due to the simplicity of its analysis on a two dimensional cross-section.

CFD modeling was performed on the typical steel skeletal frame cross-section shown in **Figure 4**, which consisted of

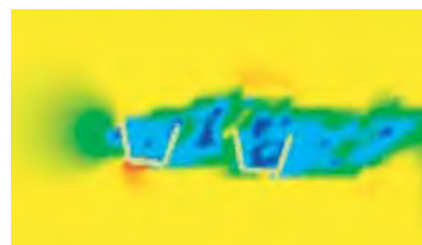


Figure 5. Wind velocity diagram for wind attack with a yaw of zero degrees

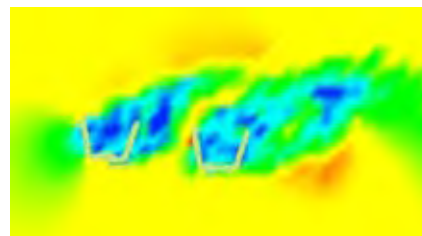


Figure 6. Wind velocity diagram for wind attack with a yaw of 10 degrees

two steel box girders, each 7'-11" deep, 11'-9" top of web spacing per box, 24'-0" center to center box girder spacing, and an 8% superelevation.

Wind was varied from -15 degrees (slightly downward) to +15 degrees (slightly upward) from the left and the right. The angle presented by the program uses a counterclockwise convention with 0 degrees being horizontally level from with wind from the left. Wind from the right will therefore be presented as being from +165 degrees (slightly upward) to +195 degrees (slightly upward) from the right.

The first series of runs were performed on the open section as shown in **Figure 4**. Wind attack with a yaw of zero degrees appears to substantiate the findings of the ASCE Task Committee on Wind Forces. **Figure 5** presents a wind velocity diagram, where the dark blue areas represent very low wind velocity, the yellow areas represent the nominal applied wind velocity and the red areas

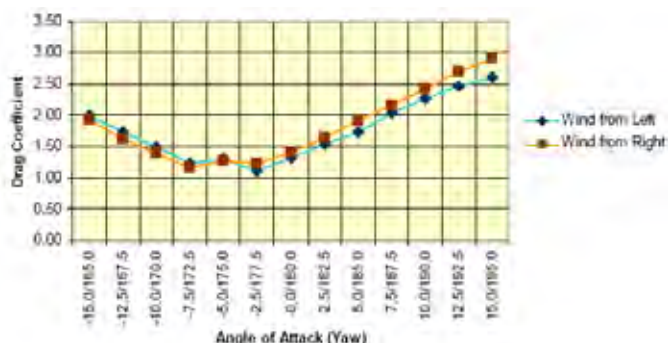


Figure 7. Drag coefficients from the CFD analysis for open cross-section

represent wind velocities approximately twice the nominal applied wind velocity. It can be seen from this figure that the areas inside and between the boxes have very low wind velocity, and therefore high stagnant pressures. The wind appears to flow over the top and bottom of the box girders as a pair.

Figure 6 presents a wind velocity diagram with a yaw angle of attack of 10 degrees. It can be seen that the wind is now flowing upwards between the boxes with significantly higher wind velocities. The wind is now acting on the two box sections as evidenced by the yellow wind trail between the boxes, again substantiating the findings of the ASCE Task Committee on Wind Forces.

The drag coefficients determined from the CFD analysis are reported in **Figure 7**. Note that the development of higher velocities associated with lower pressures in the areas between the boxes and on the leeward face of the leeward box result in higher net drag force on the bridge section. Note that the values for drag coefficient appear fairly symmetrical about the -5 degree angle. This angle corresponds to the amount of superelevation for the steel boxes. For the 10 degree upward yaw angle of wind from the left, the drag coefficient is approximately 2.3, very close to the 2.5 value originally assumed from the research.

The lift coefficients determined from the CFD analysis are reported in **Figure 8**. Again, the values for drag coefficient appear fairly symmetrical about the -5 degree angle, corresponding to the superelevation for the steel boxes. This figure also shows an unexpected flattening of the lift coefficient to approximate -0.15, indentifying a significant reduction in lift from what would be expected. It is believed that the interruption of a smooth streamlined flow over the boxes due to the missing top cover actually does not allow a suction lift to occur, thereby reducing the lift. Note that the positive lift is a downward force caused by the wind entering into the top of the boxes.

To test the conjecture regarding the reduction in lift, the same cross-section was analyzed with SIP steel forms attached to the top of the boxes, effectively creating two solid box sections, as shown in **Figure 9**.

The lift coefficients determined from the CFD analysis with the tops of boxes enclosed are reported in **Figure 10**. Again, the values for drag coefficient appear fairly symmetrical about the -5 degree angle, corresponding to the superelevation for the steel boxes. This uplift coefficient also shows vertical symmetry reflective of the geometric symmetry of the enclosed boxes as

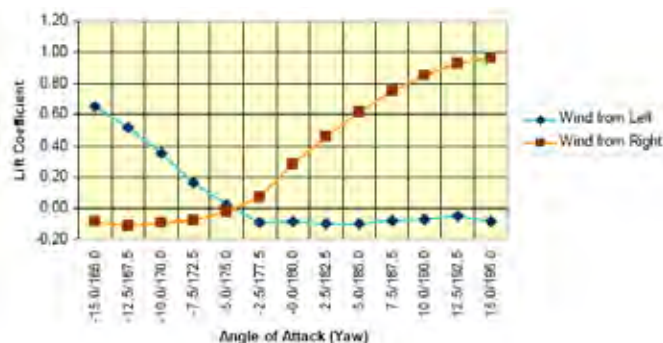


Figure 8. Lift coefficients from the CFD analysis for open cross-section

compared to the uplift for the open sections. For the 10 degree upward yaw angle of wind from the left, the drag coefficient is approximately -0.6. While this value is less than the assumed value of 0.4C_p.

Structure modeling

The analysis of the structural steel box girder system was performed to determine the impact of this higher lateral wind force. A 3D finite element analysis (FEA) model was prepared to simulate the two sample bridge units, units 10-4 and 9-5. Unit 10-4 is modeled as a 4 equal continuous span, curved, double steel box girder bridge unit. The typical span length measured along bridge centerline is 256ft with a 665ft radius of curvature. Each span is divided into 16 equal bay units with inverted-K cross frame assemblies and single diagonal lateral bracing. Unit 9-5 is a 4 continuous span curved bridge unit with 149ft-199ft-220ft-165ft span configuration with a radius of curvature transitioning from a 1700ft to 818.5ft at approximately the third point of span 2. The interior and exterior spans are divided into 20 and 16 bays, respectively, with a similar cross frame and lateral bracing system as that of Unit 10-4. The box girder components comprising of the bottom flange, web plate, interior and end plate diaphragms are simulated using quadrilateral 4-noded

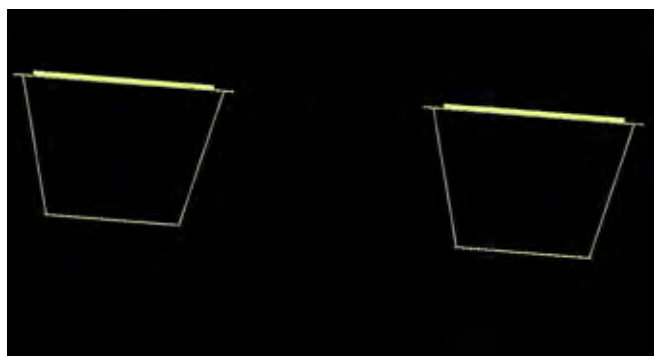


Figure 9. Typical steel skeletal frame cross section with tops enclosed

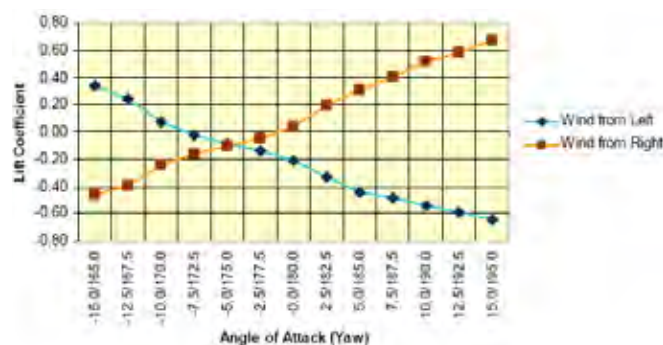


Figure 10. Lift coefficients from the CFD analysis for enclosed cross-section

shell elements. The box girder two top flanges are modeled using prismatic 3D frame elements of equivalent sectional area and flexural stiffness. A relatively fine element mesh scheme was incorporated in the model. The bottom flange width and web height was divided equally into 4 and 5 shell elements, respectively. Each bay unit was divided longitudinally into 4 equally spaced shell elements. The finite element length/width aspect ratio was maintained below 2.0. The top flange frame element is connected to the web through their common nodes.

The cross frame and the lateral brace members are simulated using axial (truss members) connected appropriately to the top flange and bottom flange element common nodal points. The connection plates at the cross frame are modeled with frame members connected to the web shell elements at their common nodal points. The web plate of the end and interior bent permanent diaphragms were modeled with shell elements while their top and bottom flanges were modeled with equivalent frame members.

Fixed supports were modeled using pinned connections. Expansion supports were modeled with longitudinal rollers. Lateral displacements transverse to the girder centerline are restrained at the expansion supports. Piers are not simulated in this model.

A 3D frame analysis model was also prepared to simulate the two bridge units 10-4 and 9-5 to compare the simple analysis method results to that of the 3D FEA model. The twin box girder bridge system is modeled with 3D frame members of equivalent axial, torsional, and flexural stiffnesses. The external diaphragms are simulated by an equivalent frame member connecting the two girders at their corresponding external brace nodes. The flexural stiffness of this frame member is equivalent to the flexural stiffness of the simulated external brace system (cross frame/diaphragm). The free bearing supports are simulated with longitudinally free and radially restrained roller supports. Fixed bearings were simulated by a completely pinned support. Piers are not simulated in this model.

A comparison of the results from these two models indicates that the results of the 3D grid model are conservative, but reasonably close to that of the 3D FEA model. The 3D grid model was adopted for the constructibility loading analysis.

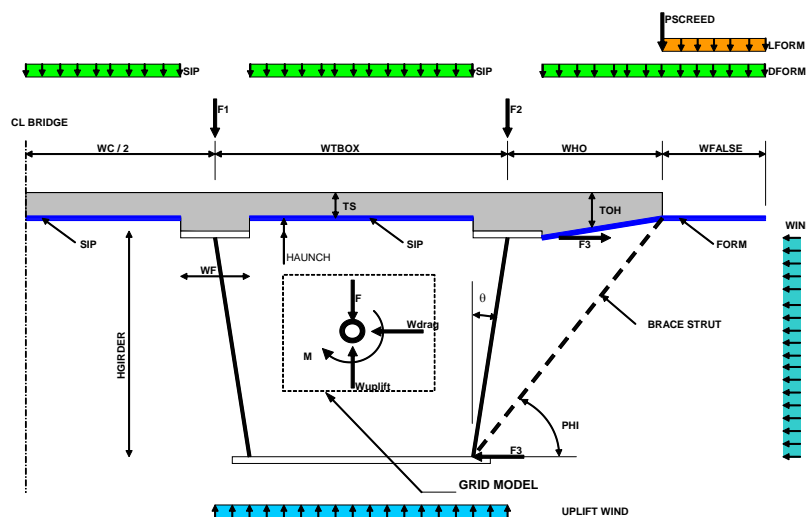


Figure 11. Distribution of non-composite and construction loads on the box girder

Applied loads

Several types of loads must be considered for the analysis of the partially constructed steel frame, including steel dead load, construction dead and live load, non-composite dead loads and wind loads. These loads are described as follows:

Steel dead load

The steel dead load is comprised of the dead weight of the structural steel skeleton under consideration.

Construction dead and live loading

The construction dead loading considered in this analysis is comprised of 20psf uniform dead weight of the metal SIP forms covering the clear distance between the top flanges of each girder and the clear distance between the inner top flanges of the two adjacent girders, 20psf uniform dead weight of the form supporting the slab overhang section and a 1.5ft wide cat walk extension on each side of the deck. See **Figure 11**.

The construction live load considered in this analysis is comprised of a 50psf uniform live load over the 1.5ft wide cat walk section. Typical screed machine linear weight is around 65–75plf. During casting operation of the deck, the construction live load does not normally co-exist with the screed machine live load. As such, the live weight of the screed machine is conservatively simulated by a non-interrupting construction live load along the girder entire length.

The horizontal component of the bracket load carrying the dead load of the overhand forms and the slab

wet concrete is also accounted for as a transverse outward pointing uniform load along the entire length of the exterior top flange.

Non-composite dead loading

The non-composite dead load is comprised of the flange tributary deck wet concrete weight including the haunch.

Wind loading

The design wind pressure of a closed deck bridge system for bridge units 10-4 and 9-5 is 75psf. An open deck bridge system wind pressure of 125psf (2.5/1.5 x 75psf) was selected throughout this study. Two wind load conditions were examined:

1. Wind load acting on the outer web of the outer girder and acting in a radial direction towards the center of curvature
2. Wind load acting on the inner web of the inner girder and acting in a radial direction away from the center of curvature

Load conditions

Five primary load conditions in accordance with the AASHTO Guide Specifications for Horizontally Curved Steel Girder Highway Bridges were considered:

LC 1: 1.4 Non-composite dead load + 1.4 Construction live and dead load for the full bridge unit (steel component stress check)

LC 2: 1.4 Steel dead load + 1.4 Wind load for the full bridge unit (steel component stress check)

LC 3: 0.9 Steel dead load + 1.4 Wind load for the full bridge unit (reactions)

LC 4: 1.4 Steel dead load + 1.4 Wind load for a partially erected bridge units (steel component stress check)

LC 5: 0.9 Steel dead load + 1.4 Wind load for a partially erected bridge units (reactions)

Load conditions LC 4 and LC 5 above consider critical construction

stages of the studied bridge unit as subsequently indicated.

The stresses in primary members due to construction factored loads shall not exceed the specified minimum yield stress in any element nor the buckling stress of any steel element subject to compression during construction. Bolted joints in load-resisting connections shall be designed to

be slip-critical for factored loads during construction. This is required to ensure permanent set or permanent inelastic deformation is controlled.

Other construction load cases similar to Load Cases "c" through "f" presented in LRFD Table 5.14.2.3.3-1 should also be reviewed. These load cases represent service wind during construction activities.

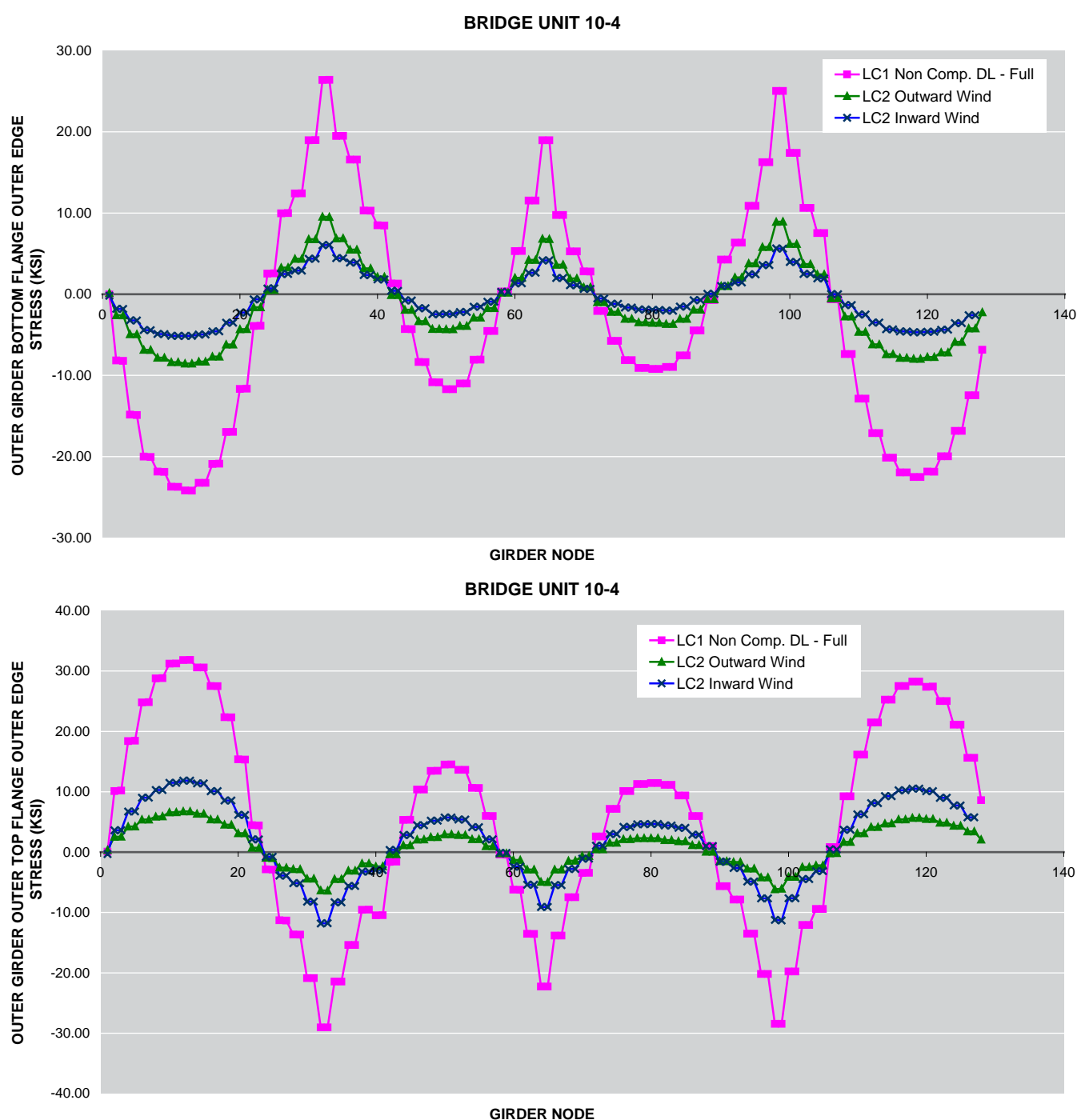


Figure 12. Unit 10-4 full bridge bottom and top flange edge bending stress distribution

Bridge unit 10-4

Construction stage (CS 1): Fully erected span 1 and partially erected span 2.

Construction stage (CS 2): Full erected spans 1 & 2 and partially erected span 3.

Bridge unit 9-5

Construction stage (CS 1): Fully erected span 1 and partially erected span 2.

Construction stage (CS 2): Full erected spans 1 & 2 and partially erected span 3.

Construction stage (CS 3): Full erected span 4 and partially erected span 3.

Summary of results

A summary of the stresses and member forces in a number of selected critical elements of the bottom flange, top flange and lateral brace members

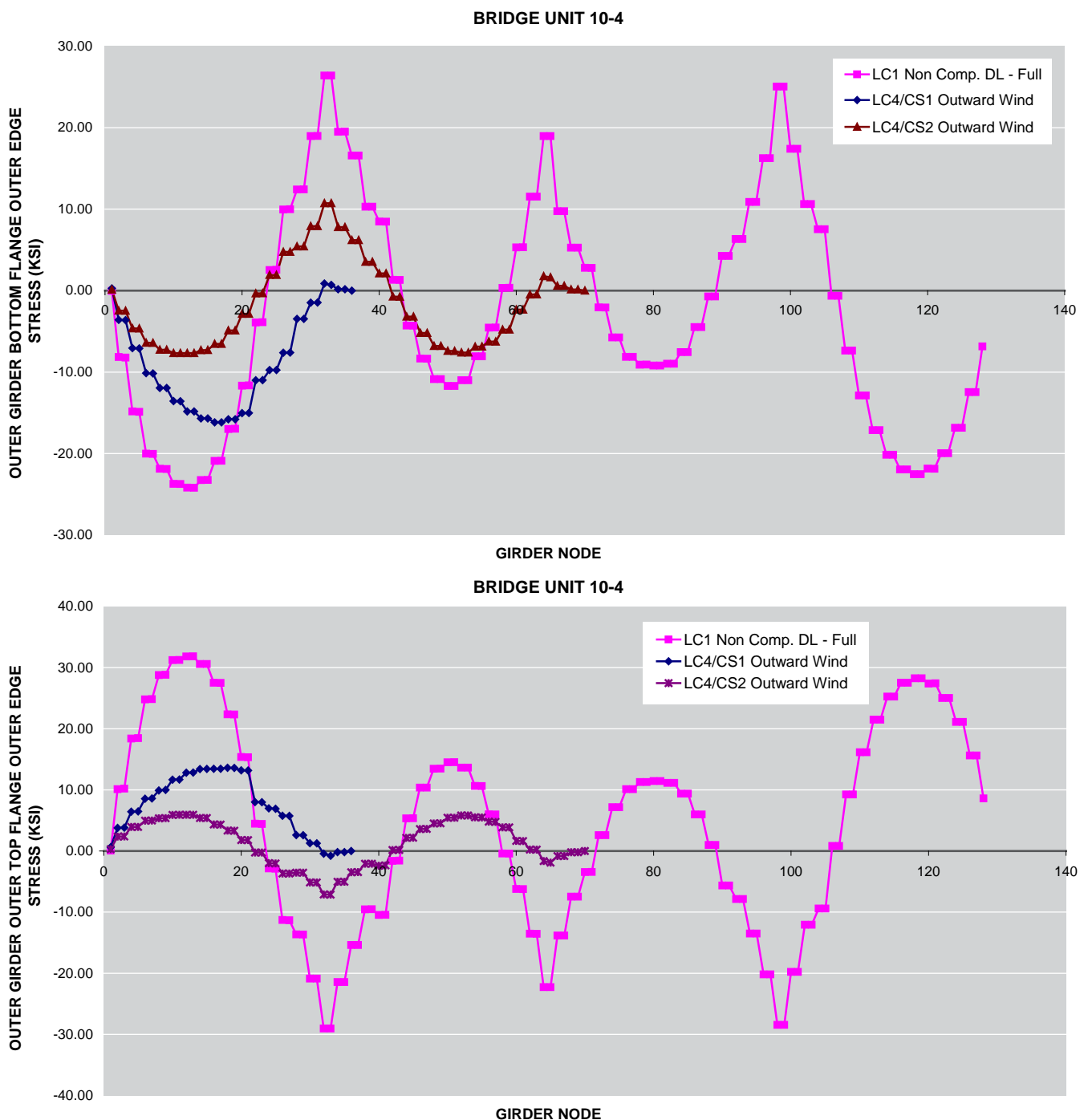


Figure 13. Unit 10-4 Bottom and top flange edge bending stress distribution. Comparison between full bridge vs. staged construction load cases

obtained from the 3D FEA analysis is presented in **Figures 12–15**.

Bottom flange and top flange stresses

The comparison of the stress levels in the selected bottom flange and top flange elements indicates that load condition LC1 simulating loading conditions during the casting of the concrete deck and the

associated dead and live construction loadings always results in a higher stress magnitude (tension or compression) than all other loading and construction state conditions. As indicated in **Figure 12**, the in-plane stresses in outer edges of the bottom and top flanges of the unit 10-4 full bridge during LC1 exceeds those during LC2 which simulates the full bridge steel dead load subjected

full hurricane level wind loading under constructability conditions. **Figure 13** presents a similar comparison of the in-plane stresses for bridge unit 10-4 between LC1 and LC4 evaluated for the two erection stages CS1 and CS2. In general, the in-plane stresses for LC1 envelopes those for LC4, and in particular for those elements located at the critical design flexure sections.

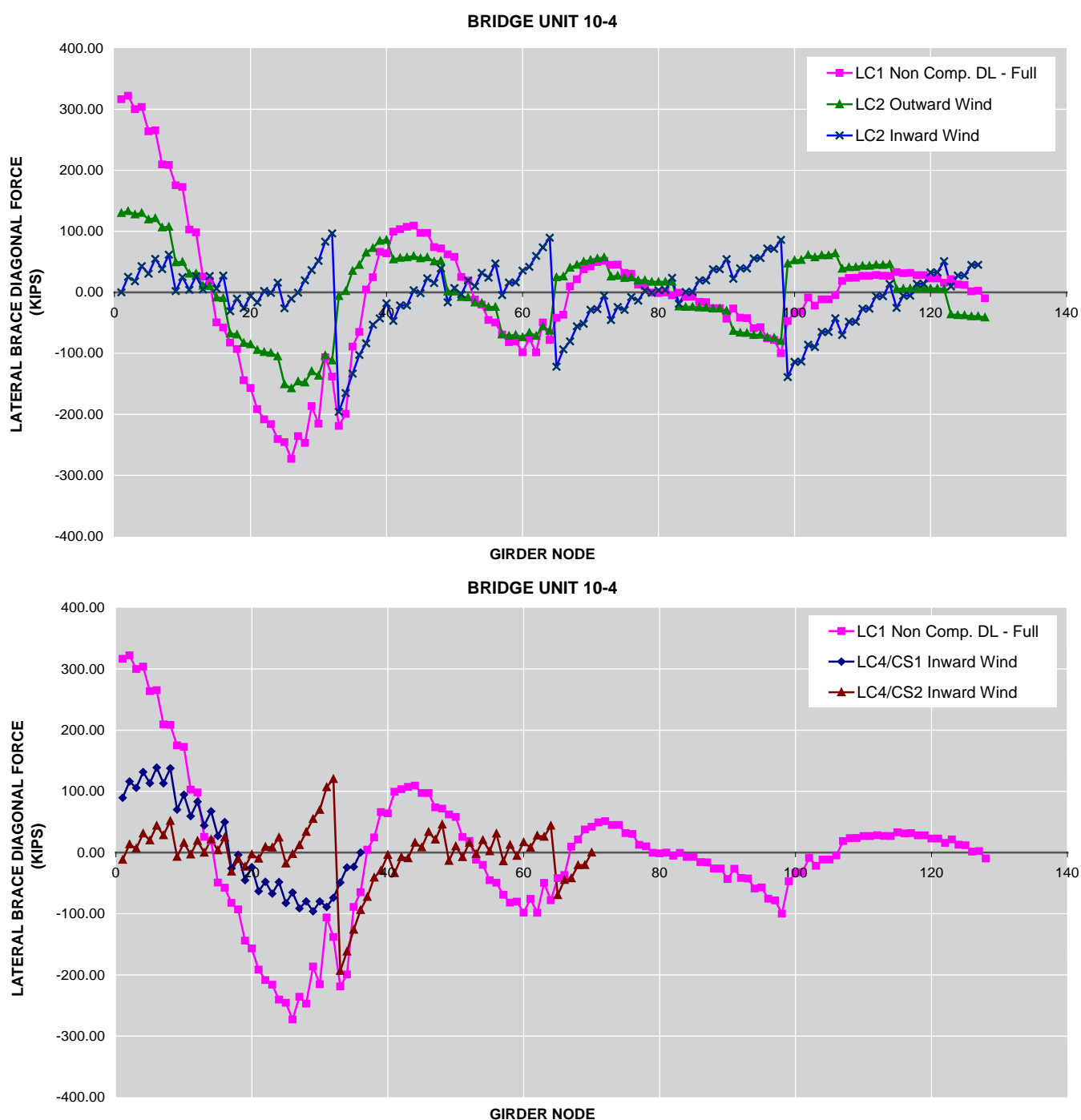


Figure 14. Lateral bracing forces unit 10-4

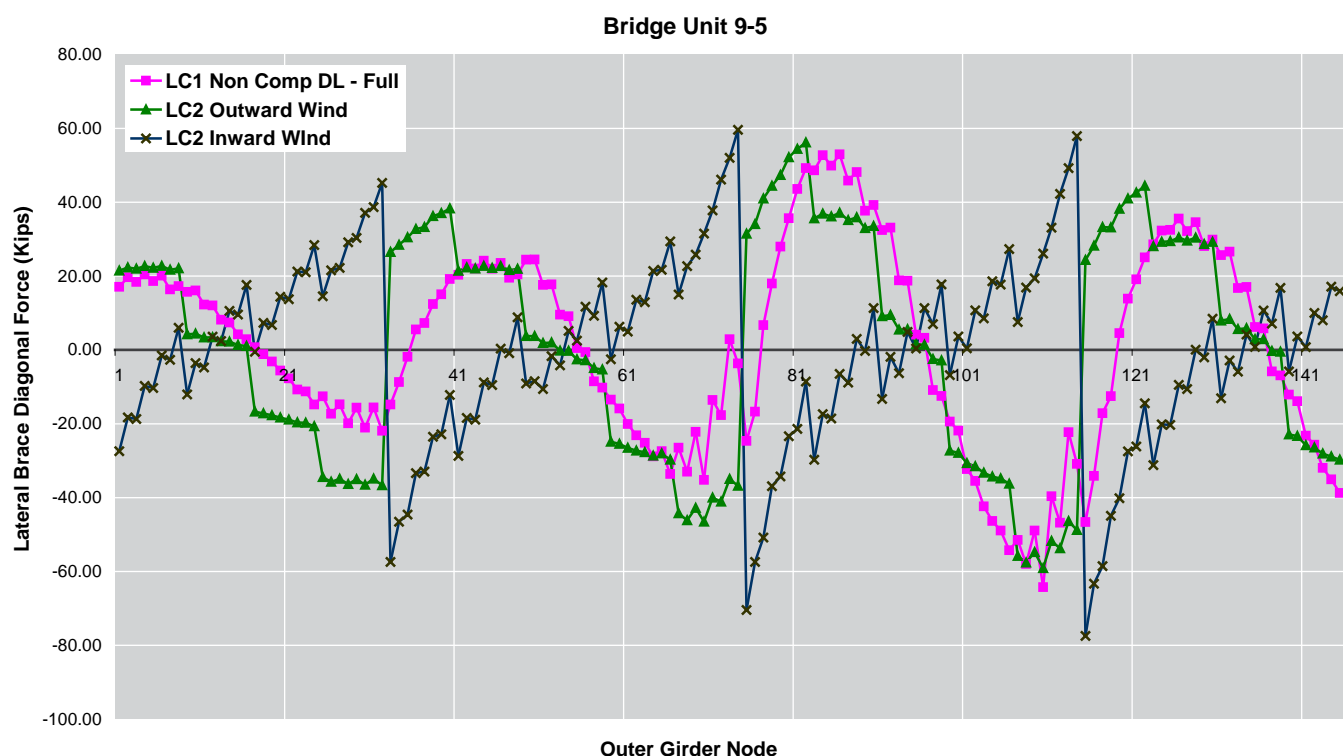


Figure 15. Lateral bracing forces unit 9-5

Lateral brace member forces

Comparison of the forces, shown in **Figures 14 and 15**, in selected lateral brace members indicates that the force level in some of these members during erection stages subjected to a hurricane level wind pressure exceeds those during the casting of the concrete deck.

A similar analysis was also performed to compare the internal brace and lateral brace member forces for bridge units 9-5, 10-4 utilizing the results obtained from the 3D grid model. The load cases considered at this stage are the first two load conditions stated above, namely fully erected superstructure steel with non composite loading case and a wind loading case. A similar trend was observed for all members of the bracing system.

Reactions

Girder reactions at the piers under load cases LC3 and LC5 indicate that uplift is a concern for the structural steel skeleton structure and should be indicated as such in the plans. These uplift forces will be extremely difficult to resist with temporary towers, but could be resisted by the concrete piers designed to support the finished structure. The contract documents shall identify these uplift forces at the piers, and provide suggested details to resist the uplift. Alternatives are temporary tie down straps, or the use of uplift resisting bearings.

Conclusion

Appropriate drag coefficients are available for completed bridges; however, drag

coefficients for partially constructed superstructure are not readily available. The results of the analysis provided herein indicate the following:

1. Drag coefficients typically assumed for completed bridges are not valid for a partially constructed structure. In general, these coefficients can be significantly higher depending on the geometry of the section.
2. Computational fluid dynamics modeling has proved to be a useful tool for the development of specific drag coefficients.
3. Wind loads during construction can be the critical load case for the design of the steel boxes, particularly lateral bracing.

References

1. AASHTO, AASHTO Guide Specifications for Horizontally Curved Steel Girder Highway Bridges 2003.
2. AASHTO, AASHTO LRFD Bridge Design Specifications, 2007 Edition.
3. American Association of State Highway and Transportation Officials (AASHTO), AASHTO Guide Design Specifications for Bridge Temporary Works, 1995 with interims through 2008.
4. ASCE, Minimum Design Loads for Buildings and Other Structures, ASCE 7-05, 2006.
5. ASCE, Minimum Design Loads for Buildings and Other Structures, ASCE 7-88, 1990.
6. Florida Department of Transportation (FDOT) Structures Design Guidelines (SDG), Florida Department of Transportation, January 2008.
7. ASCE Task Committee on Wind Forces, Wind Forces on Structures, ASCE Transactions, 1962.

**Mark Pritchard**

Civil Engineer

Hochtief (UK)
Construction Swindon,
England**Tomasz Kucki**

Senior Engineer

Atkins

**Jan de Boer**

Civil Engineer

DeBoerDC /
Mammoet UK

The design and construction of Cliffsend Underpass

Abstract

This paper presents the building challenges and final design of the Cliffsend Underpass being built under the railway near Ramsgate in south east England. Network Rail are particularly sensitive about this line as it carries the new Javelin trains which service the high speed link to St Pancras International. The challenge was therefore not only to devise a scheme which met the Client, Kent County Council's requirements, but also to develop a technique which minimises ground settlement.

The underpass is part of the new East Kent Access Road. It is 23m wide and is 125m long. For a structure of this magnitude and subject to the rail constraints highlighted above, a special box jacking concept has been developed. The jacking proposal belongs to a group of concepts based on jacking and skidding. IABSE Working Group 6 on bridge deck installation is studying the safe use and benefits of these techniques.

Introduction

Cliffsend Underpass see **Figure 1**, is the major design and build element of the East Kent Access Phase 2 contract, promoted and funded by Kent County Council (KCC) and, in part, by the Department of Transport. The contract was awarded to the VolkerFitzpatrick HOCHTIEF JV in the summer of 2009. The structure provides a route for the new dual carriageway, which sits in a 15m deep cutting either side of the railway. The proximity of local properties on both sides of the railway meant that an over-bridge solution is not viable. The overall geometry and physical location of the new structure is further constrained by significant existing statutory undertaker apparatus, under a minor road and level crossing above.

The resulting structure presented for design and build development comprised a 126m long, 23m wide and 7m high twin-cell structure. The deep approach cuttings would be formed of large diameter contiguous piled approach walls up to 15m deep, on either side. The upper deck level was dictated by the location of a large diameter sewer pipe above resulting in a 6m overburden from the top of the box deck up to the railway above.

of the structure whilst having no impact on the operation of the railway above. The new road layout and high skew of the railway makes this underpass one of the longest box jacked structures in the world.

Preliminary designs considered a conventional approach, utilising a pair of large box sections jacked into position. The major challenge of this proposal was the length and, ultimately, the required jacking capacity and control during installation. In addition, the extent of open face that would have resulted from these large box sections gave cause for concern amongst the geotechnical consultants, due to the likely extent of ground and associated railway track settlement that would have resulted.

It became apparent that the scale of the whole structure required that a different approach is considered.

Site investigation showed the main geological strata to be a lightly weathered chalk with few flints or boulders, overlain with up to 6m of (mainly) Thanet Sand strata. On this basis it was anticipated that the majority of excavation would be within the chalk, with Thanet Sand encountered over a short central length of the underpass in the top 1m of the face. Analysis suggested that the excavation slope at the shield face would be stable, without the need for ground treatment.

Design

The challenge

The challenge for the designers was to develop a structural solution which would allow the jacking of manageable sections



Figure 1. Cliffsend Underpass under construction

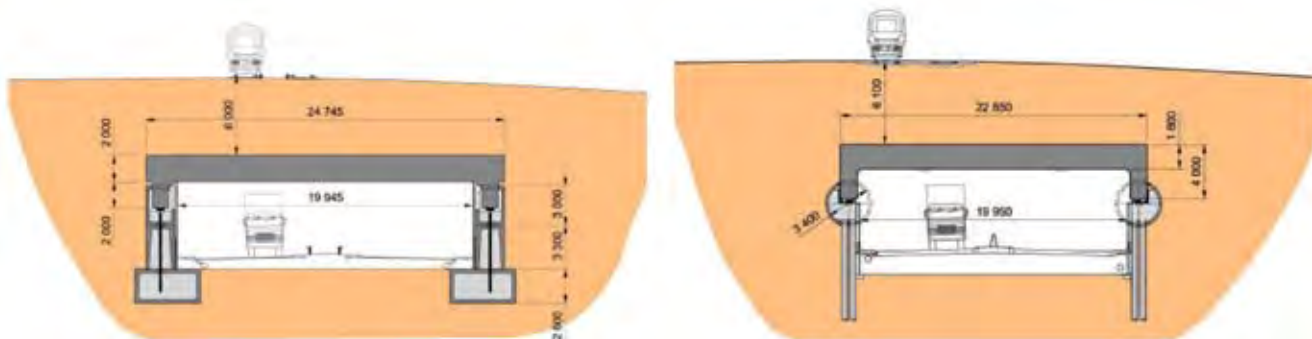


Figure 2. Cross-section of the Tender and post Tender solution

The technical solution

The Tender scheme, developed in conjunction with specialist box jacking consultants (JSG SA, from Geneva) utilised multiple jacked boxes to form abutments, see **Figure 2**. These abutments incorporated a slide path along which the main deck sections would be jacked into position.

After contract award, a series of design review meetings were held between designers, contractors and specialist jacking consultants, to further improve on this concept.

The final solution, see **Figure 2** – presented to and accepted by the Client – involves the construction of a pair of 3.05m internal diameter temporary tunnels, bored 8.50m below the railway along the lines of the underpass side walls. From within these two tunnels, mini piling rigs are used to construct rows of closely spaced reinforced concrete piles taken through the base of the tunnel and founded in the underlying chalk strata. These piles are ultimately exposed and faced to form the lower sections of side walls.

Construction sequence

Pilot tunnels and retaining walls

An earth pressure balance tunnel boring machine was employed to drive two 126m long temporary tunnels, see **Figure 3**. Track movement was continuously monitored by a set of robotic total stations detecting a total vertical settlement of less than 3mm. The tunnels were completed, within an 8 week programme, in December 2010 without any disruption to train operations or the need to apply any Temporary Speed Restriction (TSR).

From within the tunnels 530 No. 450mm diameter, bored cast in situ piles have been constructed. The piles are 14m long and reinforced for the top 8m. They



Figure 3. Western headwall with entrance of the pilot tunnels

were constructed using Klemm KR 702 limited height rigs. At peak productivity 4 No. piles were installed per rig per shift. Piling was completed in April 2011. Then the reinforced concrete pile caps were constructed within the tunnels, following which a low-friction slide track was set onto the pile cap, installed to very high geometrical tolerances.

Deck units

The underpass roof, or deck, sections comprise 6 abutting units, each 23m wide, 22m long (max) and 1.80m deep heavily reinforced concrete slabs with end down stand sections. These are being cast on site 150m west of their final location, see **Figure 4**. Each section of deck will be jacked up to the underpass portal and engaged at the front end onto the slide tracks extended from within the tunnels (as described previously). The deck sections are being constructed using a single reusable shutter. RMD formwork is being used to support the deck sections during concreting. The internal shutters to the legs are hinged for striking while the outside shutters are removable to allow fixing of reinforcement.

Each deck unit contains 1040m³ of concrete and 240 tonnes of reinforcement. The majority of the reinforcement is in a double layer of 50mm diameter high yield bars in the bottom of the slab. The high reinforcement density is a result of the



Figure 4. Casting facilities deck units

loads applied from 6m of overburden. 80% (by weight) of the reinforcement has been designed to allow prefabrication 'as beams' which are lifted into place by the 20 tonnes twin hook gantry crane which services the casting yard, see **Figure 4**.

Box jacking

Tunnelling shield

The front, or lead, deck unit incorporates a mining shield and cutting edge designed to provide intimate support and protection at the excavation face. The shield, see **Figure 5** is divided into 8 cells, each of which will contain excavation plant and miners. The shield is added to the front unit once it had been jacked into the storage area. The sheets of the anti-drag system are dispensed through slots in the front of the mining shield.



Figure 5. Impression of the Tunnelling Shield

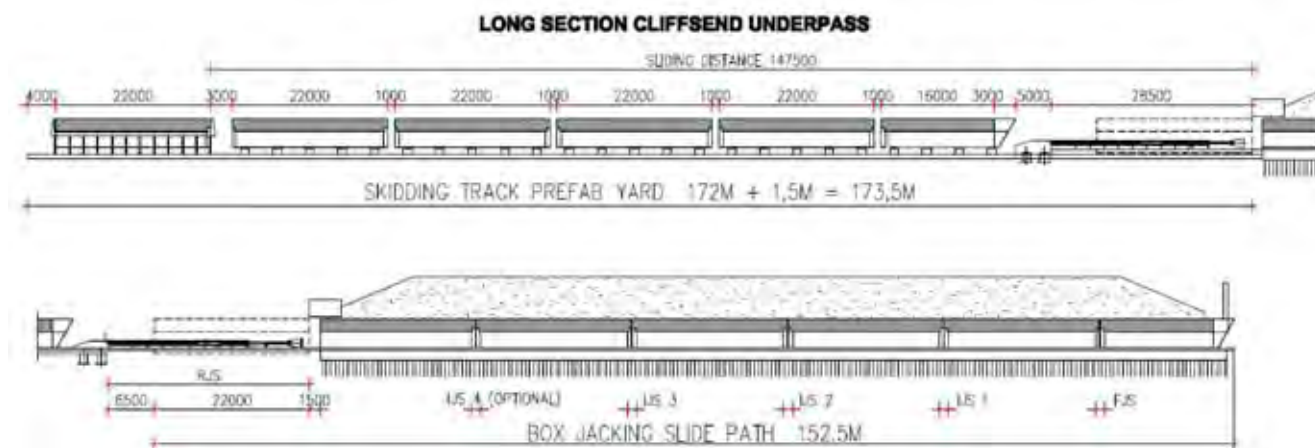


Figure 6. Long section with jacking stations 5 x 7,000t

Jacking arrangements

The deck units will be jacked under the railway using a total jacking force of 35,000t divided over 5 jacking stations, each with a capacity of 7,000t, see **Figure 6**.

The most important is the Rear Jacking Station (RJS), which consists of two groups of six 600t cylinders with a stroke of 2.20m, see **Figure 7**. Together with packers the RJS has an overall stroke of 22m, which reflects the maximum length of a single deck section. The RJS is first used to bring the lead unit into the embankment. It is then retracted to create space for the installation of the next deck section. This operation is repeated five times. Intermediate Jacking Stations (IJS) are located in the joints between the deck sections. Each IJS has a capacity of 7,000t and a stroke of 100mm. The front IJS has a stroke of 300mm.

Forward progression follows a caterpillar movement principle. The lead unit moves forward first, is followed by the next sections; the last section is moved forward by the RJS.

All jacking stations are powered by a central PPU with a flow of 72litre/minute at 450 bar. The measurement is made using digital stroke sensors. The theoretical forward movement speed varies between 370mm/hour and 140mm/hour, dependent on the number of operative IJSs.

The jacking pit

The RJS is installed in a jacking pit that acts as an abutment for the RJS. In the jacking pit, each deck section is transferred from the sliding system used in and out of the prefabrication yard onto the main sliding track system which is taken through the pilot tunnels. Resistance to the rear jacking loads is provided partly by ground anchoring of

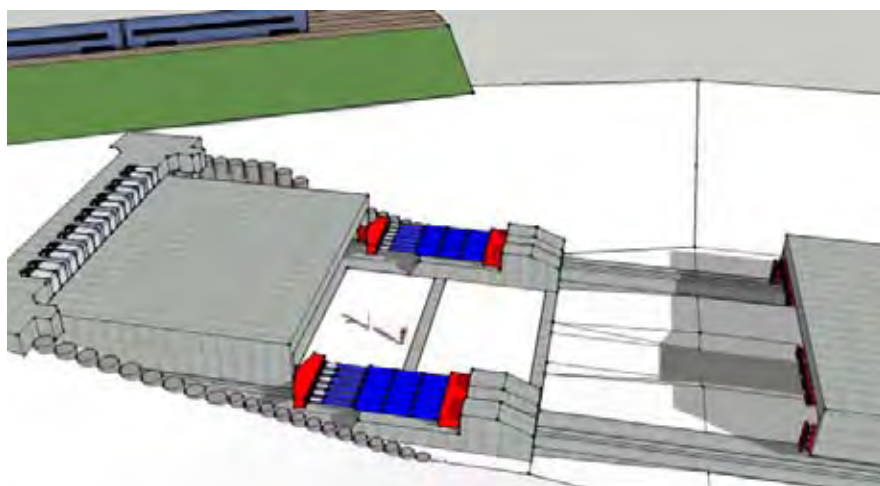


Figure 7. Rear jacking station with 12 cylinders 600t

the slide path in the jacking pit area and also by mobilisation of the tunnel/ground interface friction. The ground anchoring comprises 28 25m long multi strand systems, installed at 30° to the vertical and pre-stressed to a working load of 1220kN, see **Figure 8**.

Slide tracks and bearing systems

Mammoet are providing two separate sliding systems.

The first one is used for the transport of the six 2,500t heavy deck sections from the casting to the jacking pit area, see **Figure 9**.

This system consists of hydraulically interconnected short stroke vertical jacks supported on PTFE pads running on a stainless steel slide track. The track has been laid to a tolerance of ± 2 mm. Variation of load in the PTFE pads, as a consequence of varying track levels, is accommodated in the hydraulics which ensure that load in each jack remains constant at all times.

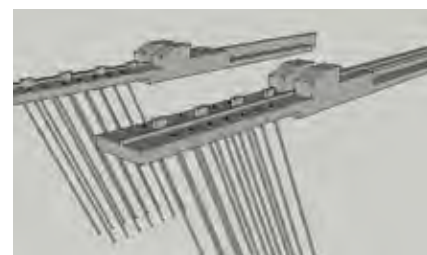


Figure 8. Thrust block with ground anchors



Figure 9. 3,200t sliding system on prefab yard

The second system operates from the jacking pit through the temporary tunnels. Here the loads are much higher as a consequence of the 6m of overburden. The total vertical load applied to this main sliding system is more than 50,000t. The system here consists of 41mm thick elastomeric bearings fixed to the underside of the deck legs. A layer of PTFE is bonded to the bottom face of the bearing. This slides on a stainless steel track on the tunnel pile caps. The only flexibility in the system is in the bearing and this is limited to approximately 2mm within the working load range of the bearing. To ensure that loads remain within design tolerance the bearing face and slide track are to be set to a tolerance of $\pm 0.5\text{mm}$.

The first system is 175m long, and the second one is 155m, with an overlapping section of 25m in the jacking pit.

Anti-drag system

To prevent migration of overburden material in the direction of deck movement and to reduce the friction between the deck unit and the overlying ground during jacking, there is an arrangement of continuous steel sheets that lie on the top of the deck units and are anchored to the west headwall, see **Figure 10**. The sheets will be dispensed through slots in the front of the mining shield from rolls suspended on the soffit of the front deck unit. Because the sheets are anchored to the west headwall, they will remain stationary relative to the overburden as the deck moves forward. This will reduce the risk of horizontal movement of the rail embankment and ensure that most of the frictional forces are generated at the interface of the top of the deck units and the anti-drag sheets. This interface will be lubricated by the injection of bentonite or high viscosity gels through grouting manifolds cast into each of the deck units.

Operations

The process of jacking (see **Figures 11 and 12**) through the embankment can be divided into several activities taking place simultaneously:

- **Mining and excavation at the shield:** the success of the whole project depends largely on the accuracy of the mining taking place. The mining determines the speed of progress, settlement of the road/railway above and the alignment of the deck.
- **Jacking of the deck units:** the operators activate the hydraulic systems to achieve forward movement and to correct possible misalignments.



Figure 10. Anti-drag system with anchored steel sheets



Figure 11. Rear jacking station during installation of the first deck unit operations

- **Anti-drag devices and lubrication of the sliding contact surfaces:** this not only reduces friction but also guarantees stability of the embankment.
- **Surveying and monitoring:** box jacking requires an attentive reaction to the slightest signal of a possible misalignment or deformation of the overgoing road. Failure to treat immediately will result in the process going out of control.

At Cliffsend the jacking process is programmed as a 24 hours a day, 7 days a week operation. After one deck section of 22m has been installed the RJS has to be temporarily removed in order to position a new deck section in the jacking pit. This operation will take 2½ days. In total the jacking of the six sections of this 126m long underpass will last approximately 10 weeks.



Figure 12. Inside the underpass during the jacking operation

Conclusions

Box jacking is a well tested technique for building tunnels and underpasses with minimal disruption to existing road and rail infrastructure.

At Cliffsend we have devised a scheme to cater for a project of great magnitude. Because of the length of the underpass (126m) and the capacity of the applied pushing equipment (35,000t) this is believed to be the most impressive example of jacking within the last ten years.

By designing a structure of these dimensions with only a roof structure and slide tracks in bored pilot tunnels, we have responded to the challenge to build Taller, Longer, Lighter structures as set by the IABSE-IASS London 2011 symposium where this paper was published.

The jacking operation has been successfully completed on 24/08/2011. The installation of all six deck units has taken 64 days and over 4000 man-hours.

**John J Orr**

Department of
Architecture and
Civil Engineering

University of Bath

**Anthony P Derby**

Senior Lecturer in
Structural Engineering

Department of
Architecture and
Civil Engineering

University of Bath

**Tim J Ibell**

Professor of
Civil Engineering

Department of
Architecture and
Civil Engineering

University of Bath

**Dr Mark C Evernden**

Lecturer in
Structural Engineering

Department of
Architecture and
Civil Engineering

University of Bath

**Mike Otlet**

Technical Director

Design & Engineering

Atkins

Concrete structures using fabric formwork

Abstract

Using fabric formwork, it is possible to cast architecturally interesting, optimised structures that use up to 40% less concrete than an equivalent strength prismatic section, thereby offering the potential for significant embodied energy savings in new concrete structures. This paper reports on the philosophy of and background to fabric formwork before techniques for the design, optimisation and shape prediction of fabric formed concrete beams are presented.

The practicality of construction with non-orthogonal elements is discussed before the results of new structural test data, undertaken at the University of Bath on 4m span elements formed in reusable fabric moulds, are presented. Potential areas of future development for fabric formwork, including the use of woven advanced composite fabrics as permanent participating formwork and the feasibility of uniform strength prestressed beams, are then discussed.

Introduction

A prismatic concrete beam, with uniform transverse and longitudinal reinforcement percentages, has a constant moment and shear force capacity at every point along its length. In all but a few locations, such a member is by definition under utilised. The ubiquitous use of orthogonal moulds as formwork for such structures has resulted in a well-established vocabulary of prismatic forms for concrete structures, yet rigid formwork systems must resist considerable fluid pressures, may consume significant amounts of material and can be expensive to construct. Moreover, the resulting member requires more material and has a greater deadweight than one cast with a variable cross section.

Simple optimisation routines, described in this paper, may be undertaken to design a variable cross section member in which the flexural and transverse force capacity at any point on the element reflects the requirements of the loading envelope applied to it. The construction of structures with complex non-orthogonal geometries is often perceived to be both difficult and expensive, yet this paper demonstrates that by casting concrete into a flexible fabric membrane, architecturally interesting, optimised structures that reduce material use and take real advantage of the fluidity of concrete can be produced.

Fabric formwork

Fabric formwork has been used in the construction of concrete structures since the early 1900s, but it was not until the 1960s that its widespread use began to grow, precipitated by the new availability of high strength, low cost fabrics¹. Initial interest in the architectural possibilities of fabric formwork can be attributed to the Spanish architect Miguel Fisac, whose work in this field culminated in a patented method for the construction of prefabricated fabric formed wall panels².

Since then, multiple design and construction methods for fabric formwork have evolved. In Japan, Kenzo Unno's 'zero-waste' system for casting fabric formed walls³ has been successful, while in North America significant savings in both material and labour costs have been recorded as a result of using fabric formwork in the construction of columns and footings⁴. Additional and ongoing research, led by Professor Mark West at the University of Manitoba's Centre for Architectural Structures and Technology (C.A.S.T.), has further considered the architectural possibilities of fabric formwork for beams and trusses, in addition to its use for shells, panels, columns and walls, **Figure 1**.

Although it has a low embodied energy (of approximately 0.90MJ/kg)⁵ concrete is used in vast quantities. In 2008



Figure 1. Research undertaken (courtesy C.A.S.T)

world production of cement amounted to approximately 2.8×10^9 t, with its manufacture estimated to account for some 3% of global CO₂ emissions⁸, providing further impetus for the design of optimised structures. Concrete volume savings in fabric formed beams, when compared to an equivalent strength prismatic member, of 40% have already been achieved^{9,10}, illustrating the potential for fabric formwork to reduce the embodied energy and carbon associated with new building structures.

Yet fabric formwork does not simply facilitate reductions in material use. Forming concrete in a permeable mould allows air and water to escape from the formwork to provide a high quality surface finish that can be readily distinguished from an identical concrete cast against an impermeable mould, as illustrated in **Figure 2**. Reductions in water:cement ratio towards the external face of structures cast in permeable moulds have been reported¹¹ and provide a surface zone with improved hardness^{12,13} and reduced porosity¹⁴.

The resulting concrete surface is more durable than one cast against impermeable formwork, with reductions in carbonation depth, chloride ingress and oxygenation reported in the literature¹¹. These results have been verified in more recent work undertaken by the authors, where accelerated tests on concrete cast in fabric formwork have shown it to provide a 48% reduction in carbonation depth; a 49% improvement in resistance to chloride ingress and up to a 20% improvement in surface hardness when compared to concrete cast against conventional formwork.

For structures where the concrete grade specified is governed by durability rather

than strength concerns, permeable formwork offers significant opportunities for embodied energy savings. For example, a C20 concrete mix cast in permeable formwork has been found to have a lower carbonation depth after 11 months than a C50 mix cast in conventional formwork¹², with such a reduction in concrete grade providing embodied energy savings of approximately 38%⁶ – in addition to those savings already achieved simply by using fabric formwork to cast a structurally optimised form. Long term cost savings for concrete cast in permeable moulds have also been reported¹⁵ and arise primarily from a reduction in maintenance and repair requirements.

Allowing water, but not cement, to drain from the surface zone is imperative when permeable formwork is used, and while Price¹¹ suggests a maximum pore size of 50µm be specified, slightly larger pore sizes have been successfully used by the authors.

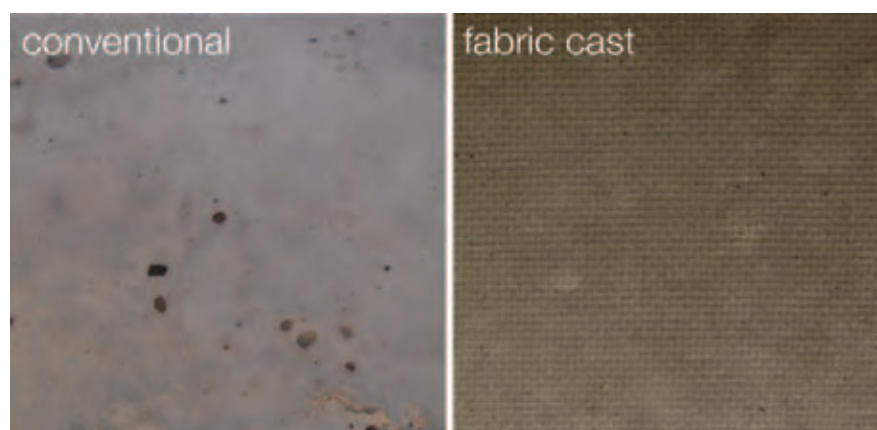


Figure 2. Identical concrete cast in impermeable (Left) and permeable (Right) moulds

The high quality surface finish of concrete cast in fabric further encourages the use of exposed internal concrete surfaces, the consequence of which is two-fold: extraneous wall and ceiling coverings can be omitted and the now exposed thermal mass may properly be used in the provision of thermal comfort.

Design

Fabric

The critical aspect of fabric formwork for determining shape and therefore aesthetic is the fabric itself. Although almost any woven fabric can be used as formwork for fabric cast concrete, tensile strengths in both warp and weft directions must be sufficient to hold the wet concrete and a low creep modulus is desirable to limit formwork deformations during casting and curing. The available literature illustrates the use of a range of fabrics as formwork, including hessian⁹ and geotextiles¹⁶, while more recent experimental work undertaken at the University of Bath has used a woven polyester fabric that has previously been utilised in the construction of underwater concrete structures.

Once a suitable fabric has been chosen, a number of methods are available to determine the final shape of the fluid filled flexible membrane. Schmitz¹⁷ used an iterative finite element based procedure to determine the form of fabric formed wall panels, while Veenendaal¹⁸ implemented dynamic relaxation to predict the final shape of fabric formed beams. Empirical relationships determined by Bailiss⁹ provide a less rigorous solution to the same problem, but have nevertheless been used successfully¹⁰, while Foster¹⁹ used a simple step-wise based method to iteratively determine the shape of the concrete filled fabric. The complete solution, which requires the use



Figure 3. Anchorage using welded end plates

of incomplete elliptic integrals, is given separately by Iosilevskii²⁰.

Reinforcement

The reinforcement of variable section members adds some complexity to the construction process, yet fundamentally does not differ from an orthogonal structure. The provision of end anchorage has been seen in previous work¹⁰ to be a crucial consideration and both externally welded steel plates (**Figure 3**) and transversely welded internal bars have been used to achieve this.

The provision of transverse reinforcement in a variable section member simply requires a varying link size, which is easily achieved but can add cost to the construction process. It is therefore imperative that any reinforcement specified is used efficiently.

Analysis

Structural design procedures for bending moment shaped beams, as developed at the University of Bath^{9,10}, are based on a sectional approach that aims to satisfy

the bending and shear requirements of the beam at every point along its length. Where open web beam sections are desired, additional consideration must be given to the effects of Vierendeel action in the member (detailed elsewhere²¹).

Flexural strength calculations are undertaken by first dividing the element into a number of equally spaced sections. By assuming that the longitudinal steel has yielded, the lever arm distance required to provide the required moment capacity at each section is quickly determined by equilibrium, (1) and **Figure 4**. This is repeated at each section along the length of the member to determine the optimised reinforcement layout for a given loading envelope.

$$z = \frac{M_{Rd}}{F_{b,H}} \quad (1)$$

Where z is the lever arm, M is the applied moment and $F_{b,H}$ the horizontal component of tension force on the section.

For a beam with just one layer of reinforcement, the resulting effective

depth is then proportional to the bending moment on the section. In such a situation, the vertical component of force in the bar will be equal to the applied shear force according to equation (2). This suggests that the inclined longitudinal bar may be used to provide both flexural and shear force capacity to the section.

$$V = \frac{dM}{dx} = F_{b,V} \quad (2)$$

Where V is the shear force, M is the applied moment, x is the position along the beam.

However, utilising a longitudinal bar to provide vertical force capacity close to the supports in a simply supported beam requires the bar to be fully anchored at its ends. The use of external steel plates to provide such anchorage is an unsatisfactory solution as it introduces the potential for brittle failure, exposes the internal reinforcement to corrosion and increases construction complexity. The difficulties associated with achieving the conditions described above are currently under investigation.

Furthermore, for a structure subject to an envelope of loads the longitudinal reinforcement position will be determined by the maximum moment on each section. Where a structure is subject to both point and uniformly distributed loads, it is feasible that the maximum moment and maximum shear forces on a section will not originate from the same load case. In such a situation, a bar placed for moment capacity will then be incorrectly inclined to provide the desired vertical force, and thus transverse reinforcement will be required. However, an inclined bar still provides some value of vertical force, which in design may often be added to the shear resistance of the section to reduce its transverse reinforcement requirements (c.f. BS EN 1992-1-1²² (cl.6.2.1)).

The assessment of shear capacity in fabric formed beams has previously been undertaken to BS 8110-12³, yet the empirical 'concrete contribution' of this method is not necessarily directly applicable to the design of variable

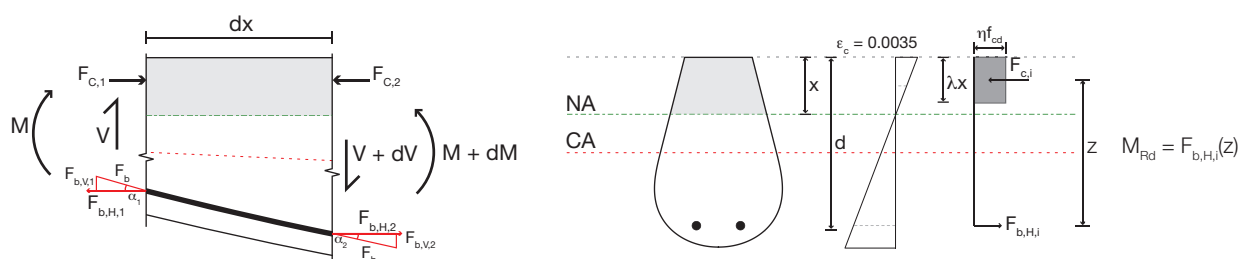


Figure 4. Steel reinforced section flexural design basis

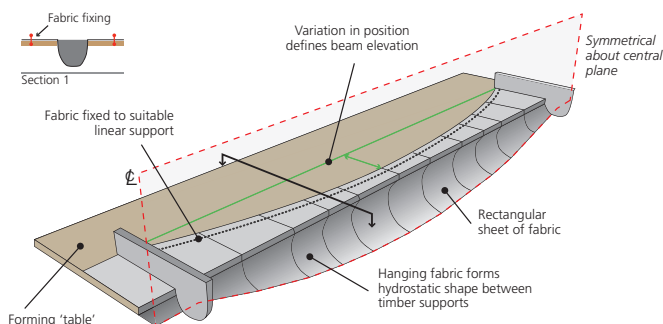


Figure 5. Construction using fabric

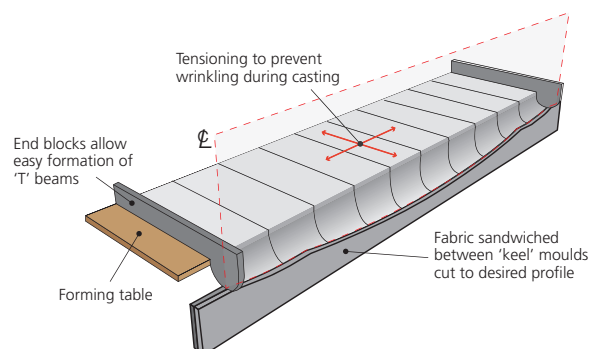


Figure 6. Construction using the keel mould

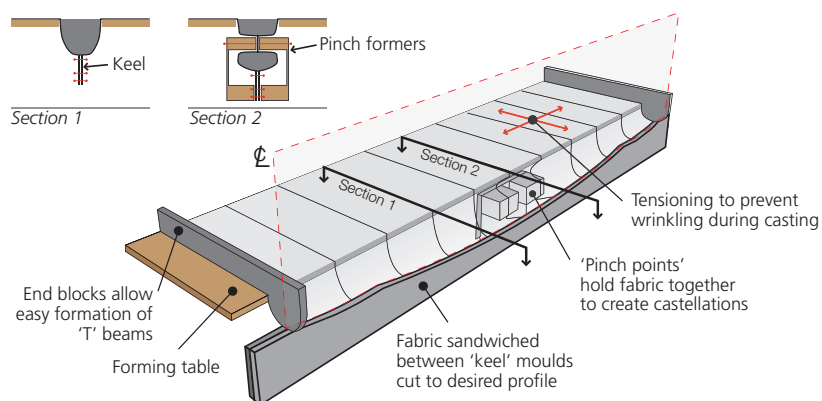


Figure 7. Construction using the pinch mould

section beams. This assertion is supported by the available test data^{9,10}, where shear has previously been seen to be the predominant failure mode.

The variable angle truss model, as adopted by BS EN 1992-1-1²² for sections with transverse reinforcement, considers only the capacity provided to the member by the reinforcement and thus avoids a reliance on empirical relationships to determine shear strength. Further work is now being undertaken by the authors to review the application of the Eurocode model to tapered beams in shear.

A potentially more attractive method for the design of non-prismatic elements is found by applying compression field

theory²⁴, which allows the detailed analysis of any cross section shape to be undertaken. However, this approach is yet to be taken up by European code writing committees.

Construction

Fabric formwork provides a fundamentally simple construction method and an optimised beam can be formed using only a sheet of fabric and modest supporting frame, as illustrated in **Figure 5**. The fabric, as discussed above, is completely reusable, either for a repeat element or in an entirely new beam geometry.

More stringent construction control is achieved through the use of the 'keel

mould' for the production of pre-cast beams, **Figure 6**. Here, the fabric is held vertically and secured to a 'keel' that has been pre-cut to the desired longitudinal beam profile. The fabric is then prestressed in two directions before being fixed in position. Prestressing the fabric prevents wrinkling during construction and minimises the volume of concrete in the tension zone.

The 'pinch mould' (**Figure 7**) may alternatively be used to create pre-cast beams and trusses with more complex geometries. Using 'pinch points' the sheets of fabric can be held together during casting, creating an opening in the resulting element. This is a potentially important consideration for the provision of building services, but requires more careful analysis.

Building services

The aesthetic appeal of variable section members, coupled with a high quality surface finish and the additional advantages of exposed thermal mass make fabric formwork an ideal means by which architectural, structural and building service requirements can be integrated.

Using the 'pinch mould' construction method, pre-cast variable section fabric formed beams can easily be created with voids in their midspan zones, **Figure 8**. Such sections are rarely used in conventional reinforced concrete design, yet provide a simple method for the

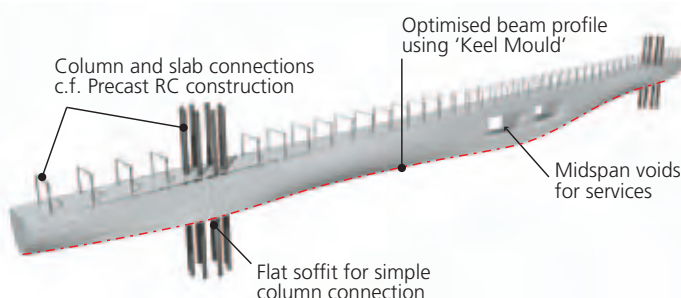


Figure 8. Pre-cast beam element

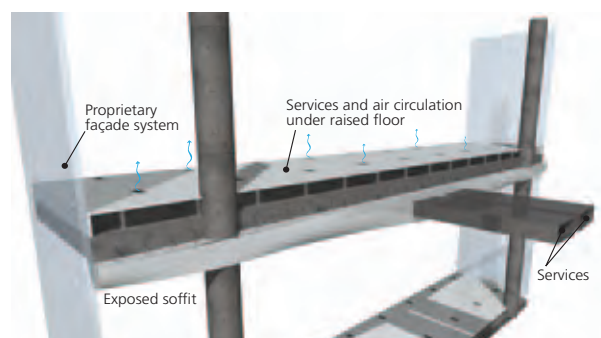


Figure 9. Integration of building services

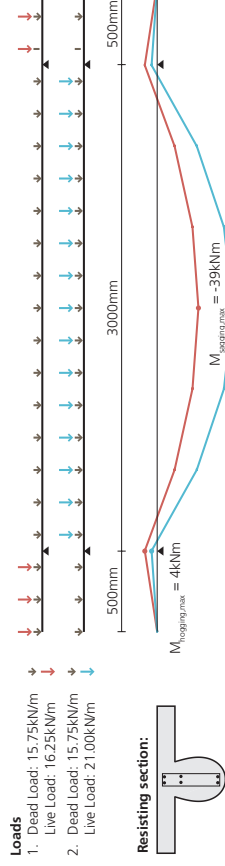


Figure 10. Load cases and resulting shear and moment envelopes

routing of service ductwork. However, such an arrangement may detract from the aesthetic appeal of exposed, fabric formed soffits and the provision of services through a raised floor may be more appropriate (**Figure 9**). Such an approach holds additional advantages for the circulation of air exposed to the concrete slab and allows the building to be easily adapted for future changes in use.

Costs

Whilst cost savings have been recorded in projects that made use of fabric formwork for the construction of columns and footings⁴, there is limited data available for the construction of more complex variable section elements. However, Pallett¹⁵ suggests that labour cost savings may be achieved as formwork stripping and work cycle times

are improved when concrete is cast in fabric. Coupled with the aforementioned material use reductions, the economic advantage of fabric formwork is increasingly apparent.

The construction of complex doubly curved concrete elements remains entirely feasible using well established computed numerically controlled (CNC) manufacturing processes to produce steel or foam moulds for use as formwork. However, such an approach is both expensive and time consuming, and is suitable only where multiple identical elements are desired. Using fabric formwork, the creation of multiple 'one-offs' from a single sheet of fabric is entirely feasible, and can be undertaken anywhere in the world using simple construction techniques.

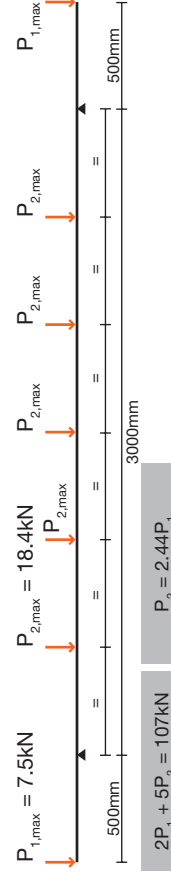


Figure 11. Test loads

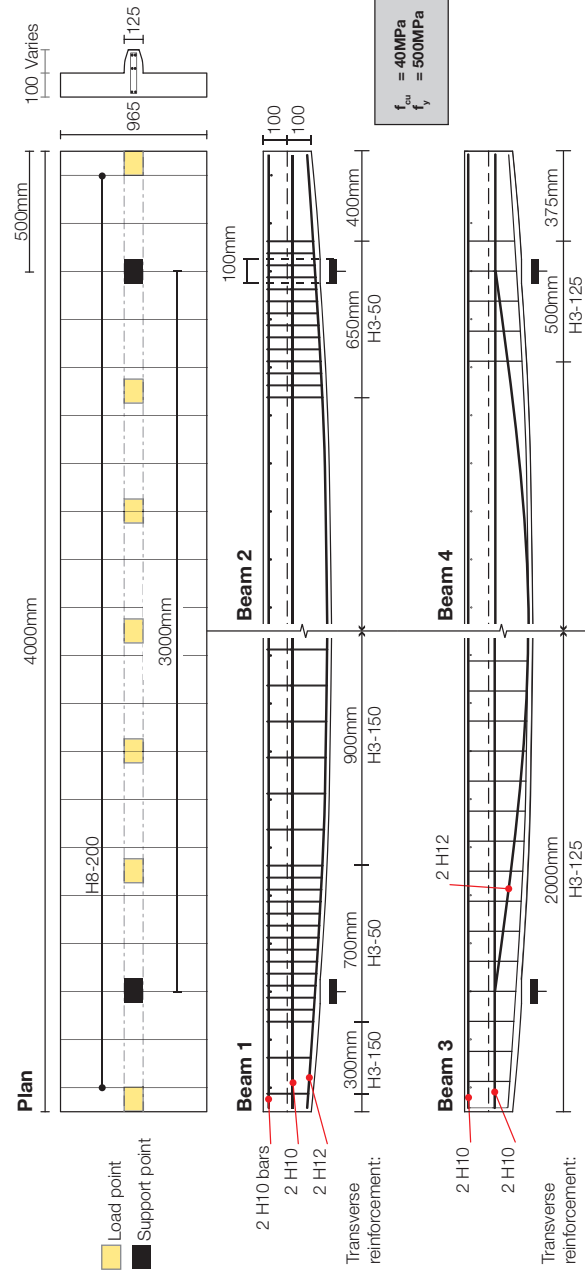


Figure 12. T-beam general arrangement

Construction examples

Whilst fabric formwork is increasingly used in North America in the construction of concrete columns and footings, there are far fewer examples of beam and slab construction. D'Aponete et al.²⁵ provide details of a number of small houses built using fabric formwork, and construction techniques for such structures are being refined in ongoing work at the Yestermorrow Design School, Vermont²⁶.

T-beams

Using the sectional analysis method described above, four 8m span fabric formed beams were recently designed at the University of Bath for use as a precast elements in reinforced concrete frame construction. These four elements were then scaled by 50% to facilitate structural testing, as described below.

The beams were designed to the envelope of loads summarised in **Figure 10**, with additional dead load being applied to account for the cubic loss in concrete volume that occurs when elements are scaled linearly (all load partial safety factors are set to 1.00). The beams were tested in nine-point bending, with the point loads required to achieve the design moment envelope given in **Figure 11**, (where a self-weight of 2.7kN/m is assumed).

The four beams had identical external dimensions and varied only in the arrangement of their transverse and longitudinal reinforcement, as illustrated in **Figure 12**. Beams 1 and 2 were designed without considering the inclination of the longitudinal tensile steel, while Beams 3 and 4 considered

the longitudinal steel to provide shear capacity at the supports. Beams 1 and 3 were transversely reinforced with minimum links according to BS EN 1992-1-1²² while Beams 2 and 4 were provided with links only where required according to an analysis using the modified compression field theory (c.f. Collins et al.²⁴).

A concrete strength of 40MPa and steel yield strength of 500MPa was assumed for design purposes, with the actual concrete strengths and steel yield strengths at the time of testing being given in **Table 1** and **Table 2** respectively.

Construction of the beams was undertaken using the keel mould, as described above and illustrated in **Figure 13**. A flat face at the supports was formed using a simple steel plate, pushed into the tensioned fabric and screwed to the plywood keel. The transverse and longitudinal steel reinforcement was bent and cut to the required shape before being tied together and placed into the mould, and a minimum cover to the longitudinal steel of 20mm was achieved using plastic spacers. The vertical sides of the top slab were cast against phenolic plywood that had first been treated with a release agent. The fabric was not treated and all casts were made in the same mould using the same fabric, which was simply brushed down after use.

Compared to an equivalent orthogonal section, and excluding the top slab, the optimised beam profile provides a concrete material saving of approximately 35%.

The beams were demoulded three days after casting and allowed to cure for at least 20 days prior to testing. Beam 1 is shown in **Figure 14**, where the disparity in concrete quality between that cast against plywood and that cast in fabric is again apparent.

The beams were tested in the loading frame shown in **Figure 15** to simulate the application of a uniformly distributed load, with the loads required to achieve the design moment envelope given in previously in **Figure 11**. The beams were all tested in load control, with a constant ratio of $P_1:P_2$ of 1:2.44 applied up to the maximum load. The load-displacement response of each beam is summarised in **Figure 16** and apposite test results are given in Table 1. The design failure load of 107kN was marginally exceeded in all tests, with these relatively small increases accounted for by the actual yield stress of

Test	Concrete strength at test (N/mm ²)	Maximum load, $2P_1 + 5P_2$, (kN)	Midspan deflection at final load (mm)	Failure mode
Beam 1	42	114	89	Flexure
Beam 2	39	119	86	Flexure
Beam 3	44	115	89	Flexure
Beam 4	33	133	89	Flexure

Table 1. Test result summary, Beams 1-4

	3mm bar		10mm bar	12mm bar
0.2% proof stress	630MPa	Yield stress	566MPa	576MPa

Table 2. Measured steel properties at test

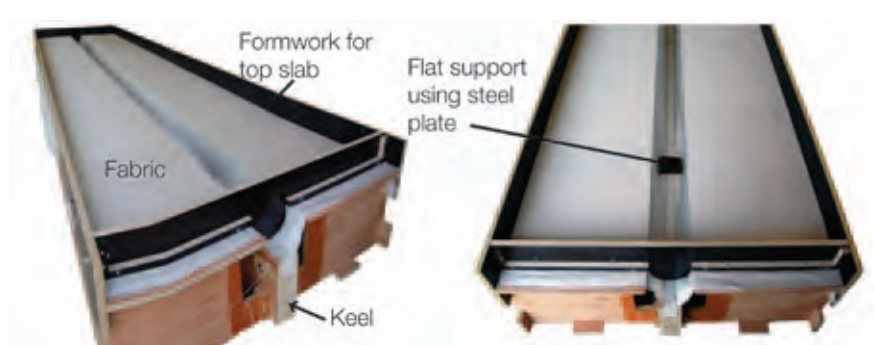


Figure 13. Keel mould table

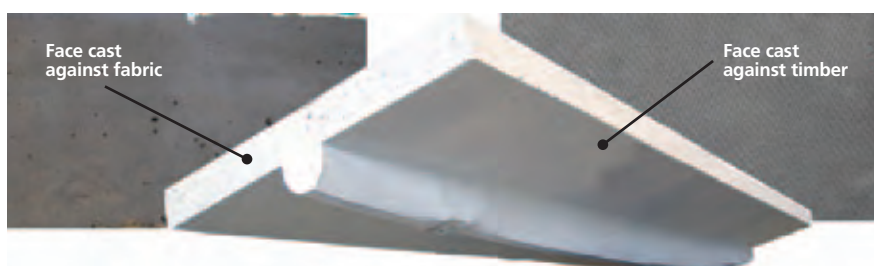


Figure 14. T-beam formed in fabric

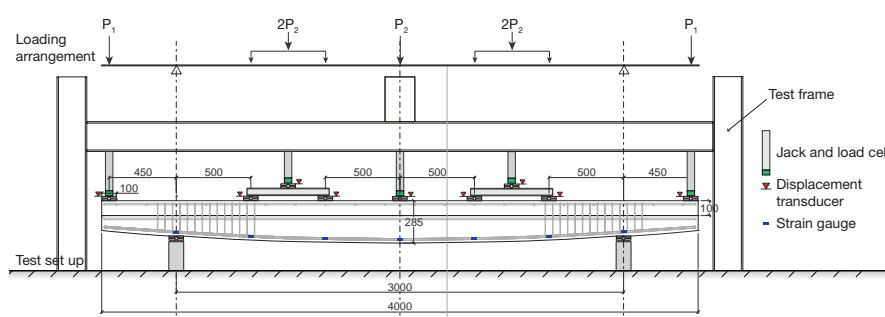


Figure 15. Test set up

the bars being higher than that assumed for design (Table 2) and the potential for small errors in the position of the longitudinal bars. In general the sectional method provides an accurate technique for determining the moment capacity of the variable section element.

Beam 1 reached a maximum load of 114kN and after displaying some ductility the cantilever loads P1 were removed. Beam 1 was then loaded by the five central point loads at a constant load of approximately 86kN up to a midspan deflection of 85mm. Subsequently, load was applied at the mid-span only, with a constant load of 54kN carried by the section up to its maximum displacement of 90mm, as shown in **Figure 16**.

Beams 2, 3 and 4 were tested in a similar manner, but after achieving ductility at their maximum load capacities (**Figure 16**) were loaded by the central point load only. Beam 4 achieved a slightly higher maximum load than the first three tests, but this increase is not considered to be significant.

All beams displayed a ductile response, with yielding of the longitudinal steel leading eventually to compression failures in the top slab. Cracking of the sections was well distributed (**Figure 17**) and no shear failures were recorded, in contrast to tests previously undertaken at the University of Bath^{9,10} in which shear was the predominant failure mode.

The four beams described above displayed similar load-deflection responses, with almost identical cracked and uncracked stiffnesses recorded. This demonstrates that the two shear design methods have relatively little effect on the overall member response, and the sectional design approach may thus be used with confidence in the flexural design of optimised beams. In addition, the keel mould has now been successfully demonstrated as a feasible construction method for fabric formed concrete structures.

The similar load capacities recorded between Beams 1-4 further suggests that transverse reinforcement design may be satisfactorily undertaken using either BS EN 1992-1-1²² or the modified compression field theory. Whilst the beams described above were designed to fail in flexure, future work will be required to comprehensively assess the shear behaviour of variable section members. This will then allow more detailed design guidance to be provided.

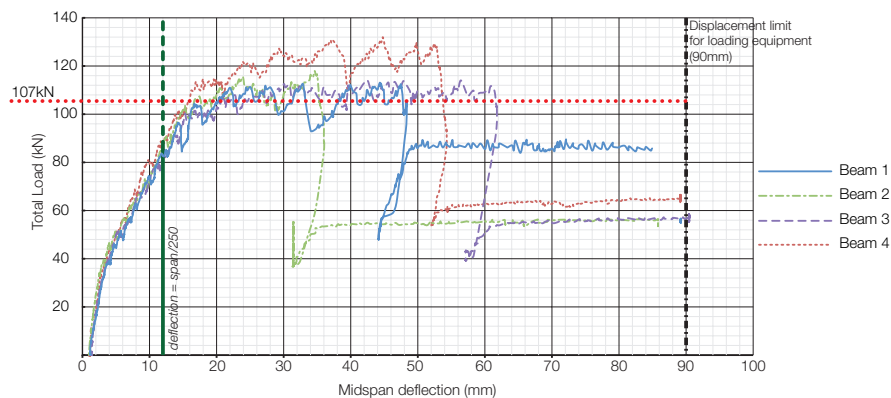


Figure 16. Load-displacement test results, Beams 1-4

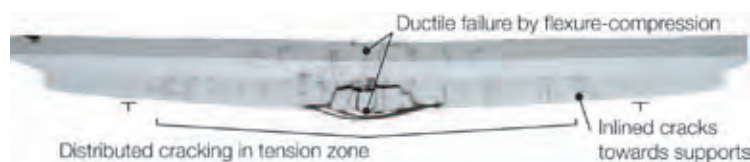


Figure 17. Typical failure mode

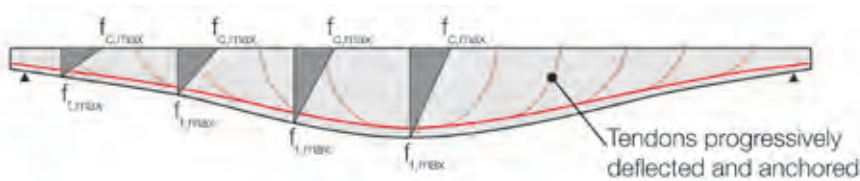


Figure 18. Uniform strength prestressed beams

Serviceability

The advantage of a prismatic beam is its constant stiffness prior to cracking. The variable section beam is inherently more flexible than its prismatic counterpart and thus the serviceability limit state may become a concern. For example, in the beams described above, applying a deflection limit of span/250 reduces the permissible load capacity by around 30%, as highlighted in **Figure 16**.

Yet stringent deflection requirements can do little except add deadweight. Designing a structure to follow the loads applied to it, without adding unnecessary material is a more sensible – moreover, sustainable – approach to structural design. For those situations where stringent deflection criteria are truly important, the use of prestressed reinforcement provides an ideal solution. With fabric formwork, uniform strength prestressed beams (as described by Guyon²⁷, where the extreme fibres at every point on the beam are at their compressive

or tensile stress limit, **Figure 18**) are entirely feasible and display excellent behaviour at the serviceability limit state. With fabric formwork, optimised, materially efficient, aesthetically pleasing structures that minimise embodied energy and encourage the appropriate use of thermal mass are possible. The construction of such structures can now be undertaken using a simple, reusable formwork system.

The future

The provision of reinforcement to a continually varying cross section has the potential to add significantly to construction time. A participating fabric system in which a composite fabric incorporating carbon fibres acts as both formwork and reinforcement may therefore be advantageous in some situations. Improvements in three-dimensional weaving capabilities may allow designers to specify carbon fibre weave directions and densities at various points along the length of a beam based

on the applied loads. The resulting formwork could then simply be filled with concrete to provide an optimised, composite reinforced structure that minimises material use.

There are, however, a number of technical hurdles to clear before such a method could be used in general construction. In addition to vandalism and fire protection, an adequate bond between concrete and reinforcement must be provided for the life of the structure and the existing architectural merit of fabric formed concrete structures must be maintained.

Flexural elements are fundamentally inefficient and it is in the design of shell structures that real material savings may be found. Using a combination of inexpensive fabric as formwork and lightweight, durable, high strength carbon fibre sheets as reinforcement, medium span shell elements such as those already produced at C.A.S.T may become a realistic alternative to existing floor and roof systems, as illustrated in **Figure 19**.

Conclusions

The design of fabric formed concrete structures has, to date, been led primarily by architectural concerns. Work to provide more complete design guidance for these remarkable structures is now well underway. Fabric formed concrete beams offer significant advantages for designers, including reductions in material

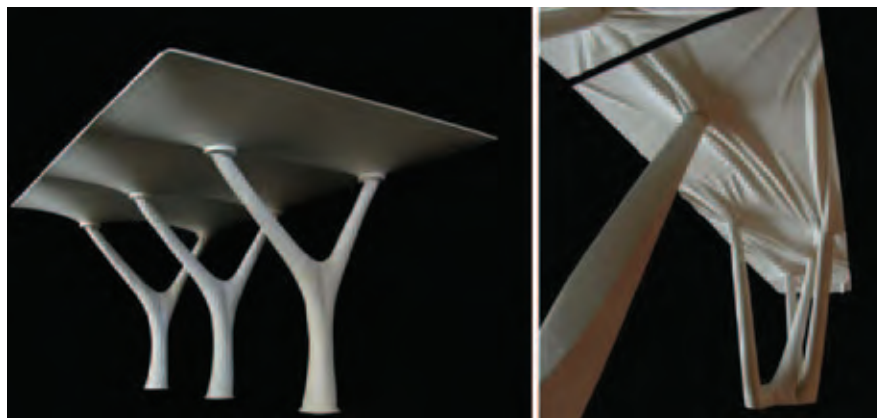


Figure 19. Fabric cast columns supporting fabric formed shells (courtesy C.A.S.T)

use, ease of construction and aesthetic appeal. Further advantages may be gained through the use of prestressed reinforcement, either steel or fibre reinforced polymers, where improvements in both serviceability and ultimate limit state behaviour can be obtained. Additional work is required to investigate the use of flexible fibre reinforced polymer fabrics and grids as both external participating reinforcement in beam structures and as internal reinforcement in thin-shell elements.

By designing optimised concrete structures, significant savings in material use can be achieved, with concomitant reductions in both embodied carbon and construction cost. Fabric formwork not only provides a simple means by

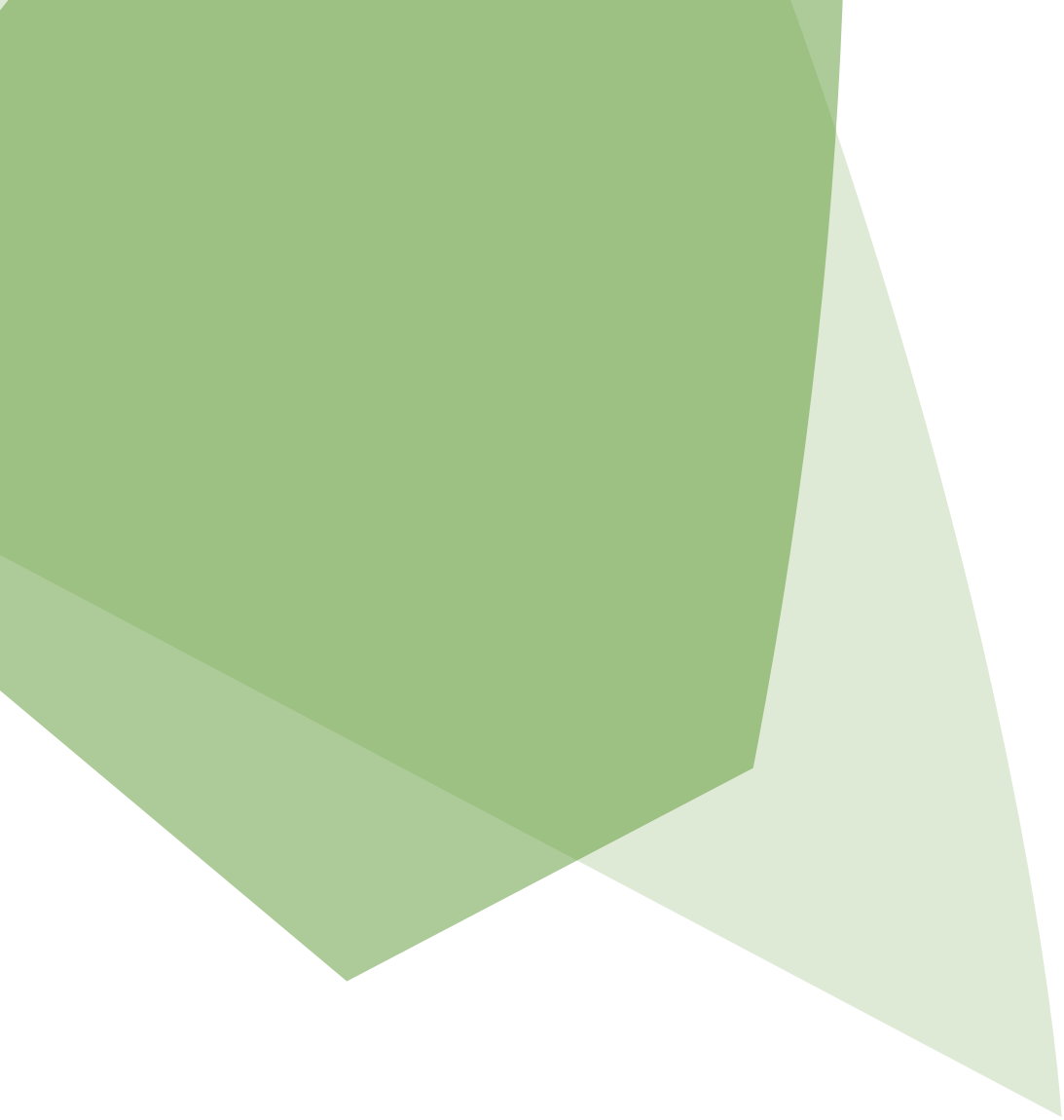
which such structures can be cast, but by allowing excess pore water to bleed from the surface of the concrete the resulting element is both durable and beautiful. Fabric formwork thus offers exciting opportunities for engineers and architects in the move towards a more sustainable construction industry.

Acknowledgments

The authors gratefully acknowledge the ongoing support of the Engineering and Physical Sciences Research Council (EPSRC) and Atkins UK Ltd, and wish to thank the technical staff in the Department of Architecture and Civil Engineering at the University of Bath for their assistance in preparing the tests described in this paper.

References

1. Lamberton, B.A.: 'Fabric forms for concrete', *Conc. int.*, December, 1989, p58-67
2. Orr, J. J., Darby, A. P., Ibell, T. J.: 'Innovative concrete structures using fabric formwork', SEMC 2010, Cape Town, South Africa, 4-8 September, 2010
3. West, M.: 'Kenzo Unno, Fabric Formed Walls', Winnipeg, University of Manitoba, Available from http://www.umanitoba.ca/cast_building/assets/downloads/PDFS/Fabric_Formwork/Kenzo_Unno_Article.pdf.
4. FabFormIndustries. Fastfoot Commercial Edging Video (online), 2010 [cited 2010 27/05]; Available from: http://www.fabform.com/products/fastfoot/fastfoot_commercial_edging_video.html
5. West, M., Araya, R.: 'Fabric formwork for concrete structures and architecture', *Int. Conf. Textile Composites and Inflatable Structures*, Barcelona, Spain, 5-7 October, 2009
6. Hammond, G. P., Jones, C. I.: 'Embodied energy and carbon in construction materials', *Proc. Instn Civil Engrs: Energy*, 161 (2) p 87-98
7. Van Oss, H. G.: 'Mineral Commodity Summaries: Cement', USGS, 2006
8. CDIAC.: Fossil-Fuel CO2 emissions (online), 2005 [cited 2010 30/03]; Available from: http://cdiac.esd.ornl.gov/trends/emis/meth_reg.html
9. Bailiss, J.: 'Fabric-formed concrete beams: Design and analysis', MEng Thesis, Department of Architecture and Civil Engineering, Bath, University of Bath, 2006
10. Garbett, J.: 'Bone growth analogy for optimising flexibly formed concrete beams', MEng Thesis, Dept for Architecture and Civil Engineering, Bath, University of Bath, 2008
11. Price, W. F.: 'Controlled permeability formwork'. London, 2000
12. Price, W. F. and Widdows, S. J.: 'The effect of permeable formwork on the surface properties of concrete', *Magazine of Conc. Res.*, 43/155, 1991, p 93-104
13. Serafini, F. L.: 'Corrosion protection of concrete using a controlled permeability formwork (CPF) system', *Corrosion and Corrosion Protection of Steel in Concrete*, Sheffield, 1994
14. Kasai, K., et al.: 'Study on the evaluation of concrete quality prepared with permeable forms and plywood forms', *Trans. Jpn Conc. Inst*, 10/1989, p 59-66
15. Pallet, P.: 'Introduction to the formworks scene', *Concrete Magazine*. 1994, p 11-12
16. West, M., Abdelgar, H. S., Gorski, J.: 'State of the art report on fabric formwork', *Concrete: Construction's sustainable option*, Sept 4-6, 2007
17. Schmitz, R. P.: 'Fabric formed concrete', 17th Analysis and Computation speciality conference, 2006 Structures Congress, St. Louis, MO, May 18-20, 2006
18. Veenendaal, D.: 'Evolutionary optimisation of fabric formed structural elements', Thesis, Civil Engineering and Geosciences, Delft, University of Delft, 2008
19. Foster, R.: 'Form finding and analysis of fabric formed concrete beams', MEng Thesis, Architecture and Civil Engineering, Bath, University of Bath, 2010
20. Losilevskii, G.: 'Shape of a soft container under hydrostatic load', *J. App. Mech.*, 77/1, 2010, p 3
21. Vierendeel, A.: *Longerons en treillis et longerons à arcades*. Louvain, Trois Rois, 1897
22. BS EN 1992-1-1, Eurocode 2: Design of concrete structures - Part 1-1: General rules and rules for buildings. 2004
23. BS 8110-1, Structural use of concrete - Part 1: Code of practice for design and construction. 1997
24. Collins, M. P., Mitchell, D., Bentz, E. C.: 'Shear Design of Concrete Structures', *The Structural Engineer*, 86/10, 2008, p 32-39
25. D'Aponte, E., Lawton, A. and Johnson, R. M.: 'Fabric Formwork for Architectural Concrete Structures', 1st Int. Conf. Conc. Techn., Tabriz, Iran, 6-7 November, 2009
26. Yestermorrow Design Build School (accessed, 01/08/10); Available from: <http://www.yestermorrow.org/>
27. Guyon, Y.: *Prestressed Concrete*. London, Contractors Record and Municipal Engineering, 1953



**Paul Groves**Network Chair
for TunnelingAtkins Middle East &
India**Eric Chui**

Divisional Director

Atkins China

**Tiffany Chan**

Principal Engineer

Atkins China

Adit mining in high permeability, interbedded sandstone, Red Line, Dubai Metro

Abstract

Adits connecting annex shafts and a bored tunnel are constructed for the Dubai Metro Red Line for the purpose of ventilation and passenger escape. A critical part of the design is to mitigate the risk of face instability due to the mining of adits to connect the bored tunnel and annex shafts, which is carried out in calcareous sandstone, whose strength and stiffness are equivalent to very densely compacted soil or extremely to very weak rock material. Overall instability due to global shear failure of the adit faces is classified as acceptably low in risk, but local piping failure due to the possible existence of weak layers of cohesionless materials could lead to overall stability problems. To limit water ingress and piping risks, dewatering via deep well pumping and horizontal drains has been proposed. Pumping trials have been carried out, with back analyses performed to create calibrated seepage models.

Introduction

The Road & Transport Authority (RTA) constructed the Dubai Metro Red Line, the first railway line in the United Arab Emirates. The Red Line, together with the Green Line, civil works were built by JTMJV (Japanese Turkish Metro Joint Venture). Atkins was Contractor's Designer responsible for all tunnel design including temporary and permanent works.

The line, which is 52.5km in length, has 26 stations, two depots, and three annex shafts. Two earth pressure balance tunnel boring machines (EPBMs) were used to construct a 5.3km long underground section.

The Dubai Metro project includes three annex shafts, each of which has two adits connected to the bored tunnel to provide ventilation (ventilation adits) and an emergency escape from the bored tunnel into the shaft (escapeway adit). The ventilation adits have a span of 8.2m and are 7.5m in height. The escapeway adit is smaller, with a span of 3.7m and a height of 5m.

The size and shape of the adits were optimised to minimise the bending moment generated on the bored tunnel

lining and to encourage the arching effect of the ground, especially for the ventilation adits, the height of which is almost the same as that of the bored tunnel. A section of the adits is shown in **Figure 1**, viewed from within the tunnel.

The adits for annex shafts 1 and 2 were constructed underneath existing roads, whereas the adits for annex shaft 3 were constructed underneath an existing six-storey building. It was important therefore to prevent excessive ground settlement due to adit excavation, especially for annex 3. The layout of annex 3 is shown in **Figure 2**.

The annex shafts were constructed using permanent diaphragm walls with the top-down excavation method. The bored tunnel was constructed by the EPBM, which passed beside the annex shafts.

The adits were constructed by the mechanical mining method with lattice girders and shotcrete for temporary support. Permanent support was provided by cast in situ reinforced concrete.

A temporary ring beam bracing system was installed within the affected section of the bored tunnel to limit deflection

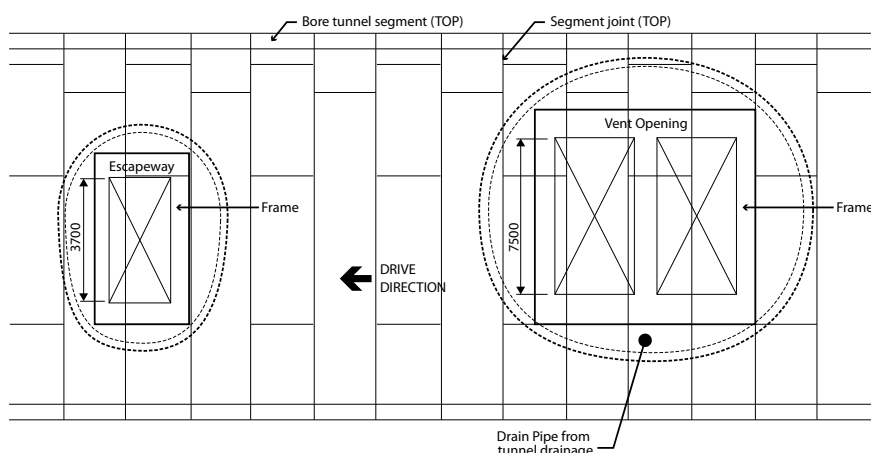


Figure 1. Typical section of adits

during adit mining and allow removal of lining segments to complete the connection. The annex shafts were drilled and mining commenced from the shaft towards the bored tunnel.

Ground conditions

In general, the adits are located in weak interbedded calcareous sandstone (CSS) that is overlain by calcareous sand (CS) and marine deposits (MD). Sandstone, although classified as rock, has strength and stiffness properties equivalent to very densely compacted soil or extremely to very weak rock material. Its fractures are close (60 to 200mm) to medium spaced (200 to 600mm), with some poorly cemented carbonate silt and sand layers noted.

The permeability of these materials is around 10^{-5} to 10^{-6} m/s; however,

structural defects such as solution cavities, joints and geological faulting could provide a pathway that would significantly increase groundwater flow. The groundwater level along the tunnel alignment is around 2 to 6m below ground level.

Geotechnical risks associated with adit mining

Based on the ground investigation information and observations during station/shaft excavation, the following key risks were identified:

- Local face instability in adit headings;
- Excessive ground movement impacts on existing structures; and
- Excessive groundwater ingress and piping (ie. running or flowing sand).

A) Local face instability in adit headings

When fully drained, sandstone and cemented sandstone material are likely to behave as firm, competent ground without noticeable movement in the adit heading face or unsupported arch. Stability analysis using the wedge failure approach indicated that the excavation face was stable and achieved the required factor of safety. Hence, it was considered unnecessary for the adit to be pre-supported with forepoling.

B) Ground movement impacts

Ground movement due to stress redistribution in the ground will occur around the advancing adit heading. However, we considered that the likelihood of large movement was low as the adits are relatively short compared to their depth. Provided that instability does not occur, settlement effects will be quite local in the area above the short adits. Having said that, local instability (eg. raveling or block failure) related to mining in drained ground is always a risk, and needs to be minimised and controlled during the work by conventional mining measures based on observational approaches; however, this is not covered in this paper.

C) Groundwater ingress and piping

When mining in sandstone below the water table, there is always a risk of significant groundwater ingress and piping, also known as running or flowing sand conditions. A comparable situation is illustrated in **Figure 3**, where excessive water inflow and possible piping have occurred in cemented sand material due to excessive hydraulic gradients and highly permeable ground.

Based on the ground investigation data and site observations during the excavation of the shafts and tunnel boring in the same area, we considered that piping and groundwater ingress were major risks of adit mining. Piping failure can be significant because it can lead to flooding, severe ground loss and possible instability, which can endanger the workforce. The phenomenon of piping occurring along a possibly weak permeable layer of cohesionless material is illustrated in **Figure 4**. Measures to reduce these risks through a structured approach are essential and discussed in the following sections.

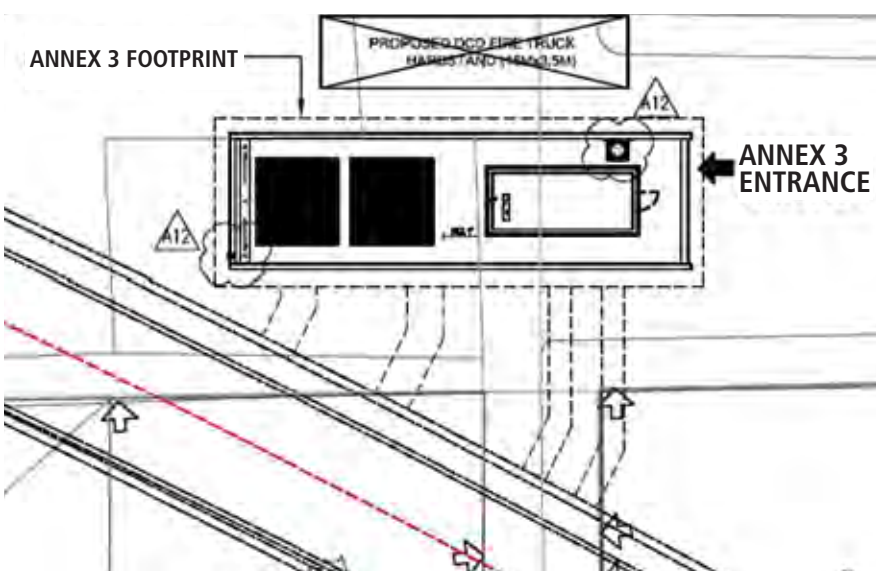


Figure 2. Layout of adits for annex 3

Risk mitigation measures

The following measures were proposed to reduce the risks due to excessive groundwater ingress and piping:

- Deep well dewatering;
- Use of a slurry wall or jet grouting from the ground surface to form a hydraulic cut-off wall;
- Horizontal gravity drains from annex shafts; and
- Other measures such as local drainage pipes, probing and grouting from the excavation face where necessary.

We considered deep well dewatering and horizontal drains to be the principal measures whereas the cut-off wall was of secondary importance because its efficiency is difficult to ascertain. The arrangement of the deep well and cut-off wall at annex 2 is shown in **Figure 5**.

Other measures that can be used just prior to or during adit mining are considered to be contingency measures against the possible partial success of dewatering and ground treatment measures.



Figure 3. Example of piping failure

Analytical approach and results

To investigate the effectiveness of deep well dewatering to reduce the pressure head at the adit level, analyses were carried out using the computer program SEEP/W. The general approach is summarised below.

Stage 1: Axisymmetrical and transient modelling – to adjust the parameters and pump rate to simulate a three-dimensional (3D) effect with two-dimensional (2D) models and to predict the time required for dewatering to reach a steady state.

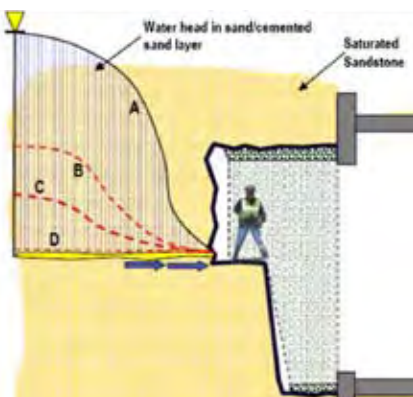


Figure 4. Significant water ingress from the strata bed

Stage 2: Initial seepage and piping risk assessment – to investigate piping risk based on the current dewatering scheme and assumed permeability of the cut-off wall.

Stage 3: Back analysis – to calibrate the model and replicate the results of the pumping trials.

Stage 4: Design of risk mitigation measures – to design final measures to mitigate piping risk based on information obtained from stage 3.

The staged analyses are described in detail below with a discussion of the results.

Stage 1 – Axisymmetrical and transient models

Before setting up the seepage models for actual layout, two calibration analyses were undertaken, as described below.

A. Axisymmetrical seepage analysis. Well dewatering is a 3D problem with different boundary conditions in the two horizontal directions. An axisymmetrical approach was adopted to simulate the deep well dewatering effect to obtain the water drawdown and hydraulic pressure. A general case of seepage into a deep well in two dimensions was then undertaken to replicate a similar dewatering pattern by adjusting the pumping rate. **Figure 6** shows results from the axisymmetrical model.

B. Transient seepage analysis. Transient analysis was carried out to evaluate the rate of groundwater drawdown, and hence the change of the hydraulic head at the adit face at different time intervals. As indicated in the analysis, approximately six days were required to achieve steady state flow for the given ground conditions.

Stage 2 – Initial seepage and piping risk assessment

Based on the stage 1 findings, 2D models were set up at each annex to give an initial idea of the piping risk and a range of factors of safety against piping.

The critical hydraulic gradient is based on the suggestion of Kiya (2000):

$$i_c = 0.179 e^{0.046 D_R} \quad (1)$$

where D_R is the relative density. For dense sand, the relative density is about

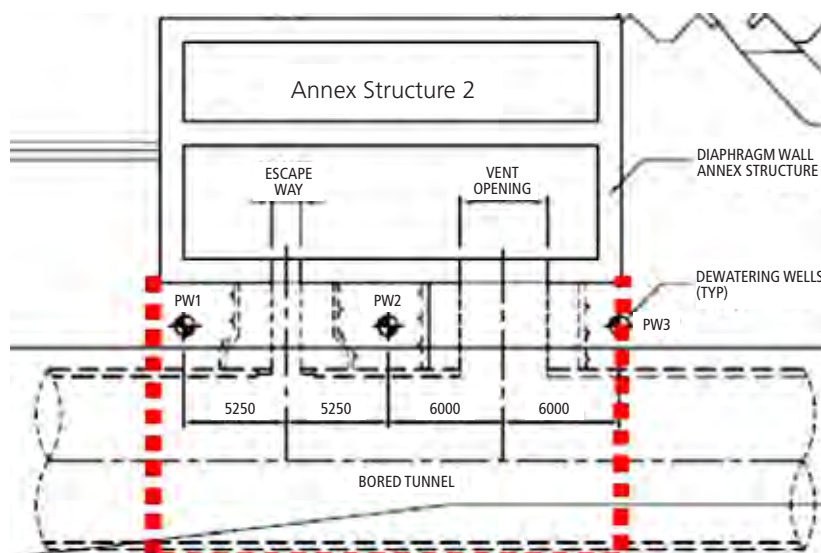


Figure 5. Plan of a deep well at annex 2

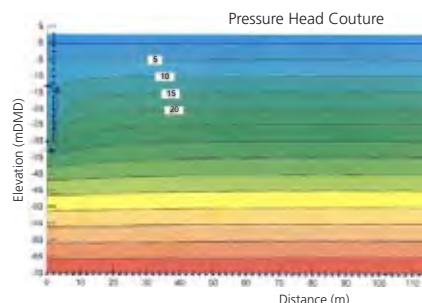


Figure 6. Axisymmetrical model

65% and therefore the critical hydraulic gradient is 3.6.

Slurry walls were constructed around the adits of annex 1 and because of site constraints, jet grouting walls were used as hydraulic cut-offs for annexes 2 and 3. To model the possibility of the cut-off wall being leaky and how that might affect the amount of groundwater ingress and piping, the cut-off wall was modelled with smeared permeability.

The results of the initial analyses suggested:

- Deep well pumping significantly reduces the hydraulic pressure head around the adit excavation and hence the piping risk. See **Figure 7**;
- With the use of piping wells, the groundwater flow was reduced by 35% for annex 2 and 67% for annex 3; and
- Piping may be a problem at the invert level.

However, the analyses were based on homogeneous soil materials with permeability of one order of magnitude. The permeability of actual ground conditions can vary, which can lead to higher groundwater inflow, and a single permeable layer can entirely change the situation. It was suggested, therefore, that trials of a deep well pumping and horizontal probe drains be carried out and the results adopted to calibrate the seepage models.

Stage 3 – Back analysis to replicate the pumping trials

Two sets of trial tests were carried out.

A. Deep wells. Flow meters were connected to each of the three pumping wells and three observation wells were installed to measure the groundwater drawdown. The procedure was as follows:

- Turn all three pumps on and monitor the water level and pumping rate until a steady state is reached.

- Cease pumping until the groundwater table recovers its natural level.
- Turn on only pump 2 and monitor the water level and pumping rate until a steady state is reached.
- Repeat step c for pumps 1 and 3.

Example results of the deep well pumping trial for annex 2 are given in **Figure 8**.

B. Probe drain pipes from segmental lining. Probes were drilled and drain pipes were installed from the bored tunnel at each adit location, and each pipe was equipped with a packer with a tap. The water pressure was measured using a pressure gauge connected to the drains

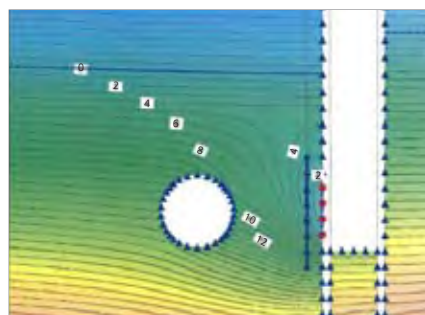


Figure 7. Analysis of the pressure head contour for annex 2

(when the tap was closed) and the flow rate from the drains was measured by the number of buckets filled per minute (when the tap was open). The trial procedure was as follows:

- Measure the pressure head with all pumps off.
- Measure the flow rate from each of the drains opened one by one with all pumps off.

- Measure the pressure head with all pumps operating.
- Measure the flow rate from each of the drains opened one by one and with all pumps operating in the steady-state mode.

Back analysis was carried out to replicate the trial results by adjusting the following parameters and assumptions:

- The permeability of the jet grout wall, which represents a partially leaky cut-off wall;
- The soil permeability; and
- The pumping rate of the deep wells.

Figure 9. shows the model replicating the trial test results from deep wells and drain pipes.

Stage 4: Design of final risk mitigation measures

The revised model, which replicated the trial test results, indicated that the hydraulic gradient might be too high to achieve a minimum factor of safety against piping of 1.5.

Therefore, in addition to the deep well pumping within the jet grout cut-off walls, a series of horizontal drains below the level of the adit inverts were proposed. The layout is given in **Figure 10** and installation **Figure 11**.

New analytical models were undertaken, taking into account the modified parameters to reflect the trial test results, adit excavation sequence and provision of the proposed horizontal drains installed from the annex shafts.

Three scenarios were studied: with horizontal drains only; with deep wells only; and with both horizontal drains and deep wells.

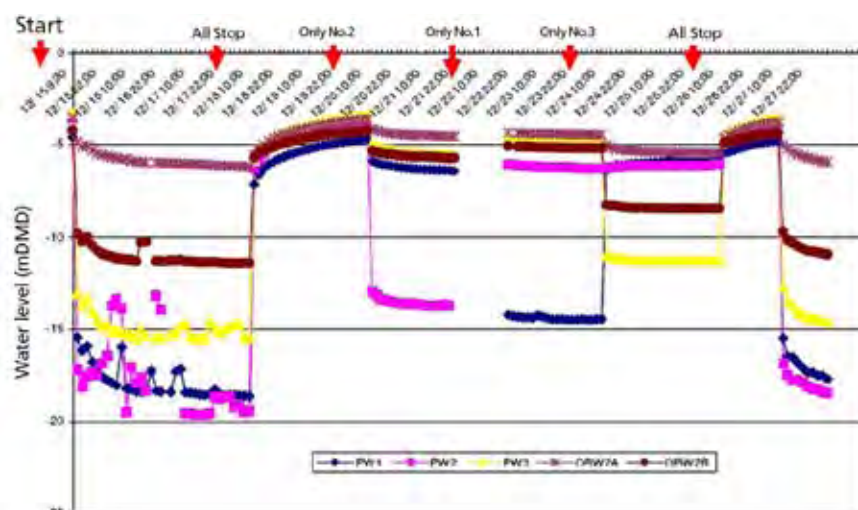


Figure 8. Analysis of the pressure head contour for annex 2

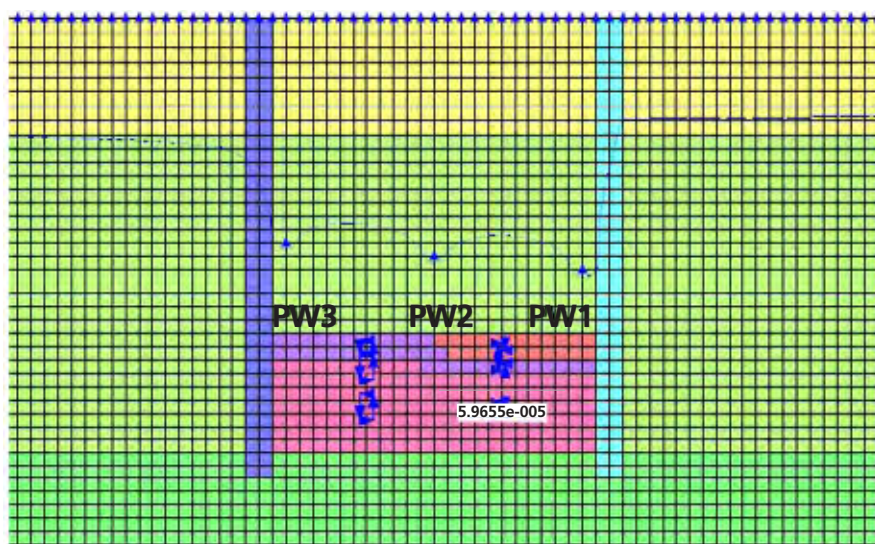


Figure 9. Back analysis model for annex 2

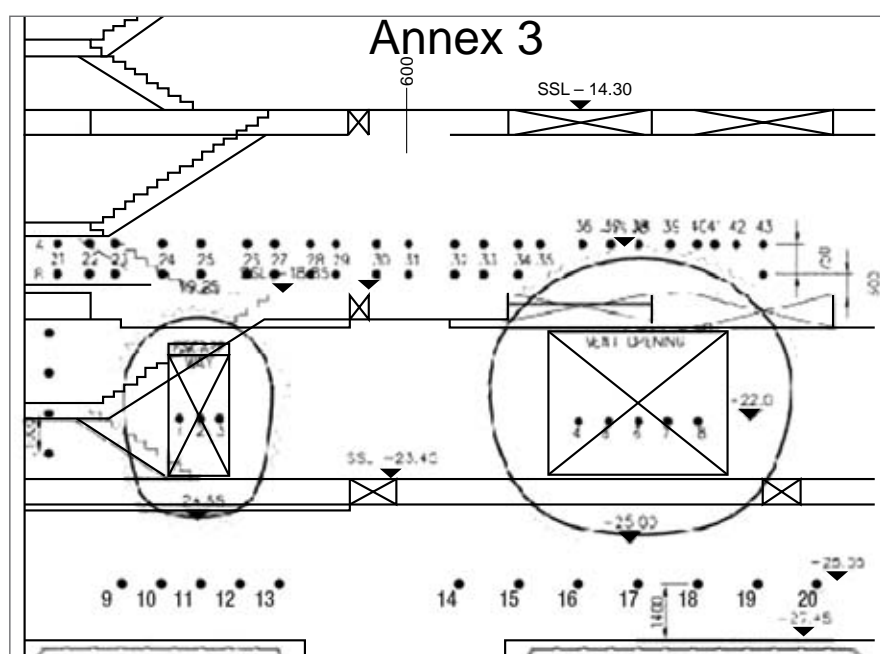


Figure 10. Layout of drain pipes installed below the adit invert of annex 3

The adit excavation was simulated by specifying that the pressure head at the adit face equal zero. The inflow of groundwater was obtained by the “flux section” around the opened face.

Phased excavation was modelled in the SEEW analysis, taking into account the construction time that would likely be required for adit mining using the heading and benching method, as illustrated in Figure 12.

The hydraulic gradient for various cases was estimated based on the SEEPW models for comparison with the critical hydraulic gradient; the factor of safety against piping and the inflow rate from

the excavation faces were also estimated from the models. The results are summarised in Tables 1 and 2.

By comparing the results of the analysis for the case with deep wells only and the case with both horizontal drains and deep wells, it is clear that dewatering around the adit via horizontal drains can significantly reduce the piping risk and initial inflow rate for adit excavation.

Verification from additional field data

Prior to the start of excavation, as planned, drain pipes were installed,



Figure 11. Installation of drain pipes installed below the adit invert of annex 3

forming part of the proposed horizontal drain holes, from the annex shaft diaphragm wall for each adit, each with a packer with a tap. The flow rate from the drains was measured based on the number of buckets filled per minute (when tap is open).

Based on the observable inflows and drawdown, further seepage back analyses were carried out to verify the design approach. The results are summarised in Table 3.

The seepage analysis generally gives a drain inflow less than that of the field measurement. The ratio between the field data and analysis results is in a range from 1.2 to 4.5, which is considered an acceptable range when compared with the possible range of permeability of sandstone, which is from 10-5 to 10-6 m/s (at least 10 times). The variation is probably due to the following:

- Variation in ground permeability.
- The 3D effect. The model carried out in the direction along the adits shows that the flow in the third direction could contribute more than 20% of the total flow.
- The uncertainty and localised effect of permeability.
- The inflow affected by the degree of leakage of the jet grout wall.

Conclusion

Although the groundwater table is above the adit crown level, the use of preinstalled horizontal drainage pipes below the adit inverts reduces pore water pressure around adit openings, resulting in the reduction of seepage ingress and the maintenance of relatively low hydraulic gradients compared with the critical gradient for piping failure.

Further back analyses based on observations were made after horizontal drain installation and immediately prior to adit break-in. These confirmed the applicability of the design approach and that the models, based on back

Analysis	During excavation	Safety factor against piping at inverts
Escapeway Adit		
With horizontal drains only	H	12
	B & I	7.2
With deep wells only	H	1.3
	B & I	1.3
With both horizontal drains and deep wells	H	12
	B & I	6.0
Ventilation Adit		
With horizontal drains only	H	4.5
	B & I	4.5
With deep wells only	H	2.3
	B & I	1.8
With both horizontal drains and deep wells	H	12
	B & I	4.5

Table 1. Summary of piping assessment for annex 3

Case	Description	Inflow into adit (L/s)		Ratio
		SEEP / W		
1	Drains at adit level only	0.5	1.85	3.7
2	Drains at adit level	0.36	0.41	1.1
	Drains at raft level	0.35	1.56	4.5
3	Drains at raft level only	0.4	1.8	4.5
4	Drains at raft level	0.34	1.53	4.5
	Drains at top level	0.57	0.88	1.5

Table 3. Observed inflows

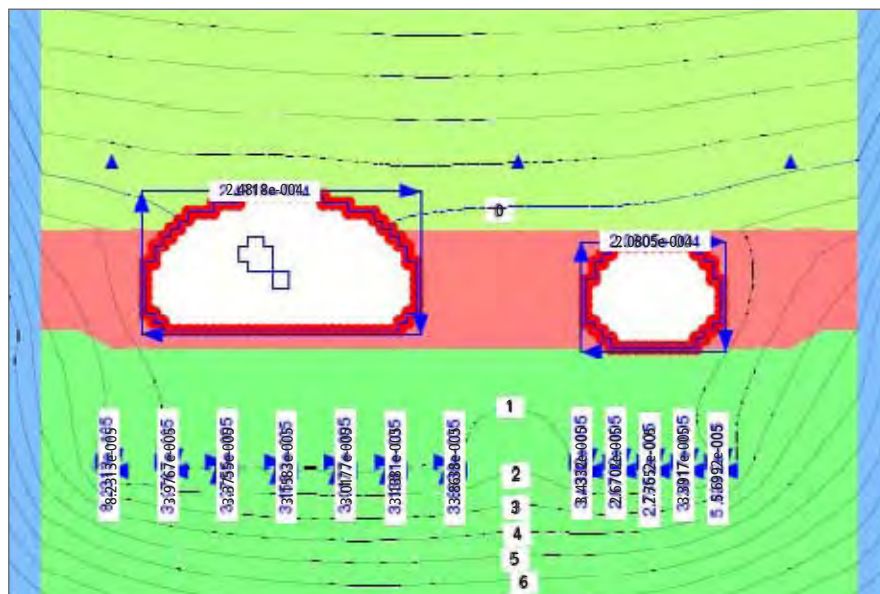


Figure 12. SEEPW model for heading excavation of annex 3

Analysis	During excavation	Groundwater inflow into adit (L/s)
Annex 3 Escapeway Adit		
With horizontal drains only	H	0.66
	B & I	0.32
With deep wells only	H	0.44
	B & I	0.17
With both horizontal drains and deep wells	H	0.21
	B & I	0.23
Annex 3 Ventilation Adit		
With horizontal drains only	H	1.25
	B & I	0.38
With deep wells only	H	0.86
	B & I	0.14
With both horizontal drains and deep wells	H	0.25
	B & I	0.26

Table 2. Summary of groundwater inflow for annex 3

analysis-calibrated models, were in good agreement with the actual cases.

The analytical approach described in this paper, involving predictions, field trials, back-analysis verifications and further calibrated analyses, helped us to gain a better understanding of hydraulic behaviour during adit excavation and how it can be affected by various risk mitigation measures related to piping and excessive water ingress.

The Red Line adits have been safely mined and are fully lined.

Acknowledgement

This paper was presented at the International Symposium on Rock Mechanics "Rock Characterization, Modelling and Engineering Design Methods" held on 19-22 May 2009 at The University of Hong Kong.

References

Kiya, H 2000. Study on the Experimental Evaluation method for Sandy Tunnel Face, Journal of the Japan Society of Engineering Geology.

**Ian Turner**

Senior Engineer

Water & Environment

Atkins

**Michael Yap**

Tunnel Engineer

Water & Environment

Atkins

Assessment of ground movement impacts on existing tunnels

Abstract

As an increasing number of tunnelling schemes are being designed and constructed in congested cities around the world, the complications involved as a consequence of tunnelling on existing sub-surface structures are becoming ever more challenging for engineers. Most would agree that the impact of tunnelling-induced ground movement on existing tunnels is an important issue, and the need for improved technical knowledge for solving this complex soil-structure interaction problem is essential. This paper initially explores the paradox of commonly used semi-empirical methods for predicting the 3D tunnelling-induced ground movements. The potential effects of these ground movements on the longitudinal and transverse response on the structural behaviour of the existing tunnels are then investigated. The shortcomings of commonly adopted assessment methods which may result in non-conservatism and mask critical issues of existing tunnels at tunnel crossings are highlighted throughout the discussion. This paper also demonstrates the use of modern computing to do powerful complex analysis to solve the complexities of soil-structure interaction and manage risks associated with tunnel crossings.

Introduction

As mass transit and other tunnelling schemes are constructed in increasingly developed urban areas, the impacts of tunnelling on existing tunnels are becoming ever more important. The problem of soil-structure interaction is relatively complex, and the need for improved knowledge of the impacts of new tunnelling works on existing tunnels is essential to obtain a thorough understanding of such issues.

This paper initially examines historic case studies that form a useful basis for predictions of likely induced movements of existing tunnels caused by tunnel construction, which often provide a database against which modelling assumptions can be verified. The use and limitations of simple semi-empirical methods for predicting the three dimensional ground displacements caused by tunnel construction are subsequently investigated. The discussion then leads on to the assessment of longitudinal and transverse (cross-sectional) behaviour of the existing tunnels. The complexity of ground movement predictions and the structural performance of the existing tunnels are examined and various methods of analysis

are assessed. Throughout the discussion, issues with non-conservative assumptions and methods of analysis are highlighted, which could potentially mask the most significant issues of existing tunnels at tunnel crossings.

Case histories

One of the challenges in understanding the effect of tunnel induced settlements on existing tunnels is the limited number of published case histories. The problems of predicting ground movements and structural performance of existing tunnels are complex and to fully understand the behaviour at these tunnel crossings, not only does the performance of an existing tunnel have to be extensively documented, details of the construction of the new tunnel are equally important. The lack of quality information adds to the dilemma as, quite often, ground movements are so small that interpreting the exact behaviour of the tunnels at the crossing point, given the accuracy of the monitoring, is not reasonably possible. Whilst such performance is without doubt desirable from the point of view of the tunnelling contractor and the

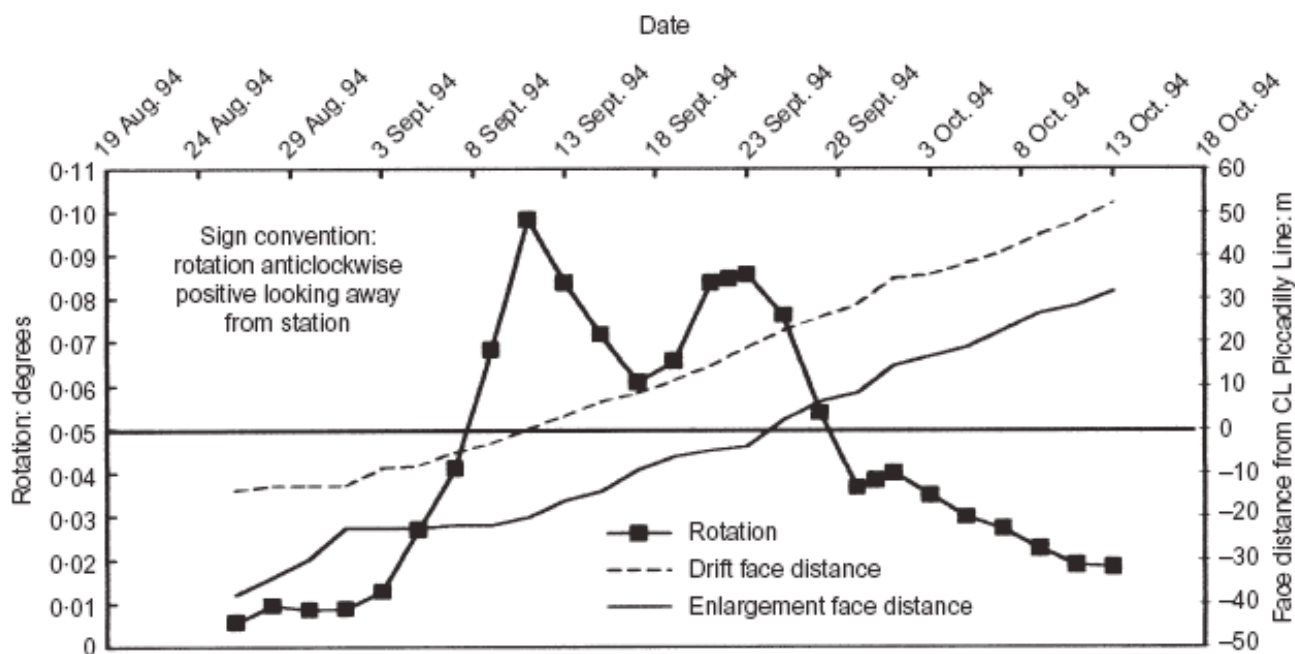


Figure 1. Rotation of Piccadilly Line tunnel as new tunnel passes beneath Heathrow³

asset owner, this poses a challenge for assessors in predicting tunnel behaviour at crossings.

Probably the most relevant example recorded in recent history is the construction of the Heathrow Express tunnels as they were driven under the Piccadilly Line at Heathrow³. This example is well documented and the movements are sufficiently large relative to the accuracy of the monitoring that reasonable conclusions can be drawn from the results. In addition, the relatively flexible behaviour of the Piccadilly Line tunnel meant that a good understanding of the ground movements could be obtained. Particular modes of response of the existing tunnels to imposed movements that were identified include the rotation of the tunnel as the face of the new tunnel passes underneath (**Figure 1**) and the large distortion that occurred on the diagonals of the tunnel. It is observed that movements of the existing tunnel could be reasonably assessed using a calibrated prediction of the tunnel-induced ground movement.

Since then, a number of other tunnel crossings have been documented. On the Channel Tunnel Rail Link (CTRL) the crossing under the Central Line was notable because of the close separation between the tunnels¹². Back analysis of the data obtained on the CTRL crossings both at the Central Line and at Highbury and Islington Stations show a wide variation in the settlement volume losses and trough width parameters (**Table 1**).

	CTRL UP		CTRL DOWN	
	K	V _s	K	V _s
GN & C southbound	0.71	0.59%	0.61	0.38%
Victoria southbound	0.55	0.44%	0.38	0.55%
GN & C northbound	0.70	0.51%	0.67	0.52%
Victoria northbound	0.45	0.44%	0.49	0.45%

Table 1. Results of back analysis of ground movement at the Highbury and Islington crossings¹²

Whilst it is not clear that this is due to soil-structure interaction resulting in a flatter trough. It is probable that higher K values were noted where the ground was stiffer due to the presence of the existing tunnel.

Similar results have been observed in other tunnel crossings in recent years such as the Thameslink 2000 tunnels under the existing Thameslink tunnel¹⁰ and where a new tunnel is driven parallel to existing tunnels⁶. Well documented examples of the behaviour of tunnels in response to ground movements have also been published^{15,3}.

Whilst considering the movements created by the construction of a proposed tunnel is important, an understanding of the existing tunnel's response to the movements is equally important. These case histories demonstrate that

the movements of existing tunnels in response to the construction of new tunnels is reasonably consistent with the movements that are predicted by using conventional technologies for predicting ground movements.

Ground movement predictions

Key to understanding the ground movement impacts on existing tunnels is being able to predict the 'greenfield' ground movements. Historically semi-empirical methods have been regularly used in the UK to predict tunnel-induced ground movements.

The most commonly used approach is the assumption of a point source leading to a settlement trough approximating to a Gaussian distribution¹⁴. Whilst

this approach has proved to be reliable for many different scenarios, there are situations where the approach has proved to have limitations.

One particular situation where this is the case is in assessing ground movements close to the source of movement generation where the assumptions appear to break down and modifications to the method are required, such as changing the trough width parameter⁹. The main reason for this is that when the existing tunnel is in close proximity to the new tunnel, the assumption of a point source is no longer valid and the shape and size of the tunnel will have an effect on the result. This often poses a challenge when considering the effects of one tunnel on another because the crossings are often close, with less than two diameters between the tunnels. At these distances, the geometry of the tunnel causing the movement becomes important to the shape of the settlement trough and therefore needs to be considered.

Solutions of predicting sub-surface ground movements close to the source of movement exist in a number of different forms. A common approach is to adopt a closed form solution for a more sophisticated source for the ground movement such as a ribbon sink method¹³. This approach assumes that the source of the ground movement is evenly distributed over the width of the new tunnel at invert level, rather than axis level, and has shown to be of better agreement to the field data obtained from the Heathrow Express trial tunnel. This results in a settlement trough very similar to the Gaussian trough when the

depth of cover between tunnels is large, but as the cover distance reduces, the predicted ribbon sink trough becomes flatter than the Gaussian trough, giving a similar response to adjusting the trough width parameter for the Gaussian trough.

An alternative approach available with modern computing power is simply to discretise the face into a number of smaller point sources (**Figure 2**), an approach that has been adopted for modelling settlement troughs due to jacked boxes. By breaking a tunnel into a number of smaller sources, the basic equations of the Gaussian trough can be used to predict the cumulative settlement due to each of the small regions. This approach has the advantage of taking into account both tunnel size and geometry, allowing unusual geometries and sequences to be considered with ease. This approach results in very similar results to the Ribbon

Sink method unless very close proximities are being considered or the tunnel has a significantly non-circular geometry.

Figure 3 shows the ground movement predictions using the Gaussian, ribbon sink and discretised methods. The two ground movement graphs are shown with depth of source taken to the axis level and to the invert level respectively. The discretised profiles are identical as they have been calculated assuming source at the centre of the each element. It is observed that the main distinction is the reduction in maximum settlement, and the flatter and wider trough when the source of ground movement is assumed to be at the invert. In hindsight, the location of the source of ground movement could perhaps be subjected to further investigation, and could potentially be influenced by various factors including the construction method of the new tunnel and ground conditions.

The current challenge with all of these approaches is ensuring that the parameters used are consistent with the technology being adopted for the ground movement prediction. Modern ground movement prediction is still fundamentally a statistical assessment method that is a subject of various influencing factors, and as such relies on databases from back analyses to give assessors reasonable input parameters for their assessment. Although all methods use the same parameters, there is no reason why for a given depth and tunnel geometry the parameters used in the assessment, the trough width parameter, K , and even the volume loss, V , should be the same.

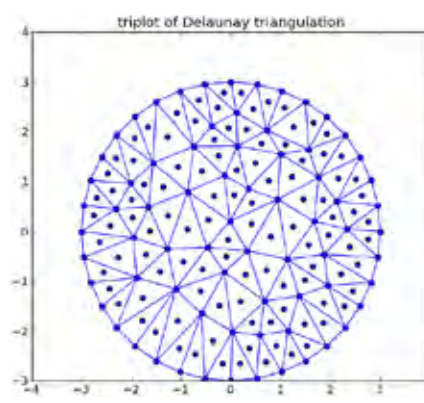


Figure 2. One method of discretising into a number of smaller point sources - using Delaunay triangulation (From Python code)

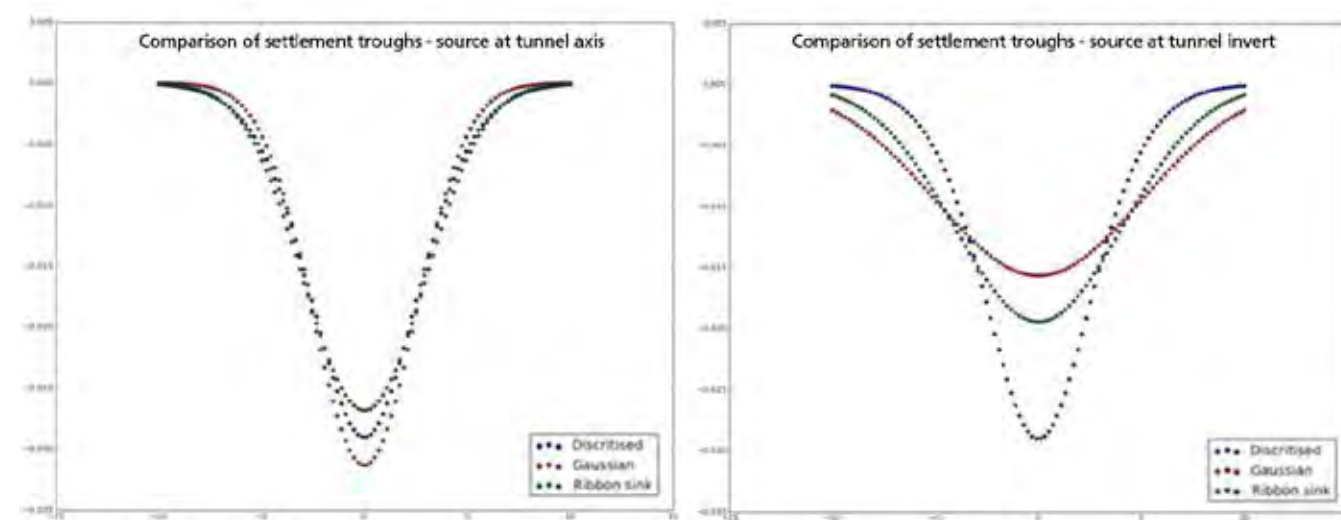


Figure 3. A comparison of ground movement predictions with source taken to axis level (left) and to invert level (right) on the same vertical scale (From Python code)

The longitudinal effect: effects of ground movements along the axis of the existing tunnel

Having predicted the 'greenfield' ground movements around the existing tunnel, an assessment of the impact of the ground movement on these tunnels is normally undertaken. One consequence of these ground movements is the structural response along the length of the existing tunnel. This section sets out to discuss the potential longitudinal structural behaviour of the existing tunnel.

As noted in historic case studies, there has been evidence that the stiffness of the existing tunnel can affect the shape of the predicted 'greenfield' settlement trough, with trough being wider and shallower as a result of the stiffness of the existing tunnel. Whilst it is typically conservative not to consider the soil-structure interaction, it is possible that not considering the interaction could result in the need to construct extensive mitigation measures which in themselves hold risks of unplanned outcomes. Not considering soil-structure interaction is also likely to result in an underestimate of the width of the settlement trough. For this reason, it is important for the assessment engineer to consider, in minimal, the implications

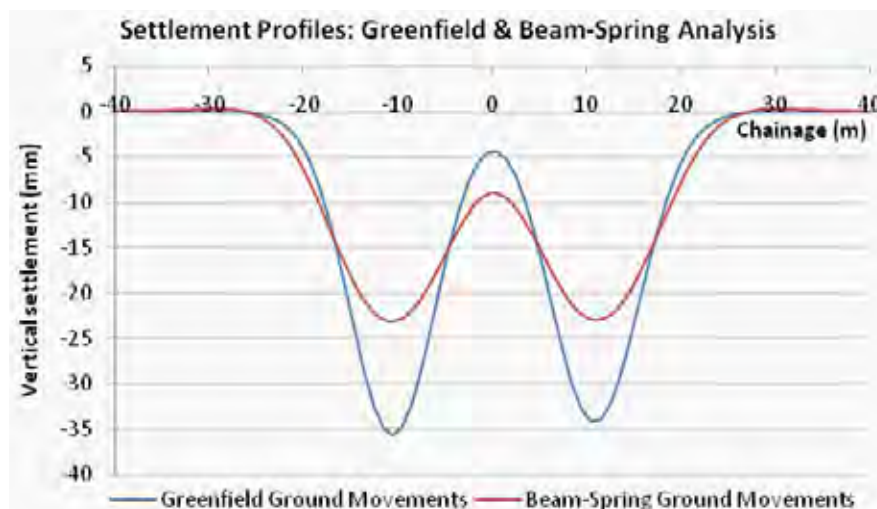


Figure 4. Comparison between Greenfield and beam-spring ground movement profiles (from MS Excel)

of soil-structure interaction, even if the final assessment is based on the 'greenfield' ground movements.

The simplest method to take into account soil-structure interaction is to adopt a beam-spring model. This methodology has been used for many years for assessing the settlement impacts on existing pipelines and other small diameter tunnels^{2,7} as well as larger diameter tunnels¹². A beam-spring model can be used to investigate this soil-structure interaction, where the existing tunnel can be modelled as a series

of beams with the appropriate sectional properties, attached to vertical and axial Winkler springs at the nodal ends. Springs are usually linear elastic, but non-linear elasto-plastic no-tension springs can be adopted for a more sophisticated model.

Greenfield ground movements are subsequently applied to these springs, either as forced displacements or by using a spring softening approach where the spring stiffness is progressively decreased by an amount proportional to the Greenfield ground movement at that

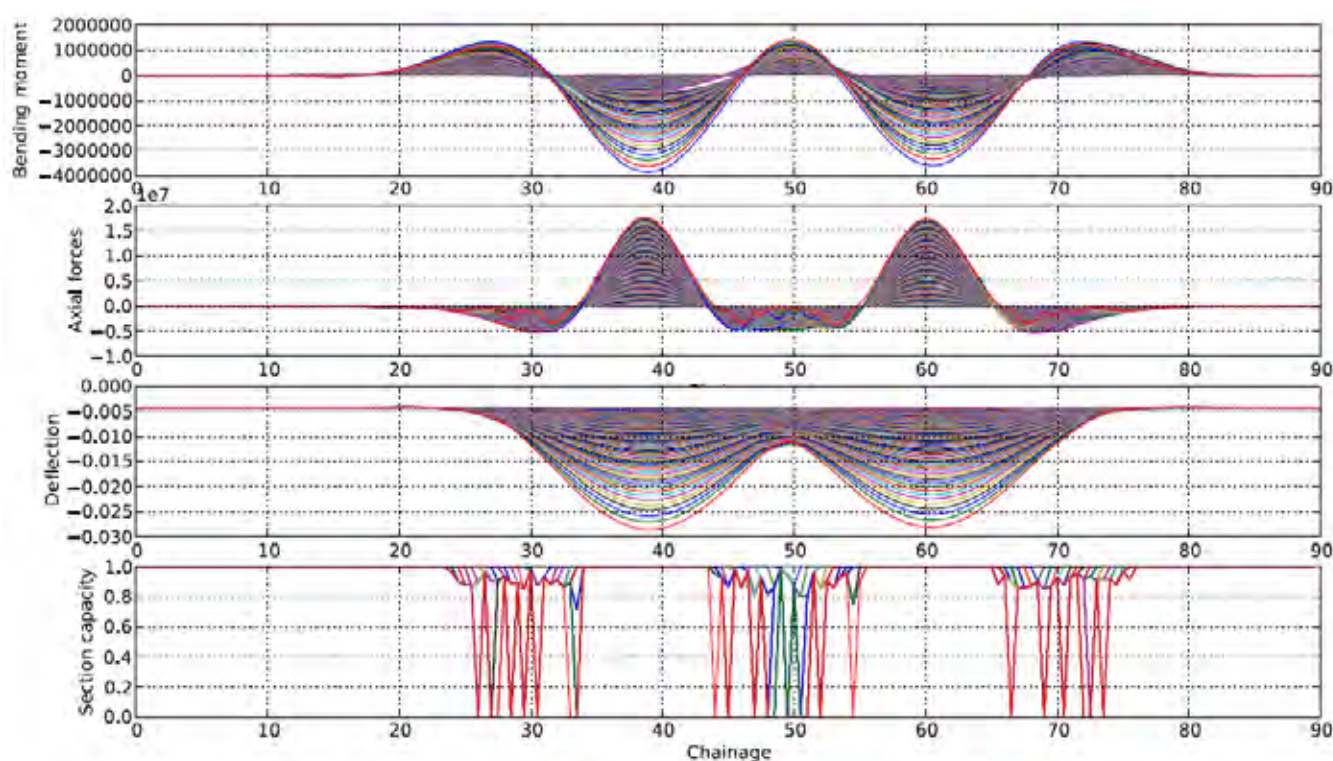


Figure 5. Results from beam-spring model which allows brittle cracking of the lining and a reduction in sectional capacity (from Python code)

location. The influence of the stiffness of an existing structure will reduce the deformation and flatten the resultant curvature in comparison to Greenfield ground movements (Figure 4).

This approach is based on assumptions of a monolithic beam distributing loads along the length of the tunnel. One of the challenges the authors have identified in using this approach has been modelling brittle tunnels where tension cracking will reduce the ability of the existing tunnel to span longitudinally over the settlement trough. To address this particular problem, a beam spring model which allows brittle cracking of the existing lining has been developed. This approach allows the tensile stress in the existing lining to reach a limiting value at which point the section gradually cracks, reducing the stiffness at this location (Figure 5).

Whilst the conventional approach to modelling materials such as masonry and unreinforced concrete is to allow no tension behaviour, this approach has some critical issues when being used in the assessment of existing tunnels. In particular, this implies that the tunnel has no longitudinal axial (tensile) force and consequently, no longitudinal bending strength at these locations. The lack of bending strength results in a more flexible tunnel which closely follows the 'greenfield' settlement trough, with no enhanced longitudinal spanning capacity as well as having a large number of small width cracks. In some cases neither of these consequences follows observed behaviour, and may, therefore, not be conservative for the assessment, so the conventional assumption of no tension may not be appropriate for some assessments.

One of the consequences of the beam-spring model which accounts for cracking of the material is that as the cracks develop they become 'strain concentrators', as seen in Figure 5. As sections of the tunnel become more flexible where cracks occur, an increased settlement induced movement is concentrated at these locations. The implications of this can be significant to the assessment, such as the development of heavily damaged sections adjacent to relatively unaffected regions, resulting in larger crack widths than might normally have been predicted. In some circumstances, the model predicts that rapid destruction of the structure through cracking can occur for relatively small changes in ground movement.

One approach to mitigate the build up of longitudinal strains along an existing tunnel is to create circumferential

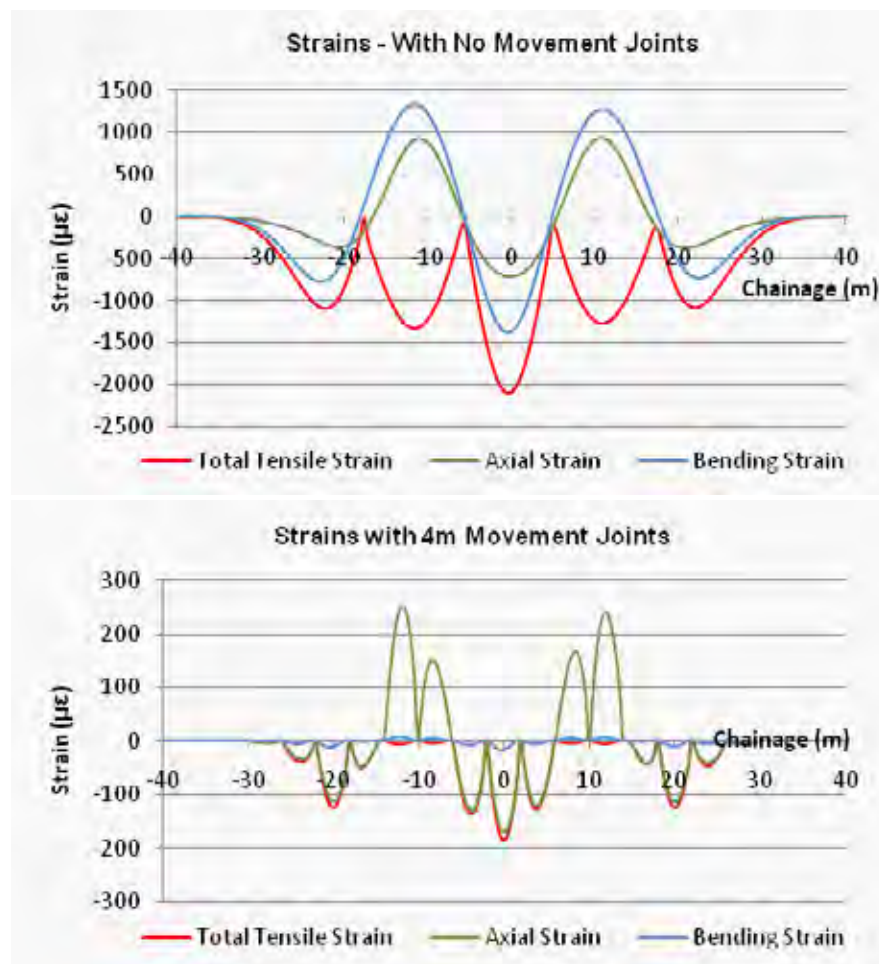


Figure 6. Comparison of results – tensile strains with and without engineered movement joints (from MS Excel)

movement joints prior to commencement of tunnelling works. This approach articulates the existing tunnel into short segments, and localises ground movement and rotation at engineered locations along the length of the existing tunnel. Strains are therefore more evenly distributed than if uncontrolled cracking behaviour was allowed to occur (Figure 6).

The creation of engineered movement joints will involve cutting or the removal of longitudinal bolts in segmental linings, or saw cutting through brickwork in masonry tunnels. A flexible liner and/or elastic joint filler can be used to maintain the water tightness of the structure if required. This approach does, however, have to be treated with caution, because the introduction of movement joints increases the flexibility of the tunnel. In some circumstances the original tunnel may have sufficient strength to avoid localised failure of the lining under longitudinal bending and so would have suffered little, if any, damage prior to the introduction of flexible elements. The introduction of the movement

joints would significantly increase the flexibility of the tunnel resulting in more movements, with the movement being localised at the movement joints. A careful risk based assessment is therefore needed to consider the best approach for protecting the existing tunnel.

The transverse effect: effects of ground movements on the cross section of the existing tunnel

Having considered the longitudinal effects in the previous section, the other main consequence of tunnelling-induced ground movements on the structural response of the tunnel is the transverse structural behaviour of the existing tunnel. This section sets out to discuss the potential effects of the cross sectional behaviour of the existing tunnel.

Case history information on the movements of the existing tunnel in the cross-sectional direction is less common than for the longitudinal movement.

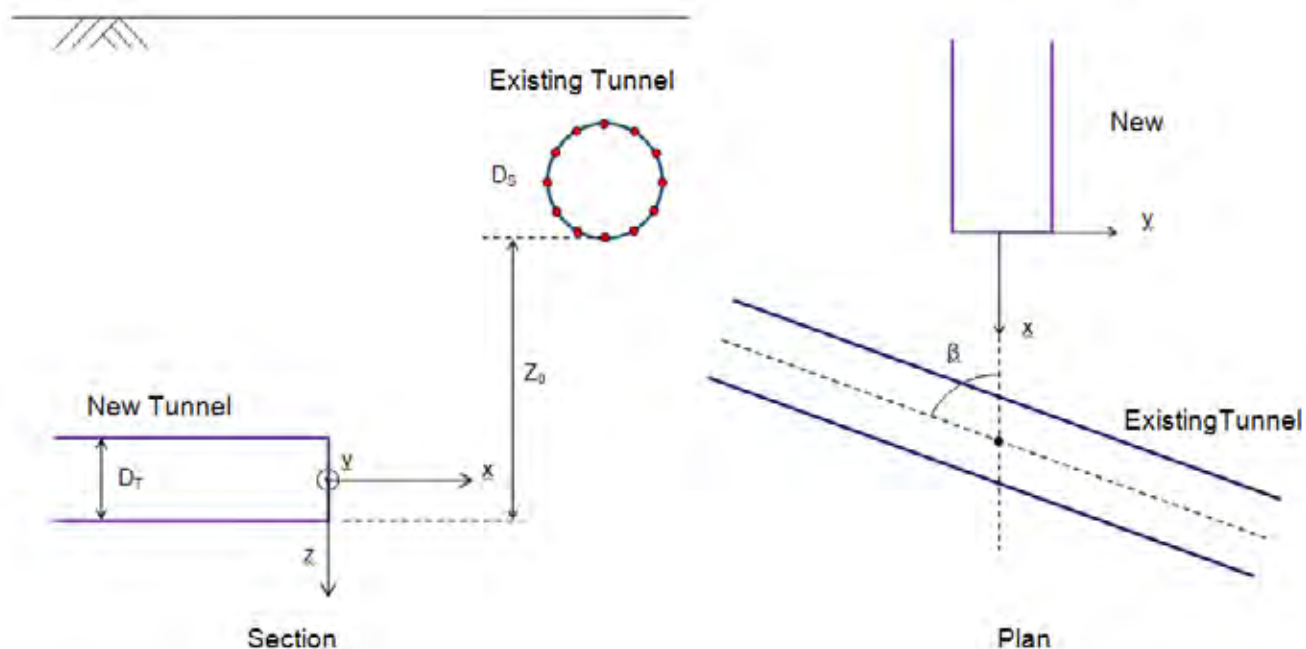


Figure 7. Simple geometric approach to cross-sectional analysis caused by tunnelling

The case histories do, however, give reasonably consistent indications that provided the tunnel is sufficiently flexible, the tunnel movements can be predicted based on the 'greenfield' movement assumptions.

The key issue to take into account with the transverse effect is that a large part of the effect occurs due to the movement of the ground around the tunnel face. Analytically, ground movements around the tunnel face are typically assumed to take the form of an S-curve defined by the cumulative normal distribution¹. Broadly speaking, based on this assumption, points in the ground tend to move towards the source of the ground movements and points closer to the source of the movement tend to move more than points further away from the source of the ground movement.

To give a complete assessment of these effects, a number of different positions for the source of the settlement need to be considered in order to account for the transitory effect as ground movements develop. Similarly, the maximum distortion of the existing tunnel often does not occur on one of the principal axes, vertical and horizontal, but on an angle as the TBM face passes. A complete assessment therefore requires the distortion to be assessed in a more comprehensive, staged manner.

A simple approach to this problem is to undertake the ground movement prediction at a number of evenly spaced points on the tunnel perimeter

at opposite ends of a tunnel diameter (**Figure 7**), to give a better understanding of the distortion in shape of the tunnel. This assessment also considers a number of different face locations for the new tunnel, giving a comprehensive assessment for the temporal changes to ground movements and consequently the shape of the existing tunnel as the new tunnel is driven beneath. Effects like skew and dip in alignment can also be considered in such an analysis.

When assessments are undertaken in this manner, some of the key effects that are observed include:

- The maximum distortion is not on the principal axes but is usually on a diagonal axis;
- The maximum distortion is temporal, with the maximum final distortion less than maximum measured distortion;
- The final distorted shape of the existing tunnel indicates that ovalisation rather than squat of the tunnel occurs, and the vertical diameter increases whilst the horizontal diameter decreases. Since most tunnels typically are more likely to be built with a vertical squat, the transverse settlement effects can be beneficial in the final condition.

Although these effects are consistent with observed behaviour such as the Piccadilly Line at Heathrow⁴, the assumption of a simple S-curve longitudinal settlement trough is, in many circumstances, a significant simplification. There are many documented cases where the longitudinal

settlement trough does not take the form of a smooth S-curve but a complex curve representing the different sources of ground movement around the face of a tunnel being constructed^{16,5,8}. So how does this non-linear behaviour affect the tunnel distortion predictions?

To assess this, a simple model has been developed to undertake assessments consistent with the approach proposed above, but where the tunnel settlement is modelled by multiple faces positioned one behind another with slightly different trough width parameters and volumes for each trough. This approach generates a complex trough in a way that makes the assessments consistent with those used for a simple S-curve trough.

As with the longitudinal effect, one issue that has to be addressed for the transverse effect is the tunnel stiffness. Whilst the approaches discussed above are appropriate for a flexible lining, if a stiff monolithic lining is considered, significant variance from the prediction could be encountered during construction. The same issues that apply to the longitudinal effect also apply to the transverse effect with respect to the stiffness of the existing tunnel. In particular:

- Stiff tunnels will provide more resistance to movement and so the simple application of the 'greenfield' ground movement predictions to a stiff tunnel will over predict the loads on the tunnel;

- Were failure to occur in a stiff, brittle tunnel, joints in the tunnel would act like strain concentrators and so additional movements, and potentially damage, would occur at these failure locations.

When the ground movement effect is being considered on a relatively stiff tunnel the 'greenfield' movements must therefore be converted to a quantitative value that will give a more credible prediction of the impact on the existing tunnel. Often the easiest way to do this is to modify the earth pressures acting on the tunnel. There are a number of ways to achieve this, for example a simple closed form solution of the stress changes in a circular tunnel in elastic ground¹¹. Having obtained the change in the loads, an assessment of the capacity of the existing tunnel to resist the additional loads due to tunnel movement can then be undertaken.

Conclusion

The ground movement effects on existing tunnels are clearly an important issue for future tunnelling, as an increasing number of urban tunnels are constructed with ever more tunnel crossings. A good understanding of the behaviour of these crossings is therefore essential to manage the risk to future construction.

The use of simple semi-empirical method for predicting the three dimensional ground displacements caused by tunnel construction is an essential tool for tunnel assessments. However, the limitations of these predictions should be recognised, whilst noting that they are fundamentally a subject of various influencing factors, and as such rely on databases from back analyses to give assessors reasonable input parameters for their assessment.

Ground movement prediction is closely related to structural performance and the interaction between the ground and the tunnel. This complexity means that normally conservative assumptions may not be appropriate and in some instances could even mask the most significant issues with particular tunnel crossings. In the assessment of the longitudinal structural behaviour of an existing tunnel, the principles of strain 'concentrators', formed naturally at points of weakness or through engineered joints are important in the understanding of the behaviour of an existing tunnel subjected to tunnel-induced ground movements. The transverse structural behaviour of an existing tunnel should be comprehensive to account for the most damaging effects which are often temporal and occur

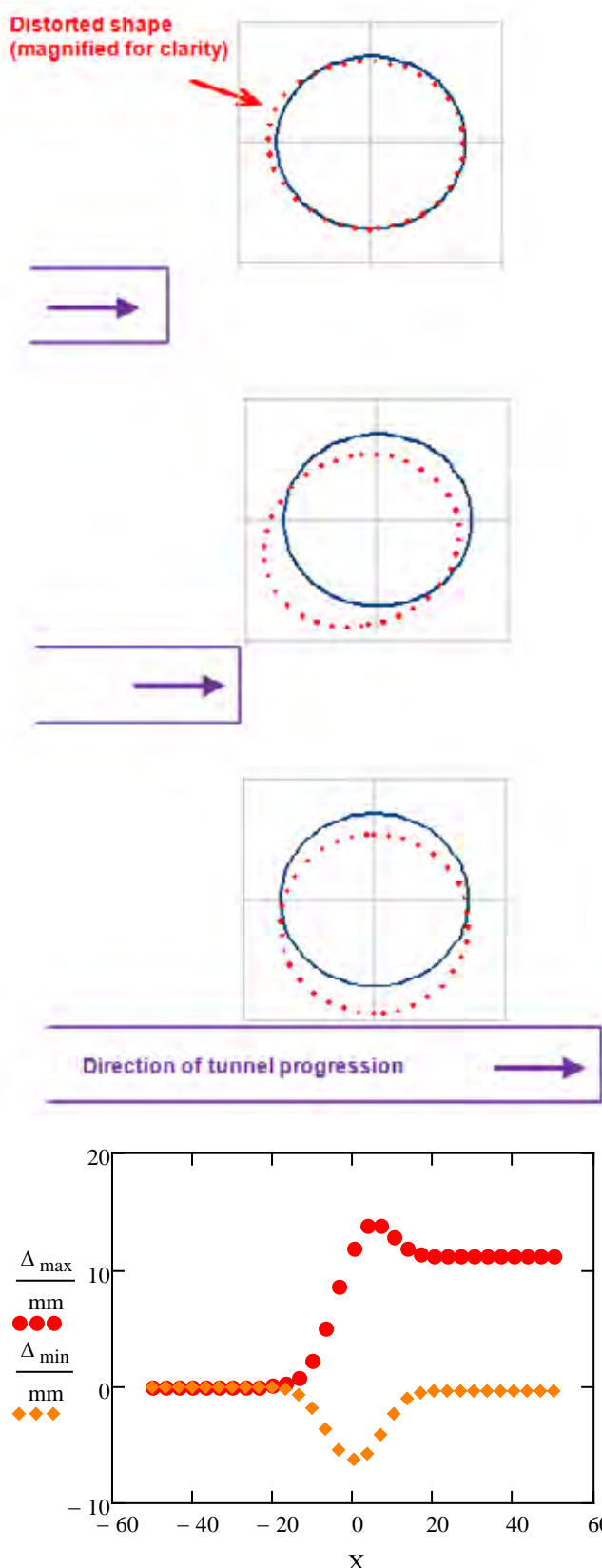


Figure 8. Distorted shape of existing tunnel as new tunnel progresses beneath. Maximum distortion is temporal and on a diagonal axis. (from MathCAD)

on a diagonal axis as the new tunnel is constructed.

The capacity of modern computing to do complex calculations quickly and easily can provide the tools to look into these complex interactions. This gives us the capability to undertake more reliable

predictions of the response of tunnels to movements as well as the ability to better manage the risk associated with these types of tunnel crossings.

References

1. Attewell, P. & Woodman, J.P., 1982. Predicting the dynamics of ground settlement and its derivatives caused by tunnelling in soil. *Ground engineering*, 15(8), pp.13 - 22.
2. Attewell, P., Yeates, J. & Selby, A.R., 1986. *Soil Movements Induced by Tunnelling and Their Effects on Pipelines and Structures*, London: Blackie and Son Ltd.
3. Cheung, L.L.K. et al., 2010. Optical fibre strain measurement for tunnel lining monitoring. *Proceedings of the ICE - Geotechnical Engineering*, 163(1), pp.1-1. Available at: <http://www.icevirtualibrary.com/content/article/10.1680/geng.2010.163.1.1>.
4. Cooper, M.L. et al., 2002. Movements in the Piccadilly Line tunnels due to the Heathrow Express construction. *Géotechnique*, 52(4), pp.243-257. Available at: <http://www.atypon-link.com/TELF/doi/abs/10.1680/geot.52.4.243.41019>.
5. Dimmock, P. & Mair, R.J., 2008. Effect of building stiffness on tunnelling-induced ground movement. *Tunnelling and Underground Space Technology*, 23(4), pp.438-450. Available at: <http://linkinghub.elsevier.com/retrieve/pii/S0886779807000922> [Accessed March 1, 2011].
6. Kim, S.-H., 1996. *Model testing and analysis of interactions between tunnels in clay*. University of Oxford.
7. Klar, A. et al., 2008. Tunnelling effects on jointed pipelines. *Canadian Geotechnical Journal*, 45(1), pp.131-139. Available at: <http://article.pubs.nrc-cnrc.gc.ca/ppv/RPViewDoc?issn=1208-6010&volume=45&issue=1&startPage=131&ab=y> [Accessed May 8, 2011].
8. Leca, E. & New, B.M., 2007. Settlements induced by tunnelling in Soft Ground. *Tunnelling and Underground Space Technology*, 22(2), pp.119-149. Available at: <http://linkinghub.elsevier.com/retrieve/pii/S0886779806001180> [Accessed February 26, 2011].
9. Mair, R.J., Taylor, R.N. & Bracegirdle, A., 1993. Subsurface settlement profiles above tunnels in clays. *Geotechnique*, 43(2), pp.315 - 320.
10. Mohamad, H. et al., 2010. Behaviour of an old masonry tunnel due to tunnelling-induced ground settlement. *Geotechnique*, 60(12), pp.927 - 938.
11. Morgan, D.H., 1971. A contribution to the analysis of stress in a circular tunnel. *Geotechnique*, 11(3), pp.37 - 46.
12. Moss, N.A. & Bowers, K.H., 2005. The effect of new tunnel construction under existing metro tunnels. In E. A. Kwast et al., eds. *Geotechnical Aspects of Underground Construction in Soft Ground*. Amsterdam: Taylor and Francis, pp. 151 - 157.
13. New, B.M. & Bowers, K., 1994. Ground movement model validation at the Heathrow Express trial tunnel. In *Tunnelling '94*. London.
14. O'Reilly, M.P. & New, B.M., 1982. Settlements above tunnel in the United Kingdom - their magnitude and prediction. In *Tunnelling '82*. pp. 173 - 181.
15. Rulu, W., Jiaping, L. & Jingya, Y., 2008. Analyses on the influence factors of metro tunnel deformation and its characteristic. In *ITA 2008*. pp. 1-9.
16. Sugiyama, T. et al., 1999. Observations of ground movements during tunnel construction by slurry shield method at the Docklands Light Railway Lewisham extension - East London. *Soils and Foundations*, 39(3), pp.99 - 112.



Luke Gorman

Senior Ecologist

Water & Environment

Atkins

Mineral extraction alongside great crested newts

Abstract

Stringent planning conditions for construction activities are putting ever more emphasis on the preservation and enhancement of biodiversity. This can often be viewed as a significant constraint to construction works but, if managed appropriately, need not be a costly exercise, nor should it delay or negatively affect a successful project outcome. Co-operation between a site operator and ecology experts has ensured that mineral extraction can continue at a quarry in Cheshire alongside a growing population of great crested newts. This paper discusses the the colonisation of an operational sand quarry by a population of great crested newts, a European Protected Species. The approach taken demonstrates that sites can be worked efficiently without adverse effects on great crested newt populations by engaging involvement of ecologists at an early stage in the project along with appropriate management, innovative mitigation measures, and a positive approach from the contractor.

Introduction

With current ecological legislation and stringent planning conditions putting ever more emphasis on the preservation and enhancement of biodiversity, mineral extraction sites are increasingly having to consider the implications on the natural environment of their work processes and restoration plans. This is often viewed as a significant constraint to works but, if managed appropriately, need not be a costly exercise, nor should it delay or negatively affect the mineral extraction process. Mineral extraction and the conservation of biodiversity often go hand in hand and appropriate management can protect the interests of the mineral extractor whilst also providing excellent opportunities for biodiversity enhancement.

This paper discusses the colonisation of an operational sand quarry by a population of great crested newts, a European Protected Species. It sets out the measures that were taken to allow the continuation of sand extraction at the site whilst also turning this potential ecological constraint into a positive factor that has enabled Tarmac to contribute towards local and national biodiversity targets.

Crown Farm Quarry

Atkins has been working as ecological consultants at Crown Farm Quarry, Sandiway, Cheshire since 2003. Crown Farm Quarry (see **Figure 1**) is a sand extraction quarry that is owned and operated by Tarmac, the largest quarrying company in the UK and now part of Anglo American. Tarmac currently has planning permission to continue extraction at the site until 2014.


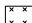

A number of ponds, pools and ditches have been created at Crown Farm Quarry as a result of historic quarrying activities. An unexpected rise in the water-table has also contributed to the formation of these waterbodies. The dynamic nature of mineral extraction sites often leads to the the creation of diverse habitats that provide excellent conditions for a range of species. Waterbodies created by mineral extraction often provide suitable aquatic habitat for amphibians and can provide habitat suitable for other species such as birds and invertebrates.

In 2003, great crested newts were discovered within some of these waterbodies in the operational part of Crown Farm Quarry following an Environmental Impact Assessment undertaken to support planning permission to extend mineral extraction

This drawing is based on the Biodiversity and Habitat Management Plan 2009 (5021100/1070/070/32682), Atkins, July 2009.

ATKINS

Legend

-  Site boundary
-  Semi-improved acid grassland
-  Semi-improved neutral grassland
-  Ephemeral (short-lived)
-  Open water
-  Scattered scrub
-  Broadleaved plantation woodland
-  Mixed plantation woodland
-  Marshy grassland
-  Native species rich hedge
-  Tall ruderal (tall plants such as nettles)
-  Bare ground
-  Inundation vegetation
-  Arable land
-  Improved grassland
-  Quarry

CROWN FARM QUARRY
CHESHIRE

BIODIVERSITY AND
HABITAT MANAGEMENT
PLAN 2009

Drawing Number
5021100/1070/070/32682

Original Scale
Not to Scale



Figure 1. Plan

at the site. Great crested newts are very mobile and will colonise new sites that provide suitable conditions.

Innovative mitigation for great crested newts in conjunction with mineral extraction

Great crested newts (see **Figure 2**) are a European Protected Species and subject to full legal protection in respect of the animals and their habitats. Therefore, once their presence on site was confirmed, it was necessary to make an application for a development licence to Natural England in order to allow the continuation of mineral extraction at the site. Such licences permit works to be undertaken in accordance with a method statement which is agreed by both the ecological consultant (in this case, Atkins), the developer (Tarmac) and Natural England. These method statements detail methods of working that must be adhered to in order to protect individual great crested newts and their habitats.

The great crested newt population at Crown Farm Quarry was found to be small but widespread in part of the site that had already been quarried and restored and was adjacent to the mineral processing area. Conventional approaches to great crested newt mitigation usually result in the use of long stretches of temporary or permanent newt exclusion fencing which requires constant inspection and maintenance so as to guarantee its integrity as a barrier to the movement of newts. It would have been extremely difficult to have segregated working areas with no newts from non-working areas with newts, by means of newt exclusion fencing, for four main reasons:

1. First, for the fencing to be effective in protecting newts, its location would have significantly disrupted quarry operations.
2. Secondly, the distribution of newts within Crown Farm Quarry and the intricacies of the quarry workings, with trackways, crossing channels and storage areas lying adjacent to breeding pools for the newts,

together with fluctuating water levels and the extent of standing water, would have raised serious issues in respect of maintaining the integrity of the newt fences in such circumstances.

3. Thirdly, the use of newt exclusion fencing would have isolated the newt population within the site and reduced dispersal opportunities which could have negatively affected the conservation status of the great crested newt population at the site.
4. Finally, the cost of extensive newt fencing would have been substantial.

An innovative approach to mitigation for newts needed to be devised which would resolve these constraints. Therefore Atkins had to devise a strategy that avoided the use of newt exclusion fencing yet would still prevent incidental injury or fatality to newts and prevent disturbance to their habitat whilst allowing great crested newts to disperse freely across the site and outside the site boundary.

No mineral extraction or other quarrying activities were expected within areas

providing the best quality terrestrial habitat for great crested newts and vehicles already utilised well established hard standing tracks which are inhospitable to great crested newts. In addition to this, it was clear that a great crested newt population had naturally established itself on an operational mineral quarry and it could be concluded that the ongoing works were not having a negative impact on the great crested newt population.

A great crested newt licence was obtained on the premise that areas of existing good quality terrestrial and aquatic habitat for great crested newts would be protected, hand searches for great crested newts would be carried out whenever work processes required the disturbance of suitable terrestrial habitats for amphibians. New refuges for great crested newts would be created and one member of the Tarmac site staff would

be trained to deal with any great crested newts found on site. The approach protected the most suitable great crested newt habitats at the quarry and enabled the efficient relocation of any newts found within work areas to a newly created refuge areas.

Tarmac has implemented habitat improvement measures devised by Atkins to help ensure that the great crested newt population on site is maintained. This included the creation of two terrestrial refuges for great crested newts near to existing breeding ponds using discarded rubble within the site. The refuges were created by site operatives under the supervision of an ecologist, the refuges consisted of mounds of loose rubble covered with soil and only took a couple of hours to construct. There were no cost implications in creating these refuges which provide additional, and safe, great crested newt terrestrial habitat that can be utilised for shelter and for hibernation over winter, whilst reducing the need for great crested newts to disperse across the quarry and into operational zones.



Figure 2. Great crested newts at Crown Farm Quarry



Figure 3. Ditch restoration work at Crown Farm Quarry

Expansion of the great crested newt population

A condition of the licence is that a survey to monitor the population of great crested newts is required every two years to ensure that the mitigation measures are working effectively and the population is not being negatively affected by the ongoing quarrying activities. The maximum length of the development licence at Crown Farm Quarry is limited to two years and the results of the great crested newt population surveys need to be submitted to Natural England in order to support applications for extensions to the licence.

Great crested newt population size class assessments were undertaken at Crown Farm Quarry during 2003, 2005, 2007, 2009 and 2011. These assessments provide an insight into the changing dynamics of the great crested newt population during this time both in response to mitigation measures, protecting them at site level and also to the natural succession of vegetation in the waterbodies which has reduced the suitability of some of the waterbodies for breeding great crested newts whilst improving the suitability of others.

The 2003 survey indicated that a small population of great crested newts was present at the site. Following the mitigation works described above, a survey in 2005 showed that the small

population was being maintained and further surveys in 2007 and 2009 indicated that a medium sized population of great crested newts was present. The 2011 survey recorded a substantially larger population than any of the previous surveys, which would be classified as a large sized population by Natural England. It is therefore considered likely that the population of great crested newts at Crown Farm Quarry is expanding.

Contributing towards Biodiversity Action Plan targets

The population assessments at Crown Farm Quarry showed that the great crested newt population is being maintained and may be expanding. The expansion of great crested newts contributes towards both national and local (Cheshire) Biodiversity Action Plan (BAP) targets which aim to ensure that there are no losses to the post 1990 range of great crested newts, increase the number of ponds suitable for great crested newts, increase the number of ponds occupied by great crested newts and to achieve an increase in the range of great crested newts. In order to continue Tarmac's contribution towards BAP targets, Atkins and Tarmac are committed to ongoing habitat improvements in the non operational areas of Crown Farm Quarry for great crested newts and biodiversity in general.

In the winter of 2009 Tarmac restored the first waterbody at Crown Farm Quarry, a linear ditch which provided important breeding habitat and an important link between great crested newt breeding ponds in the north and south of the site. Over the years, this ditch had become choked with bulrush and areas had dried out. The restoration of this ditch was undertaken during winter to reduce the chance of great crested newts being present within the ditch (great crested newts generally hibernate in terrestrial habitats). An onsite mini-digger was used to remove bulrush and to restore dry areas to open water, see **Figure 3**. This work was undertaken within a day and created approximately 150m² additional aquatic breeding habitat for great crested newts whilst improving aquatic dispersal opportunities within the quarry. The cost was for fuel for the mini-digger and the time of one site operative to man the machine.

Such relatively simple habitat management shows how meeting biodiversity targets and managing habitat for protected species need not be costly or time consuming. In fact, it is extremely easy to work these improvement measures into the day to day running of the quarry. Tarmac aim to restore or improve at least one waterbody within Crown Farm Quarry each year in order to maintain the great crested newt population on site and meet biodiversity targets.

From potential constraint to success

When great crested newts are present on a site, planners and quarry operators often face difficulties at the planning stage of extraction operations. The issue is demonstrating that the site can be worked efficiently without adverse effects on the great crested newt population and that enhancements promised at the application stage can be delivered. The discovery of a widespread population of great crested newts at Crown Farm Quarry could have been a major constraint to the operators at this mineral extraction site. However, with early involvement of ecologists, appropriate management, innovative mitigation measures, and a positive approach by Tarmac, this potential constraint has become a success story. Tarmac and Atkins have managed to allow operations at Crown Farm Quarry to continue without any delay to extraction operations. The aquatic and terrestrial habitats for great crested newts on site have been greatly improved whilst allowing the expansion of the great crested newt population with minimum expenditure, enabling Tarmac to contribute towards local and national BAP targets.



Alex Yescas

Senior Water
Resources Engineer

Atkins North America

Bank stabilization by redirective structures on the Santa Clara River, Ventura County, CA

Abstract

The Santa Clara River is one of the largest river systems (and the largest free flowing) in southern California. It flows approximately 100 miles from its headwater at Pacifico Mountain in the San Gabriel Mountains to the Pacific Ocean. In January 2005, a flood that was close to the 50-year flood event (136,000cfs at the Montalvo gage) occurred and severely eroded portions of the Santa Clara River downstream of Highway 101. The streambank in this area protects an existing golf course that was built on a landfill.

A series of measures has been implemented over the past 50 years at this location to protect the bank from erosion. Measures include rock bank protection, rock groins, and grouted rock groins confined with steel sheetpile cutoffs. Each of these measures, with the exception of the most upstream rock groin, the two most downstream rock groins, and the rock groins with steel sheet pile cutoffs, has succumbed to scour or has sunk into the riverbed. To prevent further erosion of the southern bank of the Santa Clara River and to stabilize the area to improve riparian habitat, the design team developed a concept to construct four bendway weirs and rock riprap slope protection that would function as a system with the existing groins. The bendway weirs are designed to redirect the impinging flow away from the bank of the river and guide it along the bend. This design will help encourage sediment deposits and promote riparian habitat for local fish and wildlife along the bank of the river between the bendway weirs. In addition, the bendway weir tips are designed to scour and create a self-sustaining pilot channel to train the river to migrate away from the bank of the river.

The design entailed analysis and evaluation of the hydraulics of the river for the 100-year event discharge of 226,000cfs as well as the determination of bendway weir overtopping flow conditions. Because the river and its banks are highly susceptible to scour, scour analysis was conducted to determine the magnitude of scour at the bendway weir tips and along the toe of the bank. In addition, secondary scour evaluations were conducted to determine the scour potential within the bendway weir field.

Introduction

The Santa Clara River is a challenging river to control. Instead of controlling the river, we have to be able work with the river. Throughout the years, the river has been very destructive causing hundreds of millions of dollars in damage. The Ventura County Watershed Protection District (VCWPD) selected Atkins to prepare a preliminary report to identify alternatives for a location on the Santa Clara River that continuously suffers from bank slope failure. **Table 1** summarises major repairs that have been carried out at the project site and **Figure 1** of the typical toe scour occurring along the bank.

The primary reason that the site is susceptible to scour are the encroachments of river that have taken place over the years. **Figure 2** displays the 1945 active flood channel in red and flood terrace in yellow. The blue line corresponds to an existing access road as reference to the current site.

Figure 3 displays the current alignment and containment of the river. The blue line displayed is now the active flood channel and flood terrace. The flood channel has been encroached on by several hundred feet and the flood terrace by several thousand feet. This encroachment causes an increase in flow velocity and an increase of the impingement forces along the bank of the river.

The primary cause of concern at the project site is that the river bank is adjacent to a decommissioned landfill. Further scour of the bank could lead to having the landfill leachates enter into the river causing major water quality fines to be given to the District. **Figure 4** displays the landfill boundary in red, the river is just north of the boundary.

A secondary cause of concern at the site, the section just upstream is a levee protecting the City of Oxnard, California, shown in **Figure 5**. The levee was not certified by the Federal Emergency Management Agency to provide adequate level of protection from the 100-year flood event due to toe scour evidence along the bank of the river.

Considering the major concerns at the project site, the District selected Atkins based on the experience from the experience from team and previous emergency scour protection work completed by Atkins for Ventura County. Atkins was awarded the complete engineering design report, development of design drawings and specifications, preparation of the environmental

Year	Flow (cfs)	Damages	Repairs
1969	165,000	Bank erosion	Levee repair
1978	102,200	Bank scour	½-ton rock slope protection
1980	81,400	Bank and toe scour	Toe repair and add 2-ton rock groin in 1982
1983	100,000	Bank and toe scour	Repair scour damage and protect with ½-ton rock
1992	104,000	Non documented	Construct 6 additional 2-ton rock groins
1998	84,000	Loss of 80% of 5 groins	Initiate design to repair damaged groins
2005	136,000	Additional groin loss	Construct 3 emergency groins in 2006

Table 1. Project site repair history



Figure 1. Typical toe scour along bank

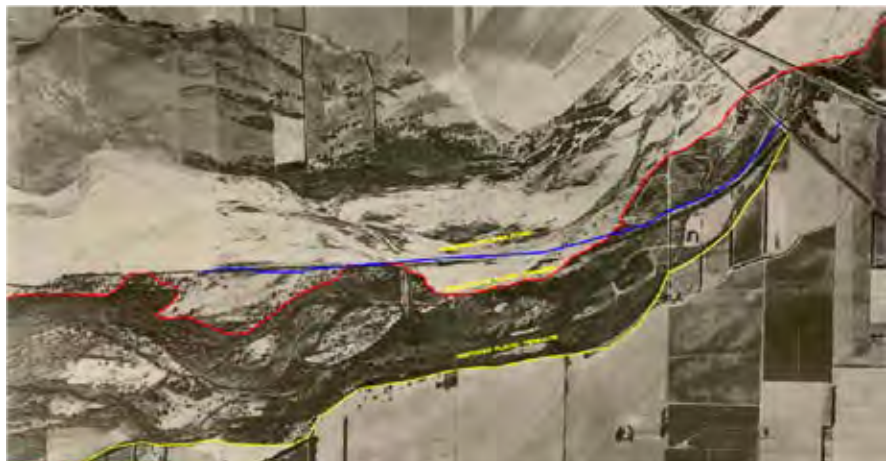


Figure 2. Santa Clara River 1945



Figure 3. Santa Clara River 2007



Figure 4. Decommissioned landfill boundary



Figure 5. Santa Clara River levee

documentation, and to provide construction support.

The objective for the project was to design a long-term innovative solution for the protection of the river bank. The design must complement the environmental surroundings and enhance the river to promote riparian habitat for local fish and wildlife. The construction of the project was scheduled out to fall outside the breeding and migrating seasons for certain wildlife.

The purpose of this paper is to present a guideline and steps recommended to carry out a successful project that identifies potential alternatives for a project and display the details to design a innovative project to resolve a long standing issue.

Design alternatives for extension of bank protection

The VCWPD Zone 2 matrix categories were reviewed to determine the most effective method to prevent further scouring of the bank. The matrix comprises four categories: effectiveness, cost, environmental, and community impacts. The matrix is developed by weighted averages and rankings. The scoring for each section under the categories ranges from 0 (least favorable) to 10 (most favorable). Effectiveness is weighted at 45%, cost at 30%, environmental at 20%, and community at 5%. The alternatives were pre-selected for review following a determination analysis of the existing conditions at the site in 2007. **Table 2** identifies the alternatives that were reviewed and scored by VCWPD and team members.

Alternatives
No project
Bendway weirs w/launching rock
Bendway weirs w/sheetpiles
Artificial armoring
Natural revetment
Longitudinal peak stone toe
Non-overtopping groins w/o sheetpiles

Table 2. Design alternatives

The evaluation matrix in **Table 3**, displays the scoring of each alternative. The no project alternative scored highest in the environmental category due to the

temporal preservation of a narrow band and erodible terrace of existing habitat susceptible to periodic erosion, it should be noted that over time stabilizing the area with bendway weirs will provide much wider band of permanent habitat resistant to erosion. With weighting, the highest ranked alternative was the bendway weirs with sheetpiles, with a score of 31.6. The bendway weirs with sheetpiles scored highly in the effectiveness category due to the potential to provide scour protection, re-direct, and train the river to migrate away from the bank towards the center of the river and was selected for the design.

Development of hec-ras hydraulic model with bendway weirs

The flood frequency discharges were obtained from the VCWPD Santa Clara River 2006 Hydrology Update. These discharges are shown in **Table 4**.

Recurrence interval	Discharge, cfs
5-year	41,900
10-year	72,800
50-year	172,000
100-year	226,000

Table 4. Flood frequency discharges

The following are assumptions that were made to develop the hydraulic models.

- The Manning's "n" coefficients were developed from composite sections. The composite sections are based from aerial imagery and field reconnaissance. The composite values ranged from 0.03 to 0.05; each cross section was analyzed uniquely;
- The downstream boundary condition was set at subcritical flow with a normal depth assumed from the river flow line slope of 0.0025;
- Multiple blocked ineffective flow areas were added to simulate gradually varied flow conditions for the 2 through 100-year flows. This was done to minimize the variations in velocities and depths along the reach;
- Four cross sections were added to model each bendway weir. Two natural cross sections at the immediate upstream and downstream limits and two with blocked obstructions representing the actual bendway weir;
- One cross section was placed in between the bendway weirs.

The hydraulic cross sections for the bendway weirs, as identified above, were placed upstream and downstream for each bendway weir. This allowed for a more accurate representation of the depth of flows and velocities within

the bendway weir flow field. The 5-year discharge caused the greatest change in flow conditions since it is approximately the bankfull discharge.

Toe scour potential for the bendway weirs

The total potential scour depth at the bendway weirs includes long-term degradation of the riverbed, general scour and local scour. Evidence of long-term degradation within the channel and at the Highway 101 and Victoria Avenue bridges was not observed during the site investigation and is not included in the scour computations. This is a valid assumption because the downstream boundary is very close to the Pacific Ocean.

General scour generally consists of contraction and bend scour for the design flood event. The bendway weirs are designed to be overtopped for the 5 through 100-year flows and do not present a significant obstruction to the 100-year flow. The channel flow area for these flowrates changes by less than three percent therefore, contraction scour is negligible and was not included. The bendway weirs divert flow away from the bend in the main channel and bend scour does not contribute to the total scour at the bendway weir.

The primary local scour component is toe scour at the tips of the bendway weirs. An exact method for determining scour depth at the toe of the bendway weir does not exist but it can be estimated using the toe-scour estimate method for rock weirs from Appendix N, Fish Passage Design for Road Crossings, California Department of Transportation, May 2007² and bridge abutment scour equations from the FHWA Hydraulic Engineering Circular No. 18⁴. The rock weir toe scour equation is empirical and was developed from laboratory and field data. The equations used in estimating scour depth for this method are given below

$$y_s = D_{xmb} - D_{mnc}$$

$$D_{xmb} = 1.14 D_{mnc} \left[1.72 + \left(0.0084 \frac{W}{D_{mnc}} \right) \right] \quad (1)$$

where y_s is the scour depth; D_{mnc} is the mean channel depth upstream of the bendway weir in feet. W is the channel water surface width upstream of the bendway weir, in feet, and D_{xmb} is the maximum water depth at the bendway weir, in feet. The values of W and D_{mnc} were obtained from the HEC-RAS model.

Evaluation matrix	Effect.	Cost	Environ.	Commun.	Weight	Rank
Alternative	Subtotal	Subtotal	Subtotal	Subtotal	Total weighted	
No Project	0	60	30	3	25.0	4
Bendway Weir w/launching rock	23	38	15	10	25.8	2
Bendway Weir w/sheetpiles	28	48	18	10	31.6	1
Artificial Armoring	9	38	14	8	19.3	7
Natural revetment	3	47	28	13	22.1	6
Longitudinal Peak Stone Toe	12	41	22	8	23.1	5
Non-Overtopping Groins w/o sheetpiles	20	41	15	10	25.3	3

Table 3. Evaluation matrix

The active channel (effective) top width was used to estimate W and the channel hydraulic depth was used for D_{mnc} .

Table 5 displays the variables and scour depths for the 100-year flood event. The computed scour depths range from 25 to 28 feet.

The Froehlich⁶ and HIRE⁷ live-bed equations are generally used to estimate abutment scour at bridges and abutment ends are analogous to the tips of the bendway weirs. The FHWA HEC-18 manual recommends both equations for clear-water scour as well. The Froehlich equation is valid when the ratio of the abutment length (L) to the flow depth (y_1) is less than 25 and HIRE when the ratio is greater than 25. The bendway weir length is used for L and the flow depth at the bendway weir for y_1 . The Froehlich equation is given below

$$\frac{y_b}{y_a} = 2.27 K_1 K_2 \left(\frac{L}{y_a} \right)^{0.43} Fr^{0.61} + 1 \quad (2)$$

where K_1 is the coefficient for abutment shape, K_2 is the coefficient for skew, A_e is the obstructed flow area, y_a is the average depth of the obstructed flow (A_e/L), Q_e is the flow obstructed by the bendway weir, V_e is the average velocity of the obstructed flow (Q_e/A_e), and Fr is the Froude number of the obstructed flow ($V_e/\sqrt{gy_a}$).

The spill-through abutment shape factor of 0.55 was used for all bendway weirs since they will be slanted, not vertical. The skew angle to the flow was assumed to be zero, resulting in a skew coefficient of 1 for all bendway weirs. Since the bendway weirs are overtopped for the 5 through 100-year events, the obstructed flow area (A_e) is just the area of the bendway weir (length multiplied by height), which remains constant for all flows. Therefore, y_a (A_e/L), which is equivalent to the height of the bendway weir, also remains constant for all flows. The flow obstructed by the bendway weir (Q_e) was estimated using the flow distribution option in HEC-RAS to compute the difference in the flow just upstream and at the bendway weir. **Table 6** displays the inputs and computed scour depths for each of the bendway weirs. The 100-year scour depths range from 27 to 35 feet.

The scour depths computed by the Caltrans method and the Froehlich equation are close. We took the larger scour depth and used that value for the design. For a scour depth safety factor, an additional 1-foot was added to the rounded scour depth value.

	W (ft)	D_{mnc} (ft)	D_{ymb} (ft)	y_s (ft)
Bendway weir 1	761.5	21.6	49.7	28.1
Bendway weir 2	737.5	21.0	48.2	27.2
Bendway weir 3	660.4	21.5	48.5	27.0
Bendway weir 4	606.2	20.7	46.5	25.7

Table 5. Caltrans rock weir toe scour results

Storm event	Q_e (cfs)	V_e (ft/s)	Fr	y_s (ft)
Bendway weir 1	9531	12.2	0.94	31.8
Bendway weir 2	7769	12.4	0.98	29.6
Bendway weir 3	10395	17.7	1.44	34.7
Bendway weir 4	6490	12.6	1.07	27.7

Table 6. Froehlich's live-bed abutment scour results

Bendway weir scour protection and design

The protection of the bendway weirs from scour was necessary for depths of scour greater than 30 feet. Sheetpiles provide a sound solution for the protection of the bendway weirs and have fewer temporary and permanent impact areas when compared to the other viable alternatives. By using sheet piles for scour protection an additional step for construction is eliminated. Typically in order to excavate in the river, the contractor would need to control the groundwater and it is common for contractors to place sheetpiles to control the groundwater and pump out the water, similar to a cofferdam. Once the pumping is done and the site is constructed, the contractor removes the sheetpiles. For this project, the contractor would leave the sheetpiles in place, eliminating the step to remove them.

Based on the design and soil parameters, a sheetpile with a PZC 13 section would be adequate for the protection of the bendway weirs (refer to **Figure 6** for PZC 13 typical section). The sheetpiles were analyzed utilizing the varying soil friction angles and scour depth potential at the tip and length of the bendway weirs. The bendway weir sheetpiles are designed to remain stable at maximum expected scour and impinging flow. The sheet piles along the tip of the bendway weirs will be driven to depths lower than the maximum expected scour depth and into a thick dense clay layer. The piles will be supported laterally utilizing tie

rods and wales along the length of the bendway weirs. The piles along the tip of the bendway weirs will be supported by intermediate piles that will help prevent the piles at the tip from rotating outwards during the maximum expected scour.

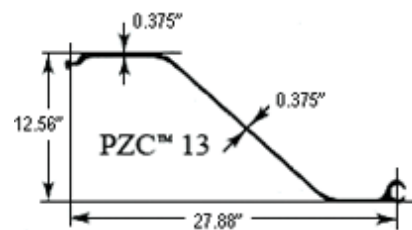


Figure 6. PZC 13 typical section

The scour depth along the length of the bendway weir (body) is in the range of 20 feet. This depth is estimated based on the scour potential for the non-cohesive soil depth to 20 feet. The bendway weirs will experience vertical (helical) flows, causing scour at the upstream and downstream face of the bendway weirs. Thus, for a scour depth of 20 feet, we chose a pile embedment depth of 25 feet along the bendway weir body to have an embedment depth of 5 feet at maximum scour. At the end of the bendway weir (tip), the depths of scour are greater than 30 feet as described above. From these values, along with the hydraulics analysis, we developed the dimensions of the bendway weirs following the FHWA Hydraulic Engineering Circular 235 and USACE guidelines⁹.

For the design dimensions of the bendway weirs, we analyzed the mean peak water surface elevations for the

Bendway weir	Crest height, riverside (ft)	Crest height, bankside (ft)	Plan view length (ft)	Plan view spacing (ft)	Key length (ft)	Top width at crest (ft)
1	5.2	8.2	150	345	43	10
2	5.0	7.5	125	360	43	12
3	4.7	7.2	125	363	38	14
4	4.3	6.7	120	-	36	14

Table 7. Bendway weir dimensions

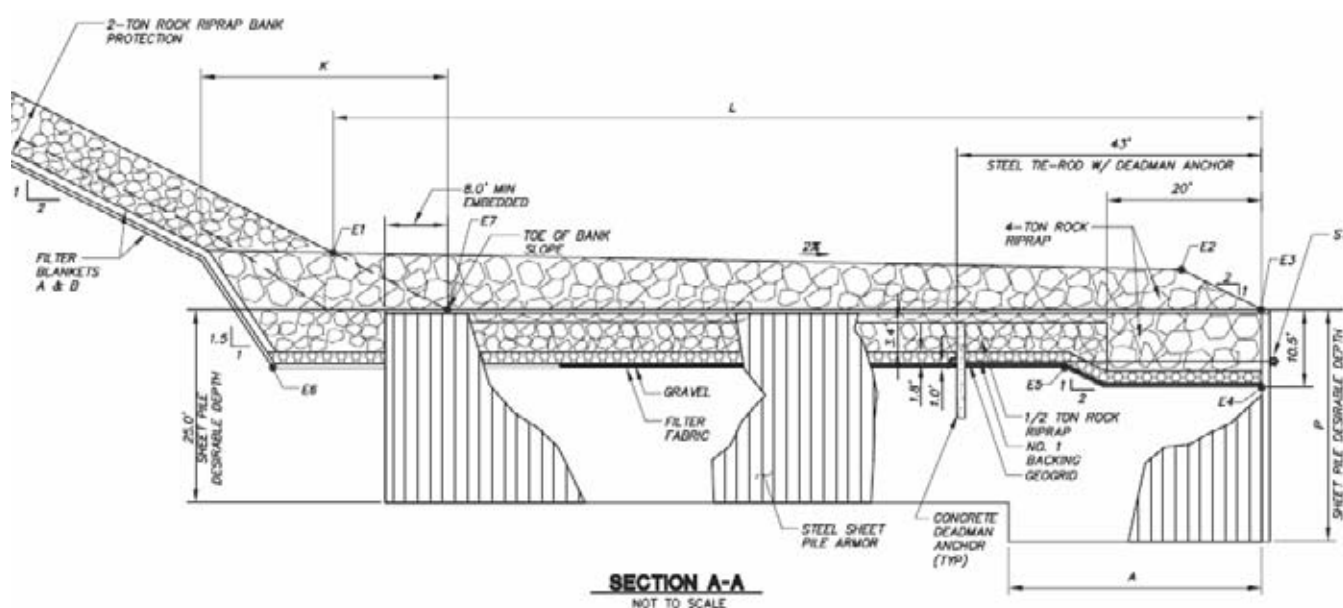


Figure 7. Bendway weir typical section

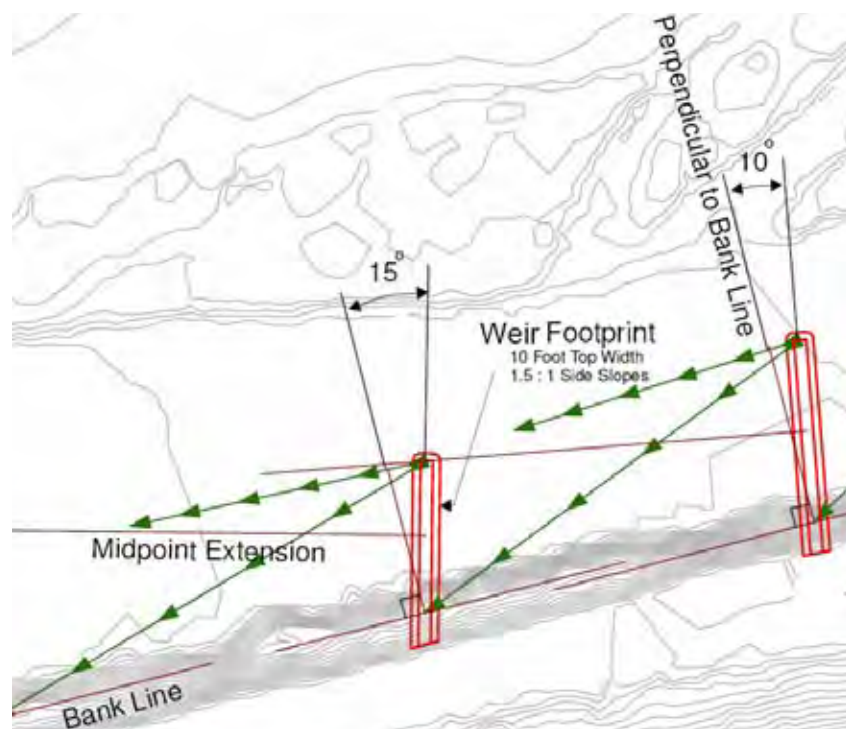


Figure 8. Bendway weir planimetric flow lines

Santa Clara River. The mean peak volume discharge for this section of the Santa Clara River is approximately 28,000cfs. For the design of the bendway weir dimensions, the Santa Clara River 5-year storm event of 41,900cfs was selected.

Refer to **Table 7** for bendway weir dimensions and **Figure 7** for a bendway weir typical section.

In addition to the dimension of the bendway weirs, skew angles are assigned. The angles are important to reduce the impinging flow at the bank by redirecting the flow away from the bank. Since the bendway weirs will be part of an existing system, we laid out the bendway weirs with all existing structures in place. The planimetric flow lines for each structure were drawn out. The flow is projected perpendicularly from the mid-point of each structure. Based on HEC-23 guidelines, the bendway weirs were placed at the tips to intercept the flow projections from the midpoint of the upstream structures. Each bendway weir was laid out until the flow projections appeared perpendicular to the bank

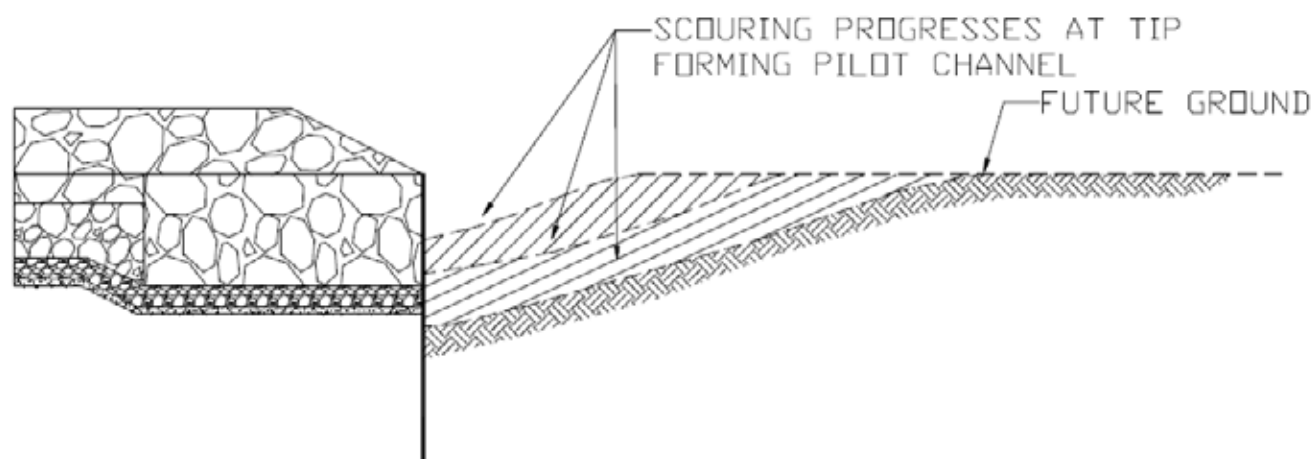


Figure 9. Estimated progression of scour



Figure 10. Upstream progression of scour



Figure 11. Upstream progression of scour

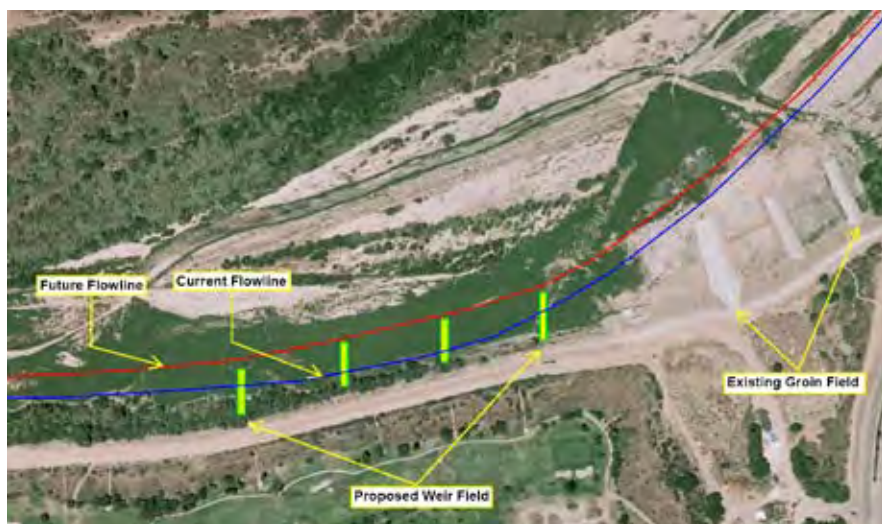


Figure 12. Bendway weir future flow line

line (refer to **Figure 8** for an example of the flow).

The tips of the weirs are meant to scour. The purpose of this is to develop a pilot channel to train the river flow away from the bank of the river. The depth of scour has been accounted for by placing the sheetpiles lower than the anticipated depth of scour, **Figures 9–11** display example of a pilot channel development.

Additional scour protection requirements

The existing bank slope protection was constructed in 1979. Currently, the bank slope is lined with 3-foot thick, ½-ton rock riprap. The design parameters utilized in 1979 for the existing bank slope protection would be insufficient for the current hydrology. In 2006, the Santa Clara River hydrology was updated, increasing the volumes of the hydrology

by 11% from a detailed hydrology study conducted in 1994. Since 1979, there have been five large peak events with three of the events over 100,000cfs. The conditions of the existing bank slope protection through the bend are unknown.

In order to protect the bank from further scour, we anticipate placing rock riprap along the slope utilizing staggered 1ton and 2ton rock riprap over granular filter blankets. We proposed 5.4feet thick 2ton rock riprap and 4.3feet thick 1ton rock riprap bank slope protection. The 1ton rock will be placed above the height of the 2ton rock. The proposed bank slope protection is designed to protect up to a 100-year storm event.

The length of improvements along the bank is critical. This segment will protect the bank slope from erosion and prevent leachates from the decommissioned landfill to enter the river. The bendway weirs are designed to be overtopped during high storm events. And alone, will not protect the bank slope from erosion. Once the depth of flow is greater than the height of the bendway weirs at the bank, the bank slope will scour without adequate protection. The bendway weirs are designed to train the thalweg (the line defining the lowest points along the length of a river bed) of the river to flow away from the bank of the river, see **Figure 12**. This is most effective during smaller flood events.

The bendway weirs are meant to be overtopped for moderate flows. The overtopping allows the thalweg to begin

adjusting laterally by scouring the tip of the bendway weirs. When a bendway weir is overtopped, it creates eddies and vortices on the downstream side. This is a natural occurrence due to the approach flow of water overtopping the bendway weir and dropping back down on the downstream side. This is considered secondary scouring effects. Protection against secondary scouring is a complex procedure.

There are no numerical or analytical widely accepted methods to determine the bank scour between the bendway weirs. To be conservative, the toe velocity along the bank was analyzed for each segment, without the bendway weirs present, to determine the magnitude of the toe scour. The flow velocity along the toe of the bank was calculated utilizing the HEC-RAS flow distribution option and determined to be in the range of 12 to 17 feet per second.

The velocity along the toe was utilized to determine the bend scour (toe scour depth) along the bank and to properly size the riprap along the bank slope. The bend scour potential was determined utilizing both the Maynard Bend Scour equation² and the Zeller General Scour⁸. Both of these methods use the inputs of the velocity, bend radius of curvature, and flow top width. The larger of the two results was taken. The bend scour potential along the toe of the bank was calculated to be in the range of 7 feet and 12 feet.

For the design, we elected to use 12 feet plus an additional 2 feet for added

safety in the event the bank toe would be exposed during a large storm event, for a total of 14 feet. This added safety margin was considered prudent because the toe's failure could result in material from the decommissioned landfill being washed downstream. The rock riprap along the bank slope was designed utilizing both the USACE riprap method from EM 1110-2-1601⁹ and the FHWA HEC-11³ riprap method to compare results. These values resulted in a riprap size D50 (median sized rock) of 3.0 feet at the toe of the bank, which equates to a 2ton rock size.

Summary

A series of measures has been implemented over the past 50 years at this location to protect the bank from erosion. The design team has developed a method to help prevent further erosion to the bank by utilizing bendway weirs. Bendway weirs are not widely used in arid regions and this project would be one of the few constructed in Southern California. As mentioned earlier, the Santa Clara River is one of the largest rivers in Southern California. Our design does not fight the river, but redirect the energy of the river to prevent bank erosion.

There are four goals for the design; 1) train the river to migrate away from the bank utilizing bendway weirs, 2) provide protection to the bank slope, 3) increase sediment deposit within the project area, and 4) encourage the development of riparian habitat for fish and wildlife.

References

1. American Society of Civil Engineers course notes (2005), "Predicting Bed Scour for Toe Protection Design for Bank Stabilization Projects." Instructors: David T. Williams et al.
2. California Department of Transportation, (2007), Appendix N, Fish Passage Design for Road Crossings.
3. Federal Highway Administration Hydraulic Engineering Circular 11 (1989) Design of Riprap Revetment.
4. Federal Highway Administration Hydraulic Engineering Circular 18 (2001), Evaluating Scour at Bridges, 4th Edition.
5. Federal Highway Administration Hydraulic Engineering Circular 23 (2001), Bridge Scour and Stream Instability Countermeasures.
6. Froehlich, D.C. (1989), Local scour at bridge abutments: Hydraulic Engineering, in Proceedings of the 1989 National Conference on Hydraulic Engineering: New York, American Society of Civil Engineering.
7. Richardson, E.V., Simons, D.B., and Julien, P.Y., (1990), Highways in the river environment participant notebook: Federal Highway Administration, Publication FHWA-HI-90-016.
8. Simons Li & Associates (1985), "Design Manual for Engineering Analysis of Fluvial Systems" prepared for Arizona Department of Water Resources.
9. United States Army Corp of Engineers (1994), "Hydraulic Design of Flood Control Channels" EM 1110-2-1601.



Claire Wansbury

Principal Ecologist

Water & Environment

Atkins



Richard Jackson

Principal Sustainable
Development &
Regeneration Manager

Olympic Development
Agency

The Olympic Park – a Biodiversity Action Plan in action

Abstract

The preparation of the London 2012 Olympic Park site included land clearance across 246 hectares in East London. The authors explore how biodiversity, the diversity of wild plants and animals, is being taken into account in this project. Planning permission was granted in 2008, and a Biodiversity Action Plan (BAP) was produced for the Olympic Park in the same year. A scheme-specific BAP is not justified in many small development projects, but for the Olympic Park the BAP was critical to ensure commitments made in the project's Environmental Statement are delivered on the ground.

Examples of the measures to protect and create wildlife-rich habitat are given in this paper. Overall, an impressive list of habitats will be created, and the Park is one of the largest new urban parks created in Europe for over a century. The production of the BAP has helped ensure that the project will create an end product that provides genuine benefits for the wildlife and people of East London.

Introduction

The London 2012 Games are styled as 'the green games', aiming to be the most sustainable Games ever held. The preparation of the Olympic Park site included clearance of large areas of industrial, and often contaminated, land across 246 hectares in East London. **Figure 1** shows the indicative map of the Olympic Park at Games time. When working on such a vast project, with a non-negotiable deadline, there could always have been a risk that the promises made when planning permission was granted could have gradually fallen by the wayside as site clearance and construction progressed. This article, based on one published in IEEM's *In Practice*, explores the history of the project to date, and shows how the production of a scheme-specific Biodiversity Action Plan has helped ensure that the opportunities provided by the transformation of the site were not missed.

Before site clearance began, the area that is being transformed into the Olympic Park was dominated by industrial development. Despite this, it was not an area devoid of biodiversity; a series of inter-linked waterways flows through the Park, see **Figure 2**, eventually joining the Thames to the south, while patches of wetland, scrub, trees and brownfield habitat formed a series of wildlife 'islands' surrounded by urban landscape, see

Figure 3. Whilst the intrinsic biodiversity of each patch may not have been of particular note in a different context, their urban setting increased their effective value. Some of the areas were covered by non-statutory designations, including water courses within two Sites of Metropolitan Importance, and wetland, woodland and wasteland within four Sites of Borough Importance (Grade I) and one Site of Borough Importance (Grade II).

The site spreads across the boundaries of four London Boroughs: Hackney, Newham, Tower Hamlets and Waltham Forest. In 2006 a new area-specific planning authority was created, the Olympic Delivery Authority (ODA). This body was created under the London Olympic Games and Paralympic Games Act 2006 and works in close consultation with the Local Planning Authorities and statutory and non-statutory consultees. The outline planning application for the Olympic Park was submitted in 2007.

It is difficult to envisage the Environmental Statement that would be required to assess the impacts of redevelopment across almost 250 hectares of land. In order to provide a meaningful assessment, the Park was divided into a series of fifteen 'Delivery Zones' so that baselines and



Figure 1. Indicative map of the Olympic Park at games time © London 2012

impacts could be described for a series of individual areas, and then viewed cumulatively. Permission was granted in 2008. However, at that stage the detailed design of individual buildings, bridges, roads and parkland areas had not been prepared. The planning permission was therefore granted subject to numerous conditions, and the planning decision notice itself totals 168 pages in length. The conditions included one specifically for biodiversity:

Biodiversity Action Plan

OD.0.11 Before 30 September 2008, the Biodiversity Action Plan, which shall be based on the Biodiversity Action Plan Framework submitted with the application, shall be submitted to the Local Planning Authority for approval. This shall clearly identify the areas of recognised wildlife habitat to be provided and the means by which these will be maintained.

Reason: To help achieve biodiversity objectives and protect habitats and species.

The production of a scheme-specific Biodiversity Action Plan (BAP) may not be justified in many small development projects, but for the Olympic Park the BAP was critical to ensure commitments made in the Environmental Statement are delivered on the ground. As detailed design progressed, the BAP, and supplementary guidance, provided clear targets, such as a specific number of bird and bat boxes to be incorporated into the design of individual bridges.

During site clearance, the requirements of the BAP meant that measures to protect wildlife were not limited to the familiar 'headline' legally protected species. For example:

- Four thousand smooth newts were translocated to new and existing ponds off site;
- Where existing habitat could be retained, clearly labelled fencing was used to demarcate protected areas. These protected areas were identified on a map as a requirement of a planning condition, so works could not impinge on them unless the ODA had given prior approval;

- At the start of site clearance a log wall was created in the north of the Park, helping to provide some temporal connectivity for the invertebrates displaced during the subsequent habitat clearance elsewhere across the site. These invertebrates should be able to spread again to colonise newly created habitat as the site matures;
- Experimental translocation of brownfield habitat was also undertaken at Thornton's Field railway sidings. Pre-clearance site surveys revealed a variety of invertebrates, such as the toadflax brocade moth. Ballast, soil and timber sleepers were carefully moved from this area to a part of the Park where they would not be disturbed;
- Across the site, a 'permit to clear' system was used, so that no area of habitat would be removed until site ecologists had confirmed in writing that any issues had been resolved.

The BAP set out commitments that had to be met as the detailed design of parkland areas evolved. It also ensured that key works were programmed in correctly, so that opportunities were not missed. One example is provided by the planting



Figure 2. Aerial view of Olympic Park © London 2012

trials on the challenging riverside areas, described by Ian Morrissey of Atkins, London 2012's official engineering design provider, in another paper. Among the terrestrial habitats, seed collection and sapling translocation were undertaken. The areas of wetland being created should be suitable for reintroduction of water voles once the habitats are well established; to prepare for this, mink monitoring is already being undertaken. As the range of otters continues to expand, occasional records are made in the London area. In order to help ensure that they can colonise the Lower Lea Valley if and when they spread that far, two artificial holts are being installed in the north of the Park.

Overall, an impressive list of habitats will be created. The Park is one of the largest



Figure 3. New brownfield habitat provided by log wall

to be created in Europe for over a century with large areas, totalling 45 hectares, planned to support BAP priority habitats. The south park will be dominated by more ornamental planting, while the north park will have more 'natural' native planting, incorporating habitats that would once have been widespread in the Lower Thames Basin. The Park will include 10 hectares of native trees and shrubs, nearly two hectares of reedbeds and ponds and over 20 hectares of species-rich grassland. Room has been found for brownfield habitats, such as the extensive log walls created at East Marsh, resisting the temptation to only create 'tidy'-looking habitats. This habitat creation will be supplemented by other activities, such as the creation of living roofs on some buildings and the installation of 675 bird and bat boxes to provide roosting and nesting opportunities as the vegetation matures.

The success of these measures is not taken for granted. A BAP monitoring programme is ongoing during construction and the Games time phase of the site. After the London 2012 Olympic and Paralympic Games, the 'transformation' phase will convert the Park into the 'Legacy' site. Monitoring will then continue under a 10 year Maintenance and Management

Plan for the Parkland and Public Realm. The overall target of the BAP for habitat creation is 45 hectares of BAP priority habitat. This will be monitored, with management adapted if needed. The aim is to reach a point where the habitats' quality is such that the 45 hectares is worthy of designation as at least a site of Borough Importance (Grade I) within the Greater London designation system.

In conclusion, while the client's and contractors' commitment to following biodiversity guidance is essential to the success of any project, another important factor is the mundane process of getting the paperwork right. On a large and complex scheme like the Olympic Park, a site-specific Biodiversity Action Plan can provide a consistent point of reference to guide design and site works. In this case, the production of the BAP has helped to ensure that the project will create an end product that provides genuine biodiversity benefits.

Acknowledgement

This paper was first published in 'In Practice' Bulletin of the Institute of Ecology and Environmental Management Number 70 • December 2010



**Kevin Sene**

Principal Scientist

Water & Environment

Atkins

**Geoff Darch**

Principal Scientist

Water & Environment

Atkins

Risk and uncertainty in hydrological forecasting

Abstract

Probabilistic techniques are widely used to assist with reducing risk and improving investment decisions in engineering applications. Examples include the use of probabilistic safety assessments and reliability analyses in the energy, rail and aerospace industries. Probabilistic approaches are also increasingly used in the water industry, and some of the earliest applications were in modelling the impacts of effluent discharges on water quality, and in stochastic modelling to assist with the design of large reservoirs. More recent examples include the use of ensemble modelling techniques in climate change impact assessments and flood forecasting applications. The availability of probabilistic outputs also opens the way to a more risk-based approach to decision making, where risk is defined as the combination of probability and consequence. This paper reviews the techniques used in a range of recent water resources, water demand, water quality and flood forecasting applications, and takes a brief look to the future of probabilistic approaches in water-related applications.

Introduction

The assessment of risk and uncertainty is an active area of research in hydrological forecasting, where the word 'forecast' is used in its widest sense to describe any model output which has a time period and location attached to it, no matter how indicative or uncertain. Some key drivers include the potential for better decision-making, and for providing greater transparency in scientific outputs. There is also an increasing trend towards seamless forecasting with estimates of uncertainty at the full range of timescales, from short-range flood forecasts from hours to days ahead to scenarios for climate change over the next few decades.

Risk is usually defined as the combination of probability and consequence, where the consequence may be expressed in terms of the economic impacts, number of people at risk, or other factors. In hydrological applications, the probabilistic component is often obtained from a model representing how changes in meteorological or catchment conditions translate into variations in water availability, demand, or quality.

Here, we review a range of approaches for estimating future probabilities with

regard to water supply, water demand, water quality and flood forecasting applications. We also briefly discuss some of the current areas of research into how best to use the resulting estimates in risk-based decision-making. The methods which are discussed include Monte Carlo, Bayesian, multi-model, ensemble, and data assimilation techniques, see **Box 1**.

Approaches to hydrological modelling

Hydrological models are widely used by national hydrological services, environmental regulators, water companies and other organisations. Typically, models representing the relationships between rainfall and river flows (rainfall-runoff models) are set up for individual sites of interest, or combined with hydrological or hydrodynamic river flow routing components into an integrated catchment model. Physically-based distributed models and data-driven models, such as transfer functions and neural networks, are also sometimes used, see **Figure 1**.

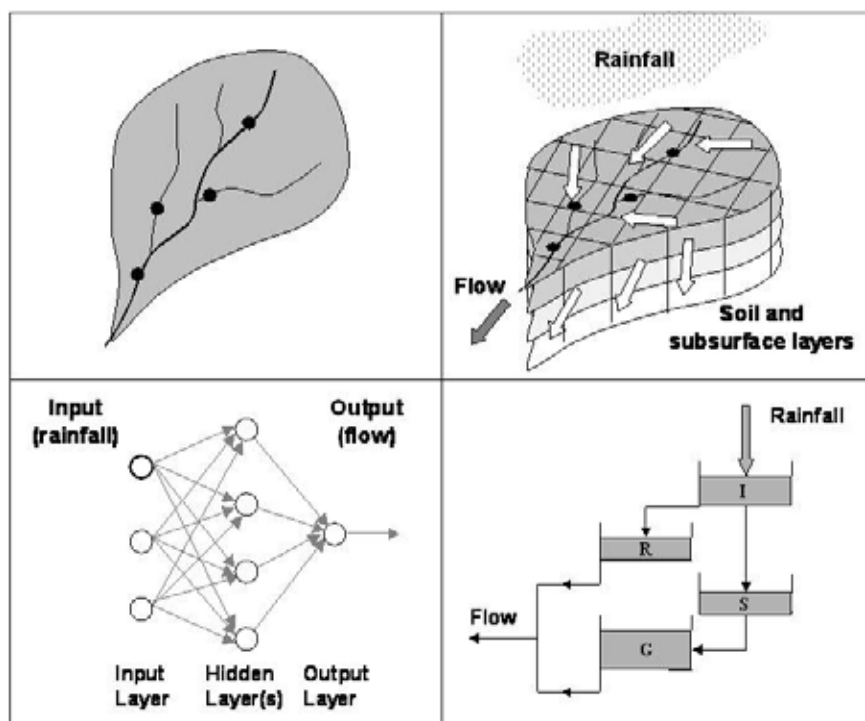


Figure 1. Some simple examples of physically-based, conceptual and data-driven rainfall-runoff models (evapotranspiration components not shown). From top left clockwise a) plan view of catchment with four river gauging stations b) physically-based model with three soil and sub-surface layers c) conceptual model with interception, soil, surface runoff and groundwater stores and d) artificial neural network model¹³ © Springer 2010.

Bayesian techniques

Methods which – using Bayes' Theorem – solve relationships between assumed (prior) and estimated (posterior) conditional and marginal probability distributions. Can include subjective prior assumptions

Cost loss

An approach to decision making which compares the costs of taking an action with the likely losses or damages. Can be related to probabilistic thresholds, and extended to non-monetary decision making e.g. using subjective Utility Functions

Data assimilation

Techniques which use recent and/or current observations to improve both the deterministic and probabilistic content of model outputs by adjusting initial conditions (model states), model parameters, input data, or model outputs

Ensemble modelling

Multiple model runs based on adjustments to initial conditions, boundary conditions, input data or model parameters

Forward uncertainty propagation

Methods which propagate ensemble members through one or more models to assess the sensitivity of model outputs to prior assumptions

Monte carlo methods

Techniques for deriving multiple model outputs which – at the simplest level – are based on random sampling from a probability distribution

Multi-model

The use of more than one model to obtain an ensemble of outputs; for example to help gauge the sensitivity of outputs to model structural errors

Sensitivity test

A 'trial and error' approach to assessing model uncertainty assuming a typical range for model parameters etc.

Statistical post-processing

Additional processing of probabilistic outputs to correct for bias and other factors, based on the historical performance of the approach. Often called probabilistic calibration or conditioning.

Some examples of this approach include the use of real-time rainfall, river level and weather radar observations in flood forecasting applications, and of the meteorological scenarios obtained from General Circulation Models (GCMs) in climate change impact assessments. In water quality modelling, the transport, interactions and decay of contaminants also need to be considered whilst, in water resources studies, predictions are also required for the likely future changes in water demand by residential, industrial and other users.

There are potentially many sources of uncertainty when a complex network of models is considered, and various types of probabilistic technique have been developed to explore the impacts on model outputs. In some cases, these methods are well established and have been used for many years: examples include stochastic modelling for the design and operation of large reservoirs²¹ and ensemble techniques for seasonal forecasting of snowmelt^{5,20}.

A more recent development has been the use of ensemble meteorological forecasts in flood forecasting applications, following the widespread introduction of this approach by meteorological services in the 1990s³. The latest climate change scenarios from the Intergovernmental Panel on Climate Change (IPCC) are also derived using a multi-model ensemble approach¹⁰.

Example applications

Climate change impacts on water supply

In the UK, as in many other countries, both public and private sector organisations increasingly need to take account of the potential impacts of climate change when considering future investments and the security of water supplies.

Whilst the fourth assessment report from the IPCC provides a continental to global overview, many countries have also commissioned more detailed local studies, and the United Kingdom Climate Projections 2009 (UKCP09) are the most recent for the UK¹².

UKCP09 is significantly more sophisticated than its predecessor (UKCIPO2) both in terms of the scientific methods used and in the tools and outputs available to the user. The main outputs include:

- Probabilistic projections of climate change over land and sea;

- Projections of sea-level rise and in storm surges;
- A weather generator for producing synthetic meteorological time series.

Projections are provided for 25km grid squares across the country using three emissions scenarios, and also for 16 administrative areas, 23 river basins and 6 marine regions.

Compared to previous assessments, the principal innovation is the probabilistic nature of the projections. Whereas UKCIP02 was based on deterministic scenarios produced using just one GCM, the UKCP09 projections are assimilated from an ensemble of over 300 model runs of the Hadley Centre GCM (HadCM3) and a selection of other IPCC GCMs. This allows exploration of alternative model parameterisations and structures.

Therefore, instead of a single 'best-guess' of change in climate, the projections provide a range of outcomes for each emissions scenario, which are converted into probability density functions using Bayesian statistics. However, the headline messages for the UK remain similar to those of UKCIP02: hotter, drier summers and warmer, wetter winters.

The major challenge in using these new scenarios is their complexity. In particular, there is co-variance between months within and between climate variables which means that the numerous probability density functions require sampling in multi-dimensions, for example using a Latin Hypercube sampling approach to derive an ensemble approximation¹⁷.

In Atkins, we are developing approaches to using the sampled output as well as techniques for using other UKCP09 products in various research projects for UKWIR, an organisation that facilitates collaborative research for UK water operators. This includes modelling the impacts of changes in rainfall, temperature and river flow on water and waste water treatment processes and their distribution networks, and the potential environmental implications.

We have also developed guidance for UKWIR on using the UKCP09 weather generator to assess changes in short duration storm events for use in sewer network modelling and are now creating a software tool based on this for use by water companies.

Water demand

In water resources assessments, estimates are often required for both the water supply and demand, looking forwards for a decade or more. There are many uncertainties in this type of analysis, and probabilistic approaches are widely used, particularly for the demand component.

In the UK, water companies update Business Plans and Water Resource Management Plans at least every five years for a 25-year planning horizon, with detailed investment proposals agreed with the regulators for fixed 5-year periods. The current Asset Management Plan (AMP5) cycle extends from 2010 to 2015. Some key sources of uncertainty in future projections include:

- Uncertainties in the base year estimate of demand;
- Uncertainties in the demand forecasts;
- Risks to supplies and uncertainties associated with those risks;
- Uncertainties associated with forecast levels of leakage;
- Outages for issues other than routine maintenance.

Starting more than a decade ago, UKWIR commissioned a series of research studies into how risk and uncertainty could be incorporated into the planning process. For example, Atkins led a study to develop guidelines on approaches to incorporating risk and uncertainty into the supply-demand balance, ranging from simple tabulated approaches to full simulation models operated on a weekly timestep¹⁶. We and others subsequently used the suggested approaches on a number of studies for water companies as part of the previous AMP4 planning cycle.

The latest water resources planning guidelines⁶ allow for the possibility of applying a probabilistic approach to estimate the influence of risk and uncertainty in assessments of supply and demand. A Monte Carlo approach is typically used, with one key consideration being the gap between supply and demand, known as the headroom.

Both target and actual headroom values are defined, with the target headroom being a minimum 'buffer' or planning margin to account for the various uncertainties in the modelling process. Water companies typically define a 90% or 95% confidence of achieving the required level of service for any given future demand situation, defined in terms of the estimated surface water deployable

output. For example, if the preferred level of service is that drought orders to ban non-essential water use should not occur more frequently than once in 35 years, and the Target Headroom is set at the 95% confidence interval, then a company can be 95% confident that it has sufficient supply provision in all years of its forecast to ensure that it can meet the level of service.

Atkins has applied these techniques for a number of water companies as part of their water resources planning process. For example, as part of the AMP4 studies for Anglian Water Services, we developed a Monte Carlo approach which could be applied at a range of spatial scales, from individual asset planning zones to the whole region, and which incorporated a component-based approach to demand forecasting. The uncertainties arising from two aspects of unplanned outages were also considered, namely pollution risks and asset failures. This overall approach provided a greater understanding of the risks and potential benefits associated with future capital works and investment decisions.

River water quality models

Water quality models are widely used to assess the impacts of pollution incidents in rivers, and for assessing the influence of industrial and sewage discharges. The influence of diffuse pollution from farmland and urban areas is also increasingly of interest.

Typically an advection-dispersion or simpler mass-balance modelling approach is used, often including rate constants to allow for the reaction or decay of constituents. The selection of models will be based on the complexity of the problem and, in some cases, a full hydrodynamic model may be used for the river flow component whereas in others a simple water balance may be sufficient. An ecological component may also be included; for example, in forecasting the spread of harmful algal blooms.

There are many potential sources of uncertainty in model development, and in the measurements used to calibrate and operate models. There is therefore a long tradition of assessing the uncertainty in model outputs, with probabilistic techniques widely used^{1, 4, 9}.

Atkins has routinely been applying Monte Carlo and other uncertainty estimation techniques on water quality modelling projects for many years. For example, in collaboration with DHV,

COWI, Sweco and Alterra, Atkins is currently contributing to the European Commission funded China River Basin Management Programme (2007-2012). This is to support the government of China in the establishment of integrated river basin management practices in the Yellow and Yangtze River basins, see **Figures 2 and 3**.

There has been considerable success in the Yellow River Basin in the application of integrated river basin planning to manage the quantity of water in the river and to control abstractions. However, the water quality situation is not currently satisfactory. Rapid industrial and urban development with weak control of discharges from industry and

little investment in urban wastewater treatment has led to the water in the main stem and tributaries of the Yellow River becoming highly polluted and unable to function as a healthy water resource for the natural ecosystem and human development needs.

Thus, one component of the programme in China is the development of approaches to reduce water pollution through the implementation of an environmentally sustainable river basin management programme. This includes the development of general (regulatory) water quality management planning and emergency (early) warning tools, together with training and development for clean technology. During 2011, we also contributed to a 4-day conference in Hangzhou organised and sponsored by the project which focussed on methods for determining pollutant carrying capacity and pollution load allocation.

There is significant interest in European approaches and so the programme has also included exploratory studies by Atkins into the potential for stochastic modelling of parameters such as Biochemical Oxygen Demand (BOD), dissolved oxygen and pH. However, at this time, a deterministic approach is being used for the main analysis work so that it is possible to more easily understand how new technologies relate to the existing procedures in China.



Figure 2. Hydrological monitoring station in the Yellow River Basin

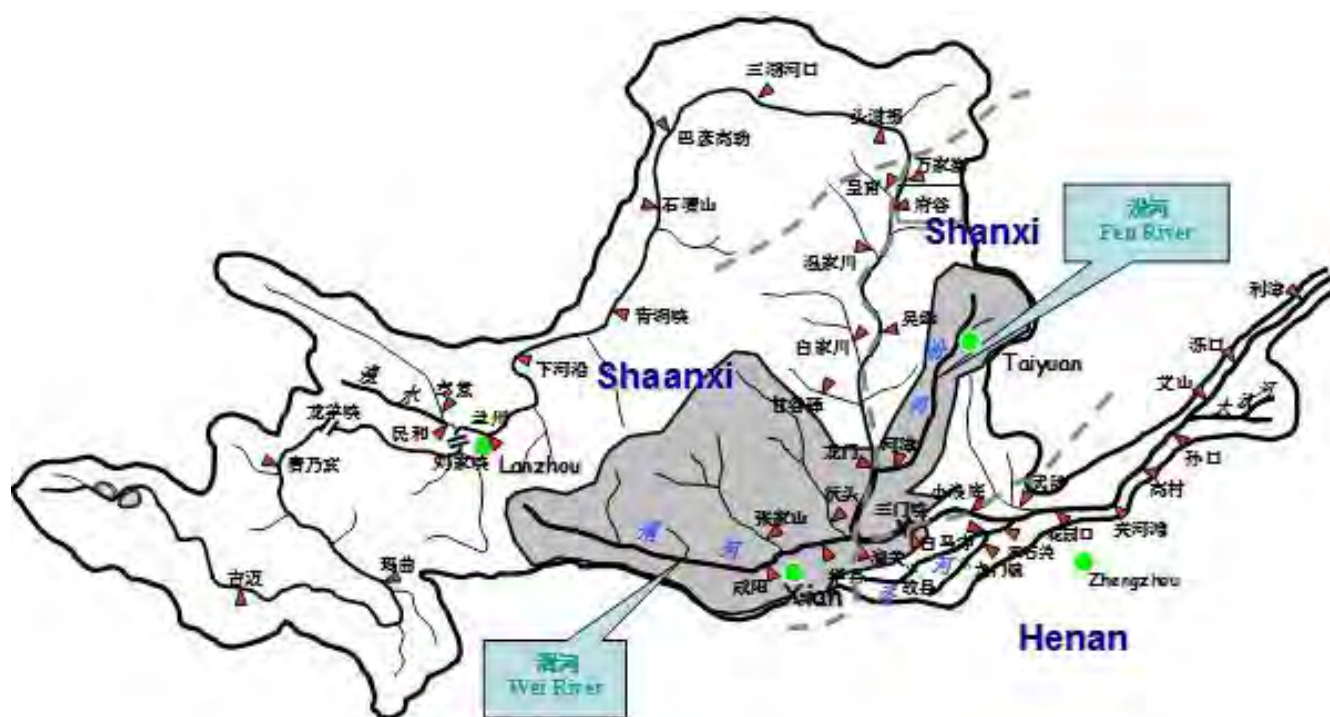


Figure 2. Hydrological monitoring station in the Yellow River Basin

Real-time flood forecasting

Flood forecasts can provide useful information to extend the lead-time and accuracy of flood warnings to householders, local authorities and the emergency services.

Typically, telemetered measurements of river levels, river flows and raingauge or weather radar estimates of rainfall are received on a 15-minute or hourly basis. These are then used as inputs to a computer-based flood forecasting system which is operated at least once a day, and more frequently during flood events. Model outputs can include forecasts for river levels, river flows, reservoir levels and other parameters from minutes to days or more ahead. Forecast lead-times can also be extended by using rainfall forecasts, and additional model components may also be included to represent complicating factors such as snowmelt and river control structure operations.

Rainfall-runoff models are a key component in many forecasting systems, and are used to estimate river flows from rainfall observations and forecasts. Air temperature values may also be used in models with a snowmelt component. For larger catchments, it often makes sense to use an integrated catchment model, and the advantage of this 'semi-distributed' approach is that spatial variations in catchment response and rainfall can be accounted for to some extent. Also, more accurate estimates can be derived for intermediate locations in the catchment. Where appropriate, the use of a hydrodynamic component allows factors such as tidal influences, structure operations and backwater effects to be represented.

Some examples of real-time models developed by Atkins range from a single rainfall-runoff model developed for a small catchment in southern England through to models such as that for the Welland and Glen catchment, which combined 55 rainfall-runoff models with a hydrodynamic model which included almost 500 weirs, gates and other structures. A key difference with the development of off-line (simulation) models is often the use of data assimilation, which is the process of using real-time data to improve the forecast. Some examples of this approach include error prediction, state updating, and parameter updating techniques, and normally a range of additional lead-time dependent model performance measures also needs to be considered. Some simplification and rationalisation of models may also be required if run-times and model stability and convergence are an issue.

Obviously, with many data inputs and models, there are also many potential sources of uncertainty, and these can propagate through the modelling network to locations further downstream. The uncertainty may arise from the data inputs, model parameters, initial conditions, boundary conditions, and other sources. Similar considerations also apply to coastal forecasting models which – at their most complex – can include hydrodynamic, wave and sea defence overtopping modules.

One approach to estimating uncertainty is to propagate estimates for an assumed range of values for individual components through the modelling network. Some examples of these so-called forward uncertainty propagation approaches include the use of sensitivity tests, 'what-if' scenarios and ensemble techniques, and these have been used for many years in off-line applications. However, this approach, although useful for exploring model performance, has some key limitations when used in flood forecasting applications. Perhaps the most important is that the probabilistic estimates are only as good as the prior assumptions which are made. Also, the number of ensemble members required can be large, and this can cause run-time issues, especially when a hydrodynamic component is included.

For real-time use, therefore, other approaches may be required, particularly if the probabilistic outputs are to be assessed against critical values, such as flood warning thresholds, or are required as inputs to cost-loss or other decision-support approaches. The main candidates are probabilistic data assimilation techniques, which use real-time data in deriving estimates of uncertainty, and statistical post-processing techniques, which adjust the outputs to account for the historical differences between observed and forecast probabilities.

Some of these approaches have recently been explored in a two-year research study for the Environment Agency as part of a project led by Atkins in collaboration with Deltares, Lancaster University, CEH Wallingford and Edenvale Young⁷. The techniques which were investigated included developments to existing ensemble Kalman filtering and Bayesian Model Averaging techniques developed by Deltares¹⁹, the Lancaster University Data Based Mechanistic (DBM) and adaptive gain approaches^{2, 8, 15}, and the CEH ARMA error prediction method¹¹. A quantile regression approach was also developed by Deltares¹⁸. User guidelines and a structured uncertainty

framework were also developed to help guide practitioners on the selection of appropriate techniques, taking account of factors such as the level of risk, catchment response times, the operational requirements for probabilistic information, and model run-times¹⁴.

Conclusions

The past few years have seen an increasing use of probabilistic and risk-based techniques in hydrological forecasting. The potential benefits have been demonstrated for a range of applications in water resources, agriculture, hydropower, flood warning, reservoir operations and other areas.

In addition to developing the underlying techniques, a key focus for research is how to make best use of the probabilistic information which is derived, and how to communicate this to end users. Whereas, with a deterministic forecast, decisions can often be made by reference to a critical threshold, in a probabilistic approach a new dimension needs to be considered, which is the probability at which actions should be taken. It is also often stated that the modelling effort should be focussed on the decision-making process, rather than using more traditional 'top-down' modelling approaches.

Many approaches to decision-making are potentially available, and ideas from decision and game theory such as cost-loss techniques and the economic value of forecasts can assist with finding an optimum solution, taking account of the risk profiles of end users (e.g. risk-taking, risk-averse). Special consideration is also required for extreme events, such as floods and droughts, since not only are the technical issues of estimating probabilities more complex, but the response and priorities of those affected may change when faced with potentially severe or catastrophic losses.

If a risk-based approach is used, the need to consider the consequences of a decision also changes the nature of the dialogue between hydrological specialists and the users of the information provided. The people best placed to estimate consequences are often those directly affected by any impacts, and this increasingly requires more of a collaborative approach, combining the skills of hydrologists and other disciplines, such as social scientists, economists, the emergency services, hydropower operators, and irrigation experts.

Acknowledgements

This paper describes projects performed by a number of people in the Strategy, Assessment and Management (SAM) group in Atkins. This work has also benefitted from research commissioned by a number of organisations, including Defra, the Environment Agency, the European Commission, and UK Water Industry Research (UKWIR). The contributions from the various project partners mentioned in the text are also gratefully acknowledged.

References

1. Beck M.B., van Straten G. (Eds.) (1983) *Uncertainty and Forecasting of Water Quality*, Springer Verlag, Berlin
2. Beven K. J. (2009) *Environmental Modelling; An Uncertain Future*. Routledge, London
3. Cloke H.L., Pappenberger F. (2009) Ensemble flood forecasting: A review. *Journal of Hydrology* 375: 613-626
4. Cox B.A., Whitehead P.G. (2005) Parameter Sensitivity and Predictive Uncertainty in a New Water Quality Model, Q2. *J. Environmental Engineering*, 131(1): 147-157
5. Day G. N. (1985) Extended Streamflow Forecasting using NWSRFS. *J. Water Resources Planning and Management*, 111(2): 157-170
6. Environment Agency (2008) *Water Resources Planning Guideline*. Environment Agency, Bristol, November 2008
7. Laeger, S., Cross, R., Sene, K., Weerts, A., Beven, K., Leedal, D., Moore, R.J., Vaughan, M., Harrison, T. and Whitlow, C. (2010) Risk-based probabilistic fluvial flood forecasts for integrated catchment models. BHS Third International Symposium, Role of Hydrology in Managing Consequences of a Changing Global Environment, Newcastle University, 19-23 July 2010, British Hydrological Society
8. Leedal, D. (2010) A Data Based Mechanistic (DBM) adapter module for the UK Environment Agency National Flood Forecasting System. International Workshop on Data Assimilation for Operational Hydrologic Forecasting and Water Management, Delft, 1-3 November 2010
9. Loucks D.P., Lynn W.R. (1966) Probabilistic Models for Predicting Stream Quality. *Water Res. Research*, 2(3): 593-605
10. Meehl, G.A., T.F. Stocker, W.D. Collins, P. Friedlingstein, A.T. Gaye, J.M. Gregory, A. Kitoh, R. Knutti, J.M. Murphy, A. Noda, S.C.B. Raper, I.G. Watterson, A.J. Weaver and Z.-C. Zhao (2007) Global Climate Projections. In: *Climate Change 2007: The Physical Science Basis. Contribution of Working Group I to the Fourth Assessment Report of the Intergovernmental Panel on Climate Change* [Solomon, S., D. Qin, M. Manning, Z. Chen, M. Marquis, K.B. Averyt, M. Tignor and H.L. Miller (eds.)]. Cambridge University Press, Cambridge, United Kingdom and New York, NY, USA
11. Moore, R.J., Robson, A.J., Cole, S.J., Howard, P.J., Weerts, A., Sene, K. (2010) Sources of uncertainty and probability bands for flood forecasts: an upland catchment case study. European Geosciences Union General Assembly 2010, Vienna, Austria, 2-7 May 2010
12. Murphy, J.M., Sexton, D.M.H., Jenkins, G.J., Boorman, P.M., Booth, B.B.B., Brown, C.C., Clark, R.T., Collins, M., Harris, G.R., Kendon, E.J., Betts, R.A., Brown, S.J., Howard, T.P., Humphrey, K.A., McCarthy, M.P., McDonald, R.E., Stephens, A., Wallace, C., Warren, R., Wilby, R. and Wood, R.A. 2009. UK Climate Projections Science Report: Climate change projections. Met Office Hadley Centre, Exeter.
13. Sene, K.J. (2010) *Hydrometeorology: Forecasting and Applications*. Springer, Dordrecht, 355pp
14. Sene, K.J., Weerts, A.H., Beven, K.J., Moore, R.J., Whitlow, C., Laeger, S., Cross, R. (2012) Uncertainty estimation in fluvial flood forecasting applications. In: K. Beven and J. Hall (eds.), *Applied uncertainty analysis for flood risk management*, Imperial College Press, London, to appear.
15. Smith, P. (2010) Adaptive correction of deterministic models to produce accurate probabilistic forecasts. International Workshop on Data Assimilation for Operational Hydrologic Forecasting and Water Management, Delft, 1-3 November 2010
16. UKWIR (2002) *Uncertainty and risk in supply/demand forecasting*. United Kingdom Water Industry Research, London.
17. UKWIR (2009). *Assessment of the Significance to Water Resource Management Plans of the UK Climate change projections 2009* (09/CL/04/11). ISBN: 1 84057 547 6
18. Weerts, A.H., Winsemius, H.C., Verkade, J.S. (2011) Estimation of predictive hydrological uncertainty using quantile regression: examples from the National Flood Forecasting System (England and Wales). *Hydrol. Earth Syst. Sci.*, 15, 255-265, 2011
19. Weerts, A.H., Seo, D.J., Werner, M., Schaake, J. (2012) Operational hydrological ensemble forecasting. In: K. Beven and J. Hall (eds.), *Applied uncertainty analysis for flood risk management*, Imperial College Press, London, to appear
20. Wood A. W., Schaake J. C. (2008) Correcting Errors in Streamflow Forecast Ensemble Mean and Spread. *J Hydrometeorology*, 9(1): 132-148
21. Yeh W. W-G. (1985) Reservoir Management and Operations Models: A State-of-the-Art Review. *Water Resources Research*, 21(12): 1797-1818



Adam Gelber
Group Manager
ED Environmental East
Atkins North America



Don Deis
Senior Scientist IV
ES IWR East
Atkins North America



Leslie Manzello
Scientist II
ED Environmental East
Atkins North America



Beth Zimmer
Senior Scientist II
ED Environmental East
Atkins North America

Long-term monitoring at the East and West Flower Garden Banks, 2004-2008

Abstract

The Flower Garden Banks (FGB) are located in the northwestern Gulf of Mexico and form part of a discontinuous arc of reef environments along the outer continental shelf. These coral reef banks are the largest charted calcareous banks in the northwestern Gulf of Mexico and are the northernmost coral reefs on the continental shelf of North America. Although coral and non-coral dominated communities exist on neighboring banks (e.g. Sonnier Bank, Stetson Bank), the reefs at Cabo Rojo, Mexico are the closest developed coral reefs in the Gulf of Mexico.

The topographic features of the FGB were created by salt diapirs of Jurassic Louann origin and the consequent uplifting of sedimentary rocks. The caps of these salt domes extend into the photic zone in clear, oceanic water where conditions are ideal for colonization by coralline algae, hermatypic corals, invertebrates, and fish species typical of Caribbean basin coral reefs. Coral species richness is lower at the FGB than on Caribbean reefs with just 31 species of scleractinian corals. The FGB also supports over 250 species of reef invertebrates, over 80 species of marine algae, and 177 species of tropical Atlantic fish. Oceanic salinity conditions prevail at the FGB and range from 28 to 38 ppt, with water temperatures ranging from 19°C (February/March) to ~ 31°C (August/September). Water clarity at the FGB is excellent, commonly 30m or more, providing light to photosynthetic organisms.

Since 1973, the Minerals Management Service (MMS) has conducted a program of protective activities at the FGB. The topographic features stipulation was designed to protect sensitive biological resources in the northwestern Gulf of Mexico, especially the FGB, from the adverse effects of oil and gas activities. The stipulation defines a No Activity Zone (NAZ) around each of the Banks and no oil or gas structures, drilling rigs, pipelines, or anchoring are allowed within the NAZ. From 1988 to 1995, the MMS monitored the FGB coral reefs on an annual basis to detect any changes that may be caused by oil and gas activities, as well as other incipient changes. In addition to the protective measures provided by MMS, the FGB were designated as a United States National Marine Sanctuary in 1992. Beginning in 1996, the National Oceanic and Atmospheric Administration (NOAA), Flower Garden Banks National Marine Sanctuary (FGBNMS), and the MMS partnered to continue the long-term monitoring at the FGB.

Clients: Bureau of Ocean Energy, Management, Regulation and Enforcement (BOEMRE) and National Oceanic and Atmospheric Administration

Sponsoring OCS region: Gulf of Mexico

Applicable planning area(s): Gulf of Mexico, Western Planning Area

Fiscal year(s) of project funding: 2004-2008

Completion date of report: September 2010

Introduction

Study objective

The objective of the study was to monitor the East Flower Garden Bank (EFGB) and West Flower Garden Bank (WFGB) located in the northwestern Gulf of Mexico and form part of a discontinuous arc of reef environments along the outer continental shelf (**Figure 1**) in accordance with the long-term monitoring protocol, ensuring that the protective measures established by MMS continue to be effective.

Monitoring programme description

For the 2004-2008 monitoring effort, cruises were conducted aboard the M.V. Fling or M.V. Spree in September and November 2004 (EFGB and WFGB, respectively), June 2005, June 2006, June 2007, August and September 2007 (EFGB and WFGB, respectively), and November 2008. The general locations of the study sites are marked by permanent mooring buoys: FGBNMS permanent mooring number 2 at the EFGB and mooring number 5 at the WFGB. Establishment of the perimeter and crosshairs subdivided each 100m x 100m study site into four quadrants (**Figure 2**).

To estimate the areal coverage of benthic components, fourteen to sixteen 10m long transect tapes were randomly positioned at each study site. Benthic coverage and the coverage of coral stressors were estimated from these transects using videography. Four coral cores were extracted from *Montastraea faveolata* colonies at each Bank in 2005 and 2007 to determine annual coral growth rates. Because *Diploria strigosa* is the second largest contributor to coral cover at the FGB, *D. strigosa* lateral growth margins were monitored and photographed to detect changes from year to year (**Figure 3**).

In order to monitor changes in coral reef community structure repetitive 8m² quadrats were photographed and analyzed for percent cover, coral condition, and growth or loss of coral tissue over time. Perimeter lines were videotaped each year to document change at known locations and to obtain a general sense of coral condition and fish populations each year (**Figure 4**). Physical and chemical characteristics of the seawater overlying the reef caps at the FGB were assessed by monitoring temperature, salinity, dissolved oxygen, pH, turbidity, photosynthetically active radiation, chlorophyll *a*, ammonia, nitrate, nitrite, total kjeldhal nitrogen (TKN), and soluble reactive phosphorous. These water quality parameters were selected to characterize

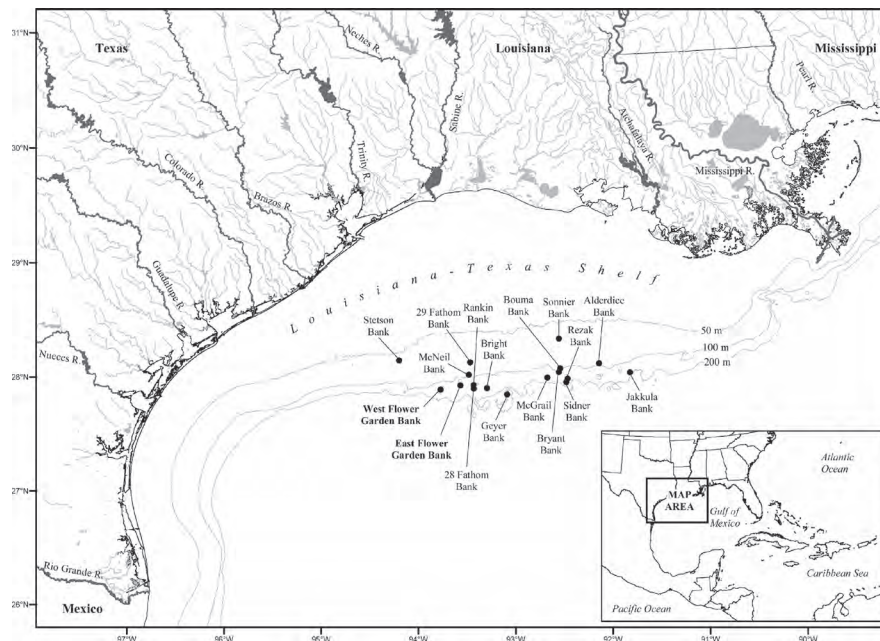


Figure 1. Map of study area



Figure 2. Establishing perimeter of study area



Figure 3. Detecting year to year changes



Figure 4. Videotaping perimeter lines



Figure 5. *Montastraea annularis* species complex

the environmental background in which the FGB coral reef resources exist. Surveys of fish assemblages were conducted to determine relative abundance and diversity of fish species. Surveys of sea urchins and lobsters were performed at night to determine abundance and distribution of populations.

In addition to the annual monitoring protocol, Hurricane Ike impacts (Hurricane Rita impacts were reported in a previous document²) quantitative coral health surveys, and notable biological and oceanographic events, such as sponge spawning, *Acropora* discoveries, coral disease, and exotic/invasive species were qualitatively assessed and documented. Coral biodiversity and taxonomy at the FGB were also evaluated.

Study results

Total coral cover, recorded by random transect videography from 2004 through 2008, ranged from $49.55 \pm 3.01\%$ to $64.13 \pm 2.70\%$ at the EFGB and from $54.41 \pm 3.13\%$ to $60.41 \pm 2.94\%$ at the WFGB. The *Montastraea annularis* species complex was the predominant component of coral cover at both Banks in all years and ranged from $26.80 \pm 4.09\%$ to $33.58 \pm 4.52\%$ at the EFGB and $31.70 \pm 2.70\%$ to $40.13 \pm 3.29\%$ at the WFGB. From 2004-2008, macroalgae were typically less abundant than crustose coralline algae, fine turf algae, and bare rock (CTB), with the exception of the EFGB in 2005 and 2008. Sclerochronology was used to measure the accretionary growth rates of *Montastraea faveolata*. When compared to the past two coring events (2003 and 2005), the 2007 core data did not appear substantially different with respect to mean growth rates. However, the range of annual growth from the 2007 samples does not show the same magnitude as the 2003 and 2005 samples. In addition, a reduction in mean annual coral growth rates was observed in the 2007 cores, which was likely related to the large-scale bleaching event that occurred in 2005. Although growth at lateral growth stations showed some significant variations and interactions, net growth was positive over the period 2003-2007. The repetitive

quadrat data showed that coral cover was consistently high during the period 2004-2008, ~64% for both Banks in all years. The coral assemblages remained stable at both Banks and dominant corals included *Montastraea annularis* species complex, *Diploria strigosa*, *Porites astreoides*, and *M. cavernosa*. Macroalgae and CTB cover showed reciprocal patterns and the incidences of bleaching, paling, and fish biting were low. There was no evidence of coral disease in the repetitive quadrats. Colonies of *M. annularis* species complex in repetitive quadrats (planimetry) showed overall positive growth from 2003-2008. Coral cover was high at the deep repetitive quadrats (32-40m or 105-131ft) at the EFGB, averaging ~77% between 2004 and 2008. The *Montastraea annularis* species complex (Figure 5) and *M. cavernosa* were the dominant species observed. The review of the 2004-2008 perimeter videos suggests that the coral communities displayed low levels of stress and high coral cover. Most distressed corals were affected by fish biting and there were few incidences of paling and bleaching. Though separate studies documented that bleaching affected up to 48% of corals in the fall of 2005, this study documented their recovery by the following spring. Fish surveys showed robust fish assemblages that were dominated by herbivorous fish and included healthy piscivore populations (Figure 6). Sea urchin surveys documented low densities of *Diadema antillarum* at both Banks from 2004-2008, except at the WFGB in 2004, 2007, and 2008; sea urchin density has not recovered to pre-1984 levels.

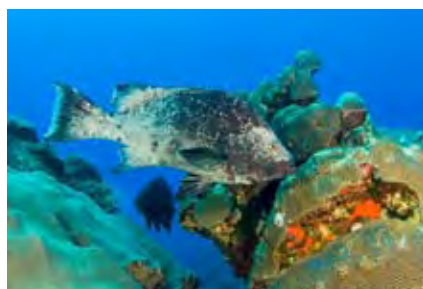


Figure 6. Healthy piscivorous fish

An estimated ~2.3m² of coral was missing from the study-site repetitive quadrat stations between June 2007 and November 2008 at the EFGB and WFGB, most likely due to Hurricane Ike. The greatest loss in terms of both the number of missing coral colonies and the total loss in area of coral cover occurred at the EFGB. Quantitative coral health surveys revealed that the vast majority of colonies surveyed were healthy. The prevalence of all coral health issues (including predation,

bleaching, ciliate infections, growth anomalies, and other miscellaneous health issues) was higher at the WFGB (9.96%) than at the EFGB (3.20%). The overall prevalence of all coral health issues at the community-wide level (EFGB and WFGB combined) was 6.78%.

Significant conclusions

The EFGB and WFGB coral reefs continue to thrive and remain the highest coral cover dominated reefs in the Caribbean and Gulf of Mexico. The reef communities have remained stable for the monitoring period 1988-2008, while other reefs in the region have declined. Continued monitoring of these reefs will document their long-term condition and be useful for studies focused on the dynamics of the robust benthic communities and the fish populations they support.

Figures 7 to 10 demonstrate the condition of the coral reef recorded and the scientific scuba diving surveys undertaken.



Figure 7.



Figure 8.

References

1. Zimmer, B., L. Duncan, R.B. Aronson, K.J.P. Deslarzes, D. Deis, M. Robbart, W.F. Precht, L. Kaufman, B. Shank, E. Weil, J. Field, D.J. Evans, and L. Whaylen. 2010. Long-term monitoring at the East and West Flower Garden Banks, 2004-2008. Volume I: Technical report. U.S. Dept. of the Interior, Bureau of Ocean Energy Management, Regulation, and Enforcement, Gulf of Mexico OCS Region, New Orleans, Louisiana. OCS Study BOEMRE 2010-052. 310 pp.
2. Precht, W.F., R.B. Aronson, K.J.P. Deslarzes, M.L. Robbart, B. Zimmer, and L. Duncan. 2008. Post-hurricane assessment at the East Flower Garden Bank long-term monitoring site: November 2005. U.S. Dept. of the Interior, Minerals Management Service, Gulf of Mexico OCS Region, New Orleans, Louisiana. OCS Study MMS 2008-019. 39 pp. + appendices. Internet URL: <http://www.gomr.mms.gov/PI/PDFImages/ESPIS/4/4318.pdf>.
3. Precht, W.F., R.B. Aronson, K.J.P. Deslarzes, M.L. Robbart, D.J. Evans, B. Zimmer, and L. Duncan. 2008. Long-term monitoring at the East and West Flower Garden Banks, 2004-2005 - Interim report. Volume I: Technical report. U.S. Dept. of the Interior, Minerals Management Service, Gulf of Mexico OCS Region, New Orleans, Louisiana. OCS Study MMS 2008-027. 123 pp. Internet URL: <http://www.gomr.mms.gov/PI/PDFImages/ESPIS/4/4322.pdf>.
4. Precht, W.F., R.B. Aronson, K.J.P. Deslarzes, M.L. Robbart, D.J. Evans, B. Zimmer, and L. Duncan. 2008. Long-term monitoring at the East and West Flower Garden Banks, 2004-2005 - Interim report. Volume II: Appendices. U.S. Dept. of the Interior, Minerals Management Service, Gulf of Mexico OCS Region, New Orleans, Louisiana. OCS Study MMS 2008-028. 1330 pp. Internet URL: <http://www.gomr.mms.gov/PI/PDFImages/ESPIS/4/4323.pdf>.
5. Precht, W.F., R.B. Aronson, K.J.P. Deslarzes, L.S. Kaufman, M.L. Robbart, El. Hickerson, G.P. Schmahl and J. Sinclair. Long-Term Reef Monitoring at the Flower Garden Banks: Status, Stasis and Change. In, Ritchie, K.B. and Brian D. Keller, eds. 2008. A Scientific Forum on the Gulf of Mexico: The Islands in the Stream Concept. Marine Sanctuaries Conservation Series NMSP-08-04. U.S. Department of Commerce, National Oceanic and Atmospheric Administration, National Marine Sanctuary Program, Silver Spring, MD. 105 pp. Internet URL: <http://sanctuaries.noaa.gov/science/conservation/pdfs/gom.pdf>.
6. Precht, W.F., Deslarzes, K.J.P., Hickerson, E. Schmahl, G.P., Sinclair, J. and Aronson, R.B. 2008. Holocene reef development at the Flower Garden Banks: recent surprises. Abstracts 11th International Coral Reef Symposium, Ft. Lauderdale, FL, p.5. Internet URL: http://www.nova.edu/ncr/11icrs/11icrs_abstractbook_final.pdf.
7. Robbart, M., B. Zimmer, L. Duncan, D.R. Deis, R.B. Aronson, K.J.P. Deslarzes, W.F. Precht, J. Sinclair, E.L. Hickerson, G.P. Schmahl, G.S. Boland. 2008. Post-hurricane assessment and recovery at the East Flower Garden Bank. Page 417 in Abstracts (Poster 18.612), 11th International Coral Reef Symposium, 7-11 July 2008. Ft. Lauderdale, USA.
8. Schmahl, G.P., E.L. Hickerson and W.F. Precht, 2008. Biology and Ecology of Coral Reefs and Coral Communities in the Flower Garden Banks Region, Northwestern Gulf of Mexico. In, B.M. Riegl and R.E. Dodge, Coral Reefs of the USA, Springer Science, 2008.
9. Zimmer, B., W.B. Precht, E.L. Hickerson, and J. Sinclair. 2006. Discovery of *Acropora palmata* at the Flower Garden Banks National Marine Sanctuary, Northwestern Gulf of Mexico. Coral Reefs (2006) DOI 10.1007/s00338-005-0054-9.



Figure 9.

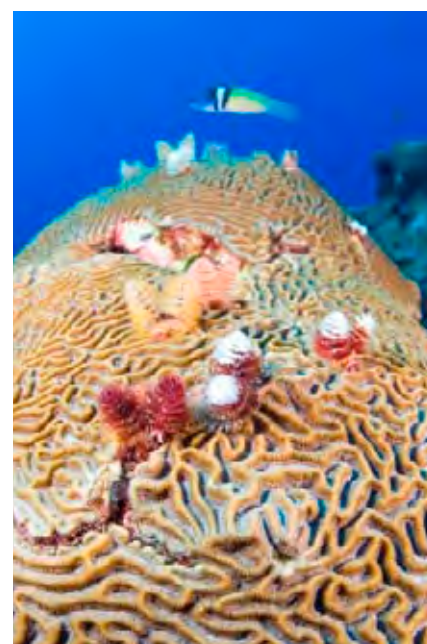


Figure 10.







ATKINS

This publication is printed on 9lives 80 paper. It is produced from 80% recycled fibre comprising: 10% packaging waste, 10% best white waste, 60% de-inked waste recycled fibre, and 20% virgin TCF (totally chlorine free) fibre sourced from sustainable forests. The supplier of 9lives 80 is accredited with the ISO 14001 standard.

www.atkinsglobal.com

© Atkins Ltd except where stated otherwise.

The Atkins logo, 'Carbon Critical Design' and the strapline 'Plan Design Enable' are trademarks of Atkins Ltd.